Mechanism of CLIC5A-Dependent Rac1 Activation and ERM Phosphorylation

by

Md Mizanur Rahman

A thesis submitted in partial fulfilment of the requirements for the degree of

Doctor of Philosophy

Department of Medicine

University of Alberta

Abstract

The chloride intracellular channel (CLIC) isoform 5A was discovered in a complex with ezrin and actin in placenta microvilli. CLIC5A is also greatly enriched in kidney glomeruli and is essential for assembly of the ezrin/NHERF2/podocalyxin complex at the apical domain of glomerular podocyte foot processes. CLIC proteins are soluble members of the GST family whose crystal structure is inconsistent with the theory that they are membrane-spanning chloride channels. CLIC5A stimulates Rac1 activity and ezrin, radixin, moesin (ERM) protein phosphorylation. The goals of this thesis are to better understand direct and functional relationships of CLIC5A with Rac1, ERM proteins and taperin in the organization of the cortical actin cytoskeleton of cells.

Though CLIC5A expression increased Rac1-GTP levels, and CLIC5A was part of the Rac1-GTP complex, I found the CLIC5A interaction with Rac1 to be indirect. Unbiased yeast two-hybrid screening revealed that radixin and taperin bind CLIC5A directly. I observed that CLIC5A interacts directly with the carboxyterminal domain of all ERM proteins, but its affinity for ezrin is the highest. Furthermore, the last 16 aa of ezrin are necessary for CLIC5A binding, and phosphorylation of ezrin at T567 markedly enhances its interaction with CLIC5A.

In renal glomeruli, endogenous CLIC5A was predominantly soluble, and Staurosporine and phospholipase C activation reduced the small proportion of CLIC5A associated with the membrane fraction. In cultured cells, triple ezrin, radixin, and moesin silencing reduced CLIC5A localization to the apical cell periphery, suggesting that CLIC5A localizes to the cortical cytoskeleton by interacting with ERM proteins.

The ezrin 432-586(T567D) mutant, which has a high affinity for CLIC5A, competitively inhibited CLIC5A-dependent phosphorylation of endogenous ERM proteins and Rac1

activation, but ezrin 432-570, which does not bind CLIC5A, was without effect. Knockdown of endogenous ezrin also reduced CLIC5A-dependent Rac1 activation, and CLIC5A expression enhanced Rho GDI/ezrin co-immunoprecipitation. These findings indicate that CLIC5A-stimulated Rac1 activation is ezrin dependent, and that CLIC5A enhances Rho GDI/ezrin binding promoting Rac1 activation.

CLIC5A-stimulated Rac1-GTP activation increased PI4P5KIα and PI5P4KIα lipid kinase precipitation with the Rac1-GTP complex, and in kidneys *in vivo*, precipitation of the PI4P5Kα3 kinase isoform with Rac1-GTP required CLIC5A. I therefore postulate that CLIC5A promotes Rac1 activation in ERM complexes, stimulating localized $PI4,5P_2$ generation by PI4P5Kα3.

Taperin. a protein phosphatase 1 (PP1) regulatory subunit, exists as isoform 1 (taperin 1, 1-711 aa) and as splice variants 2, 3 and 4, all starting at aa 307. I found that taperin isoforms 1 and 2 interact directly with CLIC5A and that residues 307-385 of taperin are sufficient for the interaction. The $_{45}$KGVVF$_{49}$ motif of CLIC5A, conserved among all CLICs, is required for its interaction with taperin. As expected, mutation of the $_{577}$KISF$_{580}$ motif of taperin 1 (1-711 aa) or 2 (307-711 aa) to $_{577}$KASA$_{580}$ abolished binding of the PP1 catalytic subunit (PP1c). In the presence of wild-type CLIC5A, immobilized GST-ezrin 432-586 captured taperin 1 and PP1c, but neither taperin nor PP1c were captured by GST-ezrin in the presence of mutant CLIC5A $_{45}$KGAVY$_{49}$. GFP-taperin 1 localized predominantly to the nucleus and the cell periphery. By contrast, GFP-taperin 2 localized exclusively to the nucleus. In the presence of wild-type CLIC5A, but not CLIC5A $_{45}$KGAVY$_{49,}$ there was a dramatic reduction in the taperin 1 nuclear localization, without effect on taperin 2, and RFP-CLIC5A co-localized with GFP-taperin 1 at the cell periphery. Interestingly, PP1cα and PP1cβ, but not PP1cγ, were captured by GST-CLIC5A even when taperin was silenced, and purified GST-CLIC5A precipitated all purified

PP1c isoforms *in vitro*, independent of taperin. Taperin knockdown did not change CLIC5A localization at the cell periphery, but reduced ERM phosphorylation. Therefore, CLIC5A brings taperin 1/PP1c into the CLIC5A/ezrin complex, and it profoundly reduces the nuclear localization of taperin 1.

To sum up, CLIC5A interacts directly with ERM proteins, and the interaction is enhanced by ERM phosphorylation. The ezrin/CLIC5A interaction enhances the sequestration of Rho GDI by ezrin to facilitate Rac1 activation. CLIC5A also brings taperin 1/PP1c into the ezrin complex and reduces the nuclear localization of taperin 1.

Preface

This thesis is an original work by Md. Mizanur Rahman.

Portions of chapter 3, 4, and 5 had been submitted in a peer-reviewed journal: **Md Mizanur Rahman**, Jong S. Kim, Laiji Li, Mahtab Tavasoli1, Zhixiang Wang, Peter M. Hwang, Barbara J. Ballermann. *A direct, functionally significant interaction between CLIC5A and ERM proteins*, Journal of Biological Chemistry, 2023, Manuscript Number: JBC-D-23-00350. The paper is ready for a new submission to the Journal of Biological Chemistry.

Md Mizanur Rahman prepared the first draft of the Journal of Biological Chemistry manuscript for publication (including the figures and the figure legends). Jong S. Kim performed experiments in Figure 1 (A, B, C), and Figure 2 (A, B, C). Md. Mizanur Rahman performed Figure 2 (D, E, F), and Figure 3 - 7, and supplementary Figure S-1, and Figure S-2 of the manuscript. Dr Barbara J. Ballermann the principal investigator supervised the studies and prepared the final draft of the Journal of Biological Chemistry paper for submission.

Md Mizanur Rahman designed and performed all the experiments in chapter 3, 4, 5, and 6 of this thesis unless otherwise stated. Dr. Barbara J. Ballermann, as the primary supervisor, supervised all the experiments.

Dr. Xin Wang performed the Rho GTPases pull down from kidney cortex tissue lysates as Figure 5.4 mentioned in this thesis.

Amy Barr prepared the Adenovirus-GFP and Adenovirus-GFP/CLIC5A vector constructs.

GFP-Rac1 constructs were kindly provided by Dr. Zhixiang Wang, Department of Medical Genetics, University of Alberta.

Dr. Laiji Li prepared the different cDNA/vector constructs of CLIC5A, different GFP-ezrin constructs, different GFP-taperin constructs, and recombinant, purified GST, GST-CLIC5A,

GST-ezrin 432-586 proteins used this study. He also provided the protocol for GST-pull-down. He trained me western blot and the use of confocal microscope and he worked together with me for capturing confocal microscopy images.

Goat-α-GFP antibody was a gift from Dr. Luc Berthiaume, Department of Cell Biology, University of Alberta.

Dedication

I dedicate my thesis to my parents and my siblings. Words cannot express how grateful I am to my loving parents, the late Md. Abul Kalam Azad and Momtez Begum, who have always loved me, supported me, and believed in me. I will always appreciate them. I would also like to dedicate this thesis to my wife, Tahmina Akhi, and my amazing and wonderful daughter Khadija Tul Kubra, who was born during my doctoral study.

Acknowledgements

First, I would like to acknowledge my supervisor, Dr. Barbara J. Ballermann for making my dream come true. Thanks Dr. Ballermann for your continuous support, supervision, and patience during my doctoral study. I am really lucky to have you as my mentor. To me, she is the perfect example of an ideal professor and a great scientist who dedicated her life to science. I did not see anyone more passionate than her for scientific research. She is the one who makes me passionate about research. She guided me through a variety of experiences, including how to design and perform my experiments and analyze the data, and she was always there to provide me with feedback to promote excellence in my project. She encouraged me when I was having trouble getting results and taught me how to do troubleshooting.

I also would like to give special thanks to my supervisory committee members, Dr. Zhixiang Wang and Dr. Peter Hwang, for their thoughtful mentoring, time, and helpful suggestions throughout my study. My sincere thanks to my past and present colleagues in the Dr. Ballermann Lab: Dr. Laiji Li, the lab manager, for providing me valuable guidance and necessary training in different assays. I also want to thank Dr. Cindy Wang, the research fellow, who also provided me with important tips. I would like to thank Dr. Salah Aburahes, who completed his Ph.D. from our lab, and Peter Kim (an MSc. student), for their friendship and encouragement. I also want to thank Dr. Abul Kalam Azad from Dr. Allan Murray's lab, Division of Nephrology, Department of Medicine, who encouraged me throughout my study. I would like to acknowledge Dr. Allan Murray for permitting me using his lab facilities.

I would like to acknowledge the funding agencies: The Canadian Institutes For Health Research (CIHR), Heart and Stroke Foundation of Canada, The Natural Sciences and Engineering Research Council of Canada (NSERC) and the Division of Nephrology-University of Alberta.

Table of Contents

List of Figures

Chapter 1:

Chapter 3:

Chapter 7:

List of Tables:

Abbreviations Used

aa	amino acids
cDNA	Complimentary DNA
CLIC	Chloride intracellular channel
DAG	Diacylglycerol
DMEM	Dulbecco's Modified Eagle Medium
DTT	Dithiothreitol
ERM	Ezrin, Radixin, Moesin
FBS	Fetal bovine serum
FERM	Band 4.1-ezrin-radixin-moesin amino terminal domain
GFP	Green Fluorescent Protein
GSH	Glutathione
GDP	Guanine diphosphate
GST	Glutathione S-transferase
GTP	Guanine triphosphate
GTPase	Guanosine triphosphatase
HRP	Horseradish peroxide
H_2O_2	Hydrogen peroxide
IAA-94	Indanyloxy acetic acid-94
KO	knock out
NHERF2	Sodium-hydrogen exchange regulatory cofactor
P -35 mm	35-mm cell culture dish
P-60 mm	60-mm cell culture dish
P-100 mm	100-mm cell culture dish
PBS	Phosphate-buffered saline
PI(3,4,5)P3	Phosphatidylinositol-3,4,5-triphosphate
PI(4,5)P2	Phosphatidylinositol-4,5-bisphosphate
p-ERM	Phosphorylated ERM (on Thr 567)
PI4P5K	Phosphatidyl-inositol 4 phosphate-5 kinase
PI5P4K	Phosphatidyl-inositol 5 phosphate-4 kinase

PKA	Protein kinase A
PKC	Protein kinase C
PLC	Phospholipase C
Rac1	Ras-related C3 botulinum substrate 1
ROCK	Rho-associated kinase
SAGE	Serial analysis of gene expression
SDS	Sodium dodecyl sulfate
siRNA	small interfering ribo-nucleic acid
SH2 domain	Src-homology domain
PAGE	Polyacrylamide gel electrophoresis
RFP	Red fluorescence protein
WT	Wild type

Symbols:

α	alpha
β	beta
γ	gamma

Prefixes:

kilo-	k-	10^3
milli-	m-	10^3
micro-	μ-	10^{-6}
nano-	n-	10^{-9}

Units:

Degree Celsius	°C
Second	sec
Hour	h
Gram	g
Litre	L
Metre	m
Moles	mol
Base pair	bp
Molarity	M = mol/L

Standard Amino Acids:

Alanine	A
Asparagine	N
Glutamine	Q
Serine	S
Valine	V
Tyrosine	Y
Aspartic acid	D
Glutamic acid	E
Phenylalanine	F
Glycine	G
Histidine	H
Isoleucine	I
Lysine	K
Leucine	L
Methionine	M
Proline	P
Arginine	R
Threonine	T
Tryptophan	W
Cysteine	C

Chapter 1

Introduction, Hypothesis and Objectives

Chapter 1

1. Introduction

The renal system consists of kidneys, ureters, bladder, and urethra. Mammalian kidneys are extremely vascularized and receive nearly 25% of cardiac output. Filtration of blood plasma occurs in kidney glomeruli, specialized capillaries that lie between afferent and efferent arterioles (1). Arterioles are contractile high resistance blood vessels that regulate the plasma flow rate and hydraulic pressure within glomerular capillaries. Kidney glomeruli filter around 150 L of blood plasma every day in healthy adult humans. To drive filtration, glomerular capillary hydraulic pressures (45-50 mm Hg) are much higher than those in other systemic capillaries (10-15 mm Hg). The degree of efferent arteriolar contraction is vitally important in maintaining a high hydraulic pressure within the glomerular capillaries. It varies depending on the physiological state and ensures a near constant renal blood flow and glomerular filtration rate (GFR). By contrast, blood in other capillary beds empties into low-resistance venules, and the degree of contraction of pre-capillary arterioles in other vascular beds can cause blood flow to be extremely variable.

Glomerular capillaries provide a large, extremely porous surface area for filtration. The glomerular filtration rate (GFR) is defined as the amount of water filtered from blood plasma across the glomerular capillary walls into Bowman's space per unit of time (2). The rate of filtration depends on the plasma flow rate, the pressure gradient between capillary and Bowman’s space, the glomerular capillary surface area, and the hydraulic permeability of the capillary wall. Hydraulic permeability is defined as the permeability to water. The GFR can be measured using substances dissolved in plasma that are freely filtered by glomerular capillaries and are not reabsorbed or secreted into the urine by the tubules. Clinically, creatinine produced

by muscle comes close to being a good substance to measure the GFR. For studies in animals infused inulin is often used. GFR = [urine concentration of creatinine or inulin)] X urine flow rate (mL/min)]／[plasma concentration of creatinine or inulin)] (2).

Accurate measurement of GFR is crucial for the diagnosis of kidney disease. The GFR in healthy people is 90 ml/min/1.73m^2 or higher, while it is less than 60 ml/min/1.73m^2 in chronic kidney disease patients (3). Although the GFR is extremely high, most of the filtered fluid is reabsorbed, in a regulated fashion, by the kidney tubules, and normally only 1-2 % of the glomerular filtrate is excreted as urine.

The glomerular capillary wall (GCW), also called the glomerular filtration barrier (GFB) acts as a molecular sieve that selectively filters blood to generate the initial urinary filtrate, which consists of water and small dissolved molecules (4). Despite the rapid flux of water and small solutes across the GCW, filtration of large proteins like albumin and immunoglobulins is extremely restricted. The GFB consists of three layers. Layer 1: the glomerular endothelial cells (glomerular ECs), lining the interior surface of the capillaries. Layer 2: glomerular basement membrane (GBM), which is thicker than the basement membrane of other vascular beds (5). Layer 3: glomerular visceral epithelial cells called “podocytes”, which cover the exterior surface of the capillaries. Other cell types that do not belong to the GFB are also present in the glomeruli. Among them are the mesangial cells and parietal epithelial cells. Mesangial cells together with mesangial matrix confer structural support for the glomerular vasculature. Parietal epithelial cells form the lining of Bowman’s capsule. Glomerular filtrate flows into Bowman’s space, then into proximal tubule and down into the loop of Henle, followed by the distal convoluted tubule, and finally into the collecting ducts. The efferent glomerular arterioles divide into peritubular capillaries, which take up fluid reabsorbed by the tubule epithelial cells,

returning it back to the body via the renal veins. The renal tubule epithelial cells contain ion and water channels and many transporters which adjust the composition of the urine through resorption and secretion. This is necessary for body water homeostasis, electrolyte and acid-base balance, mineral homeostasis (particularly Ca^{2+}, Mg^{2+} and PO_4^{2-} for bone mineralization) and resorption of amino acids, glucose, and other substances.

If the glomerular capillary pressure is elevated above normal for prolonged periods, or if there are other forms of glomerular injury, for instance, glomerulonephritis, or genetic abnormalities, glomerular cells undergo structural and functional changes to adapt. Defects in the structure and function of glomerular cells almost always disrupt the glomerular filtration barrier causing albumin and other large proteins to pass into the urine (proteinuria) and often progress to end-stage renal disease. Importantly for this thesis, injury of glomerular podocytes, which express extremely high levels of CLIC5A, always lead to proteinuria and triggers glomerular remodelling leading to glomerular sclerosis. Spot urine measurements of the albumin-to-creatinine ratios is used to define proteinuria or albuminuria (albuminuria 300 mg to 3 grams/day, normal <300 mg/day) (6). Understanding the signalling pathways that regulate the dynamic changes of the actin cytoskeleton of podocytes is promising to pinpoint new therapeutic targets to slow down proteinuria and the progression of kidney disease.

1.1. Brief summary of the main kidney functions

Kidneys are paired organs located in the retroperitoneum just below the diaphragm. Each kidney weighs 125-170 grams in adult men and 115-155 grams in adult women. Longitudinal cuts reveal two different regions in the kidney, the pale outer cortex that contains the glomeruli, proximal tubules, and distal tubules, and the darker inner medulla, that contains the loops of Henle and the collecting ducts (Figure 1) (7). The kidneys are perfused with blood through renal

arteries, which arise from the abdominal aorta. The renal arteries branch into smaller arteries and then arterioles, and finally into afferent arterioles, which empty into glomerular capillaries. Glomerular capillaries form a nearly protein-free filtrate consisting of water and small solutes at a rate of about 125 ml/minutes (8). Kidney tubules maintain body fluid homeostasis and osmoregulation despite changes in dietary intake or endogenous metabolic by-product production. They regulate osmolarity predominantly via urine diluting and concentrating mechanisms (9) by its response to vasopressin and the ability to deploy aquaporins to the luminal membrane of collecting duct cells (10). Kidney tubules also regulate the total body water content and the concentration of electrolytes, sodium (Na^+) as the main cation in the extracellular space, potassium (K^+) as the main cation in the intracellular space, chloride (Cl^-) as the main extracellular anion, and other important electrolytes like calcium (Ca^{2+}), magnesium (Mg^{2+}), bicarbonate (HCO_3^-), bisphosphate (HPO_4^{2-}), sulfate (SO_4^{2-}). The normal blood plasma Na^+ concentration is 142 mmol/L, K^+ 5.0 mmol/L, Mg^{2+} 1.5 mmol/L, ionized Ca^{2+} 2.5 mmol/L, Cl^- 103 mmol/L, $HCO3^-$ 27 mmol/L, HPO_4^{2-} 1.0 mmol/L, SO_4^{2-} 103 mmol/L. The intracellular Na^+ concentration is 15 mmol/L, K^+ 150 mmol/L, Mg^{2+} 1.0 mmol/L, Ca^{2+} 0.0003 mmol/L, Cl^- 5 mmol/L, HCO_3^- 8 mmol/L (11).

The kidneys also produce erythropoietin to stimulate red blood cells generation. They produce renin for the regulation of blood pressure. They also produce a 1-α-hydroxylase enzyme which converts vitamin D to its active form 1,25 dihydroxy vitamin D3.

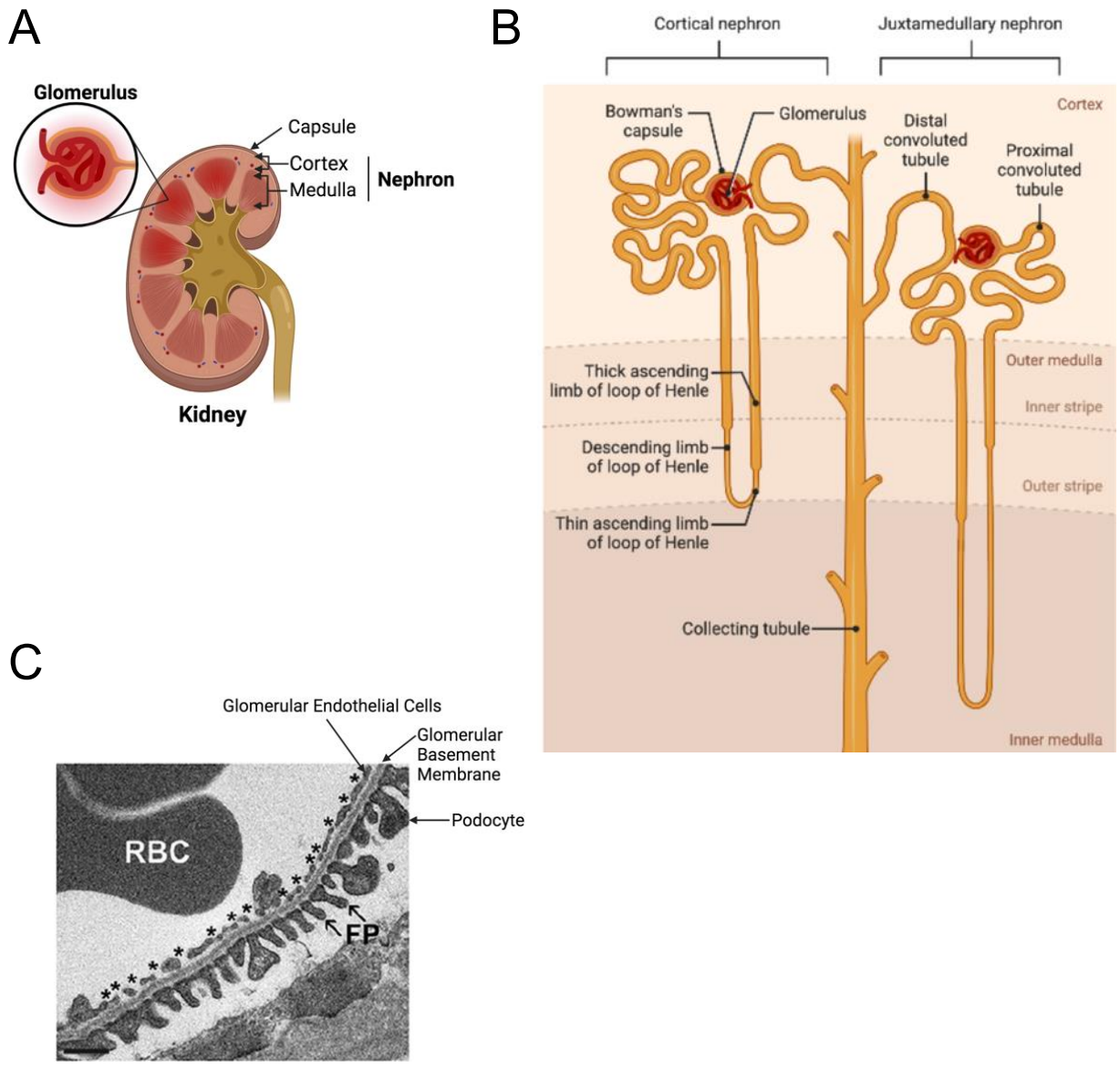

Figure 1.1: Anatomy of kidney and glomerular filtration barrier. A. Representation of kidney cortex and kidney medulla. **B.** Nephron Structure. The glomerulus, proximal tubule, loop of Henle, distal tubule and collecting duct. **C.** Transmission electron microscopic image of the GFB. FP: Podocyte foot processes. RBC: red blood cells. glomerular EC fenestrae. (Figure 1A and B created using template from Biorender.com image drawing software, 2024; Figure 1C reproduced with permission, Tavasoli M, Al-Momany A, Wang X, Li L, Edwards JC, Ballermann BJ. Both CLIC4 and CLIC5A activate ERM proteins in glomerular endothelium. Am J Physiol Renal Physiol. 2016 Nov 1:311(5):F945-F957).

1.2. Glomeruli: The filtration unit of the kidney

A human kidney contains an average of 1 to 2.5 million glomeruli (12). The glomerular capillary wall allows free passage to water and small solutes while circulating blood cells and large plasma proteins like albumin, immunoglobulins are selectively retained in the blood (13, 14).

1.2.1. Mesangial cells

Mesangial cells (MCs) are microvascular pericytes with features similar to smooth muscle cells (15). MCs represent 30–40% of the glomerular cell population (16) and are located between the capillary loops embedded in the mesangial matrix, together referred to as the "mesangium". The MCs play a role in clearing pathogens from the glomerulus, depositing matrix in cellular immune responses, and contributing to cell-to-cell signalling. The MCs are in contact with the glomerular capillary loop basement membrane at the para-mesangial angles, and they also directly contact glomerular EC without intervening basement membrane (17). During glomerular development, glomerular EC produce PDGFβ that binds MC PDGFβ receptors resulting in MC recruitment into the developing glomerular tuft (18). The MCs are in continuity with the extraglomerular mesangium and the juxtaglomerular apparatus. The MCs are not a direct component of the GFB but form a central stalk of the glomerulus where they are important contributors to glomerular structure.

1.2.2. Endothelial cells: the first layer of the glomerular filtration barrier

Glomerular ECs are the first layer of the perm-selective glomerular capillary wall and are in direct contact with blood. Similar to all endothelial cells, glomerular ECs have an anti-coagulant surface that prevents blood coagulation and acts as a barrier to prevent blood cells and large proteins from escaping into the urine. Glomerular ECs are quite flattened and much more permeable to water and small solutes than other capillary endothelial cells because they are

heavily perforated with transcellular pores, called fenestrae. Fenestrae are plasma membrane-lined pores of around 60-70 nm in diameter accounting for around 20% of the glomerular EC surface (19, 20). These transcellular pores are suitable for rapid passage of high volumes of fluid (21). Although the 60–70 nm pore size of glomerular EC fenestrae is too large to prevent the passage of proteins such as albumin, the fenestrae contain a gel-like, negatively charged glycoprotein mesh (21-23), which is a continuum of the glycocalyx that covers the glomerular EC. The glomerular EC glycocalyx is composed of proteoglycans and glycoproteins that are anchored at or in the cell membrane. The endothelial surface layer (ESL) is an associated layer of proteins, glycoproteins, and proteoglycans that adhere to the glycocalyx, but are not anchored in the membrane (4). Some of the ESL proteins, including albumin, are in equilibrium with blood (4, 24). The strong negative charge of the glomerular EC glycocalyx and its associated ESL repels negatively charged proteins like albumin and prevents their entry into the fenestrae, thus adding substantially to the permselectivity of the GFB (25).

Podocyte-derived vascular endothelial growth factor-A (VEGF-A), transforming growth factor-β1 (TGF-β1), and glomerular basement membrane-derived laminin β3/α3 are all involved in the formation of glomerular ECs fenestrae. Deletion of VEGF-A from podocytes in mice (26), TGF-β1 inhibition in developing rat kidneys (27), laminin β3 gene mutation in humans (28, 29) and laminin α3 gene deletion in mice (30), all prevent glomerular EC fenestrae formation. Also, perfusion of kidneys the drug Adriamycin induces proteinuria in mice, believed to be due, at least partly, to reduced synthesis of glomerular proteoglycans and disruption of the glomerular EC ESL (31). In rats, aging-related proteinuria also correlates with the loss of the glomerular EC ESL, and in human patients, diabetes-induced proteinuria correlates with the destruction of the glomerular EC ESL (21). Injury of glomerular ECs may promote tubulointerstitial fibrosis, a

cause of progression to end-stage renal disease (32). Diseases of the glomerular endothelium that compromise normal kidney function also include the Thrombotic Microangiopathies (TMAs), described by glomerular EC swelling, GBM splitting, fibrin and platelet deposition, and red blood cell fragmentation (33, 34).

1.2.3. The glomerular basement membrane (GBM)

The GBM is a highly ordered extracellular matrix (ECM) located between the podocytes and glomerular EC. As an integral component of the GFB, the GBM acts as an intermediary sieving matrix. It also is a sink for pro-angiogenic ligands and other mediators that provide for communication between podocytes and glomerular ECs. Electron microscopic observations revealed that GBM has an electron-dense lamina densa as its inner layer, flanked by the thinner laminae rara interna and rare externa (35). Although it is composed of the same types of macromolecules found in all other basement membranes, the GBM is thicker than most other basement membranes (36).

Proteomic analysis of purified human glomerular extracellular matrix identified 144 distinct proteins in the GBM (37, 38) the most abundant being laminin glycoproteins, type IV collagen network, heparan sulfate proteoglycan (HSPG), and nidogen. In the GBM, the major laminin trimer present is LM-521 (α5β2γ1) secreted by both podocytes and glomerular EC (39). Missense mutations in LAMB2, encoding the laminin β2 chain cause Pierson syndrome. Mice deficient in the laminin β2 chain have nephrotic syndrome (40) associated with podocyte foot process effacement, loss of slit diaphragms, as well as defective GBM formation (41). The collagen IV network is secreted as heterotrimers containing three α chains whose sequences include collagenous domains composed of many Gly-X-Y amino acid triplet repeats. The collagen IV network consists mainly of α3α4α5 heterotrimers secreted by podocytes, also some

(α1)2α2 secreted by the glomerular EC. Mutations in the collagen α5(IV) gene (COL4A5) cause Alport syndrome, a hereditary glomerulonephritis that progresses to end-stage kidney disease (42). HSPGs have a protein core with covalently attached glycosaminoglycan side chains, which are modified by sulfation to provide a negative charge to the HSPGs. Genetic studies in mice to minimize the negative charge of the GBM surprisingly failed to result in overt proteinuria (43-45). Likewise, heparanase treatment of the GBM to minimize negative charges of glycosaminoglycan also did not induce proteinuria (46). Agrin is present as the HSPG in the mature GBM (47) while perlecan and agrin co-distribute during glomerulogenesis (44). Although the HSPG abundance confers a negative charge to the GBM, which was thought, for a long time, to be a determinant of the charge selectivity of the GFB (44, 48-50), later studies indicate the GBM does not play a major role glomerular permselectivity. These studies, along with studies showing that disruption of the endothelial ESL leads to albuminuria, lead to the conclusion that the glomerular EC glycocalyx with its ESL is the main barrier to bulk albumin filtration with podocytes (see below) forming the final barrier for the small amount of large proteins that pass through the glomerular EC fenestrae and the GBM.

1.2.4. Podocytes, the final barrier for renal protein filtration

Podocytes are a major and final component of the GCW with structural and functional uniqueness. They are terminally differentiated cells whose foot processes cover outer surface of glomerular capillaries (35). Podocytes have a unique cellular morphology consisting of the cell body, long primary extensions also called major processes, from which extend secondary actin-based projections called foot processes (Figure 2). The foot processes are anchored along their length to the GBM, and their apical domain faces Bowman's space. Foot processes from one podocyte form an interdigitating structure with foot processes of adjacent podocytes (51).

Microtubules and intermediate filaments support the structure of the major processes while the actin-cytoskeleton forms the structural frame of foot processes (52, 53).

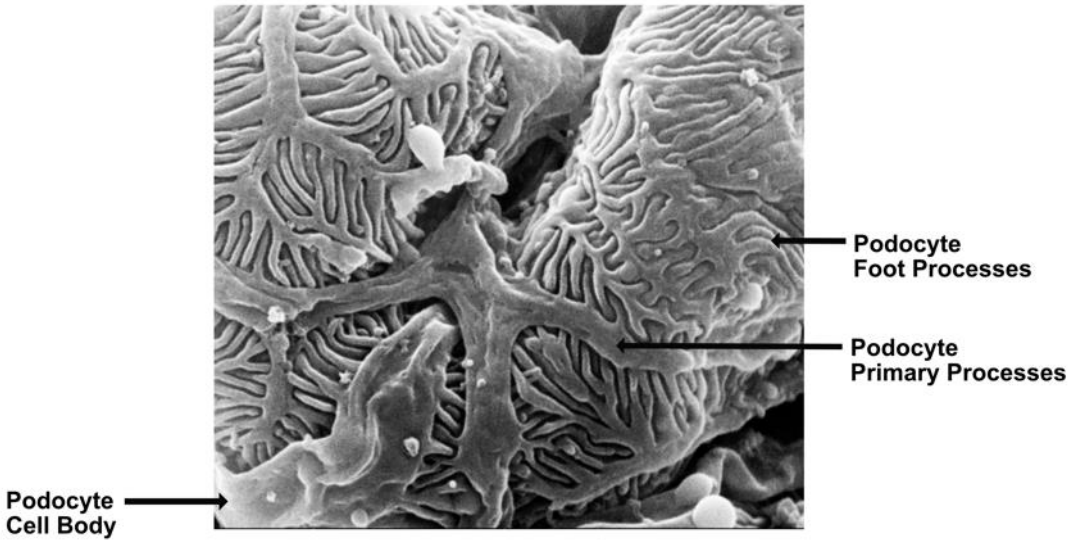

Figure 1.2: Scanning electron micrograph of mouse podocytes. Primary thick processes branch into secondary interdigitating foot processes that wrap around the capillary loops. This image was captured in our lab from a 2-month-old CLIC5-deficient mouse. Podocytes appear reasonably normal, but the number of foot processes is reduced, and they are, on average, broader.

The space between adjacent foot processes through which the glomerular filtrate flows into Bowman's space is called the filtration slit. A cell–cell junctional complex termed the "slit diaphragm" bridges adjacent foot processes (54). It is a meshwork of proteins consisting mainly of nephrin, nephrin-related protein (NEPH1), P-cadherin, FAT, neurexin and ephrin-B1. The slit diaphragm only bridges the foot processes from adjacent podocytes but not the podocyte cell bodies or adjacent primary extensions (55-57). Finnish-type congenital nephrotic syndrome (CNF or NPHS1) is an autosomal recessive disease resulting from nonsense mutations in the nephrin gene (58). NEPH1 knockout mice similarly develop podocyte foot process effacement and severe proteinuria (59). Other critical components of the podocyte slit diaphragm include P-cadherin (54), and the large transmembrane protein "FAT" (60). FAT deficient mice develop severe proteinuria(61). Neurexin and ephrin-B1 also are extracellular components of the slit diaphragm (62, 63). The slit diaphragm transmembrane proteins interact with intracellular scaffold proteins podocin, CD2AP, Par-complex molecules (Par-3, Par-6, aPKC), ZO-1, Nck, and MAGI. The podocyte glycocalyx contributes to the charge selectivity of the GFB and keeps the filtration slits open by repelling adjacent foot processes (64, 65).

Podocyte injury is the primary cause of many kidney diseases, most prominent among them membranous nephropathy, membranoproliferative glomerulonephritis, diabetic kidney disease (66, 67) and focal segmental glomerulosclerosis (FSGS). Podocyte injury often results in nephrotic syndrome characterized by severe proteinuria due to loss of glomerular permselectivity. FSGS, which is characterized by progressive scarring of glomeruli, is caused by several distinct mutations of proteins forming the podocyte actin cytoskeleton. By contrast, minimal change disease, which also causes massive proteinuria, results in reversible loss of foot processes. Calcium signaling regulates podocyte structure and slit diaphragm function. Podocyte

plasma membrane TRPC5 and TRPC6 channels promote calcium influx that results in actin cytoskeleton reorganization (68). TRPC6 binds RhoA, while TRPC5 binds Rac1. TRPC6 mutations R895C and E897K lead to increased calcium influx (gain-of-function) that leads to FSGS, but a loss of function mutation in TRPC6 is also associated with human FSGS (69). Mutations in α-actinin-4 and INF2, both of which are actin regulating proteins also results in podocyte dysfunction and human FSGS(70, 71), while mutations in nephrin and podocin cause recessive forms of steroid-resistant nephrotic syndrome. A common glomerular disease in adults, FSGS is due to mutations in essential podocyte proteins (72, 73). Acquired disorders due to viral infections, drug toxicity, diabetes, autoimmune disease and previous glomerular injury (74) can also cause podocyte injury and FSGS (75-78).

1.2.5. Protein complexes involve in the podocyte-GBM interaction

Integrin- and dystroglycan protein complexes anchor podocyte foot processes to the GBM. α3β1-integrins are the predominant integrins in mature podocytes (79-81). α3β1-integrins with distinct α and β chains are heterodimeric adhesion receptors that bind to GBM extracellular matrix type VI collagens, laminins, fibronectin, and nidogen (80, 81). Mice deficient in integrin α3 lack podocyte foot processes, have less than normal glomerular capillary loops and die within 24 hours of birth (82). Moreover, α- and β-dystroglycan, dystrophin and utrophin are also present at the basal domain of podocyte foot processes, where they bind to GBM components laminin, agrin, and perlecan. A reduction in dystroglycan expression has been reported in several mouse model of minimal change disease (83, 84).

1.2.6. Protein complexes at the apical domain of podocytes foot processes

The main objective of this thesis is to better understand the molecular mechanisms through which chloride intracellular channel (CLIC) isoform 5A participates in regulating the protein

complex that shapes the apical domain of podocyte foot processes. CLIC5A is one of the most highly expressed proteins in podocytes with transcript levels ~800 to 1000-fold higher in glomeruli compared to other tissues and cells (85). CLIC5A is necessary for ezrin activation/phosphorylation in podocytes *in vivo* (86, 87), and the assembly of the ezrin-NHERF2-podocalyxin complex that shapes the apical domain of podocyte foot processes(88, 89). Podocyte injury due to Rac1 hyperactivation is emerging as a key mechanism leading to FSGS and proteinuria. Therefore, it is critically important to define Rac1-dependent processes in podocytes. At the apical domain of podocyte foot processes, CLIC5A-dependent Rac1 activation thought to be required for phosphatidylinositol (4,5)-bisphosphate ($PI4,5P_2$) accumulation at the inner leaflet of the plasma membrane which, in turn, is required for ezrin phosphorylation, actin polymerization and hence maintenance of podocyte integrity. Thus, the CLIC5A-ezrin pathway might be a potential target for the interruption of glomerular injury. In addition, increasing evidence indicates that CLICs are not membrane-spanning chloride channels, but instead regulate Rac1 GTPase activity in the context of ERM phosphorylation. I will therefore first summarize major facts about the molecules that are part of the CLIC5A-podocalyxin-NHERF2-ezrin complex at the apical domain of podocyte foot processes, followed by a detailed description of CLIC proteins.

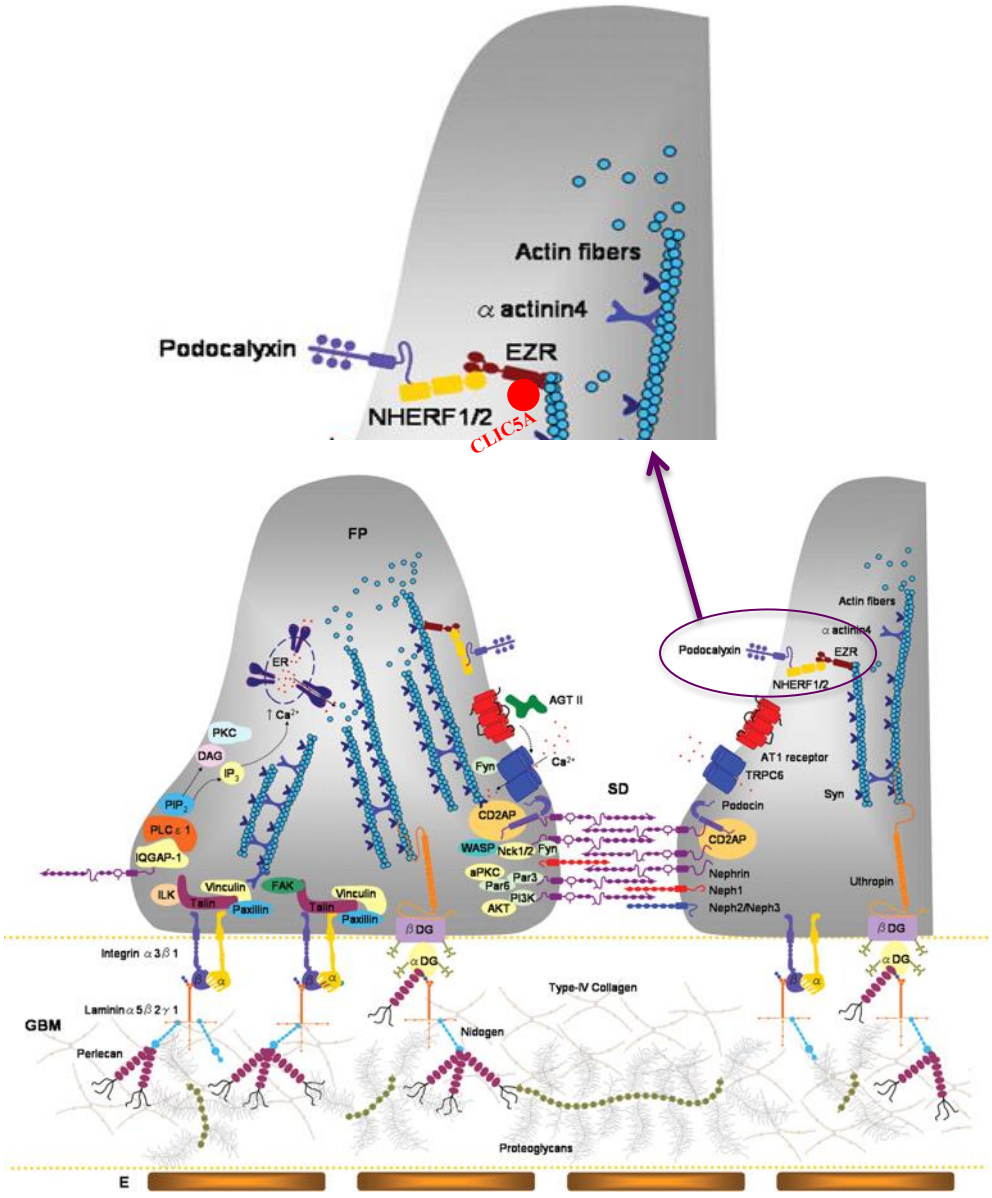

Figure 1.3: Podocyte foot processes showing protein complexes at the apical, lateral, and basal domain. (Reproduced with permission, Machuca E et al. Hum. Mol. Genet. 18:R185-R194, 2009). At the apical domain, the Ezrin-NHERF2-podocalyxin protein complex interacts with cortical actin and CLIC5A is a component of this protein complex [Wegner et al. (85)]. At the lateral domain, the filtration slit diaphragm functions as a modified adherens junction. It is composed of nephrin, podocin, P-cadherin, FAT, and CD2AP, and also interacts with the actin cytoskeleton. At the basal domain, integrins and dystroglycan interact with the GBM.

1.3. Rho GTPases: The critical regulators of actin cytoskeletal dynamics

Small GTPases are GDP/GTP-regulated monomeric switches that regulate many aspects of intracellular actin dynamics. More than 150 members of small GTPases (90) are divided into five main families: Rho, Ras, Rab, Arf, and Ran families (91). The Rho family of small GTPases is one of the most important subfamilies of the Ras superfamily. Rho GTPases are GTP-binding proteins commonly found in the eukaryotic cells (92). They consist of a GTPase domain, a short N-terminus, and a C-terminus. Rho GTPases consist of five conserved G box GDP/GTP-binding motifs G1-G5 (G1: GXXXXGKS/T, G2: T, G3: DXXGQ/H/T, G4: T/NKXD, G5: C/SAK/L/T) (93, 94). They have two variable regions- switch I (G2) region corresponding to amino acids ~28 to 40) and switch II (G3) region corresponding to amino acids 60 to 81(95-97) that serve as the nucleotide-binding pocket and interacts with Rho GEFs and Rho GAPs (98, 99). Rho GTPases switch I and switch II regions undergo structural rearrangement causing GTP-bound active/ON signal or GDP-bound inactive/OFF signal (100). Rho GTPases undergo posttranslational modifications at a cysteine residue in the CAAX motif, which is critical for their interaction with lipid bilayers and their biological activity within specific protein complexes (101).

In humans, Rho GTPases have 20 members, of which Rac1, RhoA, and Cdc42 have been extensively studied in mammalian cells. They have a crucial role in the formation of filopodia, lamellipodia, membrane ruffles, and stress fibers (102, 103). They regulate the organization of actin and microtubule cytoskeletal structures (104, 105), gene expression (106), vesicle trafficking (107-109), and cell cycle entry and progression through expression of genes involved in G1/S transition, and mitosis (110, 111).

There are three regulators of Rho GTPases, guanine nucleotide exchange factor (GEFs) that facilitate the exchange of GDP to GTP; GTPase activating proteins (GAPs) which increase GTP

hydrolysis; and the guanine nucleotide dissociation inhibitor (Rho GDI) which prevents GDP to GTP exchange (97). Over 80 Rho GEFs and 70 GAPs have been identified so far (97). Rho GEFs have limited binding specificity towards distinct Rho GTPases. Dbl and Vav 1-3 GEFs activate Rac1, RhoA, and Cdc42 and p190RhoGEF activates RhoA, RhoB, RhoC but not Rac1 and Cdc42 (97). The GTP-bound active Rho GTPases associate directly with their downstream effector proteins and thus elicit cellular responses (112). The on-off cycle of Rho GTPases ensures the appropriate spatiotemporal regulation of many cellular processes. RhoA, Rac1, and Cdc42 control actin assembly/disassembly when extracellular signal molecules bind receptors that triggers a signal cascade inside the cell. RhoA and Rac1/Cdc42 antagonistically regulate each other.

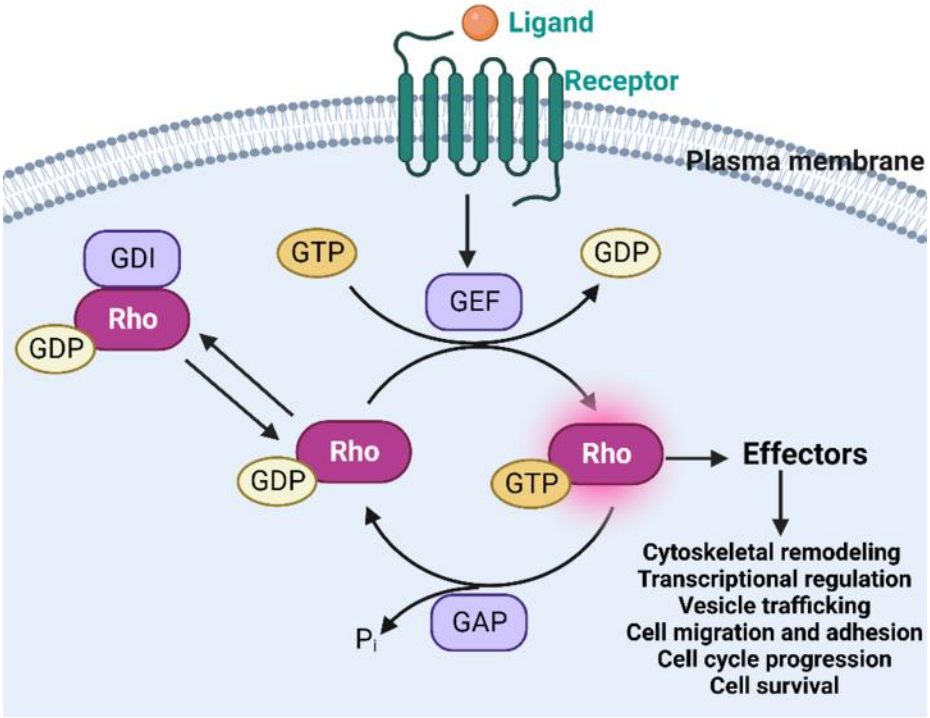

Figure 1.4: Regulation of Rho GTPases. (Reproduced with permission from Dandamudi, A.; Akbar, H.; Cancelas, J.; Zheng, Y. Rho GTPase Signaling in Platelet Regulation and Implication for Antiplatelet Therapies. Int. J. Mol. Sci. 2023, 24, 2519). GEFs activate Rho GTPases into their active, GTP bound form and GAPs inactivate Rho GTPases. Rho GDI extracts prenylated Rho GTPase from the plasma membrane by binding the isoprenoid moiety and sequestering it. Rho GTPase expression at the transcriptional level is controlled by the action of micro RNAs (miRNAs). Rho GTPases undergo posttranslational modifications by phosphorylation and sumoylation that cause the activation or inactivation of Rho GTPases depending on the cellular context. Protein levels of Rho GTPases are regulated by the ubiquitin-26S proteasome system.

1.3.1. RhoA

The Ras-related homolog (Rho) subfamily of Rho GTPases constitutes three members RhoA, RhoB, and RhoC (113). RhoA is mostly localized in the cytosol, and also at the plasma membrane and nucleus (114). The RhoA gene on chromosome 1 3p21.3 has more exons and introns than RhoB and RhoC and is suggested to be the ancestor of the latter two (115). RhoA is a monomeric protein with a molecular weight of ~21.7 kDa. RhoA prenylation at Cys190 in the CAAX-box provides stability and RhoA anchorage in the plasma membrane required for its function (115). Like other Rho GTPases, RhoA can cycle between the GTP-bound active form and GDP-bound inactive form (116) and is involved in regulating actin organization, cell morphology, and cell migration (103). Specifically, RhoA participates in the regulation of vesicle trafficking, tumor invasion, and metastasis (107, 117). In response to growth factors, RhoA is involved in the regulation of actin polymerization via effector molecule mDia and the formation of focal adhesion complexes that trigger cell motility and invasion (103). RhoA activates Rho activated kinase (ROCK) for force generation required for cell migration. ROCK, in turn, phosphorylates and inactivates myosin light chain phosphatase (MYPT) resulting in myosin II activation and actomyosin contraction (118). RhoA is active at the rear of the cell body required for rear retraction necessary for cell migration while Rac1 and Cdc42 are active at the leading edge of the cell to generate actin-based protrusion (119). While Rho regulates the myosin light chain phosphatase, RhoA and Rac1 control the synthesis of $PI4,5P_2$; both activities linked to actin organization (120).

In podocytes, RhoA is dispensable in the early developmental stage but becomes essential in enabling podocyte motility during later development (121). Appropriate localized RhoA activity stabilizes podocyte foot processes and protects them from effacement, but excessive RhoA

activity disrupts podocyte integrity. For example, podocyte-specific expression of constitutively active RhoA produces heavy albuminuria with histologic features like FSGS (122). Also, ROCK inhibition decreases podocyte dysfunction in chronic kidney disease (123) and combined angiotensin-converting enzyme (ACE) and ROCK inhibition in the 5/6-nephrectomy mouse model is more effective in reducing albuminuria than ACE inhibition alone(123). ROCK inhibition also blunts albuminuria in streptozotocin-diabetic rats (124). Such studies suggest that elevated RhoA activity in hypertensive and diabetic disease models mediate podocyte dysfunction. Conversely however, RhoA activity was found to be markedly reduced and accompanied by loss of actin stress fibers and podocyte apoptosis in the model of Lipopolysaccharide (LPS) and Adriamycin – induced injury *in vivo* (125), and siRNA mediated RhoA knockdown of and reduced actin stress fibers and enhanced podocyte apoptosis (125). Therefore, preservation of RhoA function in podocytes appears to be essential in preventing proteinuria.

1.3.2. Cdc42

Cell division control protein 42 homolog (Cdc42) is another important Rho GTPase. In humans, Cdc42 localizes to the Golgi complex, the plasma membrane, and various vesicles (126, 127). Cdc42 activation controls cytoskeletal remodeling, cell polarity, cell proliferation, cell migration, and transcription (109, 128). It has also been implicated in intracellular trafficking, regulation of malignant transformation and tumor metastasis (129, 130). The most widely studied Cdc42 isoform Cdc42u, first isolated from the placenta, is ubiquitously expressed and while Cdc42b is found in the brain (131, 132). In the GTP-bound active state, Cdc42 interacts with more than 60 effector molecules (133). Most important among these are PAK1-4 whose activation causes phosphorylation of LIM kinases 1 and 2, which phosphorylate and inactivate the actin-severing

protein cofilin (134), resulting in enhanced cell mobility. The MRCKα and MRCKβ effectors of Cdc42 phosphorylate moesin causing reorganization of the cortical actin cytoskeleton. In addition, the Cdc42 effector Par6 can induce apicobasal cell polarity. The active GTP-bound form of Cdc42 also binds and activates WASP, which, in turn activates the Arp2/3 complex (135, 136) leading to the actin polymerization and filopodia formation (137). The Cdc42 effectors ACK1 and ACK2 cause receptor endocytosis and degradation (132). Other Cdc42 effectors involved in the cellular processes are p70 S6 kinase, PI3K, PLD, PLC-β2, IQGAP1, IQGAP2, MLK2, MLK3, MEKK1 and MEKK4, ACK1 and ACK2, CIP-4, and MSE55 and BORGs (131).

In podocytes, Cdc42 plays a critical role in early development, and Cdc42 deletion from the podocytes triggers congenital nephropathy in mice (121). The lack of Cdc42 or its downstream effector N-WASP results in loss of stress fibers, podocyte apoptosis, and proteinuria apparently by decreasing expression of YAP (138). The Roundabout (ROBO) family of receptors and their ligands "SLIT glycoproteins", function as axon guidance molecules but they are also expressed in podocytes. The SLIT/ROBO/Rho GTPase activating proteins 2a (SRGAP2a) inactivates Cdc42 and RhoA but not Rac1 and helps to reduce podocyte motility and podocyte foot process effacement (139). Downregulation of SRGAP2a, expected to enhance Cdc42 activity has been detected in patients with diabetic nephropathy, and Angiotensin II or TGF-β1 treatment of podocytes increased Cdc42 activity resulting in loss of F-actin stress fibers (140). However, NMDA receptor activation reduced Cdc42 activity in mice and enhanced progression of diabetic kidney disease (141). Therefore, similar to RhoA, reduced and increased activation of Cdc42 has been linked to podocyte dysfunction implying that tight regulation of activity and localization are required to maintain normal podocyte structure and function.

1.3.3. Rac1

The Ras-related C3 botulinum toxin substrate (Rac) GTPases Rac1, Rac2, and Rac3 share 92% amino acid sequence identity and approximately 58% amino acid sequence homology with Rho family proteins RhoA, RhoB, and RhoC (142). Rac2 is predominantly found in the lymph nodes, bone marrow cells, appendix and spleen, while Rac3 expression is restricted to the brain, fat tissues and testis (143). Rac1 is expressed in most cell types, including podocytes. Rac1 regulates cell morphology, cell growth, cell migration, and gene transcription (144). Rac1 function is initiated after it anchors in the plasma membrane where it interacts with signalling lipids and effector proteins. The effector protein-binding region in Rac1 is located mostly in its N-terminus (145), and the Rac1 G-domain consists of switch regions that bind to GTP/GDP. The C-terminus includes the protein-binding domain, a CAAX motif (CLLL), and palmitoylation sites. The CAAX motif is necessary for membrane targeting (146). The inhibitor Rho GDI blocks switch I and II regions preventing Rac1 anchorage in the plasma membrane (147). Interestingly, $PI(3,4,5)P_3$ facilitates RhoGDI dissociation from Rac1 to promote GTP-bound active Rac1 (148).

In podocyte foot processes, Rac1 activation occurs in the ezrin/podocalyxin complex at the apical domain (86, 149), and it acts at the basal domain in conjunction with integrins to promote mobility and mechanosensing (150). Rac1 is not necessary for early podocyte development and but plays a role in podocyte differentiation (121). Increased Rac1 activity is associated with podocyte injury. For instance, in Adriamycin-treated mice, glomerular Rac1 activity is significantly increased, but RhoA activity remains unaltered. In LPS-treated mice, activation of Rac1 and suppression of RhoA activity were associated with severe glomerular injury. Inducible overexpression of constitutively active Rac1 (Q61L) in podocytes caused rapid onset of

proteinuria within 2 days of induction (151), and the severity of proteinuria was associated with the level of active Rac1 expression. Conversely, Rac1 inhibition considerably reduced podocyte dysfunction in chronic kidney disease (151). Rac1 activation in podocytes is also associated with proteinuria in human immunodeficiency virus-associated nephropathy (152) and in Rho GDI alpha knockout mice (153). Proteinuria due to prolonged Rac1 hyperactivation can be reduced by blocking Rac1 or blocking its downstream target aldosterone (153). In podocytes, ARHGAP24 controls the RhoA/Rac1 signalling balance, and mutations in this protein are associated with familial FSGS (154). Indeed, all gene mutations leading to Rac1 hyperactivation damage the podocyte actin cytoskeleton resulting in podocyte FP effacement (155). Conversely, podocyte-specific Rac1 deletion was protective against protamine sulphate-induced foot process effacement in mice (156). Hyper-activated Rac1 induces beta-1 integrin redistribution, decreased adhesion of cultured podocytes to laminin, and podocyte detachment in cultured cells, and foot process effacement, glomerulosclerosis, and loss of GFB integrity *in vivo* (155). It is therefore possible that the damaging effects of Rac1 hyperactivation are localized to the basal domain and result in loss of podocyte adhesion to the GBM. RNA quantification in podocytes from patients and healthy controls revealed that Rho GEF "Trio" was upregulated in FSGS podocytes, and podocyte-specific knockout of Trio decreased Rac1 activity, cell size, and motility (157). In addition, proximity-based BioID assay showed that Rho GEF β-PIX might associate with and regulate Rac1 in human podocytes (157). ARHGDIA encodes Rho GDP dissociation inhibitor RhoGDIα. Disease-causing mutations in ARHGDIA result in severe proteinuria and FSGS in humans, and ShRNA-mediated knockdown of endogenous RhoGDIα in cultured podocytes induced Rac1, but not Cdc42 or RhoA activity (158). Moreover, transient receptor potential canonical cation channels (TRPCs) drive podocyte injury and proteinuria upon Rac1 activation

(159). Therefore, as is the case for RhoA and Cdc42, Rac1 activation in podocytes can be protective or harmful. Development of therapies that selectively inhibit Rac1 will therefore require careful titration to preserve the Rac1 protective functions.

The ezrin-podocalyxin-NHERF2-CLIC5A complex is localized, in a very polarized fashion, at the apical domain of podocyte foot processes, and Rac1 is part of that complex. Rac1 activity is considerably reduced in podocytes of ezrin knockout mice, leading to protection from injury-induced morphological changes (160). Our laboratory reported that CLIC5A stimulates podocyte Rac1 (but not RhoA) activity leading to the activation of PAK and ezrin (86). Activated ezrin links cortical actin to $PI4,5P_2$ leading to the formation of cellular projections (161-163). Activated ezrin also serves as a bridge between cortical actin and membrane-spanning proteins, including podocalyxin. Our lab showed that CLIC5A-dependent generation of apical $PI4,5P_2$ at the inner leaflet of the plasma membrane as well as ezrin, radixin, and moesin (ERM) phosphorylation requires Rac1 activation (86). However, the mechanism of CLIC5A-dependent Rac1 activation is not known.

1.4. Phosphoinositides

Phosphoinositides (PPIs) are inositol-containing glycerophospholipids (164). The inositol ring, which sticks out from the lipid bilayer toward the cytosol, can be phosphorylated at different positions by distinct phosphatidylinositol kinases (PIPK) (165-167). PPIs are involved in the regulation of many cellular functions such as actin dynamics, regulation of transmembrane proteins, membrane trafficking, cell-matrix adhesion and signal transduction (168-170) (171-173). The abundance of PPIs in eukaryotic cell membranes is low but they play critical roles in cellular dynamics by recruiting multiprotein complexes (174). Phosphatidylinositol 4 phosphate 5 kinases (PI4P5K) catalyse the phosphorylation of the substrate phosphatidylinositol 4

phosphate (PI4P) to generate $PI4,5P_2$, and phosphatidylinositol 3 kinase (PI3K) causes phosphorylation of $PI4,5P_2$ to $PI3,4,P_3$. Inositol phosphatases dephosphorylate specific positions on the inositol ring. For example, PTEN dephosphorylates $PI3,4,P_3$ back to $PI4,5P_2$. Many proteins involved in organization of the cortical actin cytoskeleton, including the ERM proteins bind $PI4,5P_2$. $PI4,5P_2$ stimulates actin polymerization by inhibiting the actin filament barbed end capping proteins gelsolin and heterodimeric capping protein, and by inhibiting the actin depolymerizing factor (ADF)/cofilin and twinfilin proteins. A preponderance of $PI3,4,P_3$ is associated with cell proliferation and a preponderance of $PI4,5P_2$ at the apical plasma membrane of epithelial cells is associated with their differentiation.

Our lab has reported that CLIC5A overexpression in COS-7 cells causes a major reorganization of $PI4,5P_2$ at the apical plasma membrane into prominent clusters (89). The lab also showed that CLIC5A can interact with PI4P5 and PI5P4 kinases (89), but whether that interaction is direct is not known.

1.4.1. Rac1 interacts with PIP5KI and facilitates its activation

Rac1 interacts with PIP5KIα and weakly with PIP5KIβ and PIP5KIγ as observed from the pull-down assays relying on incubation of immobilized Rac1 with homogenates prepared from rat brain or liver, or with cell lysates (175-178). RhoA, but not Cdc42, also interacts with PIP5KIα, PIP5KIβ and PIP5KIγ. Rac1 and RhoA are also co-immunoprecipitated with PIP5KI (176). Moreover, GTP-loaded Rac1 and RhoA also directly interact with recombinant PIP5KIα and Iβ proteins (176) causing their activation. Only GTP-bound Rac1, RhoA, and Cdc42 activate PIP5KIα, Iβ and Iγ in vivo while dominant negative mutants of Rac1, RhoA, and Cdc42 failed to activate these lipid kinases (179-181). Consistent with such findings is a study from our laboratory (86) which showed that CLIC5A activates Rac1, and that the CLIC5A-stimulated

accumulation of $PI4,5P_2$ clusters in the apical plasma membrane was prevented by Rac1 inhibition or overexpression of dominant negative Rac1. We do not know whether CLIC5A-dependent Rac1 activation activates any specific phosphoinositide-metabolizing kinase isoform.

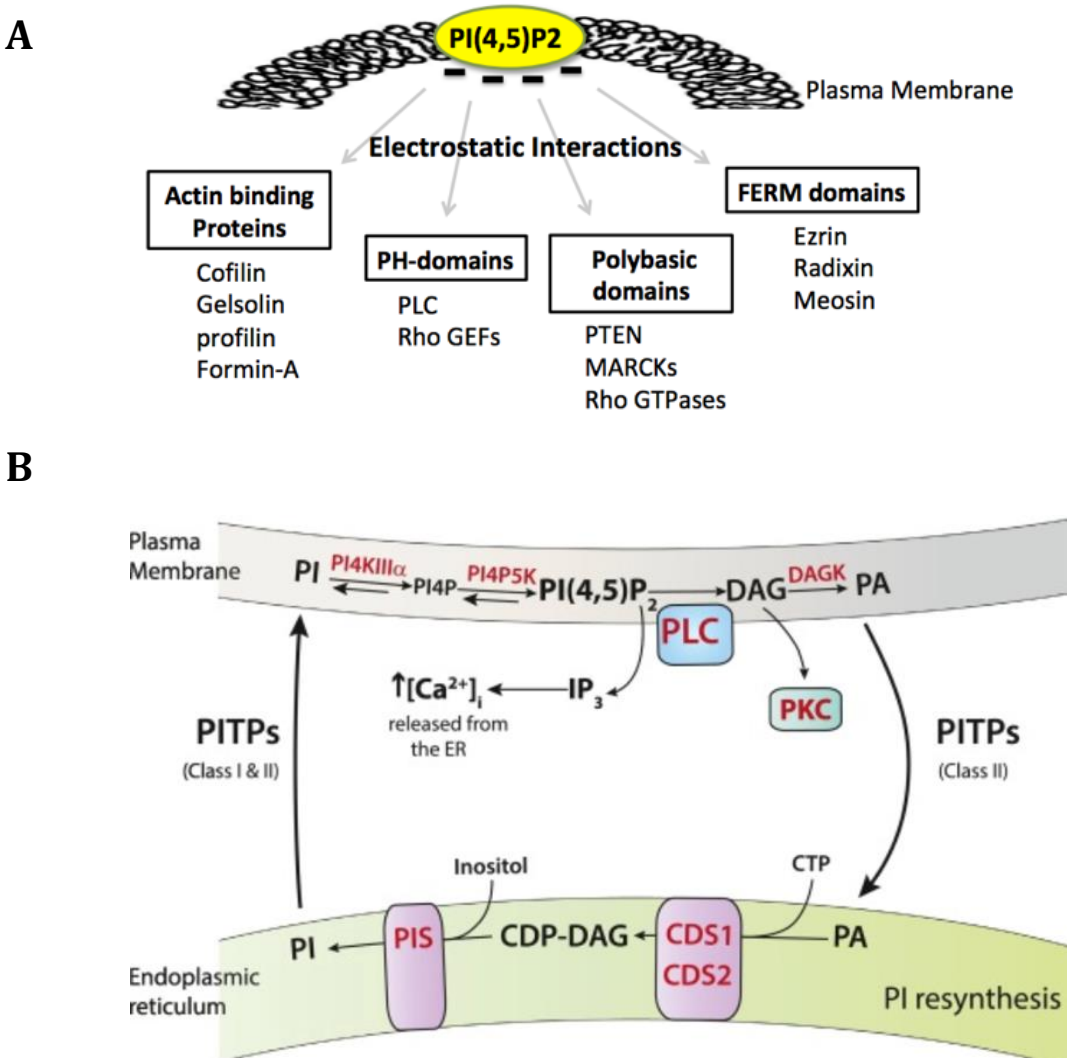

Figure 1.5: PI(4,5)P_2 cycle during phospholipase C (PLC) signaling. (Reproduced with permission, Cockcroft S. The expanding roles of PI4P and PI(4,5)P_2 at the plasma membrane: Role of phosphatidylinositol transfer proteins. Biochim Biophys Acta Mol Cell Biol Lipids. 2024, 1869(2):159394). **A.** PI(4,5)P_2 interacting proteins. ERM proteins interact with PI(4,5)P_2 through its FERM domain. **B.** PLC catalyzes the hydrolysis of PI(4,5)P_2 that produces two-second messengers, diacylglycerol (DAG) and inositol trisphosphate (IP3). DAG is converted into phosphatidic acid (PA) by DAG kinase (DAGK) and transferred to the endoplasmic reticulum by Class II phosphatidylinositol transfer proteins (PITPs). At the endoplasmic reticulum, PA is converted into the intermediate CDP-DAG by one of two CDS enzymes, CDS1 and CDS2. The final step in PI resynthesis is catalyzed by PI synthase (PIS) where CDP-DAG and inositol are combined.

1.5. Ezrin/radixin/moesin (ERM) proteins

Our laboratory showed that CLIC5A is a major protein in kidney glomeruli (85, 182, 183). Using immunogold electron microscopy CLIC5A localized in a very polarized fashion to the apical domain of podocyte foot processes, away from the filtration slit (85), exactly as was already known for ezrin and podocalyxin (184). The lab also showed that CLIC5A is part of the ezrin/podocalyxin/NHERF complex by co-immunoprecipitation of the proteins from isolated glomeruli and by near perfect co-localization of CLIC5A with ezrin (85). In addition, previous findings from our lab showed that CLIC5A and CLIC4 proteins stimulate ERM protein activation (87, 89). This is the reason for the focus on ezrin and the ERM proteins.

The ERM proteins provide regulated linkages between membrane-associated proteins and the cortical actin cytoskeleton (185, 186). They belong to the Band 4.1 superfamily, a group of proteins characterized by the presence of a ~300 amino acid residues long conserved FERM (**F**our-point-one, **ezrin**, **radixin**, **moesin**) domain, a hydrophobic cysteine-rich region (187) with a globular configuration (188). The FERM domain is located at the N-terminus of most proteins in the band 4.1 superfamily, including the ERMs, merlin, DAL-1, protein tyrosine phosphatases, talin, the Janus Kinases, focal adhesion kinase, and guanidine exchange factors. Crystal structures of ezrin, moesin and radixin suggest that FERM domains are three-lobed F1, F2, and F3(189, 190).

The ERM proteins are all involved in the regulation of actin cytoskeleton networks through their interaction with membrane proteins and other signaling molecules (191). They form a bridge between plasma membrane-associated proteins and the cortical actin cytoskeleton and play a major role in the regulation of cell morphology, migration, and cell adhesion (185, 192). They

are abundant in cell surface structures such as the membrane ruffles, filopodia, lamellipodia, microvilli, uropods, retraction fibers, and at cell adhesion sites (193).

ERM proteins are widely distributed, and many cells express more than one ERM protein. Nonetheless, each member of this family member tends to be predominant in specific tissues and cells. Ezrin is mainly expressed in the epithelial cells, including glomerular podocytes and renal proximal tubule cells (194). Ezrin was first discovered as an 80-kDa protein from the chicken intestinal microvilli and named after Ezra Cornell, a founder of Cornell University (195, 196). Ezrin-deficient mice die soon after birth and morphological abnormalities are reported in the intestinal epithelial cells in which ezrin is the only ERM protein expressed (197).

Membrane-organizing extension spike protein (moesin) was isolated from bovine uterus in 1988 and identified as receptor protein for heparin (198). Moesin expresses highly in the endothelial cells(199), while some epithelial cells also express moesin in addition to ezrin (194). Moesin is highly expressed in the lungs, spleen, and kidneys, in endothelial cells and in lymphocytes (194, 200). Defects in lymphocytes and neutrophils were observed in moesin-deficient mice, resulting in decreased microbial killing by neutrophils (201).

Radixin was identified as an actin-binding protein and highly expressed in the undercoat of adherens junctions of rat liver cells (202). Radixin is the dominant ERM protein in liver cells and is mostly concentrated at the microvilli of bile canalicular membranes where multidrug resistance protein 2 is co-localized to secrete conjugated bilirubin into bile (203). Radixin is also enriched in cochlear and vestibular stereocilia (204, 205). Radixin is also expressed in the kidney. Radixin-deficient mice are normal at birth but after 4 weeks the concentration of conjugated bilirubin increases in their serum and after 8 weeks liver injury occurs. In the inner ear hair cell stereocilia, radixin is the predominant ERM protein, and radixin-deficient mice

show progressive degeneration of cochlear stereocilia resulting in deafness but they do not display vestibular dysfunction (204). In radixin-deficient mouse cochlea, ezrin was upregulated up to post-natal day 14 and stereocilia developed normally but the cells degenerated thereafter, indicating that ezrin cannot counterbalance radixin deficiency in mature stereocilia. In contrast, up-regulation of ezrin is maintained in vestibular stereocilia after the onset of hearing and stereocilia are normal suggesting structural and functional compensation of one ERM protein by another.

1.5.1. ERM protein structure

The ERM proteins possess a high degree of amino acid sequence identity of ~85% (Appendix 1). The globular NH2-terminus of ERMs represents the first ~300 amino acid residues termed as the "N-terminal ERM association domain (N-ERMAD)" that binds to the $PI4,5P_2$ (185, 206). In their inactive state, the N- and C-termini of ERM proteins interact with high affinity, resulting in auto-inhibition. Binding of the FERM/N-ERMAD domain to $PI4,5P_2$ releases this inhibition freeing their C-terminus (the C-ERMAD domain) to bind to their transmembrane partners and actin. Unfolding of ERM proteins upon binding to $PI4,5P_2$ also promotes their phosphorylation at a highly conserved site in the C-terminus. The FERM domain forms a clover-shaped conformation and is divided into three modules F1, F2, and F3. The C-ERMAD domain includes a binding site for filamentous actin at the highly conserved last 34 amino acids common among ERM proteins (207). Also, in the C-ERMAD domain, a conserved threonine residue (T567 in human ezrin, T564 in radixin, and T558 in moesin), is a critical phosphorylation site and play a key role in the activation of ERM proteins. The C-terminus also possesses binding sites for other signaling molecules that together form complexes with the ERM proteins at the periphery of the cell cortex to provide cellular structural integrity. The FERM and C-ERMAD domains are

connected via a long α-helical linker region. The α-helical domain has three extended helices, of which two form an antiparallel coiled coil of ~7 nm in length. The α-helical linker region blocks the PI4,5P_2 binding site located in the basic cleft (208). Moreover, the ERM proteins contain a polyproline stretch the α- C-terminal regions.

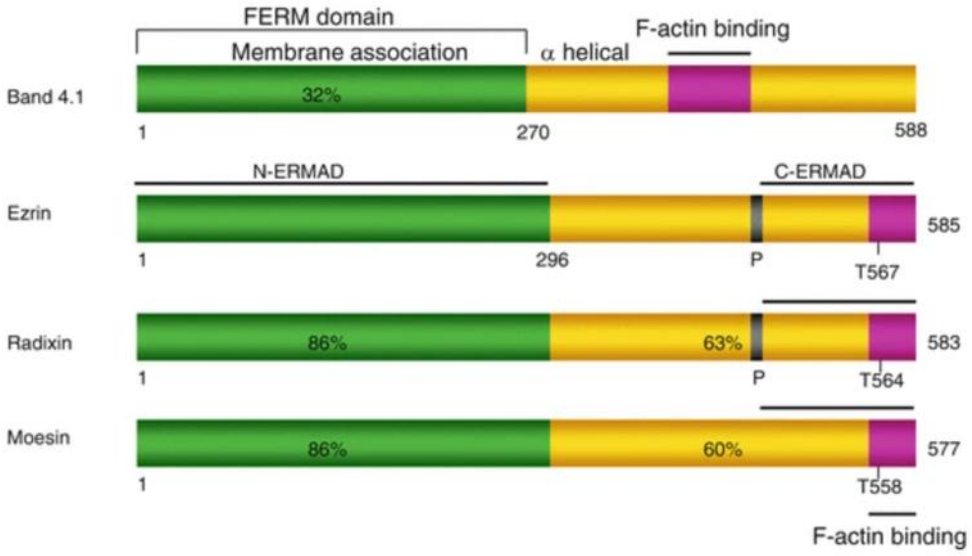

Figure 1.6: Schematic diagram of ERM protein structure. (Reprodued with permission, Ren L, Khanna C. Role of ezrin in osteosarcoma metastasis. Adv Exp Med Biol. 2014; 804:181-201). ERM proteins have three domains: a globular N-terminal membrane-binding domain (1-296 amino acids), also termed as FERM domain or N-ERMAD, the extended α-helical domain (~297-431 amino acids), followed by a positively charged C-terminal actin-binding domain (C-ERMAD). The percentage amino acid sequence identity with ezrin in N-terminal domain is indicated. P indicates polyproline region. T567 is the critical phosphorylation site in ezrin.

1.5.2. Regulation of ERM protein activation

The ERM proteins possess two different conformations: the inactive (closed) conformation and the active (open) conformation. The closed conformation results from strong intra- or inter-molecular self-association between the N-terminal and C-terminal domains. In cells, full-length ezrin interacts with plasma membrane-associated proteins via its N-terminal FERM domain, whereas the C-terminal domain interacts with the actin cytoskeleton (209). However, self-association between the N-terminal and C-terminal domains buries binding sites for plasma membrane-associated proteins as well as the C-terminal F-actin binding region (210). Dissociation of the N-terminal/C-terminal complex is triggered by docking of ERM proteins on $PI4,5P_2$ at the inner leaflet of the plasma membrane (211, 212). Mutations of basic lysine residues at K63, K64, K253, K254, K262 and K263 in the ezrin N-terminus abolishes its $PI4,5P_2$ binding and thus plasma membrane recruitment (211). Furthermore, phospholipase 2 (PLC2)-mediated depletion of PI4,5P2 reduces the interaction of ERM proteins with actin (213, 214) and overexpression of PI4P5 kinases, which produce $PI4,5P_2$ leads to increased ERM phosphorylation, cytoskeletal association, and the formation of membrane projections. Finally, osmotic cell shrinkage also triggers ERM protein activation through an increase in membrane $PI4,5P_2$ levels (215). Therefore, the interaction of ERM proteins with $PI4,5P_2$ is required for their activation and association with their protein partners (89, 216).

The extreme C-terminal ~34 amino acids of ezrin has been identified as the F-actin binding site (207), and the threonine (T567 in human ezrin) residue within the C-terminal F-actin binding site can be phosphorylated by Rho-kinase (217, 218), protein kinase C alpha (219), protein kinase C, AKT(220), and Nck-interacting kinase. This phosphorylation keeps the N-terminal and C-terminal domains apart and stabilizes the active state of ERM proteins (217, 221, 222, 223). An

exogenously expressed phospho-mimic ezrin T567D mutant induces formation of actin-based cellular projections like membrane ruffles, lamellopodia, and microvilli. In contrast, a phosphorylation-deficient ezrin T567A mutant abolished ezrin association with the actin cytoskeleton (224). Therefore, the two-step ERM activation includes recruitment of their FERM domain to the plasma membrane by $PI4,5P_2$ (186) and subsequent phosphorylation of the conserved threonine residue in the C-terminal domain (225, 226).

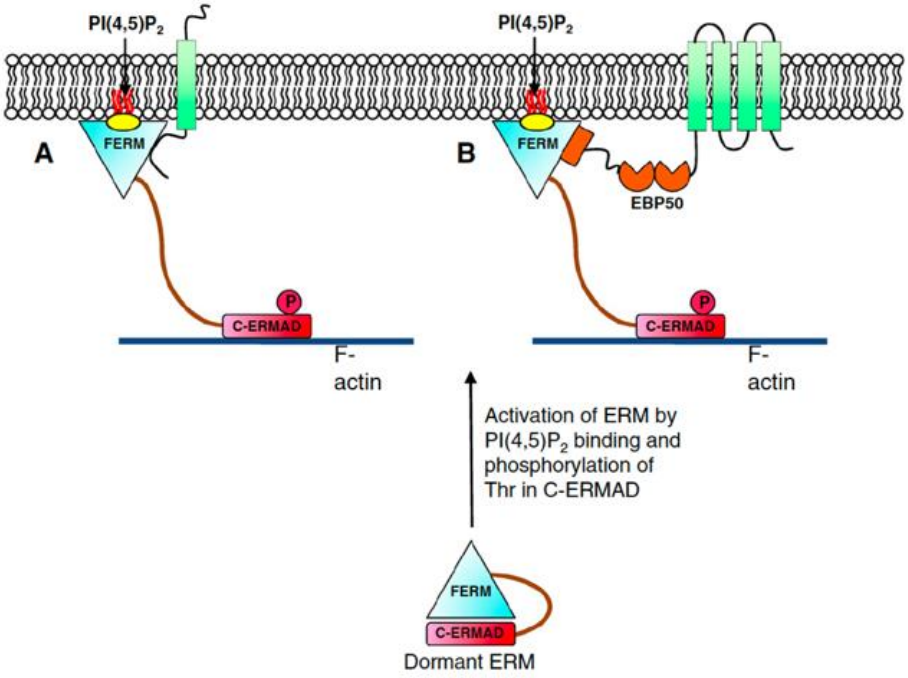

Figure 1.7: Regulation of ERM protein activation. (Reproduced with permission, Jiang et al. 2014. Biochimica et Biophysica Acta 1838: 643–657). In active/open conformation, ERM proteins function as cross-linkers by binding to cytoplasmic extensions of membrane proteins CD43, CD44, ICAM **(A)** and podocalyxin (not shown) as well as and scaffolding proteins such as EBP50 (NHERF1) and NHERF2, which then bind to membrane proteins **(B)**.

1.5.3. Interaction of ERMs with other proteins

The interaction of ERM proteins with $PI4,5P_2$ increases their interaction with the cytoplasmic domain of many membrane-spanning proteins including intracellular adhesion molecules (ICAM) 1-3, hyaluronan receptor CD44 and CD43 (227, 228). The binding of moesin to $PI4,5P_2$ augments its binding to CD93 (229). ERMs also bind to postsynaptic density protein (PDZ)-containing proteins such as transporters and ion channels through scaffolding proteins like Na^+/H^+ exchanger regulatory factors 1 and 2 (NHERF1, NHERF2), also known as ERM-binding phosphoprotein 50 (EBP50) (230, 231). ERM proteins link membrane-spanning proteins to the cortical actin cytoskeleton directly or indirectly via the scaffold protein NHERF2 (185). Podocalyxin, expressed at high levels in podocytes and endothelial cells interacts with active ezrin through a direct interaction (232) and through an NHERF2-dependent mechanism (88, 233). There is strong evidence that ERM proteins regulate the activity or Rho GTPases by binding Rho-GDI (234) and Dbl (235). Rho GDI forms a complex with the GDP-bound inactive form of the Rho GTPases and hinders their activation (236). Rho GDI contains an ERM-interacting domain at residues 391–462 (234) that directly binds the N-terminal FERM domain (amino acids 1–280) of ERM proteins (234). Binding of Rho GDI to ERM proteins prevents its interaction with Rho GTPases and markedly enhances the activity of RhoA, Rac1, and Cdc42 (234, 236-239).

1.5.4. ERM protein functions in physiology and pathophysiology

1.5.4.1. *Cellular development and differentiation*

ERM proteins are involved in asymmetric orientation and localization of the cytoskeleton, key step to the establishment of cell polarity. For example, moesin deficiency in the *Drosophila melanogaster* oocytes results in severe anterior-posterior polarity defects (240, 241). During

epithelial lumen formation ERM proteins are required to form initial cell-cell contacts. They then re-localize to the apical surface where they are crucial in the assembly of actin-rich apical structures. In *Caenorhabditis elegans* embryos, ERM-1 re-localizes from adherens junctions to the apical surface of differentiating excretory canal epithelium, and its deletion causes cyst-like structures implying defective lumen formation (212, 242).

In *Drosophila melanogaster* mutant ezrin without a C-terminal actin binding site results in epithelial adherens junction defects (243) and mutation of ezrin at the conserved C-terminal T567 prevents the formation of E-cadherin-mediated cell-cell contacts during blastocyst formation in mice (244-246). Late in development of Drosophila melanogaster epithelia, loss-of-function moesin mutants exhibit disruption in morphology and epithelial integrity (247, 248). In mice, ezrin is the only ERM expressed in intestinal epithelium (197) and in mouse embryos, ezrin is localized at cell-cell junctions before moving to the apical surface as polarity is established (242, 244). In fully differentiated epithelium, the majority of ezrin is localized at the apical surface whereas a small fraction is present at cell-cell contacts (249). Ezrin-deficient mice die soon after birth because of intestinal epithelial defects including a disorganized terminal web, microvilli, and adhesion complexes (250). In the inner ear, radixin is essential for the formation of apical actin-based stereocilia and radixin deficiency causes deafness due to progressive degeneration of cochlear stereocilia (251).

1.5.4.2. *Cell migration*

Epithelial cell migration involves cell-cell contact dissociation, followed by extension of membrane protrusions, and ERM proteins play a role in these processes. For instance, following HGF stimulation, ezrin is rapidly recruited to the lateral membrane as well as to the leading edge of migrating epithelial cells where it controls actin polymerization (249, 252). Also, upon

phorbol-ester stimulation, protein kinase C (PKC) phosphorylates and activates ezrin it to be involved in PKC-induced cell migration (219). Moreover, PKC also phosphorylates the transmembrane receptor CD44 modulating its interaction with ezrin and CD44-dependent directional cell motility (253). Hence, phosphorylation of ERM proteins recruits regulators of actin polymerization to facilitate cell migration.

1.5.4.3. *Tumor metastasis*

Even though ERM protein localization to the apical domain of polarized, differentiated epithelial cells is characteristic for epithelial cell differentiation, it turns out that ERM proteins, together with some of the membrane-spanning proteins are also involved in tumor cell mobility and metastasis. For example, in osteosarcomas in humans and mice and in rhabdomyosarcomas increased ezrin expression is associated with tumor metastasis (254, 255). Association of ezrin with CD44, a co-receptor for the hepatocyte growth factor receptor "MET", also promotes tumor metastasis (256, 257), and the ezrin-associated transmembrane sialoprotein podocalyxin can disrupt the cell-cell adhesion between MDCK cells to promote cell motility (258). Increased expression of radixin and moesin as well as enhanced ezrin phosphorylation were observed in protein profiles of pancreatic cancers with lymph node metastasis but not in those of pancreatic cancers without lymph node metastasis (212). Increased moesin gene expression was observed in patients with head and neck squamous cell carcinoma patients among other upregulated proteins (259). In a breast tumor xenograft mouse model, inhibition of ezrin activity prevented pulmonary metastasis (260). A mechanism involving an ezrin/Fes kinase interaction that stimulates HGF/Met /Src mediated cell scattering is thought to be one of the mechanisms for this tumor-related activity of ezrin (261) (249, 261). A tissue array-based immunohistochemical study showed that ezrin localizes at the apical domain of a polarized healthy breast epithelial cell but in

invasive breast carcinomas, ezrin moves to the cytoplasm or the membrane in a non-polarized fashion and is linked with significant lymph node metastasis, indicating that unusual cellular localization of ERM proteins might lead to the deregulation of several functions in tumor cells (262). Therefore, the loss of apical ERM localization may lead to an invasive phenotype. The relocation of ERM proteins from the plasma membrane to the cytoplasm could also change signal transduction by growth factors or perturb the anchoring of membrane receptors and adhesion molecules. Therefore, ERM mislocalization is one of the features of tumor metastasis.

1.5.5. ERM protein function in podocytes

Ezrin is highly expressed and localized at the apical membrane of podocyte foot processes(88, 184, 194, 233). In cultured podocytes ezrin was observed predominantly at the plasma membrane and in filopodia (263). Moreover, in wild-type mouse glomeruli, ezrin was mainly observed in the apical membrane of podocyte foot processes (184) and did not merge with podocyte markers synaptopodin or podocin (264). Ezrin is expressed in developing and mature podocytes, and its localization changes in response to podocyte injury (263). In podocytes, ezrin forms a complex with the transmembrane sialoglycoprotein podocalyxin (184) and the ezrin/podocalyxin complex is essential for the maintenance of podocyte foot processes. While NHERF2 was shown to link ezrin and podocalyxin at the apical domain of podocyte foot processes (233), NHERF2 deletion in mice did not show any noticeable renal defects (265). Proteomic profiling of glomeruli identified ezrin and NHERF2 as two down-regulated proteins in the streptozotocin model of diabetes. Podocyte ezrin expression was also reduced in diabetic patients, and ezrin knockdown in cultured human podocytes decreased insulin-stimulated actin reorganization and enhanced glucose uptake (266) suggesting that ezrin downregulation could play a role in podocyte abnormalities due to diabetes. Conditional knockout of the dicer allele to

disrupt MicroRNA-192 in podocytes altered ezrin and moesin expression leading to cytoskeletal disorganization and dedifferentiation with progressive glomerulonephritis (267). However, podocyte-specific ezrin deletion in mice was not observed to change glomerular function or podocyte morphology and had a protective effect against glomerular injury through suppression of podocyte Rac1 activity (160).

Ezrin is also highly expressed in proximal tubules (194) where it plays a significant role in solute reabsorption by regulating the apical membrane localization of several transporters (268). In proximal tubules NHERF1 links ezrin to several ion transporters (162, 268). In ezrin-deficient mice proximal tubule phosphate reabsorption is blunted, resulting in hypophosphatemia (268). Ezrin overexpression and ezrin Tyr353 phosphorylation trigger the PI3K/PI4,5P_2/Akt cell survival pathway and promote renal tubular epithelial cells proliferation (269-272), while hyperglycemia inhibits ezrin expression and Tyr 353 phosphorylation and exposes renal tubular epithelial cells to apoptotic stress (269, 271).

1.5.6. ERM proteins regulate Rho GTPases activity

Rho GDI inhibits Rho GTPase activation. The N-terminal domain of ERM proteins directly binds and sequesters Rho GDI (ARHGDIA) in podocytes enhancing GTP loading of Rac1 (158, 160, 273). In Rho-GDIα knockout mice, Rac1 hyperactivation in podocytes was associated with severe proteinuria (153). Suppression of ezrin expression and transfection of the constitutively inactive mutant of ezrin (T567A) also reduced Rac1 activity. Conversely, Rac1 activity increased when constitutively active ezrin (T567D) or the ezrin N-terminal FERM domain were overexpressed. These results are consistent with a previous study by Takahashi et al. (234) who reported that the N-terminal domain of ERM proteins plays an important role in Rac1 activation and the findings support theory that the activated form of ezrin plays an important role in the

regulation of podocyte morphology through Rac1 activation.

ERM proteins also interact with the Rho-GEFs (273). The active form of both, radixin and ezrin can bind the Rho-GEF Dbl via the FERM domain and Dbl prompted ezrin translocation to the plasma membrane through a mechanism that does not require phosphorylation of its C-terminus (273). In ezrin knockout mice glomerular RhoA activity increased and Rac1 activity was blunted relative to wild type controls, without effect on Cdc42 (160). In the models of Adriamycin and LPS nephropathy in mice, ezrin deletion was protective with higher RhoA and lower Rac1 activities (160), implying that down-regulation of Rac1 activity and up-regulation of RhoA activity confer a protective effect in the presence of podocyte injury. The association of ezrin with CD44, podocalyxin, and podoplanin can also regulate of RhoA activity positively or negatively (274, 275). RhoA activation, in turn, has been linked both positively and negatively to junctional stability, cell motility and tumour invasion, suggesting that context-dependency dictates the cellular outcome of RhoA activity (276).

1.5.7. The ezrin/podocalyxin/NHERF2 complex in the renal podocytes

1.5.7.1. *Podocalyxin is a major transmembrane protein of podocytes*

Podocalyxin belongs to the CD34 family of cell membrane-associated epithelial mucin-like glycoproteins. Podocalyxin was initially discovered in renal podocytes, but it is also abundantly expressed by endothelial cells, mesothelial cells, platelets, hematopoietic stem cells, neuronal cells, thrombocytes, megakaryocytes, and a variety of tumor cells (64, 277-283). Podocalyxin expression induces cellular morphological changes including actin recruitment, cell junction re-distribution, disruption of adhesion complexes and the formation of microvilli or foot processes (281). Podocalyxin expression is also upregulated in metastatic tumor cells (284).

1.5.7.2. *Ezrin/podocalyxin/NHERF2 complex forms at the plasma membrane of podocytes*

Podocalyxin has N-terminal extracellular mucin domain that is extensively O-glycosylated and sialylated, followed by several sites of N-glycosylation, a cysteine-containing globular domain, a juxtamembrane stalk, a single transmembrane domain, and an intracellular domain with phosphorylation sites and a C-terminal DTHL (aspartic acid, threonine, histidine, leucine) sequence for interaction with PDZ domains (88, 258). Sialylation of the podocalyxin extracellular domain confers the high net negative charge (64) resulting in anti-adhesive properties that maintain separation of adjoining foot processes keeping glomerular filtration slit open (285). Together with the filtration slit diaphragm, the negative charge density of podocalyxin also contributes to the albumin filtration barrier function of glomerular capillaries (64, 286, 287). The extreme C-terminal cytoplasmic DTHL sequence (PDZ-binding motif) of podocalxyin interacts directly with the ezrin FERM domain and with NHERF1 and NHERF2 at the apical domain of podocyte foot processes. NHERF1 and NHERF-2 are scaffolding proteins that connect plasma membrane proteins with the ERM family of proteins and thus help to link them to the actin cytoskeleton. Double immunogold labeling of ultrathin cryosections from rat kidney showed that ezrin and podocalyxin are localized to the apical plasma membrane of foot processes above the slit diaphragms (184) and can be ezrin co-immunoprecipitated with podocalyxin from glomerular detergent-extracts (88). In cultured cells, the ezrin/podocalyxin association was not disrupted by actin-depolymerizing agents cytochalasin D or latrunculin B suggesting that the interaction between them is not dependent on polymerized actin filaments (288). The C-terminal cytoplasmic domain of podocalyxin also binds the PDZ2 domain of NHERF2, which, in turn, binds the ezrin N-terminus (289). Therefore, in podocytes, ezrin couples podocalyxin directly and indirectly, via NHERF2, to actin (88). Phosphorylation of ezrin

at Thr567 is required for formation of the ezrin/podocalyxin/NHERF2 complex and its coupling to the actin cytoskeleton (217).

1.5.7.3. *Podocalyxin also involves in regulating Rho GTPase activity*

In MDCK cells, podocalyxin knockdown reduced Rac1 activity and its overexpression in human embryonic kidney (HEK293) cells up-regulated Rac1 activity. These changes were attributed to a podocalyxin-dependent association of ARHGEF7 with the ezrin-podocalyxin-NHERF2 complex (149). In HEK293 cells, full-length podocalyxin also activated Rac1, but constructs lacking the cytoplasmic domain or C-terminal PDZ binding motif did not. A construct expressing the C-terminal PDZ binding motif of podocalyxin fused to full-length NHERF1 restored full activation of Rac1. It turns out that the first PDZ domain of NHERF2 recruits a Rac1 GEF while the second PDZ domain of NHERF2 binds to podocalyxin (149). Several Rac1 GEF candidates possess a PDZ binding motif that fits favourably into the PDZ domain of NHERF2, among them Tiam-1 (tumor invasion and metastasis), ARHGEF7, known as the p21-activated protein kinase exchange factor beta (β-Pix) (290), FGD5, a Rac1-specific GEF, FGD6, a Cdc42-specific GEF, PLEKHG6, a Rho G-specific GEF that interacts with ezrin, KALRN, which conveys the signal from Arf6 to Rac and finally FLJ10357 GEF, a Rho G and Rac1-specific GEF (149). Among the candidate Rho GEFs, only GST-fusion constructs of ARHGEF7 strongly interacted with NHERF2 (149). Therefore, binding of NHERF2 to podocalyxin via its second PDZ domain facilitates anchoring NHERF2 to the plasma membrane exerting dual regulatory roles by removing the inhibitory RhoGDI and recruiting ARHGEF7 (149).

1.5.7.4. *Podocalyxin knockout disturbs podocyte foot process development*

Even though systemic podocalyxin knockout mice suffer anuric kidney failure at birth (291), podocalyxin heterozygous mice exhibit no basal phenotype but they are more vulnerable to the podocyte toxin puromycin. Puromycin is known to trigger podocyte apoptosis by inducing endoplasmic reticulum stress (292, 293). Podocalyxin loss disrupted podocyte morphogenesis and foot process formation in early development in mice and zebrafish (291, 294). Podocyte foot process effacement is associated with a reduction in the sialic acid content of podocalyxin in puromycin aminonucleoside (PAN) nephrosis. Treatment of rats with sialidase results in ezrin dephosphorylation and ezrin uncoupling from actin and neutralization of podocalyxin negative charges results in dissociation of the podocalyxin/NHERF2/ezrin complex and its association with actin leading to podocyte foot process effacement and eventually massive proteinuria (291, 295, 296). Interestingly, neutralization of the negative surface charge of podocalyxin with protamine sulfate resulted in a disruption of the NHERF2/ezrin complex from the cytoplasmic domain of podocalyxin, leaving the ezrin attached to actin filaments (88). Importantly, in podocytes of CLIC5 deficient mice the podocalyxin/ezrin/actin complex is disrupted (85, 89, 297), making CLIC5 protein a critical molecule necessary in maintaining podocyte foot process structural integrity.

1.5.7.5. *Podocalyxin upregulation in cancer*

Although podocalyxin is critical for maintenance of the structure of terminally differentiated podocytes, its expression is upregulated in many tumors and it is involved in tumor metastasis (284). The podocalyxin gene can exhibit a high frequency of missense mutations and in-frame deletions, which are associated with an increased risk of developing more aggressive prostate cancer (298). In breast and prostate epithelial cells podocalyxin functions through an ezrin-

dependent pathway (299) and possibly also NHERF1 (300-303). An anti-podocalyxin antibody PODO83 delays primary tumor growth in murine tumor models and prevents metastasis to the lung (284). Importantly, in undifferentiated cells, including cultured podocytes and tumors, podocalyxin and ezrin localize to the basal domain, reducing cell-matrix adhesion and enhancing cell motility (149, 304, 305) (306-308) (309). During polarization, redistribution of podocalyxin from the basal domain to the apical domain is initiated by its dissociation from ezrin, internalization of podocalyxin in vesicles (310), which then fuse with the apical plasma membrane, followed by re-association of podocalyxin with ezrin. Therefore, podocalyxin is considered a potential target for monoclonal antibody therapy to inhibit primary tumor growth and metastasis. Since the podocalyxin/ezrin complex is so important for podocyte function, it might be anticipated that such treatment could have side effects by disrupting the glomerular filtration barrier.

1.6. Chloride intracellular channel proteins (CLICs)

The CLIC gene family consists of six genes (CLIC1-CLIC6) in mammals. They encode proteins that belong to a subgroup of the glutathione-S-transferase (GSTs) superfamily (311). CLIC proteins have been described in all animal species and even in plants (312). *Drosophila melanogaster* has a single CLIC-like protein "DmCLIC" (313), while the nematode *Caenorhabditis elegans* has two CLIC-like proteins, Exc-4 and Exl-1(314, 315). In vertebrates, six CLIC paralogues have arisen from a single CLIC ancestor gene (316).

1.6.1. Discovery of the first CLIC protein: p64

Chloride channels are found in plasma membranes and in membranes of intracellular organelles such as the Golgi, endosomes, and lysosomes. In intracellular organelles chloride channels function parallel to H^+-ATPase, which together control in intra-organelle pH and their membrane

potential (317, 318). Searching for Cl^- channels, Landry et al. (319) identified indanyloxyacetic acids IAA-94 and IAA32 as Cl^- channel inhibitors and then purified a 64-kDa protein using an IAA-32 affinity matrix eluted with IAA-94 (320). Interestingly, the partially purified protein mixture contained another highly enriched 27-kDa protein postulated to be a Cl^- channel isoform, (320) which very likely was CLIC5A. Reconstitution of these two proteins into artificial lipid bilayers produced a Cl^- conductance (320) and incorporation into proteoliposomes conferred a Cl^- permeability that was abolished by anti-p64 antibodies (321). Also, p64 expression in cells induced anion currents (322). The fact that p64 protein was captured by a Cl^- channel inhibitor, that an antibody raised against it inhibited Cl^- flux and that an anion current was induced in cells expressing p64 led to the conclusion that p64 might be an essential component of vacuolar and membrane Cl^- channels (323). The p64 cDNA sequence was cloned by the Al Awqati and Edwards labs (321, 324), and other CLIC family members were subsequently cloned and sequenced. The p64 protein is now known as CLIC5B and was the first identified member of the "chloride intracellular channel" (CLIC) protein family. The CLIC5 gene is now known to produce two CLIC5 isoforms, CLIC5A and CLIC5B, through alternative use of exons 1A or exon 1B.

1.6.2. CLIC protein structure

Sequence alignments for the CLIC5A, CLIC4 and CLIC1 proteins are shown in Appendix 2. CLIC proteins all contain a conserved ~240 residue "CLIC" module that consists of an N-terminal thioredoxin fold, a short linker sequence, followed by a largely α-helical C-terminus. The thioredoxin-like domain contains a short hydrophobic region postulated by some investigators to be a membrane-spanning domain. The α-helical C-terminus contains a nuclear localization signal. The CLIC module adopts a GST superfamily fold structure (325, 326). Like

the omega class of GSTs, CLICs contain an elongated groove between N- and C-terminal domains (325). Glutathione (GSH) is an extremely abundant low molecular-weight thiol that maintains redox homeostasis and protects cells from oxidative damage and from toxicity of xenobiotic electrophiles. The omega GSTs possesses a monothiol G-site [Cys-Pro-Phe-Ala] that binds GSH with high affinity (327). While an active site Cys is highly conserved in all CLIC proteins, they actually have a low affinity for glutathione, and their GSH-binding site is thought to be important in targeting the CLIC to specific subcellular locations (325). The elongated groove of CLIC proteins could potentially interact with proteins distinct from GST substrates and serving as a binding site for its protein partners.

Two of the CLIC proteins, namely CLIC5B and CLIC6 (aka parchorin) also contain very long N-termini in addition to the conserved CLIC module. The crystal structures of these N-terminal extensions have not been defined so far.

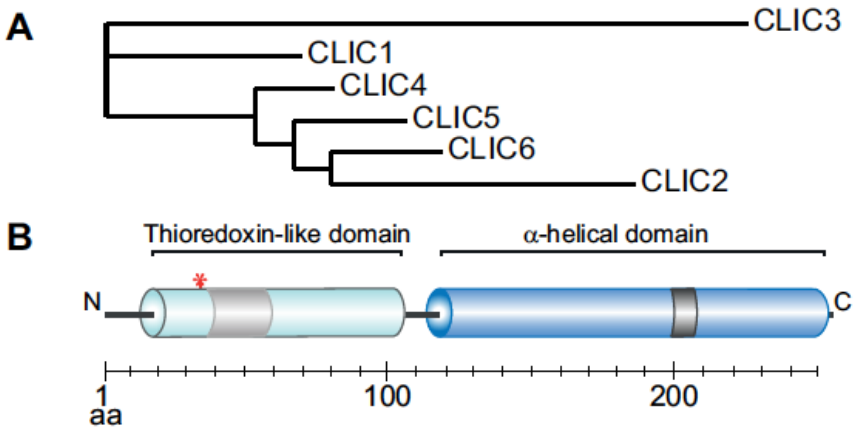

Figure 1.8: The mammalian CLIC family and schematic structure. (Reproduced with permission, Argenzio and Moolenaar (2016). Emerging biological roles of Cl^- intracellular channel proteins. J Cell Sci. 129(22): 4165-4174). **A.** Phylogenetic tree of the mammalian CLIC proteins based on sequence homology. The branch length is proportional to the number of substitutions per site. CLIC1-CLIC5A proteins are 236–253 amino acids (aa) in length. CLIC6 is different in that it is much larger (704 aa). **B.** General structure of CLICs domains. The N-terminal thioredoxin-like domain and the C-terminal α-helical domains of human CLICs are shown in light and dark blue, respectively. The thioredoxin-like domain has a hypothetical transmembrane region (light gray), and the α-helical domain has a nuclear localization signal (dark gray). The red asterisk indicates the reactive Cys residue (Cys32 in CLIC5A, Cys35 in CLIC4). The horizontal bar indicates the number of amino acids.

1.6.3. Potential molecular mechanisms of CLIC proteins

1.6.3.1. *Influence of CLICs on chloride conductance and chloride channel activity*

The initial identification of p64/CLIC5B as a potential Cl^- channel led to many publications that tested the effect of CLIC proteins on Cl^- movement across lipid membranes. The results are mixed and are summarized here. When CLIC1 was incorporated into planar lipid bilayers, it induced a voltage-dependent anion conductance inhibited by IAA-94, and reconstitution of CLIC1 into K^+-loaded phospholipid vesicles produced Cl^- efflux in the presence of the K^+ ionophore valinomycin (328). Similarly, CLIC1 was reported to insert spontaneously into preformed lipid membranes allowing anion flux inhibited by IAA-94, N-ethylmaleimide, glutathione, inactivated by heat, and sensitive to pH and membrane lipid composition (329). Also, recombinant, purified CLIC1 partitioned from the aqueous phase into artificial lipid bilayers resulting in pH-dependent Cl^- flux (330). CLIC1-induced plasma membrane Cl^- channel activity was also observed in Chinese hamster ovary (CHO) cells (331, 332). Interestingly, CLIC1 oxidation resulted in its dimerization and produced significantly greater Cl^- flux in vesicles and artificial bilayers compared to CLIC1 monomer, and a reducing environment prevented the formation of Cl^- channel activity (333). However, others found that although recombinant, purified CLIC1 auto-inserted readily into lipid bilayers, it failed to form well-defined ion channels in the presence of phosphatidylcholine and/or phosphatidylethanolamine, with or without 1 mM DTT or 10–100 μM H_2O_2 (334).

CLIC2 also induced a Cl^- conductance when inserted into an artificial lipid bilayers *in vitro* (335), but compared to the PECAM transmembrane protein (336), CLIC2 was observed in the cytoplasm and not as a transmembrane protein (337) implying that CLIC2 does not function as a Cl^- channel in the plasma membrane. Under oxidative conditions and at low pH, recombinant

CLIC1, CLIC2, and CLIC4 overexpression all stimulated poorly selective anion flux across artificial membranes, (316, 338). Kawai et al. (339) observed that CLIC3 localizes to the plasma membrane of gastric cancer cells, and patch-clamp experiments demonstrated that endogenous and exogenously expressed CLIC3 induced a Cl^- conductance. Similarly, exogenous expression of CLIC3 in LTK fibroblasts induced a Cl^- conductance (340). When CLIC4 was mixed with K^+-loaded liposomes, the potassium ionophore valinomycin triggered CLIC4-dependent Cl^- efflux(341), and CLIC4 induced a Cl^- conductance when added to artificial lipid bilayers *in vitro* (342, 343). Also, patch–clamp analysis of cells expressing exogenous CLIC4 showed increased Cl^- channel activity compared to control cells not transfected with CLIC4, findings that were interpreted to suggest that CLIC4 may be a pore-forming protein or an accessory protein closely associated with channels (344). The Cl^- efflux rate from CLIC5A-containing vesicles was also significantly greater than that from control vesicles (345). However, when purified, recombinant CLIC5A was incorporated into planar lipid bilayers, CLIC5A produced multiconductance channels that were equally permeable to Na^+, K^+, and Cl^-. The effect of CLIC5A was strongly and reversibly inhibited by F-actin. CLIC1 and CLIC4 similarly induced non-specific ion conductance but only CLIC1 and not CLIC4 was sensitive to F-actin (342, 343). P64/CLIC5B knockdown caused defects in microsome acidification, and Src-family tyrosine kinases (c-Src) phosphorylate CLIC5B activating Cl^- influx (346). Overexpressed CLIC5B in cultured cells produced a Cl^- conductance in whole-cell membrane preparations (322, 346). However, CLIC5B was not at the plasma membrane when expressed in *Xenopus* oocytes (321) suggesting that it is unlike typical Cl^- channels. CLIC6, also known as parchorin, was reported to trigger Cl^- efflux from LLC-PK1 cells, and although GFP-tagged CLIC6 was mainly cytosolic, it moved to the plasma membrane when Cl^- ion efflux was induced (347). By contrast, when the intracellular Cl^-

concentration was monitored with the Cl^--sensitive fluorophore MQAE (N-ethoxycarbonylmethyl-6-methoxy-quinolinium bromide) in CHO cells, the presence of CLIC6 had no effect on intracellular Cl^- concentrations (348). CLIC6 appears to form a multimeric complex with G-protein coupled receptors in water and hormone-secreting cells (348). CLIC6 overexpression in *Xenopus* oocyte and rat CHO cells did not enhance Cl^- efflux as observed from the voltage clamp studies (348, 349).

Therefore, there is abundant evidence that CLICs can induce redox and pH-sensitive currents in planar bilayers (330, 334, 350, 351), and that they can influence ion channel activity in cells. However, definitive studies that these proteins can form true Cl^- selective channels *in vivo* are lacking.

1.6.3.2. *Findings not consistent with CLICs chloride channel activity*

The crystal structure of several CLICs has been solved (325, 333, 335, 341, 352, 353). CLICs are globular proteins that can take on multiple folds. However, unlike bona fide Cl^- channels, they lack multiple membrane spanning domains that would be required to form ion-selective pores. Experts have therefore ruled out the possibility that CLICs are true Cl^- channels (354, 355). It has been argued that the putative single hydrophobic domain of CLICs could form a channel, but that the pore would be a primitive structure (350) since functional channels should have a minimum of four subunits. Furthermore, CLICs do not contain a signal peptide sequence, usually required to for membrane-spanning proteins. There also is biological evidence indicating that CLICs are not true ion channels. For instance, lack of CLIC1 paradoxically leads to increased plasma membrane Cl^- permeability in resting macrophages (356). Also, IAA-94, A9C, and DIDS are well-known Cl^- channel blockers. Electrophysiological investigations revealed that IAA-94 and A9C can block CLIC1 ion conductance in cells, but DIDS cannot (355, 357). To explain

experimental findings that CLICs can changes in Cl^- ion conductance, it has been postulated that CLICs might associate with, and activate endogenous ion channels (316). There also is strong evidence that other purified proteins known not be channels can induce non-specific ion currents in artificial membranes, among them amyloid peptides, and transferrin (358-361). CLICs are also unique in comparison to other ion channels in that they are dimorphic, and can exist in membrane-associated as well as cytosolic or soluble forms (338). In the cytosol, they interact with cytoskeletal filaments and other cytosolic proteins. These interactions with cytoskeletal filaments could be responsible for their functional effects (342, 362-364). How a soluble cytoplasmic protein might unfold, undergo a major structural change, and then insert into the membrane to form a functional ion-selective channel has not been explained (364-369).

1.6.3.3. *CLIC proteins show glutathione-dependent oxidoreductase activity in vitro*

Al Khamici et al. (370) measured CLIC enzymatic activity using 2-hydroxyethyl disulphide (HEDS), a specific and sensitive substrate used to assay glutaredoxin enzyme activity. They observed that CLIC1, CLIC2, and CLIC4 proteins all reduced the HEDS substrate when coupled with glutathione (GSH) and glutathione reductase (GR) in the presence of NADPH, though CLIC2 was less active than CLIC1 and CLIC4. Thioredoxins (Trx) are mostly maintained in a reduced state by accepting protons from NADPH via the enzyme Trx reductase. No oxidoreductase activity was observed for CLIC1, CLIC2, and CLIC4 when they were assayed in the presence of Trx reductase instead of glutathione reductase, indicating that they are not substrates for thioredoxin.

Cys24 is the monothiol residue within the CLIC1 enzyme active site. To determine whether Cys24 is the key cysteine residue responsible for CLIC1 oxidoreductase activity, wild type CLIC1, and CLIC1 mutated to alanine (C24A) or serine (C24S) were tested in the HEDS assay.

Wild type CLIC1 showed oxidoreductase activity but the Cys24 mutants C24A and C24S did not. Therefore, CLICs not only exhibit glutaredoxin-like oxidoreductase activity *in vitro* but the structural elements required for catalytic activities were also identified(370).

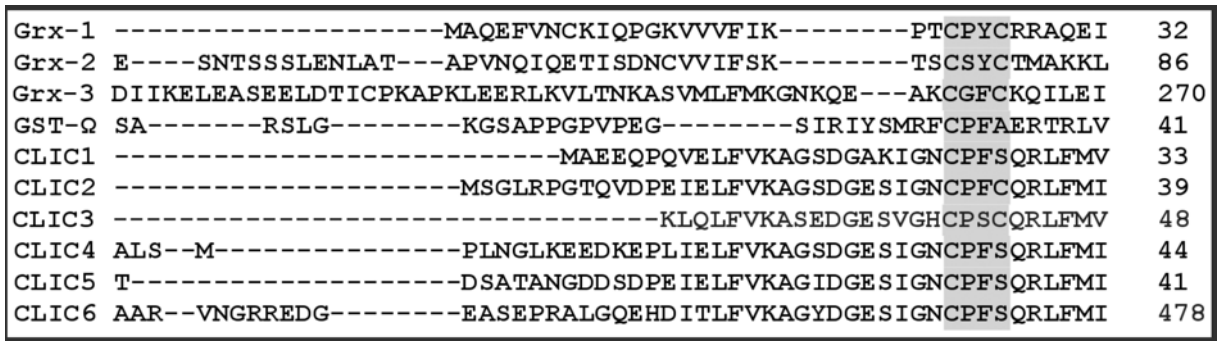

Figure 1.9: The CLIC glutaredoxin (Grx)/thioredoxin active site motif (highlighted in grey). (Reproduced with permission, Al Khamici H, Brown LJ, Hossain KR, Hudson AL, Sinclair-Burton AA, Ng JPM, et al. (2015). Members of the chloride intracellular ion channel protein family demonstrate glutaredoxin-like enzymatic activity. PLoS ONE 10(1): e115699. https://doi.org/10.1371/journal.pone.0115699). Multiple sequence alignment obtained from ClustalW using Grx1, Grx2, Grx3, GST-omega and, and human CLIC 1-6 proteins are shown. CLIC1, CLIC4, CLIC5 and CLIC6 all contain the monothiol active site motif [Cys-X-X-Ser], while CLIC2 and CLIC3 contain the dithiol motif [Cys-X-X-Cys](325). Accession numbers: Grx-1 (BAAO4769), Grx-2 (AAK83089) and Grx-3 (AAH0528289), GST-omega (AAF73376), CLIC1 (CAG46868), CLIC2 (CAG03948), CLIC3 (CAG46863.1), CLIC4 (CAG38532), CLIC5 (AAF66928), CLIC6 (NP_444507).

1.6.4. Potential cellular functions of CLIC proteins

1.6.4.1. CLIC1

CLIC1 also termed the nuclear chloride channel-27 (NCC27), was first cloned from the human myelomonocytic cell line U937 (371). CLIC1 was originally observed in the cell nuclei (371) but also localizes to the cytoplasm, nucleoplasm, and plasma membrane. CLIC1 expresses ubiquitously in many cells. It is enriched in the brush border of renal proximal tubule cells, macrophages, at the apical domain of epithelia including the luminal and glandular epithelium of human endometrium, pancreatic ducts, colon, glandular stomach, small intestine, bile ducts, airway, and epididymis (372, 373). Even though CLIC1 expresses highly in numerous epithelial cells with a diverse function; it is not necessary for morphogenesis, development, or reproduction in CLIC1 null mice. However, the absence of CLIC1 produced less reactive oxygen species that resulted in less acute kidney and pancreas injury in mice. Peritoneal macrophages from CLIC1 deficient mice generated reduced superoxide in response to phorbol ester (phorbol-12-myristate-13-acetate), whilst CLIC1 null peritoneal neutrophils show increased superoxide generation. Global deletion of the CLIC1 gene mildly affects platelet function and inhibits clotting phenotypes (374). CLIC1 global deletion also compromised phagosome acidification in macrophages and dendritic cells (375, 376). CLIC1 is recruited to the phagosomal membranes where it colocalizes with ERM proteins, Rac2, and RhoA during phagocytosis in macrophages (376). It might be possible that CLIC1 membrane association is mediated by Rac2 and/or RhoA, causing ERM protein activation via the $PI4,5P_2$ cluster generation on the cytoplasmic side of the phagosomal lipid membrane. Therefore, CLIC1 membrane association might require the function of Rho GTPases in the context of ERM protein complexes. CLIC1 expression and activity is upregulated during the cell cycle and the IAA-94 Cl^- channel inhibitor causes arrest of

the cell cycle (332). CLIC1 is expressed in endothelial cells and necessary for cultured endothelial cell growth and sprouting morphogenesis (377). CLIC1 knockdown caused decreased cell proliferation, migration, and lumen formation (377). Genetic deletion of CLIC1 in mice does not affect their viability but does result in vascular defects (378). In microglial cells from Alzheimer's patients, CLIC1 moved from the cytoplasm to the plasma membrane in response to brain β-amyloid protein stimulation along with Cl^- channel activity (351). The absence of CLIC1 protects from induced arthritis where macrophages also play a vital function (376). During angiogenesis in response to hypoxia in CLIC4$^{-/-}$ mice, CLIC1 was upregulated threefold and potentially compensates for the absence of CLIC4 expression (379).

1.6.4.2. CLIC2

CLIC2 (XAP121) was identified while mapping transcripts from the chromosome Xq28 telomere (322, 380). It is the least studied CLIC protein, partly due to its absence in the murine genome. In human male children CLIC2 gene deficiency or duplication results in developmental disability, mental retardation, and epilepsy (380-382). CLIC2 is highly expressed in skeletal and cardiac muscle where it localizes to the membrane of sarcoplasmic reticulum. In cardiac muscle CLIC2 interacts with ryanodine receptors 1 and 2 (RyR1 and RyR2), the main calcium-release channels of sarcoplasmic reticulum, amplifying intracellular Ca^{2+} signals in a redox-sensitive fashion (383). Mutant CLIC2-mediated hyperactivation of RyR1 and RyR2 and enhanced post-synaptic neurotransmitter release are associated with intellectual disability, atrial fibrillation, cardiomegaly, congestive heart failure, and seizures (384) A CLIC2 H101Q variant is similarly associated with developmental disabilities, epilepsy, and heart failure (385), the H101 residue being located in the joint loop structure of CLIC2 (335).

CLIC2 is also expressed in endothelial cells, where it co-localizes with platelet endothelial cell adhesion molecule 1 (PECAM1 aka CD31), which facilitates homophilic cell-cell interactions. CLIC2 also co-localizes with claudin 1 and other tight junction proteins including claudin 5, ZO-1 and occludin in non-tumor endothelial cells (336). Endothelial tight junction proteins regulate endothelial permeability (386, 387) and block cancer and other cells from migrating into the circulation (388). A substantial decrease claudins 1, 5, occludin, and ZO-1 as well as CLIC2 in endothelial cells of tumor blood vessels has been reported (388-390). CLIC2 may also be secreted extracellularly to bind and inactivate matrix metalloproteinase 14 (MMP14), inhibiting of MMP14-mediated extracellular matrix degradation, which would protect tight- and adherent junctions between endothelial cells which would tend to block metastasis of tumor cells (336, 391). CLIC2 knockdown in human umbilical vein endothelial cells (HUVECs) increased the fetal bovine serum-induced transmigration of human cancer cells through a HUVEC monolayer (336). Together, the findings suggest that CLIC2 plays a role in endothelial cell-cell interactions, maintaining the barrier between blood and tissues. In tumor endothelial cells, the lack of tight junctions may allow hematogenous spread of cancer cells during metastasis.

1.6.4.3. CLIC3

CLIC3 was initially identified as a binding partner with the COOH-terminal tail of extracellular signal-regulated kinase7 (ERK7) by yeast two-hybrid screen (340). Northern blot analysis showed that CLIC3 highly expresses in the placenta and less in the heart and lung, while kidney, pancreas, and skeletal muscle have minimal expression (340, 347). In A2780 human ovarian cancer cells, African green monkey cell lines COS-7 and CV-1, CLIC3 localizes to nuclei, lysosomes and endosomes (320, 347). Kawai et al. (339) showed that CLIC3 knockdown in MKN7 gastric cancer cells significantly augmented cell proliferation. Conversely, proliferation

was attenuated by the expression of exogenous CLIC3 in CLIC3 deficient KATOIII and NUGC-4 human gastric cancer cells. In a low Cl^- medium, gastric cancer cells (MKN28) and prostate cancer cells (PC3) exhibit a decrease in intracellular Cl^- concentration and attenuated cancer cell proliferation with G0/G1 arrest (392, 393). It was postulated that changes in the CLIC3 expression may disrupt intracellular Cl^- homeostasis in gastric cancer cells, leading to increased cancer cell growth. However, the mechanism of regulation of CLIC3 expression in gastric cancer cells is yet to be understood.

CLIC3 silencing in a human ovarian cancer cell line (A2780) stably expressing either Rab25 (A2780-Rab25) GTPase or a control vector (A2780-DNA3) decreases migration relative to control cells and diminished invasiveness of Rab25 expressing A2780 cells into Matrigel(394), signifying a potential role of CLIC3 in tumor metastasis. The expression of CLIC3 mRNA in bladder cancer tissues was found to be significantly higher than that in normal tissues. The cell cycle, focal adhesion, the extracellular matrix receptor interaction, and the p53 signaling pathway were significantly enriched in the high CLIC3 mRNA expression phenotype indicating that CLIC3 might be significantly associated with cell cycle, focal adhesion, the extracellular matrix receptor interaction and the p53 tumor suppressing signaling pathway (395).

CLIC3 is also necessary for macrophage activation required for the killing of *Listeria monocytogenes* by the formation of anti-intracellular bacterial phagosomes (396). An association of CLIC3 with pregnancy disorders such as fetal growth restriction and pre-eclampsia has also been observed (397). CLIC3 localizes to the syncytiotrophoblast and villous cytotrophoblast cells in the human placenta beginning in the first trimester and in term pregnancies. In Rab25 GTPase-expressing cells, CLIC3 up-regulation causes endosome acidification, a process necessary for recycling $\alpha5\beta1$ integrin-containing endosomes to the plasma membrane (394).

Additionally, CLIC3 is essential for phagosome-lysosome fusion, a process that is necessary for pathogen neutralization (396). Microarray analysis showed that changes in CLIC3 expression might affect the membrane potential, intracellular pH, and cell volume in ischemic cardiomyopathy patients (398). It seems, therefore, that CLIC3 might be important for cell proliferation, but the studies so far have not pinpointed its exact mechanism of action.

1.6.4.4. CLIC4

CLIC4 was originally identified as the human homolog of a rat brain protein termed p64H1 (134, 399, 400). CLIC4 is a mammalian homologue of EXC-4 in nematode. Mutation in ECX-4 is associated with cystic expansion of excretory canals in the nematodes (401). In mammals, CLIC4 expresses in endothelial cells in the skin, kidney, lung, liver, and brain (402, 403). CLIC4 is highly expressed in the renal glomerular endothelial cells and renal proximal tubule brush border epithelial cells (372, 401, 402), and in the microvilli of retinal epithelial cells, where it colocalizes with ezrin (400), and also in human keratinocytes (404). Localization of CLIC4 in the cytoplasm, at the nuclear membrane, the inner mitochondrial membrane, and endoplasmic reticulum has been described (316, 403-405). CLIC4 is also associated with actin-based membrane projections like membrane ruffles and lamellipodia. CLIC4 interacts with ezrin, actin, tubulin, and dynamin I (362). Knockdown of CLIC4 in the retinal epithelial cells using CLIC4-specific siRNA diminished the formation of apical microvilli, similar to the effect of ezrin deletion (406). CLIC4-null mouse embryos undergo impaired renal tubulogenesis, and in kidney proximal epithelial cells, CLIC4 is involved in luminal microvillus morphogenesis, and endo-lysosome development (401).

CLIC4 is highly expressed in all endothelial cells (377, 407) and CLIC4 knockdown in human umbilical vein endothelial cells (HUVEC) caused decreased cell proliferation, capillary network

formation, and lumen formation (377). CLIC4 is involved in endothelial cell vacuole acidification required for lumen formation of developing blood vessel (378). CLIC4 null mice are viable but they exhibit a reduction in retinal vasculature in neonates (378), and smaller kidneys with fewer glomeruli (408). These results suggest that CLIC4 is necessary for vascular development and vascular stress response.

Sphingosine-1-phosphate (S1P) is a bioactive signaling lipid produced in the intracellular membranes from sphingomyelin metabolism (409). SIP receptors are expressed in endothelial cells. Once secreted by vascular endothelial cells, S1P binds and activates the S1P receptor family of G-protein coupled receptors (410), triggering the S1P-S1PR mediated intracellular signaling that regulates endothelial cell function and vascular development. In endothelial cells, S1P promotes translocation of CLIC1 and CLIC4 from the cytoplasm to the plasma membrane. S1P-stimulated Rac1 and RhoA signaling which lead to endothelial migration, barrier control, and stress fiber formation were found to be CLIC1 and CLIC4-dependent (411).

CLIC4 is expressed at high levels in various types of cancer cells. CLIC4 expression is controlled by p53 tumor suppressor protein, tumor necrosis factor (TNF)-α, transforming growth factor (TGF)-β, and c-MYC proto-oncogene and is expressed during cell differentiation and DNA damage. Upregulation of CLIC4 is required for p53-induced apoptosis (412). Increased or reduced CLIC4 expression can induce apoptosis depending on the cell type. In keratinocytes, CLIC4 upregulation triggers an apoptotic response to an external stimulus (403). CLIC4 expression is elevated in malignant stromal cells and is associated with a worse histopathological grade of colorectal cancer (413). Therefore, CLIC4 could be a useful biological marker tracking the progression of histopathological grade of colorectal cancer. Exogenous expression of GFP-CLIC4 in NIE-115 neuroblastoma cells, followed by stimulation with lysophosphatidic acid,

thrombin receptor activating peptide, or S1-P, resulted in translocation of CLIC4 from the cytosol to the plasma membrane. Gα13-dependent RhoA activation acts in this case of CLIC4 translocation to the plasma membrane. Mutation of the CLIC4 at the hydrophobic region blocks its membrane translocation and NHERF-2 co-localization (414).

In CLIC4 knockout mice, the glomerular endothelial cell (EC) ultrastructure appears normal but these mice have fewer glomeruli and peritubular capillaries than wild type controls (408). In the renal proximal tubule epithelial cells, CLIC4 is involved in the formation of the tubule lumen and apical microvilli, through an effect on actin-dependent endosome function (401). Knockdown of CLIC4 in cultured glomerular EC using CLIC4-specific siRNA significantly reduced ERM protein phosphorylation, which was rescued by exogenous expression of CLIC4 or CLIC5(87). In either $CLIC4^{-/-}$ or $CLIC5^{-/-}$ mice, ERM phosphorylation did not decline in glomerular EC, but phosphorylation of ERM proteins in glomerular EC of dual $CLIC4^{-/-}$ and $CLIC5^{-/-}$ mice was almost completely eliminated. In dual $CLIC4^{-/-}$ and $CLIC5^{-/-}$ mice, glomerular EC fenestrae density was similar to wild-type controls at 2 months of age but was markedly decreased at 8 months of age along with a build-up of subendothelial electron-lucent material, mesangial expansion, and the onset of spontaneous proteinuria (87). The data indicate that both CLIC5A and CLIC4 stimulate ERM phosphorylation in glomerular EC, the mechanism of which is important for the maintenance of their structure and function. Furthermore, $CLIC4^{-/-}$ mice showed disrupted apical brush border of proximal tubule epithelial cells and disrupted apical microvilli. Hence, disrupted apical actin-based cellular projections from as other CLIC proteins do not compensate for CLIC4 (87, 400, 401).

1.6.4.5. CLIC6

CLIC6 was first reported in the rabbit and named parchorin (parietal choroid protein). CLIC6 is the longest among the CLIC proteins. It exists as CLIC6A (704 amino acid residues) and CLIC6B (687 amino acid residues) isoforms in humans (415, 416). The C-terminal CLIC domain has high degree of similarity with all other CLIC proteins while the CLIC6 N-terminal extension is distinct from the CLIC5B N-terminal extension (349). qPCR analysis confirmed that CLIC6 expresses highly in the lung and brain tissues as compared to other organs (417). In MDCK and COS-7 cells, overexpressed GFP-CLIC6 localizes in the cytoplasm and the perinuclear area (349), but a small fraction can redistribute to the apical membrane when cells are stimulated (418). Exogenously expressed epitope-tagged rat CLIC6 in human kidney cells was found to be localized to the cytoplasm and the plasma membrane (348), while GFP-tagged human CLIC6 was localized in the cytoplasm in a diffusive pattern when overexpressed in different kidney cell lines (349). CLIC6 expresses predominantly in the cytosol but can be recruited to the apical membrane of rabbit gastric glands when secretion is activated (418). CLIC6 is expressed in the pituitary in the posterior lobe and in cells co-expressing the dopamine receptor (DR) 2 at the border between the intermediate and anterior lobes in the pituitary gland. The neurotransmitter dopamine mediates its action via DR, particularly the D3R receptor expressed in the ventral striatum, mammillary bodies, archicerebellum, and the striatal proliferative subventricular zone of adult rat brain. D3R blocks the formation of cAMP to regulate ion channel activities and stimulate mitogenesis. In transfected HEK293 cells, CLIC6 and D3R co-localize at the plasma membrane, and they interact directly as observed from the yeast two-hybrid screen using a rat brain cDNA library (348).

1.6.4.6. CLIC5B

CLIC5B is expressed exclusively in the avian osteoclast and renal proximal tubules (419, 420) and may be involved in actin-dependent membrane remodeling (420) and bone resorption by osteoclasts (419, 420). CLIC5B in observed in the osteoclast ruffled membrane and antisense mediated CLIC5B knockdown caused decreased bone resorption in differentiating osteoclasts. Intracellular compartment acidification occurs through actions of the vacuolar proton ATPase acting in parallel with a Cl^- conductance (421). CLIC5B knockdown also caused defects in vacuolar acidification, suggesting decreased Cl^- influx. Src-family tyrosine kinases (c-Src) phosphorylate CLIC5B in its unique N-terminus and this phosphorylation activates the Cl^- influx (346). Suppression of c-Src in differentiating osteoclast abolishes the co-localization of CLIC5B with the H-ATPase (AT54). Exogenously expression of recombinant CLIC5B in cultured cells can produce chloride conductance in whole-cell membrane preparations and modification of the protein alters the Cl^- conductance (322, 346). However, the CLIC5B protein is not observed at the plasma membrane when expressed in *Xenopus* oocytes (319) indicating that CLIC5B does not resemble typical Cl^- channels.

1.6.4.7. CLIC5A

1.6.4.7.1. *Discovery of CLIC5 isoform A (CLIC5A)*

Berryman et al. (422) first identified the 32-kDa chloride intracellular channel 5 isoform A (CLIC5A) as a distinct polypeptide pulled from detergent soluble placental microvillus extract through by glutathione-agarose bead immobilized GST-ezrin 556-586. In this pull-down assay, exogenous actin added to the pull-down mixture enhanced the GST-ezrin 556-586 pull down of CLIC5A. CLIC5A and actin were found to be the most abundant microvillus proteins that bound to the immobilized GST-ezrin 556-586. Therefore, CLIC5A was first discovered in a protein

complex with ezrin, actin, and other actin-associated proteins in placenta microvilli (422). Nystrom et al. (182) produced a human glomerular transcriptome database using serial analysis of gene expression (SAGE) and found a SAGE tag (CATGAATCTGAACCAATTACC) corresponding to the 3'-UTR of the CLIC5 transcript. This transcript was predominant in the renal glomeruli and found to be identical to the 3' end of CLIC5. By SAGE analysis CLIC5 was found to be highly expressed and its expression level in human glomeruli was approximately 720-fold higher than in other tissues. A SAGE library produced from micro-dissected mouse kidney glomeruli also contained the CLIC5 transcript and its abundance was 1000-fold greater in glomeruli than in kidney tubules (423).

1.6.4.7.2. *CLIC5 Gene Structure*

The human CLIC5 gene consists of six exons (1A or 1B, 2-6) with alternative first exons 1A (CLIC5A) and 1B (CLIC5B) spanning ~144 kb of genomic DNA on chromosome 6 (422, 424). The N-terminal amino acid sequence of CLIC5A and CLIC5B isoforms vary considerably with exon 1A encoding 18 amino acids and exon 1B encoding 180 amino acids. The CLIC homology domain of CLIC5A and CLIC5B is transcribed from the same exons 2 through 6 and is therefore identical. Human and mouse CLIC5A share ~96% amino acid sequence identity. Among CLIC proteins, only CLIC6/parchorin (637 aa) and CLIC5B/p64 (437 aa) have a long N-terminal stretch.

1.6.4.7.3. *CLIC5 mRNA expression in different tissues*

A commercial northern blot containing poly(A)$^+$ RNA from various human tissues probed with radiolabelled antisense DNA corresponding to the coding sequences of CLIC5, CLIC4, and CLIC1 (422) showed a major CLIC5 transcript of 6.4 kilobases observed at high levels in skeletal muscle and heart, and moderate levels in the kidney, placenta, and lung.

1.6.4.7.4. *CLIC5 transcripts in the kidney*

CLIC5 RNase protection assay confirmed the existence of CLIC5 RNA transcript in the human kidney (85). A northern blot analysis of human kidney mRNA using cDNA probes corresponding to the open-reading frame of CLIC5A detected only a single 5.7 kilobase mRNA (85). RT-PCR analysis with the primers designed for exons 1A and 1B to evaluate CLIC5A and CLIC5B gene expression in multiple tissues from CLIC5-wild-type mice revealed that CLIC5B mRNA was detected only in mouse kidney and to a lesser extent in brain. On the other hand, CLIC5A was detected in all tissues used including the lung, brain, heart, kidney, and inner ear of mice (425).

1.6.4.7.5. *CLIC5A protein expression in cells and tissues*

Although markedly enriched in glomeruli and inner ear hair cells, the CLIC5A protein is also expressed at lower levels in heart, lungs, skeletal muscles, stomach, brain, testis, eyes, and placenta (422). When overexpressed in cells, the CLIC5A protein localizes predominantly to membrane projections, microvilli and a substantial portion is associated with the actin cytoskeleton (345). Confocal immunofluorescence and immunogold electron microscopy demonstrated that CLIC5A expresses highly in the glomerular EC and podocytes (85). Cell fractionation studies suggest that CLIC5A is mostly soluble and can translocate to the plasma membrane as a peripheral protein (426).

1.6.4.7.6. *CLIC5A is necessary for the maintenance of inner ear hair cell stereocilia*

Gagnon et al. (425) identified the naturally occurring “jitterbug” mutation in the CLIC5 gene causing mouse deafness and vestibular dysfunction. They demonstrated that only the CLIC5A isoform is expressed in the inner ear, and that the CLIC5A protein localizes to the apical stereocilia sensory hair cells of the cochlea and vestibular apparatus in the mouse and in the

chicken utricle (425). The inner ear hair cell stereocilia are giant microvilli that act as mechanoreceptors for hearing and balance (427). Detailed analysis revealed that initial development of the stereocilia is normal but that their structure degenerates with age resulting in impaired hearing and deafness at 7 months in the CLIC5A deficient mice (425). Importantly, a similar phenotype is observed with loss-of-function radixin gene mutations (204). It turns out that CLIC5A co-localizes with radixin at the base of stereocilia where the radixin abundance increases when CLIC5 is absent. CLIC5 deficiency causes a fused base in the hair cell rootlet. Therefore, CLIC5A thought to associate with the radixin–actin complex in the stereocilia stabilizing the link between the plasma membrane and actin cytoskeleton (428).

In humans, a homozygous nonsense mutation in the CLIC5 gene similarly leads to autosomal recessive hearing loss starting in early childhood and becoming severe before the second decade. The hearing loss in humans is associated with vestibular areflexia and mild renal dysfunction (429).

1.6.4.7.7. *In glomeruli, CLIC5 localizes to podocytes and glomerular EC*

Immunoblot analysis of whole cell lysates prepared from isolated glomeruli showed that both CLIC5A and CLIC5B were present in the $CLIC5^{+/+}$ mice and lacked $CLIC5^{-/-}$, with a lower abundance of CLICB compared to CLIC5A in $CLIC5^{+/-}$ glomeruli. Immunofluorescent labelling of adult mouse kidney section with anti-CLIC5 antibody demonstrated that CLIC5 is mainly observed in podocyte cell body and foot processes. Immunogold electron microscopy of mouse kidney section with anti-CLIC5 antibody also showed that CLIC5 predominantly localizes to the apical domain of foot processes (85). Fluorescence confocal microscopy imaging of cultured primary mouse podocytes after 14 days *in vitro* showed that CLIC5 is localized at the tips of actin filaments and also has a punctate labelling pattern at regions of cell–cell contact (297).

1.6.4.7.8. *CLIC5 regulates the expression of ERM proteins and podocalyxin*

Western blot analysis using whole cell lysates prepared from isolated glomeruli of $CLIC5^{+/+}$ and $CLIC5^{-/-}$ mice showed that the major podocyte proteins ERM proteins, podocalyxin and to a lesser extent, nephrin abundance were reduced in $CLIC5^{-/-}$ but not in the $CLIC5^{+/+}$ mouse glomeruli (85, 297), and phosphorylation of ERM proteins was profoundly reduced in glomeruli of $CLIC5^{-/-}$ mice (86), ezrin strongly colocalized with CLIC5, and podocalyxin co-immunoprecipitated with CLIC5 (85). These data indicate that CLIC5 regulates the abundance of ezrin as well as maintains the level of ERM phosphorylation in podocytes *in vivo*.

1.6.4.7.9. *CLIC5A stimulates ERM protein phosphorylation and actin polymerization*

Phosphorylation of ERM proteins increased in COS-7 cells overexpressing CLIC5A compared to vector-transfected cells (89), enhancing the association of ezrin with the cytoskeletal fraction. This effect of CLIC5A was not altered by the non-specific Cl^- inhibitor IAA-94. Moreover, scanning electron microscopic imaging demonstrated cell surface ruffling in COS-7 cells overexpressing CLIC5A, and actin polymerization increased.

1.6.4.7.10. *CLIC5A-expression increases plasma membrane $PI4,5P_2$ abundance*

Live-cell confocal imaging using the PH-PLC biosensor for $PI4,5P_2$ showed a substantial increase in $PI4,5P_2$ clusters at the dorsal plasma of CLIC5A-overexpressing cells (89). Plasma membrane $PI4,5P_2$ is a substrate for phospholipase C (PLC) – mediated $PI4,5P_2$ hydrolysis. Depletion of $PI4,5P_2$ with the PLC activator m-3M3FBS for 5 minutes reduced ERM phosphorylation in COS-7 cells which could not be rescued by CLIC5A expression (89). These results are consistent with the possibility that CLIC5A actually increases the association of ERM proteins with the plasma membrane through increased production of $PI4,5P_2$ causing greater ERM activation.

1.6.4.7.11. *PI4P5Kα silencing reduces CLIC5A-stimulated ERM phosphorylation*

It turns out that CLIC5A colocalizes with the P(4,5P_2-generating kinases PI4P5Kα and PI5P4Kα, and that these enzymes can be pulled from cell lysates by purified, immobilized GST-CLIC5A suggesting that they are in the same protein complex. Knockdown of endogenous PI4P5Kα with PI4P5Kα-specific siRNA reduced CLIC5A-stimulated ERM phosphorylation in COS-7 and HeLa cells (89). Deletion mutants of CLIC5A lacking the first 21 aa (22-251 aa) or the last 19 aa (1-232 aa) did not co-localize with PI4,5P_2 generating enzymes and failed to stimulate PI4,5P_2 accumulation as well as ERM phosphorylation. These observations would be consistent with CLIC5A-mediated stimulation of PI4P5K activity, causing PI4,5P_2 generation and consequent ERM activation.

1.6.4.7.12. *CLIC5-deficiency disrupts the ezrin-NHERF2-podocalyxin complex in glomeruli*

The CLIC5A protein is extremely abundant in glomeruli (182, 423), and it colocalizes with ezrin in podocytes (85, 297). Active, phosphorylated ezrin interacts with podocalyxin(184) directly and via NHERF2, coupling podocalyxin to the actin cytoskeleton (233). In CLIC5-deficient mice, ezrin phosphorylation is nearly absent (86, 87, 89). In wild-type mice glomerular NHERF2 is largely cytoskeleton-associated, whereas in CLIC5$^{-/-}$ mice NHERF is mostly soluble (89). This finding suggests that CLIC5A is necessary to maintain intact ezrin-NHERF2-podocalyxin complexes, and its deficiency disrupts the complex causing NHERF2 to dissociate from the actin cytoskeleton.

1.6.4.7.13. *CLIC5A expression stimulates Rac1 activation, but not Cdc42 and RhoA*

Ectopic expression of CLIC5A increases the level of Rac1-GTP without a change in total Rac1 abundance in COS-7 cells, without change in Cdc42-GTP and RhoA-GTP levels (86). Phosphorylation of Pak1 and -3, effectors of Rac1 and Cdc42, was also significantly higher in

COS-7 cells expressing CLIC5A compared to vector-transfected cells, whereas Pak2 phosphorylation did not change. Similarly, in cultured mouse podocytes, which do not express CLIC5A at baseline, CLIC5A expression stimulated ERM and Pak1,3 phosphorylation. The Rac1 inhibitor NSC 23766 treatment or expression of dominant negative Rac1 N17 abolished CLIC5A-stimulated ERM and Pak1,3 phosphorylation (86). These data suggest strongly that activation of Rac1 by CLIC5A is upstream of ERM as is Pak1,3 phosphorylation. $PI4,5P_2$ is the docking site for ERM proteins at the inner leaflet of cell membrane and CLIC5A-stimulated ERM phosphorylation cannot occur when $PI4,5P_2$ generation is disrupted (89). The Rac1 inhibitor NSC 23766 abolished CLIC5A-dependent $PI4,5P_2$ cluster formation (86) indicating that CLIC5A-stimulated apical $PI4,5P_2$ cluster generation also requires Rac1 activity.

1.6.4.7.14. *CLIC5 deficiency makes mice more susceptible to glomerular injury*

Scanning and transmission electron microscopic evaluation of the glomerular ultrastructure revealed that glomerular podocyte cell bodies are smoother and foot processes are shorter and fewer in number in $CLIC5^{-/-}$, than in wild-type mice (85, 297). The foot processes in $CLIC5^{-/-}$ mice were disorganized but did not undergo effacement and the slit diaphragm remained intact. Nonetheless, there was an increase in albuminuria in $CLIC5^{-/-}$ mice compared to the $CLIC5^{+/+}$ mice (85). However, there was no glomerulosclerosis (297) and blood urea nitrogen and serum creatinine concentrations were not elevated even in 12-month-old $CLIC5^{-/-}$ mice (85). Interestingly, transmission electron microscopic also revealed the presence of large vacuoles in many glomerular EC in $CLIC5^{-/-}$ mice though the glomerular EC fenestrae were normal (85).

Adriamycin (doxorubicin) is an anthracycline antibiotic used in cancer therapy, and it causes predictable glomerular injury in mice (430). Albuminuria was detected in both $CLIC5^{+/+}$ and $CLIC5^{-/-}$ mice littermates three weeks after Adriamycin injection, but the albumin/creatinine ratio

was 560 ± 135 μg/mg in CLIC5$^{+/+}$ mice and 1,691 ± 350 μg/mg in CLIC5$^{-/-}$ mice (85). This nearly 3-fold greater level of albuminuria in Adriamycin-treated CLIC5$^{-/-}$ mice indicates greater the vulnerability of mice to Adriamycin-induced glomerular injury when CLIC5 is absent.

Uninephrectomy (UNx) combined with deoxycorticosterone (DOCA) administration and a high salt intake is a well-established model for systemic and glomerular capillary hypertension in rodents (431). In UNx-DOCA/salt hypertensive CLIC5$^{-/-}$ mice, the fraction of glomeruli with microaneurysms was doubled compared to the UNx-DOCA/salt hypertensive CLIC5$^{+/+}$ mice and the albumin/creatinine ratio was 1720 ± 960 μg/mg after 21 days of DOCA/salt administration in CLIC5$^{-/-}$ mice, compared to only 91 ± 31 μg/mg in UNx-DOCA/salt hypertensive CLIC5$^{+/+}$ mice (mean ± SD, n = 5, $P < 0.05$), even though the degree of hypertension was similar in both strains of mice. This finding indicates that CLIC5-deficient mice are much more susceptible to hypertension-induced glomerular microaneurysm formation and albuminuria than CLIC5$^{+/+}$ mice (87). UNx-DOCA/salt hypertension also led to a very significant increase in glomerular Pak phosphorylation, which was abolished when CLIC5 was absent (86). Taken together, these results showed that CLIC5 is necessary for the maintenance of podocyte structural integrity and GFB function. Moreover, in the absence of CLIC5A glomeruli are much more susceptible to injury by Adriamycin and hypertension, suggesting that glomerular CLIC5A and CLIC5A-dependent Rac1/Pak activation play an important role in resisting glomerular injury.

1.7. Taperin

CLIC5A plays a significant role in the regulation of actin-associated protein complexes. The actin multiprotein complex consisting of CLIC5A, radixin, taperin, myosin VI (MYO6), as well as the tyrosine phosphatase receptor Q (PTPRQ) is necessary for the proper positioning and maintenance of the stereocilia shaft by organizing membrane-cytoskeletal attachment at the base

of the hair cell stereocilia (428). CLIC5A colocalizes with taperin, radixin, and MYO6 at the base of hair cell stereocilia (428). The deafness-associated proteins radixin, PTPRQ, and taperin were mislocalized in fused stereocilia of CLIC5-knockout mice (428). Therefore, a CLIC5A-taperin interaction might play a significant role in CLIC5A function.

1.7.1. Human taperin isoforms

Autosomal recessive nonsyndromic hearing loss is very common in humans, involving about 60 loci in a total of 113 genes. The taperin gene, also known as the "C9orf75" gene, is one of the genes for which loss-of-function mutations have been causally linked to autosomal recessive nonsyndromic hearing loss in two separate families (432, 433). The human taperin primary RNA transcript undergoes alternative splicing to produce four known taperin isoforms. Isoform 1 (1-711 aa) has calculated molecular weight of ~75.6 kDa. Isoforms 2 and 3 lack the N-terminal 1-306 aa found in isoform 1. Isoform 2 consists of 405 aa (starting at residue 307 relative to isoform 1) and has a calculated molecular weight of ~44.12 kDa. Isoform 3 and 4 are similar to isoform 1 with minor sequence variations. All taperin isoforms have a PP1c binding motif (KISF) at 577–580 aa in isoform 1, and at position 271–274 aa in isoform 2. Mass spectrometry detected all four isoforms in HeLa cells (434).

1.7.2. Taperin expression and subcellular localization

The taperin protein is widely expressed in mammalian tissues, most notably in the cochlea of the inner ear (434). Immunolocalization revealed that the taperin gene product was mainly observed at the taper regions of inner ear hair cells stereocilia and thus annotated as taperin (433). Taperin can also translocate between the nucleus and cytoplasm and is found to be complexed with PP1c in both sub-cellular locations (434). Endogenous taperin is mostly observed in the nucleus of immune-stained HeLa cells, and live-cell confocal imaging showed that exogenously expressed

GFP-tagged taperin 307-711 aa (isoform 2) in the HeLa and U2OS cells is also observed at the nucleus (434).

1.7.3. Potential taperin interacting proteins

Searching for taperin interacting proteins in the interaction network (IntAct, Interaction network, EMBL-EBI, ebi.ac.uk), shows that taperin is predicted to interact with CLIC proteins, specifically CLIC5, CLIC4, CLIC2, and CLIC1 as well as protein phosphatase 1 catalytic subunits (PP1c) PP1cα, PP1cβ, and PP1cγ. A yeast 2-hybrid screen in which CLIC1 was used as bait identified a partial cDNA clone corresponding to a C-terminal fragment (amino acids 307–711) of taperin (435). Crosslinking immunoprecipitation approach revealed that GFP-tagged CLIC5 and Xpress-tagged taperin were co-immunoprecipitated(434).

1.7.4. Taperin regulates PP1 activity

Endogenous taperin co-immunoprecipitated with PP1cα but not PP1cβ, and PP1cγ from the HeLa cell extracts, and mutation of the KISF mutated to KASA abolished the taperin/PP1cα interaction. A quantitative proteomics approach also detected taperin as a nuclear PP1c interacting protein (436). Taperin binds and blocks PP1cα activity toward glycogen phosphorylase, indicating that taperin acts as a strong inhibitor of PP1cα activity (434). An "RVRW" peptide with high affinity for PP1c blocked its binding to the taperin KISF motif, whereas a control "RARA" peptide was without effect (436). These studies indicate that taperin is a PP1 regulatory subunit that binds the catalytic PP1c subunits via its KISF motif.

1.7.5. Taperin is part of a multiprotein complex consists of CLIC5A and radixin

Hearing and balance depend on the deflection of actin-based stereocilia of inner ear hair cells which act as mechano-transducers to convert mechanical stimuli into electric impulses conveyed to the brain (437, 438). Mutations in CLIC5, radixin (RDX), taperin (TPRN), protein tyrosine

phosphatase receptor Q (PTPRQ), and myosin VI (MYO6) genes all lead to disruption of inner ear stereocilia (439-442) (205, 425, 428, 433). These proteins concentrate at the base of the inner ear hair cell actin bundles during embryonic development (204, 439, 443, 444). In $CLIC5^{+/+}$ mice inner ear hair cells, radixin is enriched at the base of stereocilia by postnatal day 17, but in $CLIC5^{-/-}$ mice, radixin was found to be dissociated from stereocilia (428). Similarly, in $CLIC5^{+/+}$ mouse inner ear hair cells, taperin was concentrated at the base of the stereocilia, but in $CLIC5^{-/-}$ mice taperin staining was scattered and distributed throughout both fused as well as unfused stereocilia (428). These results indicate that CLIC5A is necessary for the proper localization of radixin and taperin at the base of inner ear hair cell stereocilia. Furthermore, taperin, CLIC5A and radixin form a complex to establish a link between the plasma membrane and the subjacent actin cytoskeleton at the base of inner ear hair cell stereocilia, stabilizing the plasma membrane and actin cytoskeleton linkage.

1.7.6. Taperin regulates actin dynamics

Taperin has an overall 34% amino acid sequence similarity to phostensin that can cap the pointed end of actin filaments (433). Taperin is observed at the basal domain of stereocilia where many peripheral actin filaments with pointed ends terminate, indicating that taperin might act as an actin regulator in inner ear hair cells stereocilia (205, 428, 433). In fact, taperin overexpression results in rod-shaped actin organization in >50% of COS-7 and HEK293 cells (445). Therefore, the evidence so far suggests that taperin, like CLIC5A and radixin regulate actin dynamics, but the mechanisms by which these proteins function in conjunction with each other is not understood.

2. Hypothesis and Objectives

Rationale

In my thesis, I focus on possible mechanisms of CLIC5A-dependent Rac1 activation and ERM phosphorylation to gain insights into CLIC5A function in renal glomerular podocytes. Since previous findings indicate that CLIC5A is part of the ezrin/podocalyxin/NHERF2 complex in podocytes (89) and since Rac1 is activated by CLIC5A (86), it seems likely that CLIC5A interacts directly with one or more of the proteins in the ezrin/podocalyxin/NHERF2 complex. Also, since CLIC5A is part of the radixin/taperin complex at the base of stereocilia in the inner ear (428), it seems likely that the function of CLIC5A toward radixin and ezrin is conserved. While it is established that CLIC5A expression is functionally important for Rac1 activation and ERM phosphorylation, the underlying mechanisms are unclear and directly interacting protein partners of CLIC5A through which CLIC5A exerts its biological functions were not previously identified. I expect that my investigation of CLIC5A functions in cells will apply generally to the mechanism(s) of action of other CLIC proteins.

Hypothesis

CLIC5A-stimulated Rac1 activation and ERM phosphorylation require a direct CLIC5A-Rac1 or CLIC5A-ezrin interaction. Localization of CLIC5A near the cell membrane depends on a direct interaction between CLIC5A and its direct binding partner(s). CLIC5A and taperin also interact directly and this interaction is functionally important for the subcellular localization of taperin.

Objectives

1. Determine whether CLIC5A, Rac1 and ezrin are part of the same protein complex.

2. Determine the direct interacting partners of CLIC5A.

3. Determine whether CLIC5A interacts directly with Rac1, and ezrin, radixin, moesin (ERM) proteins.

4. Determine the subcellular distribution of CLIC5A in isolated glomeruli.

5. Determine the consequence of CLIC5A expression on the subcellular localization of ezrin.

6. Determine whether CLIC5A stimulates Rac1-dependent specific PI4P5 kinase or PI5P4 kinase isoforms.

7. Determine whether ezrin phosphorylation increases its interaction with CLIC5A.

8. Determine the functional consequence of blocking the CLIC5A/ezrin interaction.

9. Determine whether CLIC5A-stimulated Rac1 activation requires ezrin.

10. Determine whether CLIC5A and other CLICs interact directly with taperin.

11. Determine the consequence of CLIC5A expression on the subcellular localization of taperin.

12. Determine whether taperin binds a specific PP1c isoform in the CLIC5A protein complex.

13. Determine whether CLIC5A-dependent ERM phosphorylation is altered by taperin.

Chapter 2

Materials and Methods

Chapter 2: Materials and Methods

2.1. Chemicals and reagents

All the chemicals and reagents were prepared and used according to the manufacturer's instructions unless otherwise stated.

Table 1: List of chemicals and reagents and their sources

Chemical/Reagent/	Source	Catalogue #
Dulbecco's Modified Eagle Medium	Sigma-Aldrich, St Louis, MO, USA	D5796
Fetal bovine serum	Life Technologies, Burlington, ON, Canada	12483-020
Penicillin/Streptomycin	Life Technologies, Burlington, ON, Canada	15140-122
Tryspin-EDTA	Life Technologies, Burlington, ON, Canada	25300-054
EBM-2 medium	Lonza, Walkersville, MD, USA	CC-3156
EGM-2 MV Bulletkit growth media	Lonza, Walkersville, MD, USA	CC-3162
Quick Coating Solution	Angio-Proteomie, Boston, MA, USA	cAP-01
Lipofectamine 2000	Invitrogen, Carlsbad, CA, USA	11668-027
Lipofectamine 3000	Invitrogen, Carlsbad, CA, USA	L3000015
Polybrene	EMD Millipore, Billerica, MA, USA	TR1003
Opti-MEM I medium	Life Technologies, Burlington, ON, Canada	31985-070
Dulbecco's PBS	Life Technologies, Burlington, ON, Canada	25300-054
Cell lysis buffer	Cytoskeleton Inc. Denver, USA	GL36
Protease inhibitor cocktail	Cytoskeleton Inc. Denver, CO, USA	PIC02
Phosphatase inhibitor	Roche Diagnostics, Mannheim, Germany	4906837001
2X Laemmli buffer	BioRad laboratories, Inc. Hercules, CA, USA	1610737
Glutathione-Sepharose 4B	Global life sciences, Marlborough, MA, USA	17075605
1x proteinase inhibitor cocktail	Roche Diagnostics, Mannheim, Germany	04693116001
β-mercaptoethanol	Bioshop Canada Inc. Burlington, ON, Canada	MER002.100
Calyculin-A	Millipore Sigma, Billerica, MA, USA	208851
m-3M3FBS	Millipore Sigma, Billerica, MA, USA	525185
RPMI 1640 medium	Sigma-Aldrich, St Louis, MO, USA	R8758
Collagenase IV	Worthington, Lakewood, NJ, USA	LS005275
Digitonin	Millipore- Merck KGaA, Darmstadt, Germany	300410
Novex™ 8-16% Tris-Glycine gel	Invitrogen, Carlsbad, CA, USA	XP08165BOX
Western blocker solution	Sigma-Aldrich, St Louis, MO, USA	WO138
Imobilon®–P PVDF membranes	Millipore-Sigma, Oakville, Ontario, Canada	IPVH00010
No-Stain Protein Labeling Reagent	Invitrogen, Carlsbad, CA, USA	A44449
ECL solution	Cytiva, Buckinghamshire, UK	RPN2106
Tween-20	Sigma-Aldrich, St Louis, MO, USA	P7949
RIPA lysis buffer	EMD Millipore, Burlington, MA, USA	20-188
10X RIPA buffer	Abcam, Waltham, MA, USA	ab156034
Pierce Glutathione agarose bead	Life technologies, Burlington, ON, Canada	78602
Protein G plus/protein A-agarose	Muillipore Calbiochem, San Diego, CA, USA	IP0515ML
Rac1 activation assay Biochem kit	Cytoskeleton Inc. Denver, USA	BK035
Rac1 G-LISA activation assay kit	Cytoskeleton Inc. Denver, USA	BK128
TnT® Quick coupled Transcription /Translation Systems	Promega Corporation, Madison, WI, USA	L1170
Control siRNA	Santa Cruz Biotechnology, Dallas, TX, USA	sc-35349

Human ezrin siRNA	Santa Cruz Biotechnology, Dallas, TX, USA	sc-37007
Ezrin siRNA	OriGene Technologies, Rockville, MD, USA	SR305077
Radixin siRNA	OriGene Technologies, Rockville, MD, USA	SR304025
Moesin siRNA	OriGene Technologies, Rockville, MD, USA	SR305077
Human Taperin siRNA	OriGene Technologies, Rockville, MD, USA	SR317309
Scrambled Negative control siRNA	OriGene Technologies, Rockville, MD, USA	SR30004
Commercial human kidney cDNA	Ambion, Texas, USA	
Matchmaker® Gold Y2H system	Takara Bio USA Inc. San Jose, CA, USA	630489
pCDNA3.1/V5-His-TOPO vector	Invitrogen, Burlington, ON, Canada	K480040
pTARGET plasmid DNA	Promega, Madison, WI, USA	TM044
pGEX-3 plasmid DNA	GE Healthcare, Piscataway, NJ, USA	28-9546-54
pEGFP-C1 plasmid DNA	Clontech, Mountain View, CA, USA	6084-1
Escherichia coli BL21 Gold (DE3)	Agilent Technologies, Santa Clara, CA, USA	230132
IPTG	Invitrogen, Carlsbad, CA, USA	15529019
Rac1 inhibitor NSC23766	Santa Cruz Biotechnology, Dallas, TX, USA	sc-204823
QIAgen MaxiPrep kit	Qiagen, Germantown, MD, USA	12162
QIAgen MiniPrep kit	Qiagen, Germantown, MD, USA	27104
QIAgen PCR purification kit	Qiagen, Germantown, MD, USA	28104
QIAgen gel extraction kit	Qiagen, Germantown, MD, USA	28704
QIAgen DNeasy blood & Tissue kit	Qiagen, Germantown, MD, USA	69504
PrimeSTAR GXL DNA Polymerase	TaKaRa Bio. Co. San Jose, CA, USA	R050A

2.2. Primary antibodies

Table 2: Primary antibody sources and dilutions are listed in the following table:

Primary Antibodies	Host	Catalog #	Source	WB	IF	IP
CLIC5	Rabbit	ARP35263	Aviva, San Diego, CA, USA	1:4000		
CLIC1	Rabbit	SC134859	Santa Cruz Biotech. Dallas, TX USA	1:500		
CLIC4	Rabbit	SC130723	Santa Cruz Biotech. Dallas, TX USA	1:500		
Rac1	Mouse	ARC03-S	Cytoskeleton Inc, Denver, MA, USA	1:1000		
Ezrin FL	Rabbit	3145S	Cell Signaling, Danver, MA, USA	1:4000	1:200	1:200
Ezrin C-ter	Rabbit	Ab40839	Abcam, Waltham, MA, USA	1:4000		
Radixin	Rabbit	MA5-14886	ThermoFisher Sci. Waltham, MA, USA	1:4000		
Moesin	Rabbit	3150S	Cell Signaling, Danver, MA, USA	1:4000		
pERM	Rabbit	Ab76247	Abcam Inc. Waltham, MA, USA	1:4000		
FLAG	Mouse	F1804	Sigma-Aldrich, Oakville, ON	1:4000		1:100
HA	Rabbit	3724S	Cell Signaling, Danver, MA, USA	1:1000		
GFP	Rabbit	2956S	Cell Signaling, Danver, MA, USA			1:2000
GFP	Rabbit	N/A	Dr. Luc Berthiaume, Cell biology, University of Alberta	1:4000		
Podocalyxin	Goat	AF1556	R&D Systems, Minneapolis MN USA	1:500		
NHERF2	Rabbit	9568S	Cell Signaling, Danver, MA, USA	1:2000		
Nephrin	Goat	AF3159	R & D Systems Minneapolis, MN, USA	1:2000		
N-Cadherin	Rabbit	4061S	Cell Signaling, Danver, MA, USA	1:2000	1:200	
Taperin	Mouse	sc-515824	Santa Cruz Biotech. Dallas, TX USA	1:2000		
PP1c α (c-19)	Goat	Sc-6104	Santa Cruz Biotech. Dallas, TX USA	1:2000		
PP1c β	Rabbit	PA1-12379	Invitrogen, Carlsbad, CA, USA	1:2000		
PP1c γ	Rabbit	Ab134947	Abcam, Waltham, MA, USA	1:2000		

Pan-PP1c	Mouse	Sc-7482	Santa Cruz Biotech. Dallas, TX USA	1:2000		
RhoGDI α	Mouse	Sc-373724	Santa Cruz Biotech. Dallas, TX USA	1:2000		
GAPDH	Rabbit	2118S	Cell Signaling, Danver, MA, USA	1:5000		
β-Actin	Mouse	A2228	Sigma-Aldrich, Oakville, ON, Canada	1:1000		

Table 3: Secondary antibody sources and dilutions are listed in the following table:

Secondary Antibodies/ Reagents	**Conjugate**	**Catalog #**	**Source**	**WB**	**IF**
Streptavidin	HRP	3999S	Cell Signaling, Danver, MA, USA		
Goat anti-mouse IgG(H+L)	HRP	115-035-003	Jackson ImmunoResearch Lab Inc. West Grove, PA, USA	1:1000-1:50000	
Goat anti-Rabbit IgG(H+L)	HRP	32460	ThermoFisher Sci. Waltham, MA, USA	1:5000-1:10000	
Donkey anti-goat IgG(H+L)	HRP	705-035-003	Jackson ImmunoResearch Lab Inc. West Grove, PA, USA	1:5000-1:10000	
Rabbit anti-mouse IgG (H+L)	Alexa Fluor 594	A11032	ThermoFisher Sci. Waltham, MA, USA		1:500-1:1000
Donkey anti-Rabbit IgG (H+L)	Alexa Fluor 594	A21207	ThermoFisher Sci. Waltham, MA, USA		1:500-1:1000

2.3. Cell culture, transfection, and cell lysis

2.3.1. COS-7, HEK293, and HeLa cells

COS-7 cells are the African green monkey kidney cell line (446) that is widely used for efficient transfection of plasmid vector constructs. COS-7 cells do not express CLIC5A at baseline (89). These are the reasons for using COS-7 cells to study the functions of the overexpressed CLIC5A protein, as no endogenous CLIC5 would interfere. The human embryonic kidney cell line (HEK293) is also widely used for efficient transfection of plasmid vector constructs and was used in my studies. The HEK293 cell line is a permanent cell line developed from the human primary embryonic kidney and transformed with sheared human adenovirus type 5 DNA (447). HeLa is also commonly used for efficient transfection of plasmid vector constructs to study the

functions of overexpressed proteins. HeLa cells are an immortalized cell line, derived from cervical cancer cells from Henrietta Lacks, a 31-year-old African American mother of five, who died of cancer on October 4, 1951, and after whom the cell line was named (448). COS-7 cells (Thermo Fischer Scientific, USA), HEK293 cells (Thermo Fischer Scientific, USA) and HeLa cells (Thermo Fischer Scientific, USA) were cultured in Dulbecco's Modified Eagle Medium (DMEM) containing 10% v/v fetal bovine serum (FBS) and 1% v/v penicillin/streptomycin at 37°C in humidified air containing 5% CO2. DMEM medium containing 10% v/v FBS was used for cDNA transfection. One day before transfection, cells were dissociated from the culture plates with 0.05% w/v trypsin-EDTA treatment and re-plated. ~70% confluent cell monolayer was used for transfection. Transfections were performed with Lipofectamine 2000 according to the manufacturer's protocol using varying concentrations of plasmid DNA constructs. 48 hours after transfection, cells were washed twice with ice-cold phosphate-buffered saline (PBS) and lysed with standard RIPA buffer or TX-100 lysis buffer (Triton X-100 0.5%, HEPES 10 mM, NaCl 0.1 M, β-mercaptoethanol 14 mM, EGTA 2.5 mM, MgCl2 5 mM) containing protease inhibitor cocktail (Roche) and phosphatase inhibitor "PhosStop" (Roche). The lysed cells were scraped from the culture plates and collected into the pre-chilled centrifuge tubes, centrifuged at 14,000 X g and the supernatants collected were used for different assays. To use as input, 100 µl of supernatant was mixed with 100 µl of 2 X Laemmli buffer. To prepare total cell lysate (TCL), 100 µl of the lysed cells was mixed with 100 µl of 2 X Laemmli buffer and boiled for 5 minutes. To prepare detergent-insoluble pellet fractions, the supernatants were removed, and the pellets were suspended in 100 µl of 2 X Laemmli buffer and boiled for 5 minutes.

2.3.2. Human glomerular endothelial cells

Mycoplasma-free primary human glomerular endothelial cells (EC) were purchased from Angio-proteomie (Boston, MA, USA). Human glomerular EC are not suitable for transfection with cDNA vector construct; therefore adenoviral vector-mediated transfection method was conducted as previously used by Tavasoli et al. (2016). Cultured human glomerular EC do not express CLIC5A. Culture plates were first coated with the "Quick Coating Solution". Human glomerular EC were then cultured in EGM-2 MV Bulletkit growth medium containing 5% FBS and 1% penicillin/streptomycin at 37°C in humidified air containing 5% CO2. CLIC5A was expressed from the adenoviral vector pAdTrack-GFP/CLIC5A that expresses GFP and CLIC5A from separate promoters. Control pAdTrack-GFP was used as adenoviral-mediated vectors to infect cells. human glomerular EC cells were dissociated from the culture plates with 0.05% w/v trypsin-EDTA treatment and re-plated in p35 mm culture plates at a density to achieve ~70% confluent cells 24 hours later. The cells were then infected with 30 MOI (**M**ultiplicity **O**f **I**nfection) in 1 ml EGM-2 culture medium containing 5µg/ml polybrene. After 48 hours, the cells were lysed with cell lysis buffer (Cytoskeleton Inc. 50 mM Tris pH 7.5, 10 mM $MgCl_2$, 0.5M NaCl, and 2% Igepal) containing protease inhibitor (Cytoskeleton Inc.) and phosphatase inhibitor "PhosStop" (Roche) and supernatant was collected for the G-LISA assay.

Nonspecific negative control siRNA and human ezrin-specific siRNA were transfected on ~70% confluent human glomerular EC in 35-mm plates using 1 ml penicillin/streptomycin antibiotic-free EBM-2 medium. 5 µl Lipofectamine 3000 and siRNA were mixed with 200 µl of Opti-MEM I medium and incubated for 10 minutes at room temperature and mixed with 1 ml EBM-2 medium to achieve a final siRNA concentration of 10 nM. 6 hours after siRNA transfection, 1.0 ml antibiotic-free EBM-2 containing 10% FBS was added. 24 hours after transfection, the

medium was changed to complete EGM-2 medium containing growth factors, antibiotics, and 5% FBS. 48 hours after transfection, cells were washed with ice-cold PBS and lysed with cell lysis buffer (Cytoskeleton Inc.) containing protease inhibitor cocktail (Cytoskeleton Inc.) and phosphatase inhibitor "PhosStop" (Roche) and the supernatants were used for the G-LISA assay.

2.3.3. Human podocytes

Podocytes naturally do not proliferate *in vivo* (449). To make them proliferative, podocytes transformed with a thermo-sensitive SV40 large T antigen mutant tsA58U19 were used (tsT podocytes) (450, 451). As the tsA58 mutant T antigen is temperature sensitive (452), a strict culture temperature of 33°C is required. Cell culture plates were coated with the "Quick Coating Solution" first. The conditionally immortalized human podocytes were cultured using RPMI 1640 medium containing 10% *v*/*v* FBS, 1% *v*/*v* penicillin/streptomycin and 0.025 μg/ml doxycycline at 33°C in humidified air containing 5% CO_2. When the cells became ~80% confluent, they were washed twice with ice-cold PBS and lysed with RIPA lysis buffer containing protease inhibitor (Roche) and phosphatase inhibitor "PhosStop" (Roche) to prepare cell lysates for western blot analysis.

2.4. Experimental animals

All protocols involving mice were approved and performed according to the guidelines developed by the University of Alberta Animal Care and Use Committee (protocol # AUP00000222).

2.4.1. Generation of CLIC5$^{-/-}$ mice

CLIC5$^{+/+}$ and CLIC5$^{-/-}$ jitterbug mice (CLIC5$^{-/-}$ or CLIC5$^{jbg/jbg}$) on the CH3/HeJ background were purchased from Jackson laboratories (Bar Harbor, ME 04609, USA). These mice were discovered because of their head bobbing and circling behavior typical for defects in the

vestibular apparatus, these mice are called as "jitterbug" (jgb). The jbg/jgb mice have a spontaneous mutation due to an intragenic deletion in exon 5 of the CLIC5 gene that results in the absence of the CLIC5A and CLIC5B proteins (425). They develop progressive inner ear hair cell degeneration causing gradual hearing impairment (429). The jgb mutation on the CH3/HeJ background was backcrossed for >10 generations into C57BL/6J background in our lab. Breeding heterozygous CLIC5$^{-/+}$ females with CLIC5$^{+/+}$ or CLIC5$^{-/-}$ males produced CLIC5$^{+/+}$ and CLIC5$^{-/-}$ mice. For genotyping, genomic DNA was isolated from tail clipping as described by Truett et al. (453) from ~2-3 week-old mice, or from ear-punch biopsies. The CLIC5 exon 5 genome sequence was then PCR amplified with forward primer 5'-CAATGACGAGAAGCGACTCA-3' and reverse primer 5'-GCTGTCCAGATTCCTCATAAACA-3'. These primer sequences are homologous to intron sequences surrounding exon 5. The PCR products for CLIC5$^{+/+}$ and CLIC5$^{-/-}$ were 326 bp and 229 bp, respectively. CLIC5$^{+/-}$ resulted in both 326 bp and 229 bp PCR products.

2.5. Cloning and generation of vector constructs

2.5.1. CLIC5A cloning

The full-length human CLIC5A coding region from the human kidney cDNA library (Gen Bank accession no. DQ679794) was cloned into the pCDNA3.1-vector (85) and used as the template for subcloning into other vectors. The GFP-CLIC5A vector construct was generated by PCR-amplification of human CLIC5A encoding the complete open reading frame from the pcDNA3.1-CLIC5A template DNA using the forward primer 5'-CGCACTCGAG**ACCATG**GGGCATCATCATCATCATCATACAGACTCGGCGACAGCTA AC-3' and reverse primer 5'-CCGGGATCCTCAGGATCGGCTGCGTTTGGC-3', and subcloned into the XhoI/BamHI restriction endonuclease site of the pEGFP-C1 vector. One

Kozak consensus sequence (bold) was added in the forward primer (bold and underlined) to enhance expression and 6xHis tag sequence (italic and underlined) was integrated for protein detection. CLIC5A full length (1-251 aa) was also cloned into the NdeI/BamHI restriction endonuclease site of the yeast-two-hybrid bait vector pGBKT7 using commercial human kidney cDNA as template. N-terminal CLIC5A 22-251 amino acids (aa) and C-terminal CLIC5A 1-232 aa deletion mutants were also cloned into the NdeI/BamHI restriction endonuclease site of the bait vector pGBKT7 using pGBKT7-CLIC5A 1-251 aa as template. N-terminal FLAG-, and GST-epitope tagged CLIC5A fusion constructs were prepared in pTARGET, and pGEX-3 vectors, respectively. For all vector constructs, restriction digestion and sequencing of inserts were conducted to confirm sequence fidelity and appropriate orientation.

Human CLIC5A $_{45}$KGVVF$_{49}$ to $_{45}$KGAVY$_{49}$ point mutant was prepared using Q5 Site-Directed Mutagenesis Kit (New England Biolabs, Cat# E0554S). To generate RFP-CLIC5A-KGAVY, the pmCherry-C1 plasmid vector (Clontech, PT3975-5, Cat# 632524) was used, and GFP-CLIC5A-KGAVY was generated using the pEGFPC1 vector. The PCR amplified products and plasmid vectors were digested with XhoI and BamHI, and then prepared as vector or inserts respectively, followed by ligations and transformations. All constructs generated by mutagenesis and cloning were sequenced to confirm the nucleotide sequence successes of mutations and sequence fidelities (Molecular Biology Services Unit, Dept. Biology, University of Alberta).

2.5.2. Preparation of recombinant, purified GST- and GST-CLIC5A proteins

Transformation of cloned pGEX-3-GST, or pGEX-3-GST-CLIC5A wild type and KGAVY constructs were conducted into *Escherichia coli* BL21 Gold (DE3), followed by induction with 0.2 mM IPTG and grown at 37°C for 4 h. Bacteria were harvested in PBS containing 1X proteinase inhibitor cocktail (Roche), followed by sonication and addition of 1% Triton X-100 to

collect crude protein extracts. The crude protein extracts were subjected to affinity chromatography purification of GST, and GST-CLIC5A recombinant, pure proteins on glutathione-Sepharose 4B according to the manufacturer's instructions.

2.5.3. Adenoviral vector constructs

To generate CLIC5A producing adenovirus "pAdTrack-GFP/CLIC5A" vector, the plasmid vector pcDNA3.1-CLIC5A was used as a template for PCR amplification of CLIC5A using the forward primer: 5'-CGCA**GTCGAC**GCCACCATGACAGACTCGGCGACAGCTAAC-3', and reverse primer: 5'-CCGAAGCTTTCAGGATCGGCTGAGGCGTTTGGC-3'. Sal I (bold) and Hind III restriction endonuclease sites (underlined) were added upstream of the start codon (ATG) in the forward primer, and downstream of stop codon in the reverse primer, respectively. The CLIC5A PCR product was sub-cloned into the Sal I/Hind III restriction endonuclease site of pAdTrack-CMV (Gift from Amy Barr, University of Alberta). pAdTrack-CMV control vector itself encodes GFP under a distinct promoter. In the "pAdTrack-GFP/CLIC5A" vector, CLIC5A expresses separately from GFP and is not a fusion protein with GFP. Sequence orientation and fidelity of these two adenoviral constructs were confirmed by full sequencing. The pAdTrack-CLIC5A construct was linearized by restriction endonuclease digestion of PmeI, followed by transformation into *E. Coli* (BJ5183) containing the adenoviral backbone plasmid pAdEasy-1 for the purpose of homologous recombination and PacI restriction endonuclease analysis was conducted to confirm the recombinant plasmid. PacI treated linearized recombinant plasmid was transfected into the adenovirus packaging cell line HEK293A. The prepared adenoviruses were propagated, harvested, purified and finally the viral titer was calculated (87).

Table 4: Templates and primers for CLIC5A mutagenesis

Constructs	Template for PCR	Primers	PCR annealing temperature °C
GFP-CLIC5A-C32A	GFP-CLIC5A-WT	Forward: 5'-AGCATCGGCAACGCTCCT TTCTCTCAG -3' Reverse: 5'-TTCTCCATCGATTCCAGCCTTCAC-3'	65
GFP-CLIC5A-KGAVY	GFP-CLIC5A-WT	Forward: 5'-TGGCTGAAAGGAGCAGTGTACAATGTC ACCACT-3' Reverse: 5'-GAGGATCATGAAGAGGCG CTGAGA-3'	65
GST-CLIC5A-KGAVY	GST-CLIC5A-WT	Forward: 5'-TGGCTGAAAGGAGCAGTGTACAATGTC ACCACT-3' Reverse: 5'-GAGGATCATGAAGAGGCG CTGAGA-3'	65

2.5.4. CLIC4 and CLIC1 cloning

The cDNAs encoding the human CLIC1 (hCLIC1) (GenBank AAH64527)) or human CLIC4 (hCLIC4) (GenBank ID: BC012444.1) open reading frame was PCR-amplified from human kidney cDNA (Ambion, 3331G, lot 065R053977A, TX). The PCR primers are listed in Table 6. In the forward primers, a Kozak consensus sequence (bold) was incorporated to enhance expression. The PCR product was then cloned into the mammalian expression vector pTARGET vector. One Kozak consensus sequence (bold) was added into the forward primer to enhance CLIC1 expression. pTARGET vector without cDNA insert was served as the control. pTARGET-CLIC4 cDNA was used as a template to clone CLIC4 into the bait yeast vector pGBKT7 (PGBKT7-CLIC4). pTARGET-CLIC1 cDNA was used as a template to clone CLIC1 into the bait yeast vector pGBKT7 (PGBKT7-CLIC1). For cloning of hCLIC1 and hCLIC4 cDNA into the yeast bait vector, the NcoI and Bam HI restriction endonuclease sites were integrated into the forward and reverse primers, respectively to enhance the downstream cloning

efficiency. The PCR primers are listed in Table 6. The PCR products were cloned into the bait vector pGBKT7 containing GAL4-DNA-BD. Restriction enzyme digestions and sequencing verified the hCLIC1 and CLIC4 cDNA orientation and the fidelities of the sequences. All the plasmid vector constructs were reproduced in *E. coli* DH5α using the QIAgen MiniPrep kit.

2.5.5. Cloning of ezrin and taperin

Full-length human ezrin 1-586 (GenBank accession no. AAH13903) coding region was used to design primers, PCR amplification and cloning into the XhoI/BamHI restriction endonuclease site into the pEGFP-C1 vector using commercial human kidney cDNA as template. The PCR primers are listed in Table 6. pEGFP-C1-ezrin 1-586 plasmid DNA was served as the template for PCR amplification and cloning of ezrin 1-296, ezrin 432-586, and ezrin 432-570 DNA inserts into the pEGFP-C1 plasmid vector.

Ezrin 1-586 was also PCR amplified and cloned into the NdeI/XhoI restriction endonuclease site of the pGADT7 prey vector using commercial human kidney cDNA as template. Ezrin fragments 1-296, ezrin 297-586, ezrin 432-586, ezrin 432-570, ezrin 432-550, ezrin 432-516, ezrin 480-540, ezrin 516-586, and ezrin 550-586 were PCR amplified and cloned into the NdeI/XhoI restriction endonuclease site of the pGADT7 prey vector using pGADT7-ezrin 1-586 plasmid DNA as template. The primer sequences used for PCR amplification are listed in Table 6.

Taperin isoform 1 (1-711 aa) could not be PCR amplified due to its high GC content. Therefore, codon optimized commercial synthesis of taperin 1-711 aa and the taperin fragment 272-385 aa cloned into the pGADT7 yeast-two-hybrid prey vector as well as the pEGFP-C1 vector were conducted by GeneScript (Piscataway, NJ, USA). The coding region for human taperin (GenBank accession no. BC098411) was used for successful PCR amplification of taperin 307-

711 aa (isoform 2) using a human kidney cDNA library as template. The PCR product was then cloned into the NdeI/XhoI restriction endonuclease site of the pGBKT7 yeast-two-hybrid bait vector. Taperin 307-711 was also cloned into the pEGFP-C1vector using pGADT7-taperin 307-711 aa as template. The primer sequences used for PCR amplification are listed in Table 6.

To obtain the constructs of GFP-tagged taperin 1-306, taperin 272-385, and taperin 272-306 in the pEGFPC1 plasmid vector, the common template GFP-taperin-1-WT (GenScript, Piscataway, NJ USA, codon optimized form unless specified) was used for PCR amplification (Primers in Table 6). The PCR reactions were carried out using PrimeSTAR GXL DNA Polymerase (TaKaRa Bio USA, Inc.) according to the manufacturer's instructions. Because special DNA polymerase and specific annealing temperature were used, the primer sequence and the annealing temperatures are listed in a separate table for taperin 1-306, 272-385, and 272-306 (Table 5).

Table 5: Primers used to perform the PCR reaction of taperin

Name	Primers	PCR Annealing temperature °C
GFP-TPN-1-306	Forward primer: 5'-TTC**GAATTC**TATGGCCGCT CTGGGCAGGCCTGGC-3' Reverse primer: 5'-GAT**GGATCC**CTCACACGGG CTTAGGAGCGGGCCGGAT-3'	60
GFP-TPN-272-385	Forward primer: 5'-TTC**GAATTC**TCCTGCC AGCCCTCCTGCGAGCGCC-3' Reverse primer: 5'-GAT**GGATCC**CTCATGGGCT TTTGCCCAGGGCGGGTGC -3'	60
GFP-TPN-272-306	Forward primer: 5'-TTC**GAATTC**TCCTGCC AGCCCTCCTGCGAGCGCC-3' Reverse primer: 5'-GAT**GGATCC**CTCACACGGG CTTAGGAGCGGGCCGGAT-3'	60

Table 6: Primer sequences for PCR amplification

Plasmid constructs	**PCR Primer sequences**	
hCLIC5A 1-251	Forward primer	5'CGCACTCGAGACCATGGGGCATCATCATCATCATACAG ACTCGGCGACAGCTAAC-3'
	Reverse primer	5'-CCGGGATCCTCAGGATCGGCTGAGGCGTTTGGC-3'.
pEGFP-hCLIC5A 1-251	Forward primer	5'-CGCACTCGAGCCATGACAGACTCGGCGACAGCTAAC-3'
	Reverse primer	5'-CCGGGATCCTCAGGATCGGCTGAGGCGTTTGGC-3'
pGBKT7-hCLIC5A 1-251	Forward Primer	5'-GCCCATATGATGACAGACTCGGCGACAGC -3
	Reverse Primer	5'-GCGGGATCCTCAGGATCGGCTGAGGCGTTTG-3
pGBKT7-hCLIC5A 22-251	Forward Primer	5'-GCCCATATGGCTGGAATCGATGGAGAAAGCATCG -3'
	Reverse Primer	5'-GCGGGATCCTCAGGATCGGCTGAGGCGTTTG-3'
pGBKT7-hCLIC5A 1-232	Forward Primer	5'-GCCCATATGATGACAGACTCGGCGACAGC -3'
	Reverse Primer	5'-GCGGGATCCTGCACAGGTGTTGGTGAACTC-3'
pGBKT7-hCLIC5A 1-251	Forward Primer	5'-GCCCATATGATGACAGACTCGGCGACAGC -3
	Reverse Primer	5'-GCGGGATCCTCAGGATCGGCTGAGGCGTTTG-3'
pTARGET-hCLIC4 1-253	Forward Primer	5'-CCACCATGGCGTTGTCGATGCCGCTGAAT-3'
	Reverse Primer	5'-CCGGGATCCTTACTTGGTGAGTCTTTTGGCTAC-3'
pEGFP-hCLIC4 1-253	Forward Primer	5'CGCACTCGAGCCATGGCGTTGTCGATGCCGCTGAAT-3'
	Reverse Primer	5'-CCGGGATCCTTACTTGGTGAGTCTTTTGGCTAC-3'
pGBKT7-hCLIC4 1-253	Forward Primer	5'-CATATGGCCATGGAGATGGCGTTGTCGATGCCGCTGAAT-3'
	Reverse Primer	5'-AGGTCGACGGATCCCTTACTTGGT GAGTCTTTTGGCTAC-3'
pTARGET-CLIC1 1-241	Forward Primer	5'-CCACCATGGCTGAAGAACAACCGCAGGTC-3'
	Reverse Primer	5'-CCGGGATCCTTATTTGAGGGCCTTTGCCACTTG-3'
pGBKT7-CLIC1 1-241	Forward Primer	5'CATATGGCCATGGAGATGGCTGAAGAACAACCGCAGGTC-3'
	Reverse Primer	5'AGGTCGACGGATCCCTTATTTGAGGGCCTTTGCCACTTG-3'
pEGFP-Ezrin 1-586	Forward Primer	5'-GCCCTCGAGATGCCGAAACCAATCAATGTCCG -3'
	Reverse Primer	5'-GCGGGATCCTTACAGGGCCTCGAACTCGTCG-3'
pEGFP-Ezrin 1-296	Forward Primer	5'-GCCCTCGAGATGCCGAAACCAATCAATGTCCG-3'
	Reverse Primer	5'-GCGGGATCCCTTCCTGCGGCGCATATACAAC-3'
pEGFP-Ezrin 432-586	Forward Primer	5'-GCCCTCGAGGAAGAGGCGCGGAGGCGCAAG -3'
	Reverse Primer	5'-GCGGGATCCTTACAGGGCCTCGAACTCGTCG-3'
pEGFP-Ezrin 432-570	Forward Primer	5'-GCCCTCGAGGAAGAGGCGCGGAGGCGCAAG -3'
	Reverse Primer	5'-GCGGGATCCTTACTGCCGCAGCGTCTTGTACTTGTC-3'
pGADT7-Ezrin 1-586	Forward Primer	5'-GCCCATATGATGCCGAAACCAATCAATGTCCG -3'
	Reverse Primer	5'-GCGCTCGAGTTACAGGGCCTCGAACTCGAT-3'
pGADT7-Ezrin 1-296	Forward Primer	5'-GCCCATATGATGCCGAAACCAATCAATGTCCG-3'
	Reverse Primer	5'-GCGCTCGAGCTTCCTGCGGCGCATATACAAC-3'
pGADT7-Ezrin 297-586	Forward Primer	5'-GCCCATATGCCTGACACCATCGAGGTGCAGCAG -3
	Reverse Primer	5'-GCGCTCGAGTTACAGGGCCTCGAACTCGTC-3'
pGADT7-Ezrin 432-586	Forward Primer	5'-GCCCATATGGAAGAGGCGCGGAGGCGCAAG -3
	Reverse Primer	5'-GCGCTCGAGTTACAGGGCCTCGAACTCGTC-3'
pGADT7-Ezrin 432-570	Forward Primer	5'-GCCCATATGGAAGAGGCGCGGAGGCGCAAG -3
	Reverse Primer	5'-GCGCTCGAGCTGCCGCAGCGTCTTGTACTTG-3'
pGADT7-Ezrin 432-550	Forward Primer	5'-GCCCATATGGAAGAGGCGCGGAGGCGCAAG -3
	Reverse Primer	5'-GCGCTCGAGGTGGGTCCTCTTATTCTCATCTC-3'
pGADT7-Ezrin 432-516	Forward Primer	5'-GCCCATATGGAAGAGGCGCGGAGGCGCAAG -3'
	Reverse Primer	5'-GCGCTCGAGCTTCTCCTCATTGCGGTCATCCC-3'
pGADT7-Ezrin 480-540	Forward Primer	5'-GCCCATATGCCGGTGAGCTACCATGTCCAGGAG -3'
	Reverse Primer	5'-GCGCTCGAGCTGGGACAGCTCGCTGCTC-3'
pGADT7-Ezrin 516-586	Forward Primer	5'-GCCCATATGAAGCGCATCACTGAGGCAGAG -3'
	Reverse Primer	5'-GCGCTCGAGTTACAGGGCCTCGAACTCGTC-3'
pGADT7-Ezrin 550-586	Forward Primer	5'-GCCCATATGAATGACATCATCCACAACGAGAAC-3'
	Reverse Primer	5'-GCGCTCGAGTTACAGGGCCTCGAACTCGTC-3'
pEGFP-Taperin 307-711 WT	Forward Primer	5'- CGCACTCGAGCCATGGAGACCATCCCCTTGGGGGAC-3'
	Reverse Primer	5'-CGCGGTACCTCAGAAATACAGGGCTGGCTCGCT-3'
pEGFP-Taperin 307-711 optimized (OP) WT	Forward Primer	5'- CGCACTCGAGCCATGGAAACCATCCCTCTGGGCGAC -3'
	Reverse Primer	5'- CGCGGTACCTCAGAAGTACAGGGCGGGTTCGCT -3'

pEGFP-Taperin 307-711 OP KASA mutant	Forward Primer	5'- CGCACTCGAGCCATGGAAACCATCCCTCTGGGCGAC -3'
	Reverse Primer	5'- CGCGGTACCTCAGAAGTACAGGGCGGGTTCGCT -3'
pGADT7-Taperin 307-711	Forward Primer	5'-GCCCATATG ATGGAGACCATCCCCTTGGGGGAC-3'
	Reverse Primer	5'-GCGCTCGAGTCAGAAATACAGGGCTGGCTC -3'

2.6. Western blot (WB) analysis and quantification

2.6.1. Sample preparation

The cell culture plates were placed on ice. Cells in the culture plates were washed twice with ice-cold PBS and harvested with RIPA lysis buffer (50 mM Tris-Cl pH 7.5, 150 mM NaCl, 1% Nonevent P-40, 0.5% sodium deoxycholate) containing complete protease inhibitor cocktail (Roche) and phosphatase inhibitor "PhosStop" (Roche), or cell lysis buffer (cytoskeleton Inc.) or other cell lysis buffer where appropriate. After 15 in the lysis buffers, the cells were dislodged with a cell scraper and collected into prechilled centrifuge tubes, followed by rotation incubation at 4°C for 15 minutes, and centrifugation at 14,000 rpm for 15 minutes at 4°C. The supernatants were collected and placed in new prechilled centrifuge tubes. Protein concentrations were measured by Bradford assay. The input lysates were mixed with the same volume of 2 X Laemmli buffer containing 5% β-mercaptoethanol, boiled for 3 minutes, and stored at -80°C.

2.6.2. SDS-PAGE

The prepared samples were loaded onto the 8-16% gradient polyacrylamide gel lanes for SDS-PAGE at room temperature initially running at 50 volts for ~20 minutes to move the samples through the stacking gel and enter into the separating gel, followed by 130 volts running until the dye front reached the bottom of the gel.

2.6.3. Protein transfer and total protein imaging

Proteins were transferred onto the polyvinylidene fluoride (PVDF) membranes overnight at 40 volts at 4°C. The membranes were washed twice with distilled water for 2 minutes. Membranes were then incubated with No-Stain® Protein Labeling Reagent prepared according to the

manufacturer's protocol, imaged using the iBright 750 imager (ThermoFisher Scientific), and analyzed by the ImageJ software (NIH, USA). The membranes were again washed with distilled water (3 X 2 min) for subsequent immunoblotting.

2.6.4. Blocking and antibody incubation

PVDF membranes have a high affinity for proteins. To block the non-specific binding, unoccupied sites on the membranes were blocked overnight by gentle shaking incubation with Western Blocker® solution (Sigma) at 4°C (454). The western blocker solution consists of proprietary blocking proteins and other components in Tris-buffered saline (TBS), pH 7.75, and containing 0.1% Triton X-100, and 600 ppm Kathon CG/ICP (an antimicrobial agent). The membranes were incubated with primary antibody, diluted to the appropriate concentration Western Blocker®, with gentle shaking overnight at 4°C. The primary antibodies were then removed, the membranes washed three times with TBST buffer for 30 min at room temperature to remove unbound primary antibodies and incubated with HRP-conjugated secondary antibodies (diluted 1:10000 in Western Blocker®) specific to the species of the primary antibody with gentle shaking at room temperature for 1 hour. The membranes were washed again three times with TBST buffer for 30 minutes at room temperature.

2.6.5. Protein detection

The membranes were incubated with the enhanced chemiluminescence (ECL) solution (according to the manufacturer's instructions for 2-3 minutes. Membranes were exposed to X-ray film (FujiMedical X-Ray Film Super Rx, Fujifilm) or imaged by iBright 750. Band densities were determined by ImageJ and normalized to total protein or GAPDH on the same membrane.

2.7. Live cell confocal microscopy

HeLa cells were plated into 35-mm culture dishes containing a cover slips (25 mm diameter, Cat# 72223-01, Electron Microscopy Sciences, Hatfield, PA USA) at ~20 10^4 cells one day prior to transfection. They were then transfected with different cDNA constructs using Lipofectamine 2000 (Invitrogen) according to the manufacturer's instructions. The cell membranes or nuclei of living cells were labeled by CellBrite™ Steady membrane labeling kit (Cat# 30107) or NucSpot Live 650 Nuclear stain (Cat #40082) (Biotium, Fremont, CA, USA), respectively, according to the manufacturer's instructions. Briefly, the CellBrite™ Steady membrane labeling or NucSpot Live 650 dyes were added to the culture medium followed by incubation at 37°C for 30 or 10 min, respectively. Living cells were examined with an Olympus Spinning Disk Confocal microscope. Image acquisition and processing were conducted using Volocity software (Version 6.4, Perkin Elmer, Waltham, MA USA) (Cell Image Core, Faculty of Medicine and Dentistry, University of Alberta). The images were captured randomly and all cells in each image were measured and analyzed. Representative images are shown in the figures.

2.8. GST-/GST-CLIC5A pull-down assay

The GST-/GST-CLIC5A pull-down assay was performed according to the method described by Berryman and Bretscher (422) and Al-Momany et al. (89). Briefly, cells were washed twice with cold PBS and scraped from the plates into the chilled centrifuge tubes. The cells were then evenly suspended in lysis buffer (1% Triton-X 100, 20 mM HEPES pH 7.4, 0.6 M KCl, and 1 mM EDTA) containing proteinase inhibitor cocktail (Roche) and phosphatase inhibitor PhosStop™ (Roche), incubated for 15 minutes at 4°C with end over end rotation, followed by centrifugation for 15 minutes at 14,000 X g. The supernatants were collected and 50-µl cell reserved for total cell lysate "input". The remaining supernatants were first pre-cleared for 30

min by end-over-end rotation with glutathione beads, followed by centrifugation for 5 min at 12,000 X g. The resulting supernatants were incubated with 12.5 µg GST or 25 µg GST–CLIC5A (approximately equimolar concentrations) and captured by glutathione beads by end over end rotation incubation for 3 hours at 4°C. The beads were then washed twice with cold PBS/0.1% Tween-20 and twice with cold PBS. Bound proteins were eluted with 2 X Laemmli buffer and boiled for 3 min. Eluted proteins were separated by SDS-PAGE and subjected to WB analysis.

2.9. Immunoprecipitation

Immunoprecipitation (IP) was performed as described by Takeda et al. (88) with some modifications. Briefly, cultured cells were washed twice with ice-cold PBS, and harvested with cold IP-lysis buffer (50 mM Tris-HCl, pH 7.4, 150 mM NaCl, 1.0% NP-40, 0.5% sodium deoxycholate, 30 mM sodium fluoride, 40 mM β-glycerophosphate, 20 mM sodium pyrophosphate, 1 mM sodium orthovanadate, 100 nM Calyculin-A, complete protease inhibitors (Roche), and phosphatase inhibitor PhosStop™ (Roche). Cells were homogenized on ice and centrifuged at 14,000 X g for 15 min at 4°C. The supernatants were removed, and 50 µl were kept as total cell lysate input controls. The remaining supernatants were pre-cleared for 30 min with 30 µl protein G^+/protein A-agarose beads at 4°C, and centrifuged 12,000 rpm, for 5 minutes. The collected supernatants were mixed with control IgG or goat anti-GFP IgG antibody (1 µg), followed by end over end rotating incubation for ~2 hours. Then, 60 µl protein G plus/protein A-agarose beads from a 1:1 slurry were added followed by overnight end over end rotating incubation at 4°C. The beads were sedimented at 3,500 rpm for 5 minutes; washed twice with IP wash buffer I, twice with IP wash buffer II, and once with IP wash buffer III(455). Finally, the beads were sedimented at 3,500 rpm for 5 min and resuspended in 60 µl of 2 X

Laemmli buffer and boiled for 10 min. Eluted proteins were separated by SDS-PAGE, and subjected to WB analysis.

2.10. Rac1-GTP pull down and Rac1-GTP quantification assay

The Rac1 activation assay uses the Cdc42/Rac Interactive Binding (CRIB) region (also called the p21 Binding Domain, PBD) of the Cdc42/Rac effector protein, p21 activated kinase I (PAK). The PBD protein motif binds the GTP-bound form of Rac and Cdc42 protein in a highly specific fashion (456). To determine Rac1-GTP abundance, the PAK-PBD pull down assay was used according to the manufacturer's instructions (Cytoskeleton, Inc.). Cultured cells were harvested very rapidly with 1 ml lysis buffer (Cytoskeleton, Inc.) from 100 mm culture plates and sedimented at 10,000 X g, for 1 minute. 50 µl of the resulting supernatants were reserved for total cell lysate input controls. The remainder of the supernatants were subjected to end over end rotating incubation with 40 µg of GST-PAK-PBD immobilized on glutathione beads for 2 hours at 4°C and precipitated using 3,500 X g for 3 min at 4°C. The beads were washed once with wash buffer (Cytoskeleton, Inc.) and again precipitated at 3500 X g for 3 min at 4°C. The beads were then resuspended in 40 µl of 2 X Laemmli buffer and boiled for 3 min followed by western blot analysis.

For precise quantification of the Rac1-GTP concentration (ng), the G-LISA® assay (Cytoskeleton, Inc.) was used according to the manufacturer's instructions. Cells were lysed as described above, and the protein concentration in the supernatants was determined by the Bradford assay. 20 µg of total lysate protein was used for each per data point. To deplete supernatants of Rac-GTP, they were incubated at room temperature overnight. The Rac-GTP depleted lysates were used to define the background and to establish the standard curve (0, 1, 3 and 6 ng constitutively active Rac1).

2.11. Isolation of mouse glomeruli

Mouse glomeruli were isolated by differential sieving method according to the method of Rops et al. (457), with slight modifications. Kidneys from C57BL/6J-CLIC5$^{+/+}$ and C57BL/6J-CLIC5$^{-/-}$ mouse kidneys were rapidly removed; stripped of their capsules, followed by collection of kidney cortex. The kidney medulla was discarded. The kidney cortex was finely minced, suspended in RPMI 1640 medium containing 1.0 mg/ml collagenase IV (with or without 10 nM Calyculin-A) and digested at 37°C for 1.0 hr. The digested tissue was passed through stacked 100 μm, 70 μm and 40 μm cell strainers (BD Falcon, Durham, NC, USA) using gentle pressure with cell lifter. Accumulated glomeruli on the surface of the 40 μm cell strainer were collected and placed into 100 mm cell culture plates in 15 ml RPMI 1640 medium containing 0.5% FBS and 10 nM Calyculin-A and incubated in a cell culture incubator containing 5% CO_2/air for 10 minutes. Contaminating tubules adhere preferentially to cell culture plastic and were removed by incubating the glomerular suspension three times on 100 mm cell culture plates. Each time, the medium containing the the non-adherent glomeruli was transferred to a new cell culture plate. Glomerular preparations were examined for purity by light microscopy and were used for experiments only if they were free of tubules (>99% pure). The glomerular numbers were quantified. The glomeruli were sedimented by centrifugation at 4,500 rpm for 5 minutes at 4°C and washed twice with cold PBS to use for differential detergent fractionation.

To prepare glomerular cell lysates, they were resuspended in 250 μl of lysis buffer (50 nM Tris-HCl pH 7.5, 150 mM NaCl, 1% Nonidet P40, 0.5% sodium deoxycholate, 1 X protease inhibitor (Roche), 1 X phosphatase inhibitor PhosStop™ (Roche), and 100 nM calyculin-A), incubated for 20 minutes, then passed through a 28 1/2-gauge needle three times and centrifuged at 14,000 X g for 15 min. The supernatants were used to detect endogenous soluble proteins.

2.12. Differential detergent fractionation

The subcellular localization (cytosol, membrane, pellet) of exogenously expressed CLIC5A, endogenous ezrin, mutant ezrin, GAPDH and N-Cadherin in COS-7 and HeLa cells, and of endogenous CLIC5A, ezrin, NHERF2, nephrin, and podocalyxin in isolated mouse glomeruli were determined by differential detergent fractionation. In this assay cells are first treated with cytoplasmic protein extraction buffer containing digitonin then a detergent (Triton X-100)-containing membrane protein extraction buffer followed by collection of the insoluble pellet fraction that contains cytoskeleton and nuclei. A sample of total cell lysate was reserved from washed COS-7 and HeLa cells, and washed glomeruli (~5000 per assay) and lysed with 2X Laemmli buffer. The remaining washed and pelleted COS-7 and HeLa cells or isolated glomeruli were resuspended in cytoplasmic protein extraction buffer [200 μg/ml digitonin (COS-7 and HeLa cells), or 100 μg/ml digitonin (glomeruli) in 40 mM PIPES, 1.2 M sucrose, 400 mM NaCl, 12.5 mM MgSO4**.**H2O, 5 mM EDTA, 1 X protease inhibitor cocktail, 50 nM Calyculin A, pH 6.8] and incubated by rotary shaking for 10 minutes (COS-7 and HeLa cells) or 15 minutes (glomeruli) at 4°C. Subsequently, they were centrifuged at 2,000 X g for 10 min at 4°C. The supernatants were collected and designated as the digitonin soluble cytoplasmic fraction. The pellets were washed once with ice-cold PBS by centrifugation at 6,000 X g for 10 min at 4°C, resuspended in membrane protein extraction buffer (0.5% *v*/*v* Triton X-100, 50 mM HEPES, 150 mM NaCl, 5 mM EDTA, 1 X protease inhibitor cocktail, 50 nM calyculin A, pH 7.4), incubated for 30 min on ice with intermittent vortexing, followed by centrifugation at 6,000 X g for 10 min at 4°C. The resulting supernatants were designated as the Triton X-100 soluble membrane protein fraction, and the pellets were designated as insoluble cytoskeletal fraction (P). The volume of incubation of extraction buffers was 400 μl for COS-7 and HeLa cells and 100 μl for

isolated glomeruli. For WB analysis, each fraction was adjusted to represent equivalent starting material.

2.13. **siRNA knockdown**

Transfection with siRNA was performed using Lipofectamine 2000™ (Life technologies) in the human glomerular EC cells. Control siRNA (Scramble, cat. # sc-35349) and human ezrin siRNA (cat # sc-37007) were purchased from Santa Cruz Biotechnology. Briefly, human glomerular EC cells were cultured in p-35 mm plates and split to achieve ~70% confluence for transfection. The EGM2 medium was replaced with same medium without antibiotic just before siRNA transfection. 10 nM control or ezrin siRNA and 100 µl Opti-MEM I medium was mixed (Mix A). 1 µl Lipofectamine 2000™ and 100 µl Opti-MEM medium I was mixed (Mix B). Mix A and B were combined and incubated for 20 minutes at room temperature, and then added to the cells. After 7 hours, 1 ml complete EGM2 medium was added on the cells.

Triple ERM silencing and taperin silencing were performed using siRNA according to the manufacturers instructions (OriGene technologies, USA). Briefly, HeLa cells in the log phase of growth were plated into 24-well plates at 10 10^4 cells/well in 500 µl complete DMEM medium. 16 – 24 hours later, 50 µl transfection buffer, 5 – 50 nM siRNA, 1.2 µl siTran™ 2.0 transfection reagent were mixed and incubated for 15 minutes at room temperature and then applied to the cells. Cells were studied 48 hours later.

2.14. Yeast-two hybrid assay

Screening was conducted by Hybrigenics™ (Evry, France) service to identify potential direct interacting proteins using full-length human CLIC5A (1-251 aa) as bait and an adult mouse kidney protein domain library (~80,000 protein domains) as prey. To confirm and map the regions of ezrin and taperin that interact directly with CLIC5A, the Clontech Matchmaker

GAL4-based yeast two-hybrid (Y2H) assay was used according to the manufacturer's instructions. In the Matchmaker GAL4-based Y2H system, the DNA-binding domain (DNA-BD) and activation domain (AD) must come into close proximity to trigger transcription of the reporter genes MEL1 and AUR1-C. MEL1 encodes the α-galactosidase enzyme. The α-galactosidase expressed and secreted by the yeast cells, hydrolyzes the chromogenic substrate X-α-Gal, turning the yeast colonies blue. The AUR1-C gene encodes the enzyme inositol phosphoryl ceramide synthase. AUR1-C expression in the Y2HGold yeast strain induces resistance to the highly toxic antibiotic Aureobasidin A (AbA^r).

For yeast mating, an aliquot of the yeast Y187 strain (MATα) containing prey vector is mixed with an aliquot of the Y2H Gold strain containing bait vector. The mated strains are then cultured overnight and plated on selective agar plates deficient in leucine and tryptophan [-Leu/-Trp (DDO)]. Only successfully mated colonies containing both bait and prey vectors grow on DDO medium. The DDO medium containing X-α-Gal with or without Aureobasidin A is used to define whether direct interactions between bait and prey proteins have turned on the expression of the reporter genes. To rule out false-positive direct interactions and to map the minimum regions of ezrin and taperin that directly bind CLIC5A, I first cloned different CLIC5A constructs into the bait vector pGBKT7, and different ezrin and taperin constructs into the prey vector pGADT7. I also cloned CLIC4 and CLIC1 into the bait vector pGBKT7. I prepared the Y2HGold and Y187 yeast competent cells according to the manual. Cloned bait vectors were transformed into the Y2HGold yeast competent cells and allowed to grow for 3 days at 30°C on synthetically defined agar medium (SD) without tryptophan (Trp^-). Cloned prey vectors were transformed into the Y187 yeast competent cells and allowed to grow for 3 days at 30°C on SD agar medium without leucine (Leu^-). For mating, a colony of bait and a colony of

prey yeast were placed into a single 1.5 ml centrifuge tube containing 500 µl of 2 X YPD medium (yeast extract, peptone, glucose), mixed gently by vortexing, and incubated with shaking at 200 rpm, 30°C for 20-24 hours. From the mated culture, 100 µl of 1/10 or 1/20 or 1/500 dilutions were spread on the Leu^-/Trp^- agar medium (DDO), Leu^-/Trp^- agar medium containing X-α-Gal (DDO/X), or Leu^-/Trp^- agar medium containing X-α-Gal and Aureobasidin A (AbA) antibiotic (DDO/X/A) and incubated for ~3-5 days at 30°C. Yeast transformed with pGBKT-7/p53 (bait) and pGAD-T7 /SV40 large T antigen (prey) served as positive control, and yeast transformed with pGBKT-7/Lamin (bait) and pGADK-T7/SV40 large T antigen (prey) served as negative control. A direct interaction between bait and prey results in blue colonies on DDO)/X-α-Gal and DDO/X-α- Gal/Aureobasidin A agar plates. No interaction prevents growth on plates containing Aureobasidin A.

2.15. *In vitro* transcription/translation-based protein synthesis assay

The TnT® quick coupled transcription/translation system was used for eukaryotic cell-free protein synthesis. The system is suitable for the expression of genes cloned downstream from either the T7 or SP6 RNA polymerase promoters (458). The proteins produced are soluble, post translationally modified, and are not purified but used directly for GST pull-down to study protein-protein interaction *in vitro*. I synthesized hemagglutinin (HA)-tagged ezrin and taperin proteins using different ezrin and taperin vector constructs in the pGADT7 plasmid as templates. Upon removal from storage at -70°C, the TnT® quick master mix was rapidly thawed and placed on ice. 40 µl TnT® T7 quick master mix, 2 µl Methionine 1 mM, pGADT7-ezrin or pGADT7-taperin plasmid cDNA templates (600 ng) and nuclease free water were added to make a 50 µl reaction volume. The reaction components were mixed gently by pipetting and incubated at 30°C for 90 minutes. Western blot analysis using 1 µl of the reaction mixture and anti-ezrin, anti-HA

and anti-taperin antibodies was used to confirm successful synthesis of the desired proteins. The reaction products were then used for GST-/GST-CLIC5A pull down assay. To examine ezrin-CLIC5A interactions, 5 µl of the reaction mixture containing synthesized HA-tagged ezrin 1-586 aa and the N-terminal ezrin fragment 1-296 aa, or 40 µl of the reaction mixture containing synthesized HA-ezrin fragments 297-586 aa, ezrin 432-586 aa, or ezrin 432-570 aa, were incubated with purified 20 µg GST or 40 µg GST-CLIC5A (approximately equimolar concentrations) in ice-cold Tris-HCl (20 mM, pH 7.5) buffer to make a volume of 500 µl. Similarly, 40 µl of synthesized taperin isoform 2 (307-711) aa, the taperin fragment 272-385 aa, or 160 µl of synthesized full-length taperin isoform 1 (1-711 aa; Gene script synthesized cDNA construct) were added to 20 µg purified GST or 40 µg purified GST-CLIC5A (approximately equimolar concentrations) in ice-cold Tris-HCl (20 mM, pH 7.5) buffer to make a volume of 500 µl. The pull-down mixtures were allowed to undergo rotation incubation for 1 hour, followed by addition of 60 µl glutathione beads (bead: PBS 1:1) and rotation incubation overnight at 4°C. The pull-down mixtures were then centrifuged at 3,500 rpm for 5 minutes, the supernatant was discarded, and the beads were washed twice with ice-cold PBS. 40 µl 2 X Laemmli buffer was added to the washed beads and heated to 95^{o}C for 5 minutes prior to SDS-PAGE and western blot analysis.

2.16. Statistical analysis

Biological replicate samples were examined at least three times or more. GraphPad Prism software was used for all statistical analysis. Data are presented as mean ± SD. For the comparison of the two groups, the Student t-test was used. For comparison of more than two groups, analysis of variance (ANOVA) was used, followed by the Bonferroni post-hoc test for individual differences. The limit of statistical significance was defined as $p < 0.05$.

Chapter 3

CLIC5A interacts directly with the ezrin, radixin, and moesin

Chapter 3

CLIC5A interacts directly with the ezrin, radixin and moesin

3.1. Introduction

The cell cortex, also known as the actomyosin cortex, is a layer of cytoskeletal proteins just beneath the cell membrane. It plays a crucial role in defining the cell structure and for the transmission of signals from the plasma membrane into the cell. ERM proteins help organize the cortical actin cytoskeleton by linking plasma membrane components to filamentous actin. They are necessary for the development of cytoskeletal structures like filopodia, lamellipodia, stereocilia, microvilli and podocyte foot processes (222, 459-461) and take part in intracellular signal pathways (193). In podocytes, ezrin interacts with podocalyxin directly, and also indirectly through NHERF2, linking podocalyxin to actin. As a major podocyte protein, CLIC5A is part of the ezrin/NHERF2/podocalyxin complex (85).

CLIC5A is one of the most highly expressed proteins in glomeruli with transcript levels nearly 800 fold higher in glomeruli compared to other tissues (182) and 50-fold higher in glomerular EC compared to other EC (183). CLIC5A was first discovered in a protein complex with ezrin, actin, and other actin-associated proteins in placental microvilli (422), suggesting that the association of CLIC5A with actin-based cytoskeletal structures is important for their assembly or maintenance. In podocytes, CLIC5A localizes to the apical plasma membrane of foot processes, identical to the distribution of podocalyxin, and ezrin (85, 184). In glomeruli, CLIC5A is also found in the porous fenestrated region of glomerular EC, and it co-localizes strongly with ezrin and podocalyxin in human renal glomeruli (85).

This lab has shown that CLIC5A expression causes ERM protein phosphorylation (activation) in glomerular podocytes *in vitro* and *in vivo* (86, 87, 89). CLIC5A also stimulates Rac1, but not

Cdc42 or RhoA activity (86). CLIC5 deletion in mice decreases ezrin phosphorylation and results in dissociation of the ezrin/NHERF2/podocalyxin complex in renal glomeruli (89). CLIC5 deletion in mice also results in podocyte foot process disorganization, glomerular EC vacuolization and makes glomerular capillaries more vulnerable to Adriamycin and hypertension-induced injury (85, 86, 297). CLIC5A is also expressed in the basal region of inner ear hair sensory hair cell stereocilia, and CLIC5 deletion results in degeneration of these actin-based cellular projections, resulting in vestibular disturbances and progressive deafness (425). A Turkish family with renal disease and deafness due to an inactivating CLIC5 mutation has been reported (429).

While it seems quite clear that CLIC5A is functionally important for the activation of Rac1 and ERM proteins, I aimed to identify the immediate protein partners of CLIC5A together with which CLIC5A functions in cells. Therefore, the objective of this chapter is as follows:

To determine whether CLIC5A interacts directly with Rac1, and ezrin, radixin, moesin proteins.

3.2. Results

3.2.1. CLIC5A, ezrin and Rac1 are part of the same protein complex

Since CLIC5A expression stimulates ERM phosphorylation (activation) (89) and Rac1 activation (86), I first sought to determine whether CLIC5A, ezrin and Rac1 are in the same protein complex. A single pilot experiment reported in the PhD thesis of M. Tavasoli (506) had previously suggested that CLIC5A co-precipitates with non-hydrolysable GTPγS-loaded Rac1 in the PAK-protein binding domain (PAK-PBD) pull-down assay. COS-7 cells, which do not express CLIC5A at baseline, were therefore transfected with Flag- or Flag-CLIC5A cDNA constructs. 48 hours later lysates were prepared from the cells and subjected to pull-down with immobilized PAK-PBD beads. In COS-7 cells expressing Flag-CLIC5A, I observed that Rac1-GTP levels were higher than those in cells transfected with the Flag-control vector, consistent with previously published work by Tavasoli et al. (89). Furthermore, Flag-CLIC5A and endogenous ezrin co-precipitated with Rac1-GTP in CLIC5A expressing cells (Figure 3.1. A), consistent with the pilot experiment in the Tavasoli thesis (506). Similarly, when COS-7 or HeLa cells were transfected with GFP- or GFP-CLIC5A cDNAs, and treated with or without the specific Rac1 inhibitor NSC 23766 (100 μM) for 10 minutes, Rac1-GTP levels increased in the absence, but not in the presence of NSC 23766, and GFP-CLIC5A and endogenous ezrin co-precipitated with Rac1-GTP from both cell types in the absence, but not in the presence of the Rac1 inhibitor (Figure 3.1.B). I was therefore able to conclude that CLIC5A, ezrin and Rac1-GTP are part of the same protein complex, and that the co-precipitation of CLIC5A and ezrin in this assay was not due to nonspecific binding of ezrin or CLIC5A to the PAK-PBD beads. Other proteins that bind Rac1-GTP would also be expected in these PAK-PBD pull-downs (see Chapter 5) but were not identified here.

3.2.2. CLIC5A interacts with Rac1, but they do not interact directly

As CLIC5A precipitates with Rac1-GTP, it became important to determine whether CLIC5A binds Rac1-GTP directly. Wild-type GFP-Rac1, constitutively active GFP-Rac1 Q61L, and dominant negative GFP-Rac1 D17N overexpressed in COS-7 cells were all pulled from COS-7 cell lysates by GST-CLIC5A without apparent preference for constitutively active GFP-Rac1 (Fig. 3.2.A). Moreover, live cell imaging of HeLa cells co-transfected with RFP-CLIC5A and wild-type GFP-Rac1 cDNAs showed that RFP-CLIC5A partially co-localized with GFP-Rac1 (Fig. 3.2.B). However, purified, recombinant His-Rac1 loaded with GTPγS or GDP (Fig. 3.3.A) did not bind recombinant, purified GST-CLIC5A immobilized on glutathione beads (Fig. 3.3.B). These results indicate that CLIC5A and Rac1-GTP interact at or near the cell membrane, but this interaction appears to be indirect.

3.2.3. Identification of CLIC5A binding partners in mouse kidney library

We next used unbiased screening of a mouse kidney protein domain library to search for direct CLIC5A binding partners. This library was chosen because CLIC5A is expressed at very high levels in mouse kidney podocytes. The screening was done for us by Hybrigenics® (Evry-Courcouronnes, France) using Yeast-Two-Hybrid (Y2H) library screening technique. The library consisting of >80,000 independent protein domain fragments ("prey") was screened against full-length CLIC5A as the "bait". The Y2H library screening results are as follows:

Table 7: The Y2H library screening results using CLIC5A as bait

	Domain	Function
Bait: CLIC5A	Full-Length	Part of the ezrin/podocalyxin complex in podocytes and inner ear hair cell sensory stereocilia.
Prey: Proteins identified that interact directly with full-length CLIC5A:		
Radixin	C-terminus 330-586 amino acids	The C-termini of radixin and ezrin are highly homologous. **Radixin and CLIC5A interact in inner ear stereocilia**. Ezrin and CLIC5A are part of the NHERF2/podocalyxin complex in podocytes.
Taperin	Central domain 312-424 amino acids	Protein phosphatase 1α (PP1α) regulatory subunit and suppresses PP1α phosphatase activity, **component of the CLIC5A/radixin complex in the inner ear hair cell** stereocilia and mutation causes hearing loss, has 78% amino acid sequence similarity with human taperin 272-385 fragments.
Shank2	C-terminus 951-1262 amino acids	Recruits a Rac1 GEF "Rho guanine nucleotide exchange factor 7 (ARHGEF7), also known as βPix (Pax-interacting exchange factor beta", thus modulates GTPase activity.

It is well known that the radixin and ezrin C-termini are highly homologous and that these ERM proteins couple transmembrane proteins to actin (Appendix 1 for ERM proteins alignment) (151, 207). Also, radixin and CLIC5A are in the same protein complex in the inner ear (425), while in the kidney, CLIC5A strongly co-localizes with, and activates ezrin (85, 89). Therefore, I postulated that the finding of a direct interaction between CLIC5A and radixin suggest that a similar interaction may exist between CLIC5A and ezrin.

3.2.4. CLIC5A binds directly to ezrin C-terminus (amino acids 432-586)

To confirm and map the direct interaction between CLIC5A and ezrin, I cloned CLIC5A full-length (FL) 1-251 amino acids (aa), CLIC5A 22-251 aa (N-terminal deletion mutant), and CLIC5A 1-232 aa (C-terminal deletion mutant), CLIC4 FL (1-253 aa) and CLIC1 FL (1-241 aa) into the bait vector and different ezrin domains and fragments into the prey vector of the Y2H assay. A direct interaction between the bait and the prey results in blue colonies in "Double Drop-out (DDO)/X-α-Gal as DDO/X plates" and DDO/X-α-Gal/Aureobasidin A (A) antibiotic" agar plates as DDO/X/A plates. If there is no direct interaction between the bait and the prey proteins, yeast colonies cannot growth on DDO/X/A agar plate containing the Aureobasidin A antibiotic.

I observed that CLIC5A FL 1-251 aa interacts most strongly with the ezrin C-terminal domain 432-586 aa. CLIC5A also interacts with ezrin 297-586 aa, weakly with ezrin 516-586 aa, and very weakly with ezrin 550-586 aa (faint blue colonies) as evident from the growth of blue colonies on the DDO/X/A plate (Figure 3.4). However, in the Y2H assay CLIC5A does not interact directly with FL ezrin 1-586 aa, the ezrin N-terminal domain 1-296 aa, ezrin 432-570, ezrin 432-550 aa, ezrin 432-516 aa, or ezrin 480-540 aa based on the absence of blue colony growth on the DDO/X/A agar plates (Figure 3.4). Ezrin 297-586 aa, which includes both the coiled coil domain (297-431 aa) and C-terminal domain (432-586 aa), showed a direct interaction with CLIC5A FL 1-251 aa as evident from the growth of weak blue colonies, but not as strongly as ezrin 432-586 aa, suggesting that the coiled coil domain slightly hinders the CLIC5A/ezrin direct interaction and 297-431 aa is not the region of ezrin that binds CLIC5A. My finding that the last 16 amino acids of the ezrin C-terminal domain are required for the interaction with CLIC5A indicate that this region of ezrin is critical for binding to CLIC5A. The

CLIC5A N-terminal (22-251 aa) and C- terminal deletion mutants (1-232 aa) failed to interact with ezrin 432-586 aa as observed from the absence of yeast colony growth on the DDO/X/A plates. Diploid yeast colonies did grow on the DDO/X plates devoid of Aureobasidin A antibiotic, meaning that mating was successful and that the colonies contained both constructs, but the colonies did not turn blue when CLIC5A N- and C-terminal deletion mutants (bait) and ezrin 432-586 (prey) were evaluated (Figure 3.5). Therefore, the N-terminal and C-terminal domains of CLIC5A are necessary for direct binding of ezrin.

3.2.5. CLIC5A interacts directly with the ezrin, radixin, and moesin

Using the Y2H assay, I observed that expression of CLIC5A as bait together with the C-terminus of ezrin 432-586 aa, or radixin 432-583 aa, or moesin 432-577 aa as prey, induced expression of the MEL1 reporter encoding α-galactosidase and resulting in blue colonies in the presence of X-α-gal on the DDO/X agar plates, indicating direct interactions between CLIC5A and the C-terminal domains of ezrin, radixin, and moesin (Figure 3.6). Yeast colony growth on the antibiotic Aureobasidin A containing plates, which requires induction of the reporter AUR1-C through a direct bait/prey interaction, was also observed for the combination of CLIC5A as bait and the ezrin, or radixin or moesin C-terminal domains as prey (Figure 3.6). However, the number and size of blue colonies in the presence of X-α-gal and Aureobasidin A antibiotic were consistently (n = 3 distinct experiments) greater for the CLIC5A/ezrin 432-586 aa combination than the combination of CLIC5A/radixin 432-583 aa or CLIC5A/moesin 432-577 aa, which produced fewer and smaller blue colonies (Figure 3.6). This suggests that the affinity of CLIC5A for ezrin 432-586 is greater than its affinity for radixin 432- 583 aa or moesin 432-577 aa. Ezrin was therefore studied in detail.

3.2.6. CLIC4 and CLIC1 do not interact directly with ezrin in the Y2H assay

CLIC1 and CLIC4 proteins are the most studied CLIC proteins, and they are highly homologous with CLIC5A (see sequence alignments, Appendix 2). Therefore, we were also interested to determine whether CLIC1 and CLIC4 interact directly with ezrin. Y2H assay using FL CLIC5A (1-251 aa), FL CLIC4 (1-253 aa), or FL CLIC1 (1-241 aa) as bait, and FL ezrin 1-586 aa or ezrin 432-586 aa as prey, showed that CLIC5A interacts directly with ezrin 432-586 aa as evident from growth of blue colonies on the DDO/X/A agar plates, but neither CLIC4 nor CLIC1 were found to interact directly with ezrin 1-586 aa or ezrin 432-586 aa based on the absence of growth of yeast colony on the DDO/X/A agar plates (Figure 3.7). These results suggest that CLIC5A might be unique among the CLIC proteins in the context of ezrin complex in cells, or that CLIC5A has a significantly higher affinity for the ezrin C-terminus than CLIC1 or CLIC4.

3.2.7. Validation of Y2H mapping results of CLIC5A/ERM direct interaction

I next used the GST pull-down method to validate the Y2H results. I observed that endogenous ezrin, radixin, and moesin were all pulled from the COS-7 cell lysates by GST-CLIC5A immobilized on glutathione bead (Figure 3.8), suggesting that CLIC5A can interact with these proteins in their active conformation and consistent with the interaction between CLIC5A with ezrin, radixin, and moesin by Y2H assay in Figure 3.6. To rule-out possible false-positive interactions by Y2H, I also validated the mapping results, using the GST-CLIC5A pull down and co-immunoprecipitation assays, of ezrin protein constructs expressed in COS-7 cells and synthesized *in vitro*. When GFP-ezrin constructs were expressed in COS-7 cells, GST-CLIC5A pulled down GFP-ezrin 432-586 aa, but not GFP-ezrin 1-586 aa or GFP-ezrin 432-570 aa from the cell lysates (Figure 3.9), consistent with the Y2H findings in Figure 3.4. However, unlike the Y2H findings, the ezrin FERM domain (aa 1-296) was also pulled from the cell lysates by GST-

CLIC5A. Ezrin phosphorylation at Thr 567 (human ezrin sequence) is critical for its activation and thus I also overexpressed phosphomimetic ezrin 432-586 aa T567D mutant for GST-CLIC5A pull-down (Figure 3.10). Compared to other GFP-ezrin constructs, much more of the phosphomimetic form of ezrin 432-586 aa T567D was pulled down by GST-CLIC5A (Figure 3.10). When co-expressed with GFP-CLIC5A in COS-7 cells, HA-ezrin 1-586 aa, HA-ezrin 432-586 aa, but not ezrin HA-432-570 aa were co-immunoprecipitated with GFP-CLIC5A from the lysates (Figure 3.11). Since interactions observed by GST-pull-down from cell lysates or co-immunoprecipitation can be indirect, I also determined whether ezrin proteins synthesized *in vitro* using the TnT® transcription/translation system interact with purified GST-CLIC5A. Consistent with the Y2H mapping results, immobilized GST-CLIC5A effectively precipitated the *in vitro* synthesized the HA-tagged ezrin 297-586 aa and ezrin 432-586 aa fragments, but not the ezrin 432-570 aa fragment or full-length ezrin 1-586 aa (Figure 3.12.A). However, unlike the Y2H findings, GST-CLIC5A also precipitated the *in vitro* transcribed and translated the HA-Tagged ezrin 1-296 aa fragment representing the FERM domain. (Figure 3.12.B). In addition, immobilized GST-CLIC5A pulled down *in vitro* synthesized radixin 300-583 aa, radixin 432-583 aa and moesin 432-577 aa (Figure 3.12.C). Therefore, for the direct interaction of CLIC5A with ezrin, the last 16 amino acids of the ezrin C-terminus are required. The finding that the ectopically expressed ezrin N-terminal FERM domain (ezrin 1-296 aa) and the *in vitro* synthesized HA-tagged ezrin 1-296 aa binds GST-CLIC5A suggests a false negative result for ezrin 1-296 aa in the Y2H assay, possibly due to retention of this ezrin fragment at the yeast plasma membrane. The finding that FL ezrin 1-586 aa co-immunoprecipitated with GFP-CLIC5A when both proteins were expressed in COS-7 cells (Figure 3.11), but failed to interact with CLIC5A in the Y2H or the *in vitro* transcription/translation assays, is consistent with the

high-affinity auto-inhibitory interaction between ezrin N-terminal FERM domain and its own C-terminal tail (210) that would block the C-terminus of ezrin preventing it from binding CLIC5A.

Figure 3.1

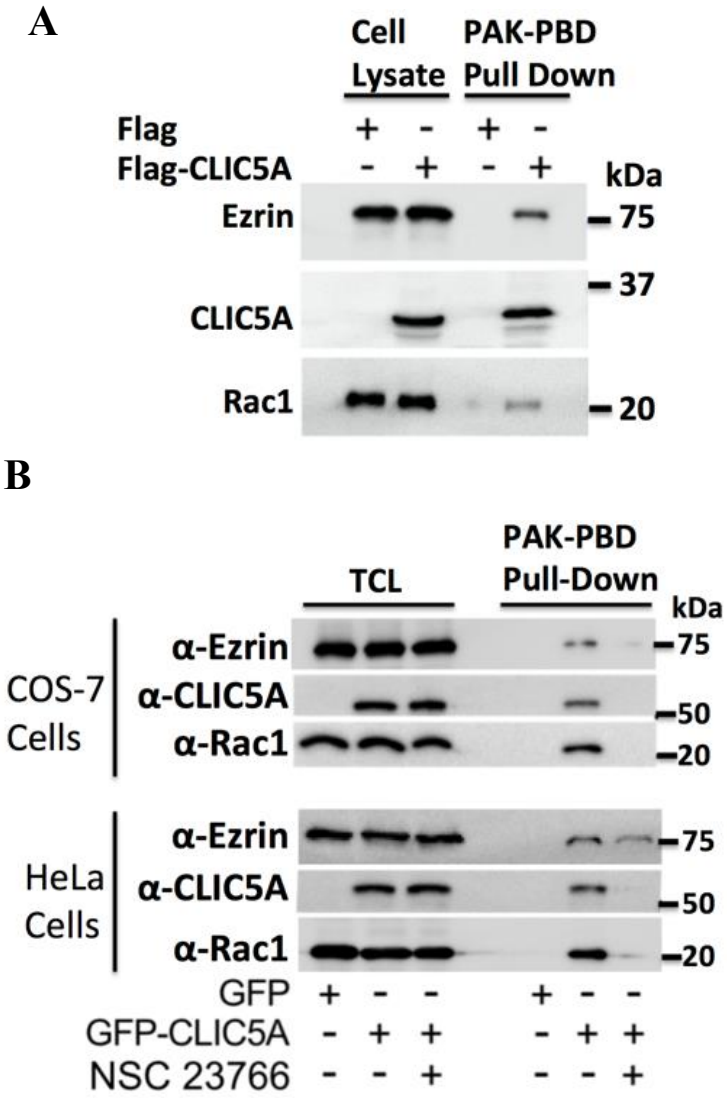

Figure 3.1: CLIC5A and ezrin are part of the Rac1-GTP complex. A. Western blot (WB) analysis with anti(α)-ezrin, α-CLIC5A and α-Rac1 antibodies of cell lysate and proteins pulled down by immobilized PAK-protein binding domain (PAK-PBD) beads from lysates of COS-7 cells transfected with Flag- or Flag-CLIC5A cDNAs constructs. **B.** WB analysis with α-ezrin, α-CLIC5A and α-Rac1 antibodies of total cell lysates (TCL) and proteins captured by immobilized PAK-PBD beads from lysates of COS-7 and HeLa cells transfected with GFP or GFP-CLIC5A cDNAs constructs. The GFP-CLIC5A cDNA expressing COS-7 and HeLa cells were treated with or without the Rac1 inhibitor NSC23766 (100 μM, 10 minutes).

Figure 3.2

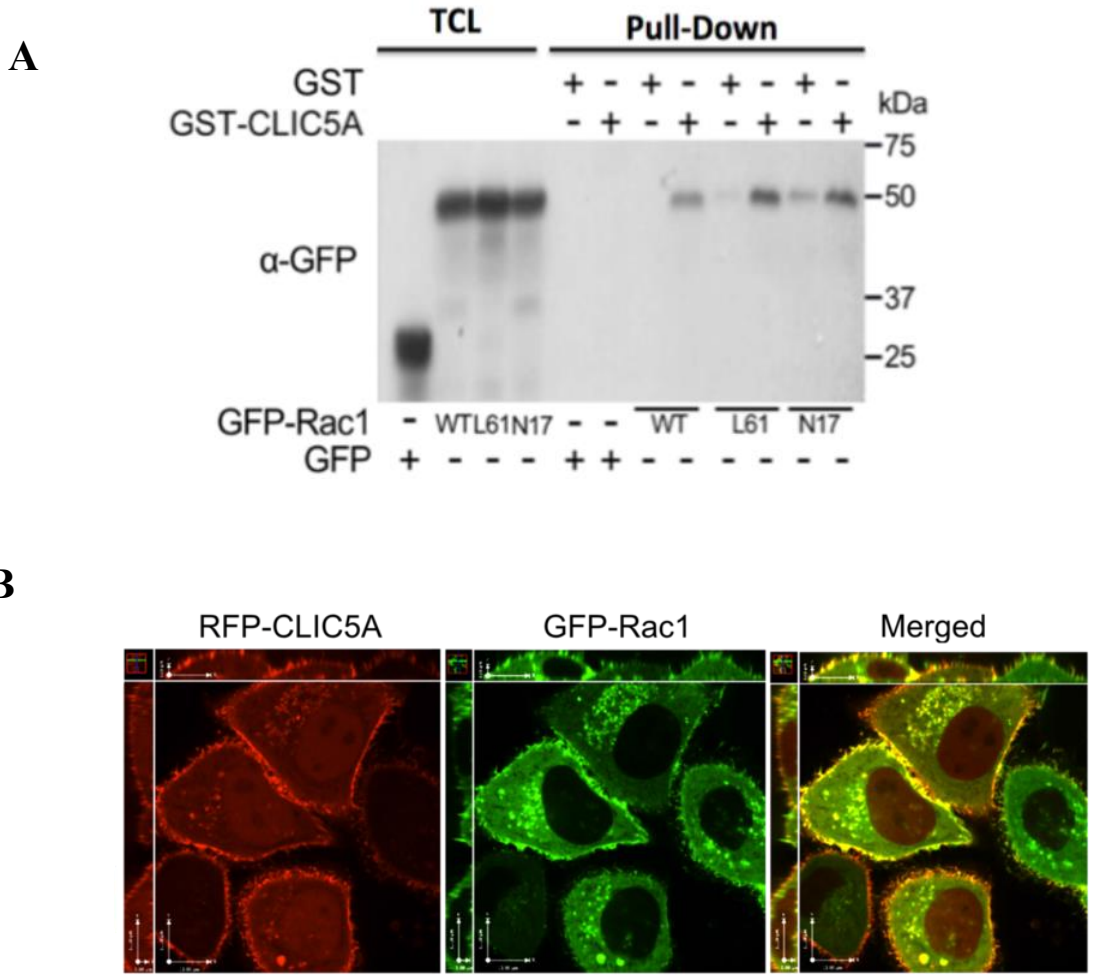

Figure 3.2: CLIC5A interacts with Rac1. **A.** WB analysis with α-GFP antibody of total cell lysate (TCL) and proteins pulled down by GST- or GST-CLIC5A immobilized on glutathione bead from lysates of COS-7 cells transiently transfected with wild-type (WT), constitutively active (L61) or dominant negative (N17) GFP-Rac1 cDNAs constructs. **B.** Live cell imaging of HeLa cells transiently transfected with RFP-CLIC5A (red) and wild-type GFP-Rac1 (green) cDNAs constructs. Co-localization (yellow) in the merged image is observed at the cell periphery and in the perinuclear location.

Figure 3.3

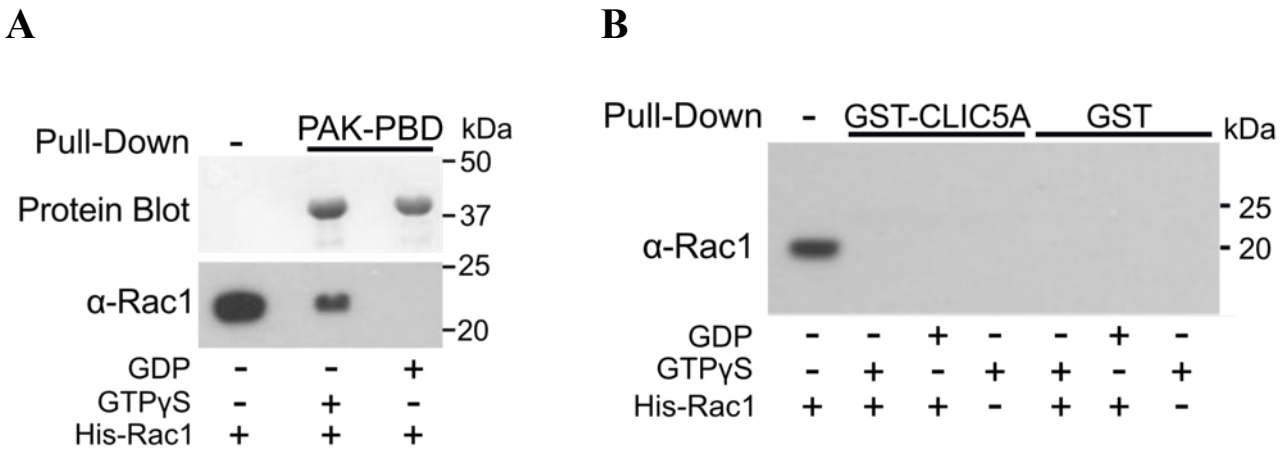

Figure 3.3: CLIC5A does not interact directly with Rac1. **A.** *In vitro* loading of purified, recombinant His-Rac1 with GTPγS. 500 ng of His-Rac1 was loaded with GTPγS or GDP, followed by affinity capture of Rac1-GTPγS by immobilized PAK-PBD bead. Top Panel: Protein blot. Bottom panel: WB with anti-(α)-Rac1 antibody. **B.** WB of purified His-Rac1 from GST- or GST-CLIC5A pull-downs from cell-free solutions (Tris-HCl, 20 mM, pH 7.4) containing Rac1-GTPγS or GDP loaded Rac1. His-Rac1 wild-type (5 ng) was used as input (extreme left lane).

Figure 3.4

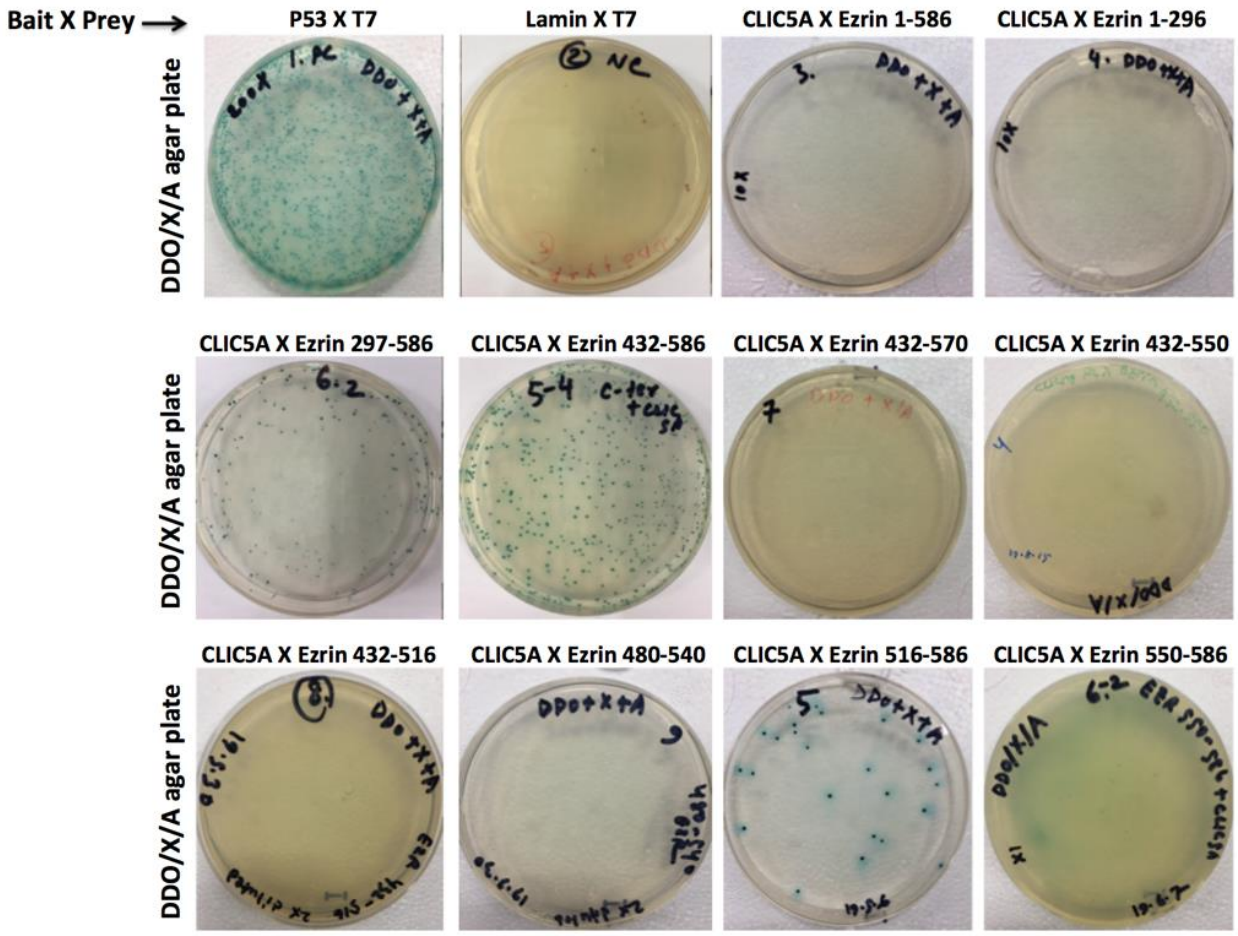

Figure 3.4: Yeast two-hybrid mapping showing direct interaction of CLIC5A and ezrin 432-586 aa. Y2H assay with wild-type full-length CLIC5A 1-251 as bait and distinct ezrin fragments as prey. DDO: Leucine/Tryptophan deficient medium. DDO/X: DDO medium containing X-α-gal substrate; DDO/X/A: DDO medium containing X-α-gal substrate and Aureobasidin A antibiotic. Blue colonies and growth on Aureobasidin A containing agar indicates induction of the reporters due to a direct interaction between bait and prey. The P53/T7 combination served as positive, and the Lamin/T7 combination as negative control.

Figure 3.5

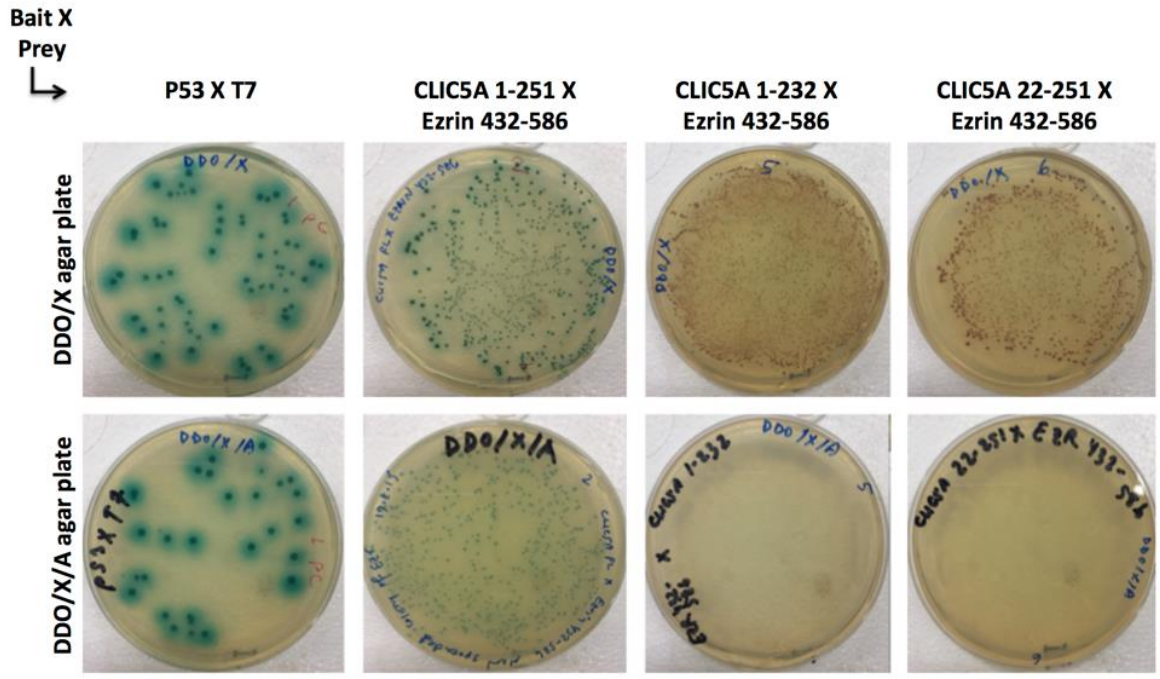

Figure 3.5: CLIC5A C-terminal and N-terminal mutants do not interact directly with ezrin. Yeast two-hybrid mapping using wild-type full-length CLIC5A 1-251 aa, or CLIC5A 1-232 aa C-terminal mutant, or CLIC5A 22-251 aa N-terminal mutant as baits, and ezrin 432-586 aa as prey. DDO/X: DDO medium containing X-α-gal substrate; DDO/X/A: DDO medium containing X-α-gal substrate and Aureobasidin A antibiotic.

Figure 3.6

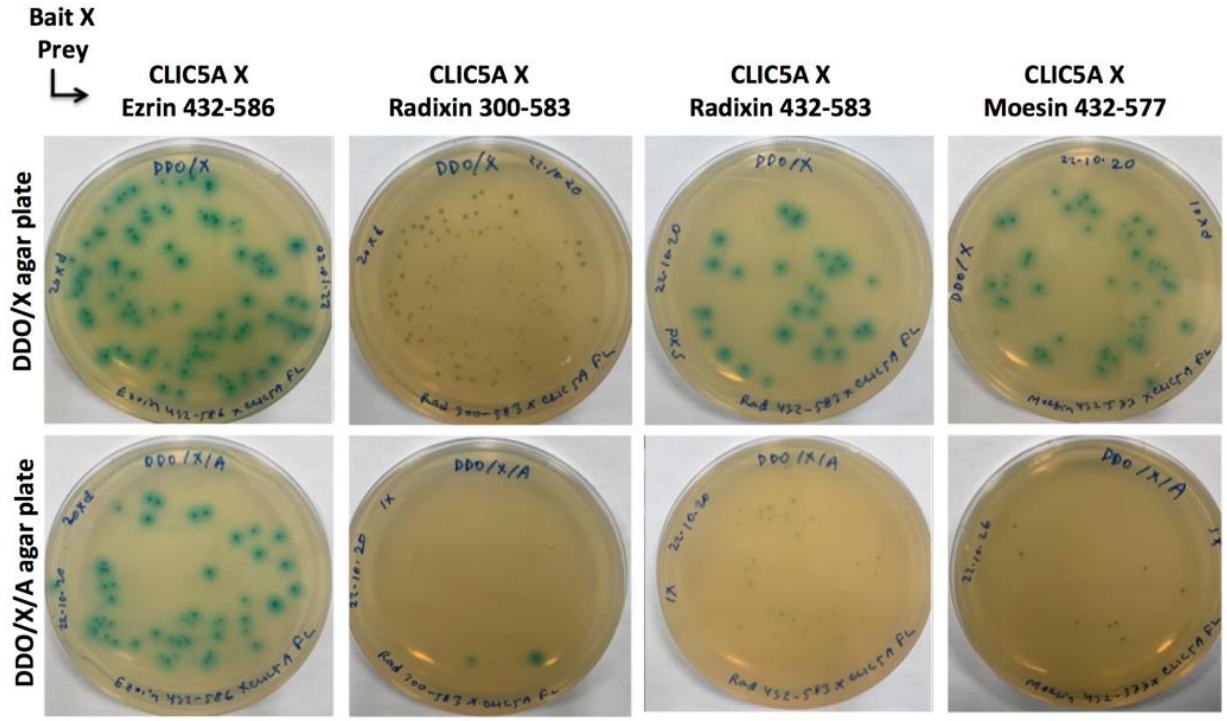

Figure 3.6: Yeast two-hybrid assay showing direct interactions of CLIC5A and ezrin, radixin, moesin C-terminal domains. Plates contain yeast colonies expressing untagged full-length CLIC5A 1-251 amino acids (aa) in the "bait" vector and C-terminal domain of ERM proteins (ezrin 432-586 aa, or radixin 432-583 aa, or moesin 432-577 aa) in the "prey" vector. Colony growth on double deficient medium (DDO, lacking leucine and tryptophan) indicates both vectors are present. Blue colonies indicate α-galactosidase activity in the presence of X-α-gal (DDO/X plate) due to direct interactions between bait and prey proteins. Growths on plates containing the antibiotic Aureobasidin A (DDO/X/A) indicates a direct interaction between bait and prey proteins resulting in Aureobasidin A resistance.

Figure 3.7

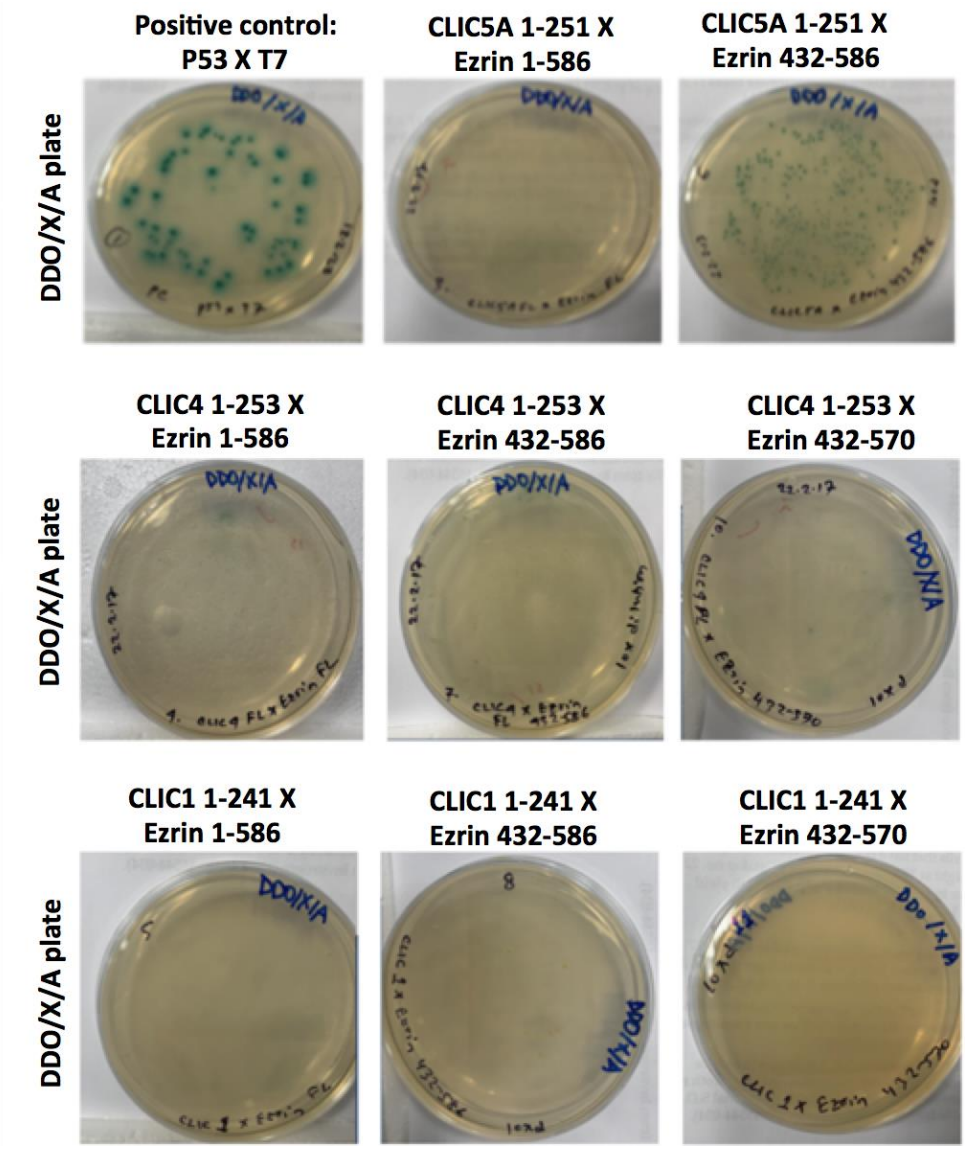

Figure 3.7: CLIC4 and CLIC1 do not interact directly with ezrin in yeast two-hybrid assay. Yeast two-hybrid assay showing blue yeast colonies growth on DDO/X/A plates indicates a direct interaction. Baits p53, CLIC5A, CLIC4, CLIC1 in the bait vector, and prey T7, ezrin 1-586, ezrin 432-586, and ezrin 432-570 in the prey vector were used for Y2H assay. Blue colonies indicate α-galactosidase activity in the presence of X-α-gal on the DDO/X/A plates due to direct interactions between bait and prey protein. P53 X T7, and CLIC5A X ezrin 432-586 were used as the positive controls.

Figure 3.8

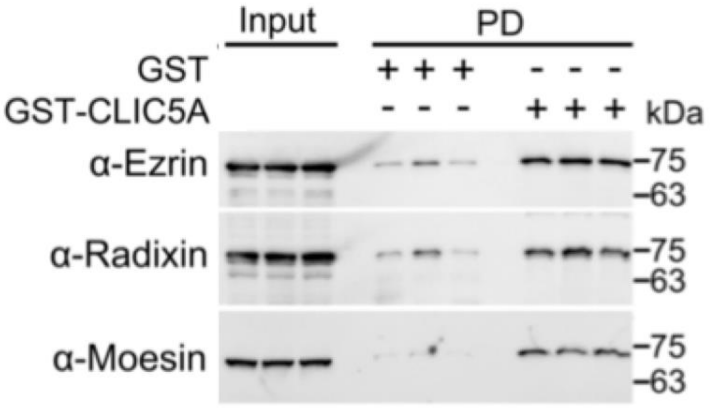

Figure 3.8: Immobilized GST-CLIC5A pulls endogenous ezrin, radixin and moesin from cell lysates. WB analysis with anti(α)-ezrin, α-radixin and α-moesin antibodies of total cell lysates (Input) and proteins from GST- or GST-CLIC5A pull-downs (PD) using lysates from untransfected COS-7 cells. Equimolar amount of GST and GST-CLIC5A were used.

Figure 3.9

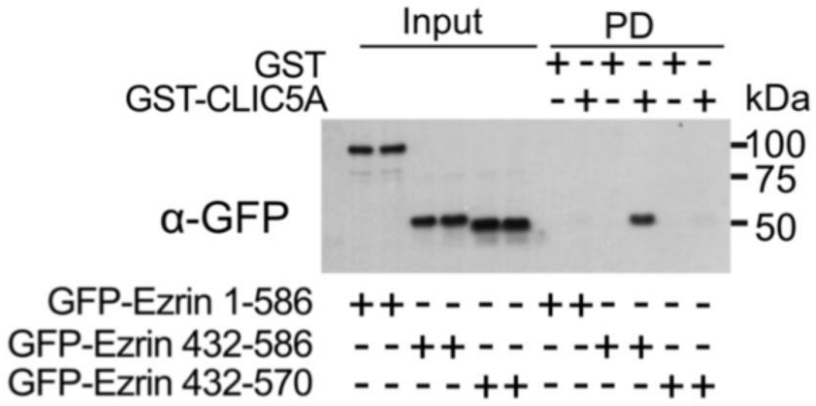

Figure 3.9: CLIC5A pulls down ezrin 432-586, but not ezrin 432-570. WB analysis with α-GFP antibody of total cell lysate (input) and proteins pulled by GST or GST-CLIC5A immobilized on glutathione bead from the lysates of COS-7 cells transiently transfected with the full-length GFP-ezrin 1-586, GFP-ezrin 432-586 and GFP-ezrin 432-570 cDNA constructs.

Figure 3.10

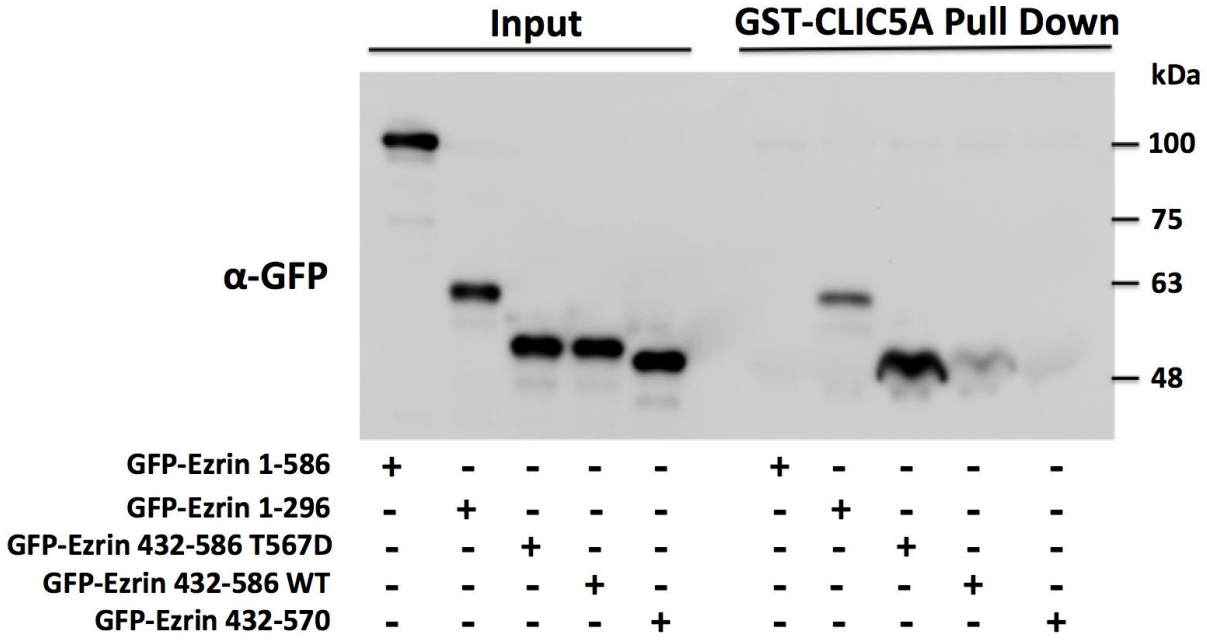

Figure 3.10: GST-CLIC5A pulls down GFP-ezrin 1-296 and GFP-ezrin 432-586, but not GFP-ezrin 1-586 or 432-570. WB analysis with α-GFP antibody of total cell lysate (input) and proteins pulled by immobilized GST-CLIC5A on glutathione bead from the lysates of COS-7 cells transiently transfected with the full-length GFP-ezrin 1-586, GFP-ezrin 1-296, GFP-ezrin 432-586 T567D phosphomimetic point mutant, GFP-ezrin 432-586 wild type, and GFP-ezrin 432-570 cDNA constructs.

Figure 3.11

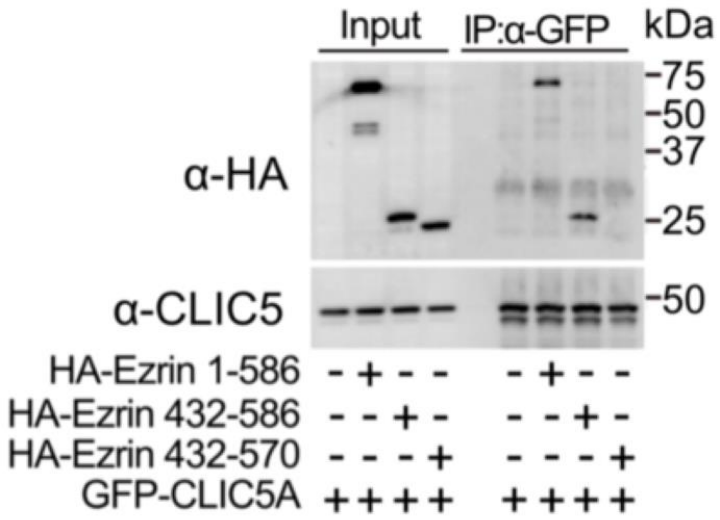

Figure 3.11: CLIC5A co-immunoprecipitates with ezrin 1-586 and ezrin 432-586, but not with ezrin 432-570. Western blot with α-HA and α-GFP antibodies of input (total cell lysate) and proteins from co-immunoprecipitation (IP) with Goat α-GFP antibodies using lysates of COS-7 cells co-transfected with HA-ezrin 1-586, or HA-ezrin 432-586, or HA-ezrin 432-570, and GFP-CLIC5A cDNA constructs.

Figure 3.12

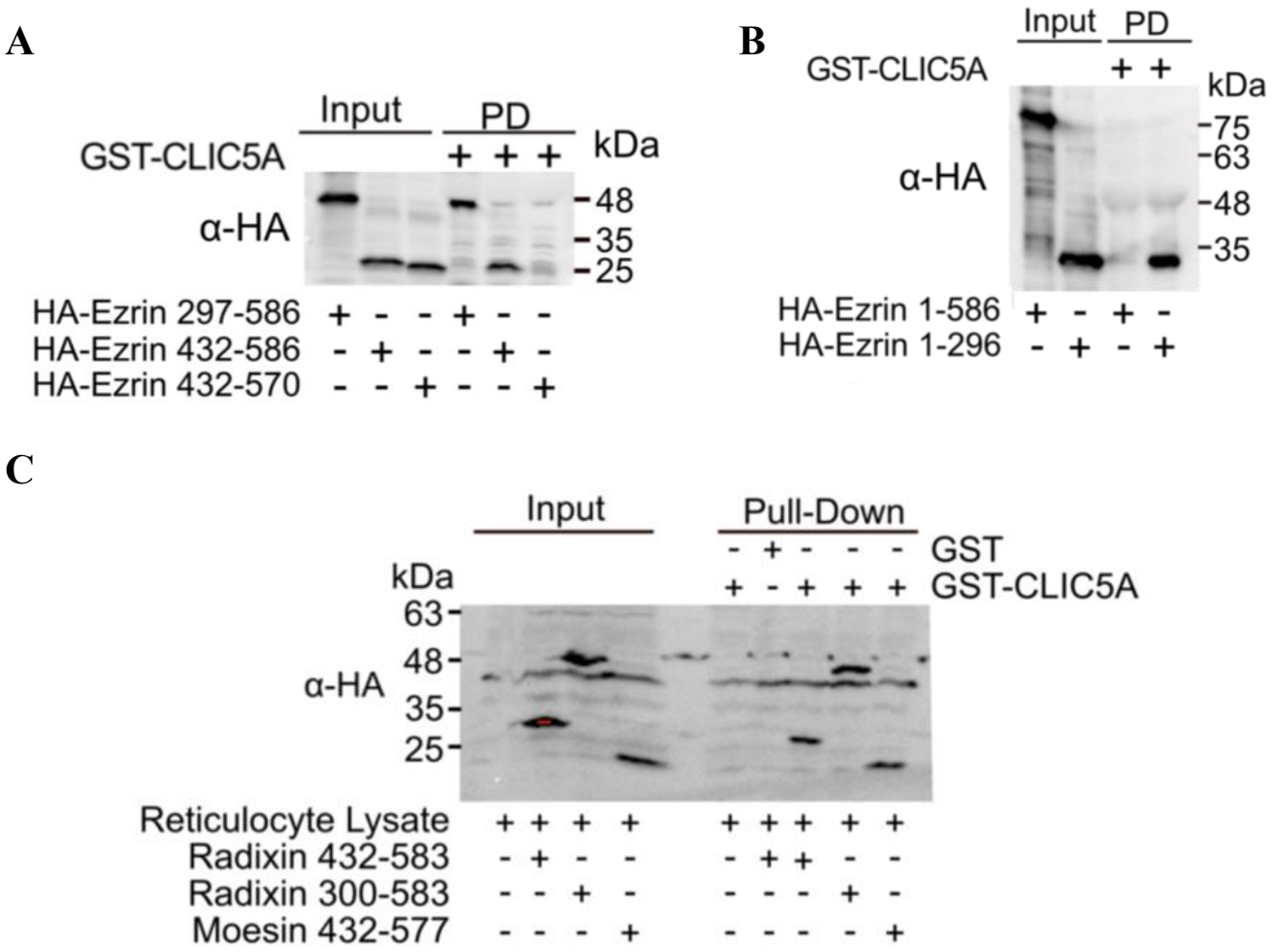

Figure 3.12: CLIC5A binds directly to the C-terminal domain of ezrin, radixin and moesin *in vitro*. A. WB with α-HA antibody of input and proteins pulled by GST- or GST-CLIC5A from *in vitro* transcribed/translated mediated synthesized HA-ezrin 297-586, HA-ezrin 432-586, and HA-ezrin 297-570 proteins using the TnT® reticulocyte lysate system. **B.** WB analysis with α-HA antibody of input and proteins pulled by GST- or GST-CLIC5A from *in vitro* synthesized of HA-ezrin 1-586 and HA-ezrin 1-296 proteins using the TnT® reticulocyte lysate system, followed by GST- or GST-CLIC5A pull-down. **C.** WB with α-HA antibody of input and proteins pulled by GST- or GST-CLIC5A from *in vitro* transcribed/translated mediated synthesized HA-radixin 432-583, HA-radixin-300-583, and HA-moesin 432-577 proteins using the TnT® reticulocyte lysate system to determine the protein-protein interaction.

3.3. Discussion

CLIC5A is part of the ezrin complex in glomerular podocytes and placental microvilli and also part of the radixin complex in inner ear sensory hair cell stereocilia (85, 345, 422, 425) , but a direct interaction between the ERM and CLIC proteins, though postulated (462) had not previously been shown. I report a direct interaction between CLIC5A and ERM proteins in this chapter and show that CLIC5A interacts directly with the C-terminal domain of ezrin, radixin and moesin. It was also previously reported that CLIC5A expression leads to enhanced Rac1, but not RhoA or Cdc42 activation (86). I observed here that although Rac1-GTP, CLIC5A and ezrin are part of the same protein complex, the interaction between CLIC5A and Rac1-GTP seems to be indirect.

The observation that CLIC5A and ezrin co-precipitate with Rac-GTP in the Rac1 GTPase pull down assay, first suggested that Rac1-GTP might interact with CLIC5A. Non-specific adhesion of CLIC5A was ruled out given that CLIC5A did not bind PAK-PBD beads when CLIC5A-stimulated Rac1 activation (Rac-GTP) was inhibited by NSC 23766 (Figure 3.1.B). CLIC5A also co-localized with Rac1 at the cell periphery (Figure 3.2B). However, I found that GST-CLIC5A could pull down constitutively active, wild-type as well as dominant negative Rac1 from lysates of cells in which these Rac1 constructs were expressed (Figure 3.2A), suggesting that any CLIC5A/Rac1 interaction does not require activation of Rac1. These findings then led me to determine whether CLIC5A interacts directly with Rac1. I was able to load purified, recombinant Rac1 with GTPγS, but observed that GST-CLIC5A could not interact directly with the GTPγS- or GDP loaded His-Rac1 *in vitro* (Figure 3.3). Although the interaction between CLIC5A and Rac-GTP appears to be indirect, the result does indicate that Rac1-GTP is present in the CLIC5A/ezrin protein complex.

It is known that ezrin can sequester the Rho guanine nucleotide inhibitor (Rho GDI), enhancing the activity of associated Rho GTPases like Rac1 (234, 235). Therefore, we wanted to determine whether ERM proteins and other proteins are the direct interacting proteins of CLIC5A. The unbiased Y2H protein domain screen suggested that the mouse radixin C-terminal domain can interact directly with CLIC5A. This finding was encouraging since a functional interaction of radixin and CLIC5A in the inner ear hair cells was previously reported (425). My Y2H mapping revealed that CLIC5A interacts with the ezrin C-terminal domain 432-586 aa strongly and that ezrin 432-570 with the last 16 amino acids deleted failed to interact directly with CLIC5A.

Ezrin FL (1-586 aa) takes on an auto-inhibited (inactive) conformation when it is not bound to plasma membrane PI4,5P2, due to a high-affinity interaction between the ezrin N- and C-terminal domains that prevent the C-terminus from interacting with other proteins (186). Therefore, FL ezrin would only be expected to interact with CLIC5A when it is in the active PI4,5P2 -bound conformation. In the Y2H system, the closed conformation of ezrin would therefore not be able to interact with CLIC5A. Sequestration of active ezrin bound to PI4,5P2, at the membrane would also preclude an interaction with the CLIC5A bait in the yeast nucleus where activation of the reporter genes has to take place. In the GST-CLIC5A pull down assay or of *in vitro* transcribed/translated ezrin 1-586 would also be in the closed/autoinhibited state (210) making the C-terminal tail of ezrin inaccessible for binding CLIC5A and actin. Endogenous FL ezrin was pulled down by GST-CLIC5A (Figure 3.8), but overexpressed FL ezrin was not pulled from cell lysates by GST-CLIC5A (Figure 3.8, 3.9). Also, when FL HA-ezrin (1-586 aa) was co-expressed with GFP-CLIC5A (Figure 3.11), the HA-ezrin (1-586 aa) was co-immunoprecipitated with GFP-CLIC5A. The best way to explain these apparently contradictory results is that some of the endogenous ezrin in cell lysates must be available for binding to GST-CLIC5A, and that

co-expressed CLIC5A and ezrin must be able to form a complex in the cells. By contrast, overexpressed full-length ezrin probably exists mostly in the auto-inhibited, soluble form in the absence of CLIC5A. Therefore, my finding that the C-terminal domains of ezrin 432-586 aa interact directly with CLIC5A strongly suggests that FL CLIC5A only interacts directly with ezrin when ezrin is in the open (active) conformation.

The Y2H assay showed that the C-terminal domain of ezrin, radixin and moesin all interact directly with CLIC5A, though the interaction seems to be strongest for ezrin (Figure 3.6). For ezrin, I showed that this interaction requires the C-terminal last 16 amino acids (Figure 3.4). Our observation of the direct interaction between CLIC5A and ezrin is supported by the observation by Berryman et al. (345, 422) who discovered CLIC5A in a cytoskeletal protein complex precipitated with an immobilized GST-tagged ezrin C-terminal (556-586) peptide.

While the Y2H assay was negative when CLIC5A was used as bait and the ezrin N-terminal domain (1-296 aa) as prey, the ezrin 1-296 aa was precipitated by immobilized GST-CLIC5A when it was expressed in COS-7 cells (Figure 3.10) or produced *in vitro* in the cell-free transcription/translation system (Figure 3.12.B), suggesting that CLIC5A may independently bind the ezrin N-terminal FERM domain, when ezrin is in its active conformation. Moreover, N-terminal deletion of first 22 amino acids or C-terminal deletion of last 20 amino acids from full-length CLIC5A (1-251 aa) makes it nonfunctional in terms of interacting with ezrin (Figures 3.5). This deletion was previously shown to abolish the ability of CLIC5A to localize at the cell periphery and it was unable to stimulate ERM phosphorylation (89).

CLICs can functionally interact with ERM proteins (462) and particularly CLIC4 and CLIC5A have been shown associated with ezrin and induce cell surface microvillus formation in epithelial cells (162, 345). CLIC4 was also identified in the interactome of the ezrin N-terminal FERM

domain (463) and when produced in a cell-free system, the N-terminal FERM domain of ezrin interacted with recombinant CLIC4. Since the ezrin N-terminal domain binds plasma membrane PI4,5P2, it seems likely that the Y2H assay could not detect the interaction, as activation of the reporters requires nuclear localization of the interacting proteins in this assay. The two extensively studies CLIC proteins; CLIC4 and CLIC1 surprisingly did not interact directly with ezrin in my Y2H assay. Taken together with findings by others, it seems conceivable that direct interactions of the ERM proteins occur via the FERM domain, and that CLIC5A might have a distinct function that makes it unique in that it also interacts with the C-terminal domain of ERM proteins.

However, the results of this chapter leave open the following questions: Is CLIC5A a cytosolic protein unlike membrane spanning channel proteins? If CLIC5A is a peripheral membrane protein, can it dissociate from the membrane fraction? Does CLIC5A require ERM proteins for its cell membrane localization? These questions are investigated in chapter 4. Also, what are the functional consequences of the CLIC5A/ERM proteins direct interaction, and how does CLIC5A activate Rac1 and enhance phosphorylation of ERM proteins? These questions are investigated in chapter 5.

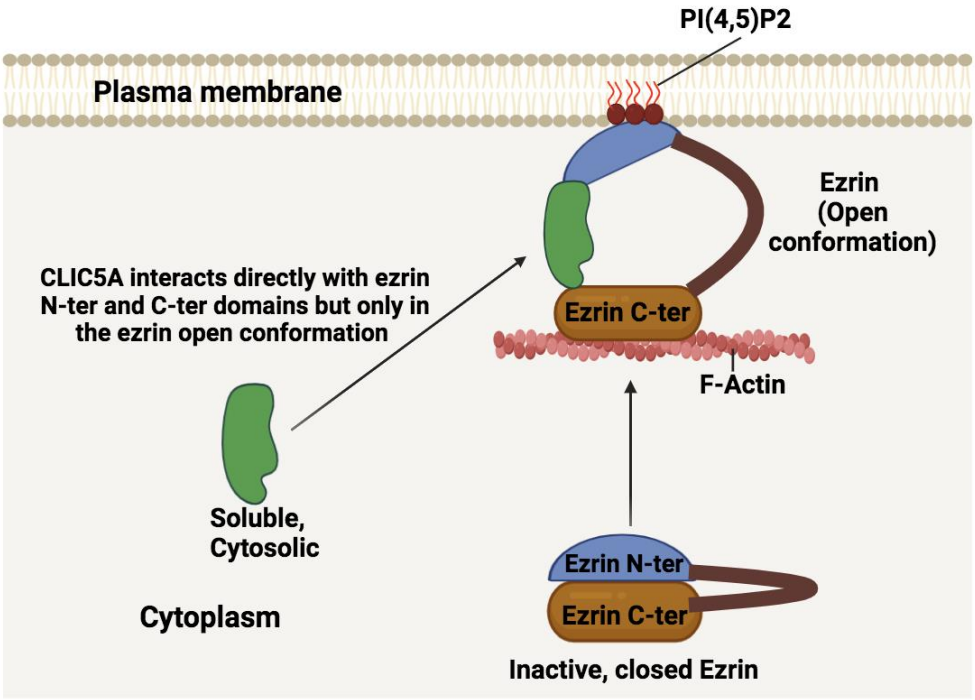

Figure 3.13: Model: CLIC5A interacts directly with the N- and C- terminal domains of ezrin. The open, active conformation of ezrin is accessible for direct binding of CLIC5A, while the inactive closed conformation of ezrin cannot bind CLIC5A.

Chapter 4

CLIC5A is predominantly a cytosolic protein and can be displaced from the cell periphery

Chapter 4

CLIC5A is predominantly a soluble protein and can be displaced from the cell periphery

4.1. Introduction

Experts studying chloride channels have concluded that CLIC proteins were misnamed because they cannot form transmembrane channels with chloride-selective pores *in vivo* (354, 355), but this issue is still highly controversial. Overexpressed CLIC5A and CLIC5B proteins partition into artificial lipid bilayers and facilitate non-selective ion movement across the bilayers down electrochemical gradients (342, 343, 345), as also observed for other members of the CLIC family (316). However, even though transiently expressed CLIC5A localizes at or near the apical plasma membrane in cultured cells, its presence in cells does not alter anion efflux (345). CLIC proteins are produced without signal peptide and crystal structures of the closely related CLIC1 (325), CLIC2 (335), and CLIC4 (341) family members predict that they are soluble proteins that do not possess even a single predicted transmembrane helix, therefore not resembling classic ion channels that contain multiple membrane-spanning segments.

CLIC proteins were initially annotated as chloride intracellular channels after the first mammalian CLIC protein, p64 (CLIC5B) was affinity purified from bovine kidney microsomes with IAA-94, a non-selective chloride channel inhibitor (324). Reconstitution of purified, recombinant CLIC5A into artificial lipid bilayers produced a dose-dependent chloride conductance *in vitro* that, although sensitive to the non-selective chloride channel blocker IAA-94 (345), but was not inhibited by the more selective blockers of classic chloride channels, 4,4'-diisothiocyanatostilbene-2,2'-disulfonate (DIDS) and 4-acetamido-4'-isothiocyanato-2,2'-stilbenedisulfonic acid (SITS) (355). Moreover, CLICs do not have sequence homology to any known channel family, they can readily dissociate from the plasma membranes and their

structure is not compatible with the formation of ion-selective pores (316, 354, 355). The size of CLIC1−CLIC5A is only ~25-29 kDa, which is much smaller than typical ion channels. To explain their effect on ion conductance, it has been suggested that CLICs undergo a redox-sensitive unfolding transition producing oligomers that can spontaneously insert into artificial lipid bilayers, similar to the bcl proteins (311). CLICs could also adopt multiple conformational folds, and the transitions between them might be associated with their translocation to their diverse subcellular locations. However, although CLIC5A is found in association with the plasma membrane, surface labeling studies indicate that CLIC5A is not detected on the cell surface and thus is not an integral membrane-spanning protein (496). Nonetheless, the function of CLIC5A and other CLICs as bona fide ion channels is still controversial and has been disputed (354, 355).

CLIC5A is observed in actin-rich projections of the plasma membrane and in glomerular podocytes (85). In the inner ear, CLIC5A co-localizes with radixin (425, 428). Both, ezrin and radixin are peripheral membrane proteins through their association with PI4,5P2 (189, 206, 464). Ectopically expressed CLIC5A also co-localizes with PI4,5P2 and PI4P5 kinases at the dorsal plasma membrane in COS-7 cells (89), and I showed that CLIC5A can interact directly with ERM proteins, (Chapter 3). Nonetheless, whether CLIC5A expressed in glomeruli is cytosolic or membrane-bound remains unknown. In this chapter, I report my experiments to investigate the association of endogenous CLIC5A with distinct membrane fractions using isolated glomeruli from CLIC5$^{+/+}$ (wild-type) mice. Therefore, the objective of this chapter is:

To determine the subcellular distribution of native, endogenous CLIC5A and to determine whether CLIC5A can be displaced from the membrane-associated form.

4.2. Results

4.2.1. CLIC5A is predominantly cytosolic in differential detergent fractionation

I first determined whether endogenous CLIC5A is soluble, membrane- or cytoskeleton-associated using differential detergent fractionation of freshly isolated glomeruli from $CLIC5^{+/+}$ mice. Endogenous nephrin and podocalyxin were used as the control for integral membrane proteins, and GAPDH as the control for soluble, cytosolic proteins. Ezrin and NHERF2 were used as the control for peripheral membrane proteins. The sum of the fractions was equivalent to the input loading control. Western blot analysis of digitonin-soluble cytoplasmic fraction, Triton X-100 soluble "membrane" fraction and insoluble/pellet "cytoskeletal" fractions showed that endogenous CLIC5A was recovered predominantly in the digitonin-soluble cytosolic fraction (~55%) (Figure 4.1), which is consistent with the findings by Kim et al. (496) who showed that exogenously expressed Flag-tagged CLIC5A is mostly observed in the cytosolic fraction in COS-7 cells. Digitonin is a mild detergent that complexes with membrane cholesterol introducing large pores, thus cytosolic proteins can be extracted. GAPDH was found only in the digitonin soluble cytosolic fraction, as expected. NHERF2, which is a peripheral membrane protein, was recovered predominantly from the Triton X-100 soluble membrane fraction. Ezrin was found in the membrane fraction, as well as in the soluble fraction and in the insoluble cytoskeletal fractions. Nephrin and podocalyxin are integral membrane proteins and were mostly recovered from the membrane fraction as expected. The results suggest that endogenous CLIC5A is mostly a soluble protein, though a significant portion was also found associated with the Triton-X 100 soluble and the insoluble pellet fractions.

4.2.2. Ser/Thr phosphatase inhibition failed to shift CLIC5A to the membrane fraction

I next determined whether phosphorylation could change the abundance of endogenous CLIC5A in different subcellular locations. Glomeruli isolated from CLIC5$^{+/+}$ mice were treated with DMSO or 50 nM Calyculin-A, which is a Ser/Thre phosphatase inhibitor (465), for 30 minutes before differential detergent fractionation. Calyculin-A treatment did not significantly increase the membrane retrieval of CLIC5A from the Triton X-100 soluble membrane fraction (~38%) compared to vehicle (DMSO) (~34%). (Figure 4.2: A, CLIC5A blot; and B, % CLIC5A in each fraction). There was a small shift of endogenous CLIC5A from the digitonin-soluble cytosolic fraction from ~42% to 38% in response to Calyculin-A, consistent with the ~4% increase of membrane fraction associated CLIC5A in response to Calyculin-A (Figure 4.2: B, % CLIC5A in each fraction). But this ~4% increase of CLIC5A from the cytosol to the membrane fraction in response to Calyculin-A did not reach statistical significance. Therefore, acute Ser/Thr phosphatase inhibition in freshly isolated glomeruli does not have a clear-cut effect on the proportion of CLIC5A associated with the membrane fraction. Moreover, the increased pERM abundance in response to Calyculin-A treatment (Figure 4.2: A, pERM blot) indicates that Calyculin-A effectively protected ERM proteins from de-phosphorylation in glomeruli when compared to the vehicle treatment. However, even though ERM phosphorylation is known to stabilize their binding to the cortical actin cytoskeleton (223, 224), in the isolated glomeruli the % ezrin in each fraction did not change significantly in response to Calyculin-A. Also, there was no significant change in the association of the integral membrane proteins podocalyxin and nephrin, or the peripheral membrane protein NHERF2 in response to Calyculin-A (Figure 4.2: A). These results indicate that acute inhibition of Ser/Thr de-phosphorylation does not alter the

membrane-association of CLIC5A or any of the proteins in the ezrin/podocalyxin/NHERF in isolated mouse glomeruli, so the experiment was not very informative.

4.2.3. Staurosporine reduced CLIC5A abundance from the membrane fraction

I also determined the effect of Staurosporine-mediated dephosphorylation on the location of endogenous CLIC5A in different subcellular fractions. Isolated glomeruli from CLIC5$^{+/+}$ mice were treated with vehicle (DMSO) or Staurosporine (100 nM, 30 minutes, 2 independent experiments) (89). At the concentration used, Staurosporine is a broad kinase inhibitor (466, 467) that can abolish the critical phosphorylation of Thr567 of ezrin (223, 224). In two experiments I observed that Staurosporine treatment decreased the abundance of CLIC5A in the membrane fraction and raised its proportion in the digitonin soluble cytosolic fraction (Figure 4.3). Staurosporine treatment reduced ERM protein phosphorylation as expected and resulted in ezrin dissociation from the cytoskeletal fraction and association with the membrane and the cytosolic fractions. As ezrin Thr567 was dephosphorylated with Staurosporine treatment, the decrease in ezrin abundance in the insoluble fraction, which contains cytoskeletal proteins, was not surprising. However, a clear-cut association of endogenous CLIC5A with ezrin could not be established by this approach.

4.2.4. m-3M3FBS significantly decreases CLIC5A abundance in the membrane fraction

Isolated glomeruli collected from CLIC5$^{+/+}$ mice were also treated with vehicle (DMSO) or phospholipase C activator m-3M3FBS (468) (800 nM, 30 minutes) to investigate whether hydrolysis of PI4,5P2 could change the association of endogenous CLIC5A, ezrin, and NHERF2 with different subcellular fractions. The PLC activator hydrolyzes PI4,5P2 at the inner leaflet of the plasma membrane. Differential detergent fractionation followed by western blot analysis of different fractions showed that treatment of glomeruli with m-3M3FBS significantly shifted

endogenous CLIC5A, ezrin, and NHERF2 to the digitonin soluble cytosolic fraction (Figure 4.4). These effects are consistent with previous imaging studies that showed complete loss of PI4,5P2 from the plasma membrane and the dissociation of expressed GFP-CLIC5A from its dorsal membrane location in COS-7 cells in response to PLC-activation (86, 89). NHERF2 is a peripheral membrane protein that binds ezrin. Treatment with m-3M3FBS also displaced NHERF2 from the membrane fraction but PLC activation. These findings indicate that a significant portion of endogenous CLIC5A that associates with the Triton X-100 soluble lipid and insoluble pellet fractions is PI4,5P2 -dependent. For ezrin, the shift to the soluble fraction was mainly from the cytoskeletal portion, while the membrane-associated fraction was slightly, but not significantly reduced. The displacement of endogenous CLIC5A from membrane and cytoskeletal fractions in response to PLC activation could be due to its association with ezrin, other PI4,5P2-associated proteins like G-protein coupled receptors, proteins involved in vesicle cycling, membrane transporters, and cytoskeletal proteins like gelsolin, profilin and N-WASP (469), or to an association of CLIC5A itself with PI4,5P2.

4.2.5. Ezrin 432-586 blocks CLIC5A plasma membrane abundance

As ezrin 432-586 (T567D) binds FL CLIC5A directly and strongly, I reasoned that ezrin 432-586 (T567D), which lacks the N-terminus/FERM domain and therefore cannot associate with the plasma membrane, might bind and block the association of CLIC5A with the endogenous membrane-bound ezrin-containing protein complex. For these experiments I expressed GFP-ezrin 432-586 (T567D) in COS-7 cells together with GFP-CLIC5A. GFP-ezrin 432-570, which cannot bind CLIC5A served as control (Figure 4.5 and 4.6). Ezrin 432-586(T567D) significantly decreased the abundance of CLIC5A in the membrane fraction and raised the proportion of GFP-CLIC5A in the digitonin soluble cytosolic fraction (Figure 4.5). By contrast, ezrin 432-570

expression did not alter the association of GFP-CLIC5A with the membrane fraction (Figure 4.6). I interpret these findings to indicate that ezrin 432-586(T567D) reduces the association of CLIC5A with membrane-bound ezrin by competing with endogenous ezrin for CLIC5A binding.

4.2.6. CLIC5A localization at the cell periphery is partly mediated by ERM proteins

I next wanted to determine whether the peripheral localization of CLIC5A is due to its direct binding to ERM proteins in HeLa cells. Since ezrin, radixin and moesin are all pulled from cell lysates by GST-CLIC5A (Figure 3.8), and since they all interact with CLIC5A in the Y2H assay (Figure 3.6) and *in vitro* pull-down assays (Figure 3.12.C), we determined whether triple siRNA-mediated knockdown of ezrin, radixin and moesin changes the subcellular distribution of CLIC5A. In HeLa cells, GFP-CLIC5A strongly localized to the dorsal plasma membrane domain, as previously reported for COS-7 cells (86, 89). When ezrin, radixin, and moesin were silenced simultaneously, a significantly larger proportion of GFP-CLIC5A was observed in the cytosolic compartment when compared to cells treated with nonspecific siRNA (Figure 4.7: A-D). Even so, a significant portion of CLIC5A remained localized at the cell periphery. Therefore, the localization of CLIC5A at the cell periphery in HeLa cells partly depends on ERM protein expression, but a significant portion of the CLIC5A-association with the cell periphery is independent of ERM proteins.

Taken together, these results suggest that CLIC5A is predominantly a cytosolic protein that can be displaced from the membrane fraction, unlike the typical chloride channel proteins. The findings are consistent with the view that CLIC5A is NOT a membrane-spanning protein but instead is a peripheral membrane protein because of its direct interactions with ERM proteins.

Figure 4.1

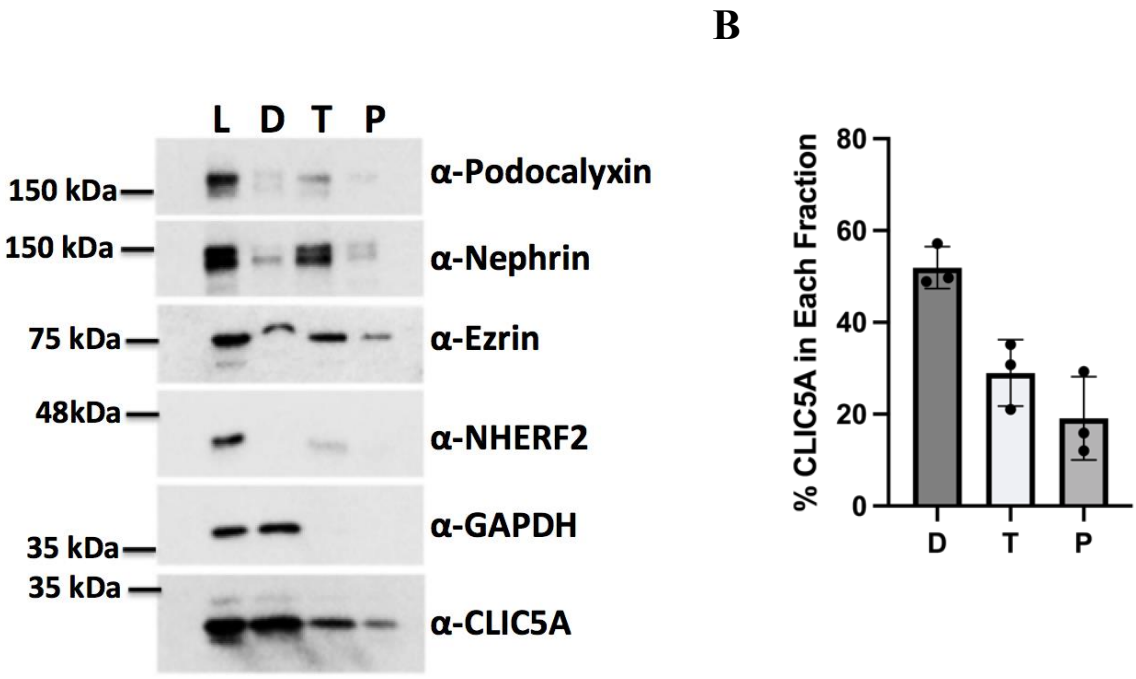

Figure 4.1: CLIC5A observed predominantly in the soluble cytoplasmic fraction. A. Differential detergent fractionation followed by western blot of glomerular lysate isolated from CLIC5$^{+/+}$ mice. GAPDH serves as control for cytoplasmic protein, ezrin and NHERF2 as control for peripheral membrane proteins, and nephrin and podocalyxin as controls for integral membrane proteins. **B.** The % of total CLIC5A in the digitonin (D) (cytoplasmic) fraction, Triton X-100 (Tx) soluble membrane fraction, and insoluble pellet (P) or cytoskeletal fraction. (100% = sum of D + T + P; n = 3 independent experiments, mean ± SD). L represents total cell lysate.

Figure 4.2

A

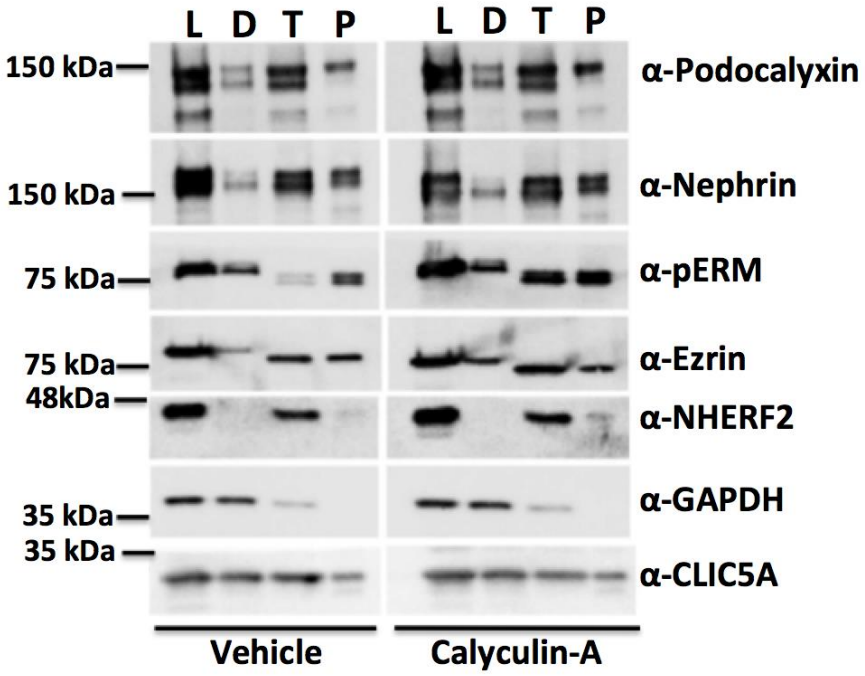

B

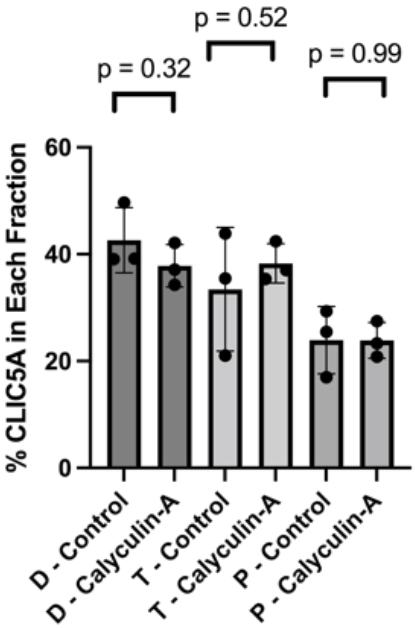

C

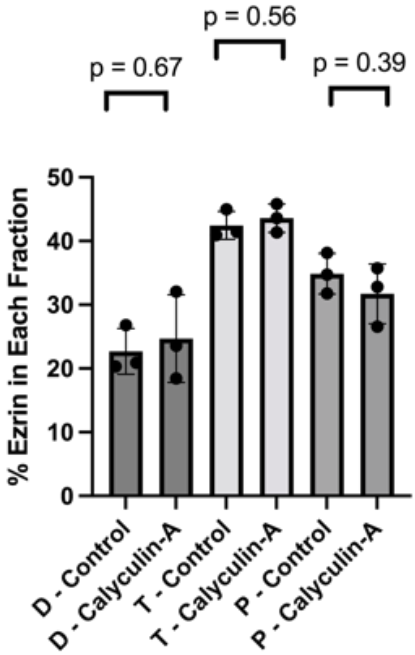

Figure 4.2: Ser/Thr phosphatase inhibition by Calyculin A does not translocate cytosolic CLIC5A to the membrane fraction in CLIC5$^{+/+}$ mouse **(Figure 4.2 continues next page)**

glomeruli. A. Differential detergent fractionation followed by western blot analysis of glomerular lysate isolated from CLIC5$^{+/+}$ mice treated with control (DMSO) or Calyculin-A 50 nM. GAPDH serves as control for cytoplasmic protein, ezrin and NHERF2 serve as control for peripheral membrane proteins, and nephrin and podocalyxin serve as integral membrane proteins. pERM serves as the calyculin-A treatment control. **B & C**. The % of total CLIC5A and the % of total ezrin graphs in the digitonin (D) fraction (cytoplasmic fraction), Triton X-100 (T) soluble membrane fraction, and insoluble pellet (P) or cytoskeletal fraction. (100% = sum of D + T + P; n = 3 independent experiments, mean ± SD, * <0.05, ** < 0.01, *** <0.001, two-way ANOVA and post-hoc Bonferroni tests). L represents total cell lysate.

Figure 4.3

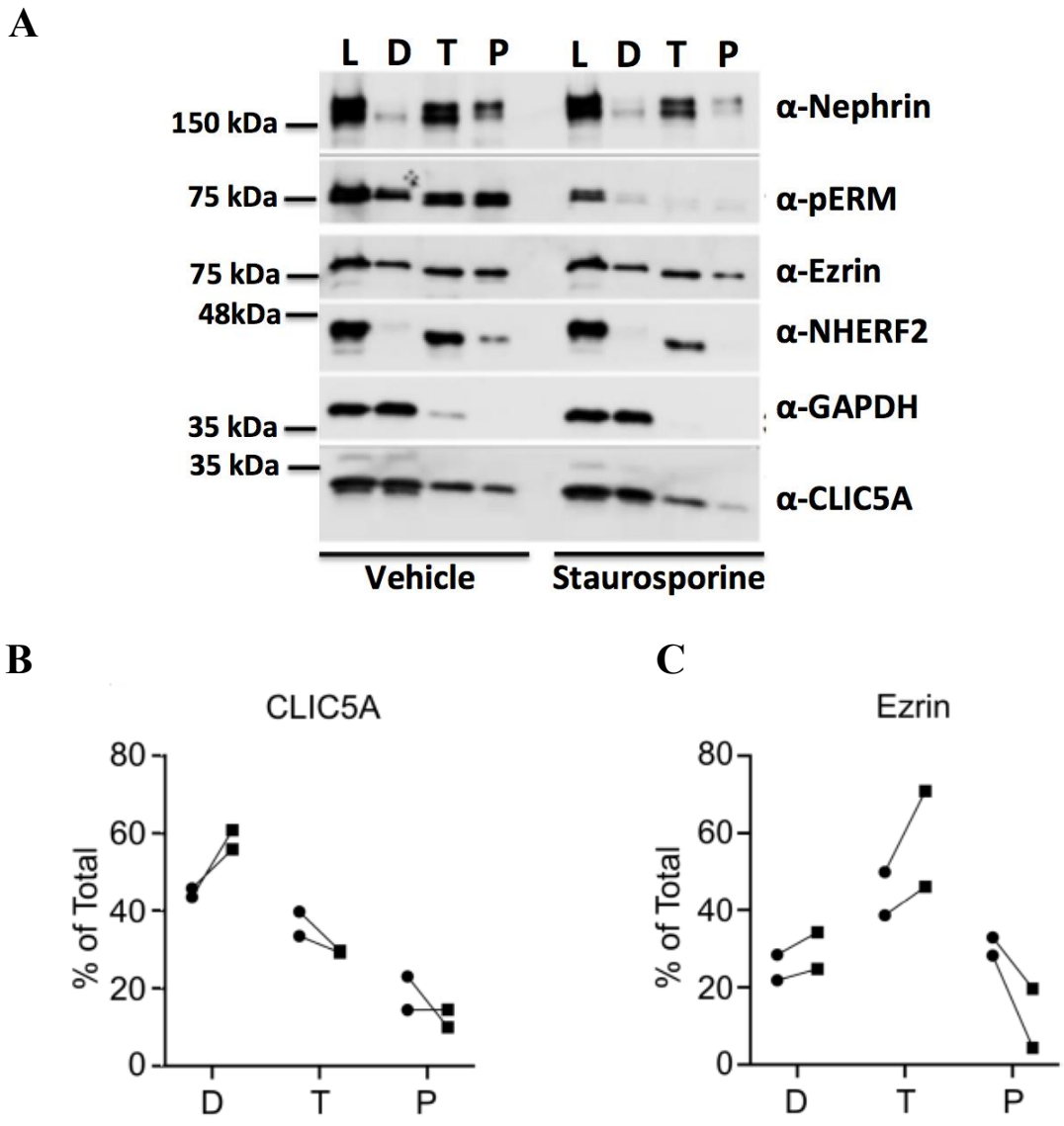

Figure 4.3: CLIC5A membrane association decreased with Staurosporine treatment in CLIC5$^{+/+}$ mice glomeruli. **A.** Differential detergent fractionation followed by western blot of lysate from isolated glomeruli of CLIC5$^{+/+}$ mice pre-treated with vehicle (DMSO) (•) or Staurosporine 100 nM (■) for 30 minutes. GAPDH: cytoplasmic protein control, ezrin and NHERF2: peripheral membrane proteins, and nephrin and podocalyxin: integral membrane proteins. pERM abolish serves as the Staurosporine treatment control. **B & C**. The % of total CLIC5A (left) and ezrin (right) graphs in the digitonin (D) fraction (cytoplasmic fraction), Triton X-100 (T) soluble membrane fraction, and insoluble pellet (P) fraction. L is total cell lysate.

Figure 4.4

A

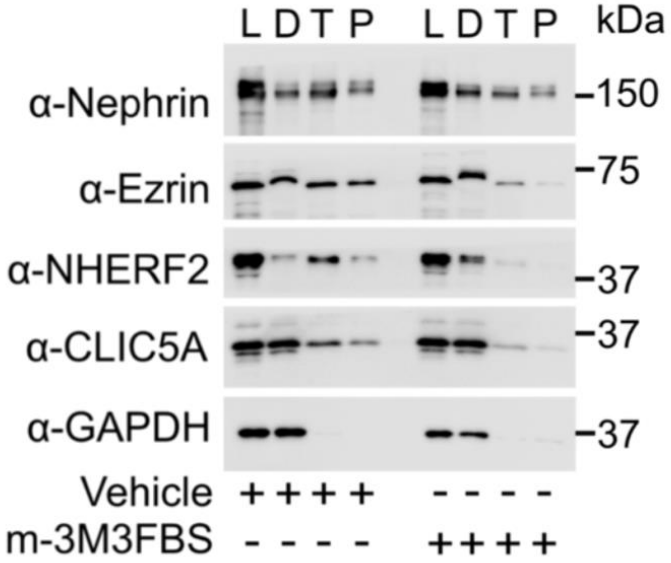

B

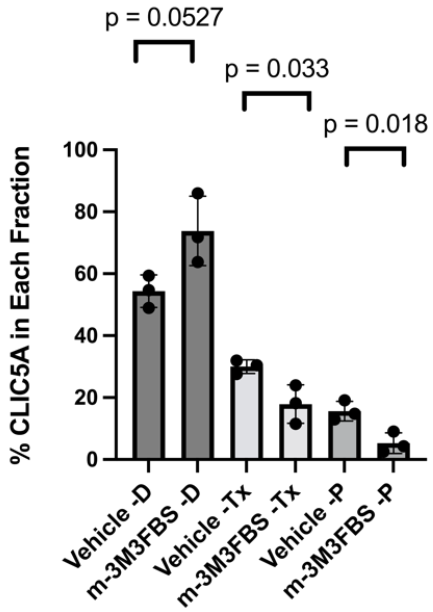

C

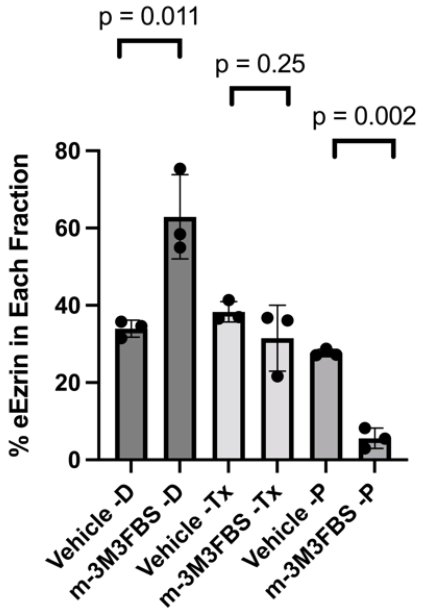

Figure 4.4 continues next page

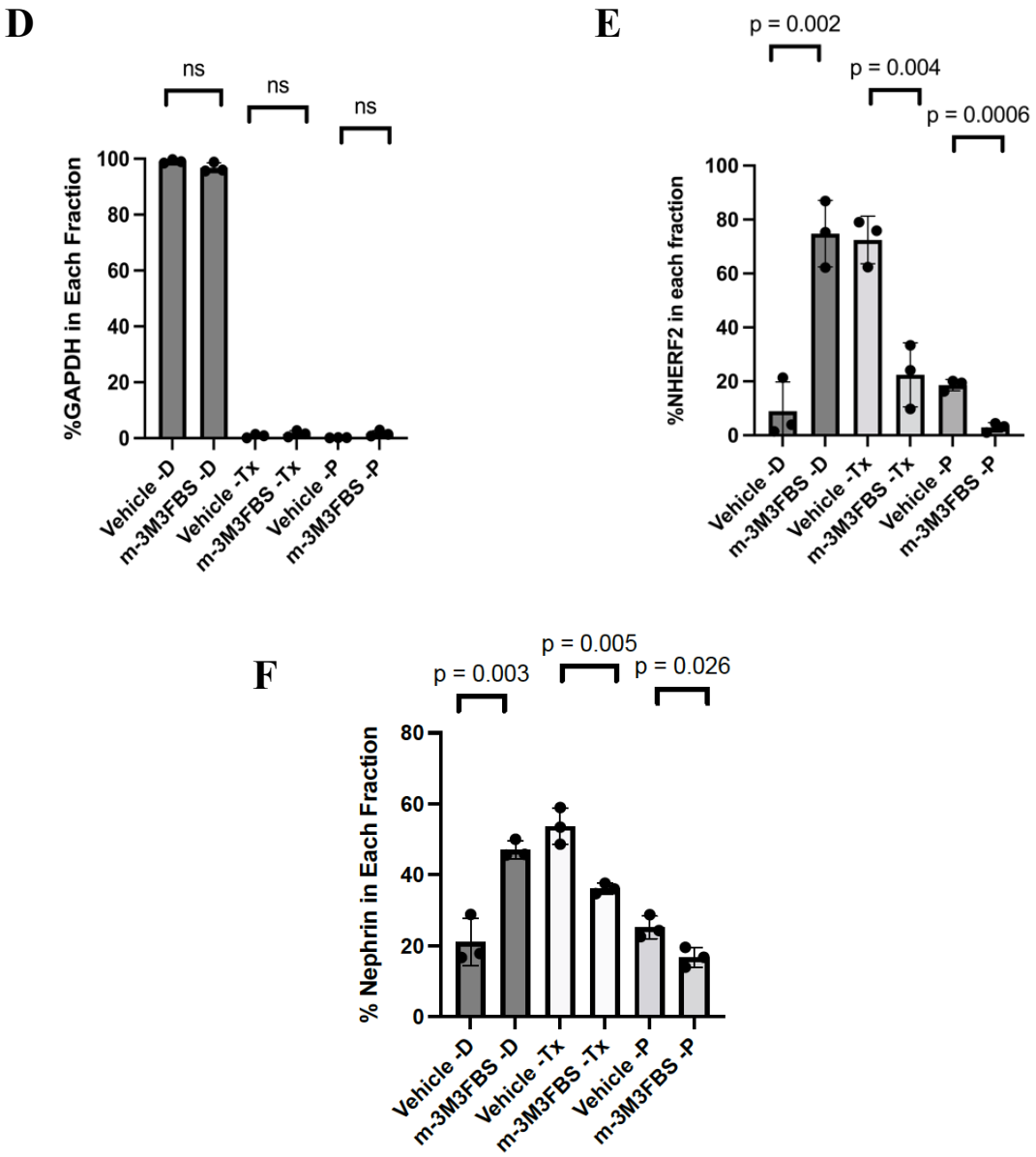

Figure 4.4: CLIC5A plasma membrane localization significantly reduces with PLC activator m-3M3FBS treatment. A. Differential detergent fractionation followed by western blot analysis of lysate from isolated glomeruli of CLIC5$^{+/+}$ mice treated with vehicle or the PLC activator m-3M3FBS (800 µM) for 30 min. Nephrin and podocalyxin serve as control for integral membrane proteins, NHERF2 and ezrin serve as control for peripheral membrane proteins, and GAPDH serves as control for soluble proteins. **B - F**. The % of total CLIC5A, ezrin, GAPDH, and NHERF2 proteins in the digitonin (D), Triton X-100 (T) and insoluble pellet (P) fractions. (100% = sum of D + T + P; n = 3 independent experiments, mean ± SD, * <0.05, ** < 0.01, *** <0.001, two-way ANOVA and post-hoc Bonferroni tests).

Figure 4.5

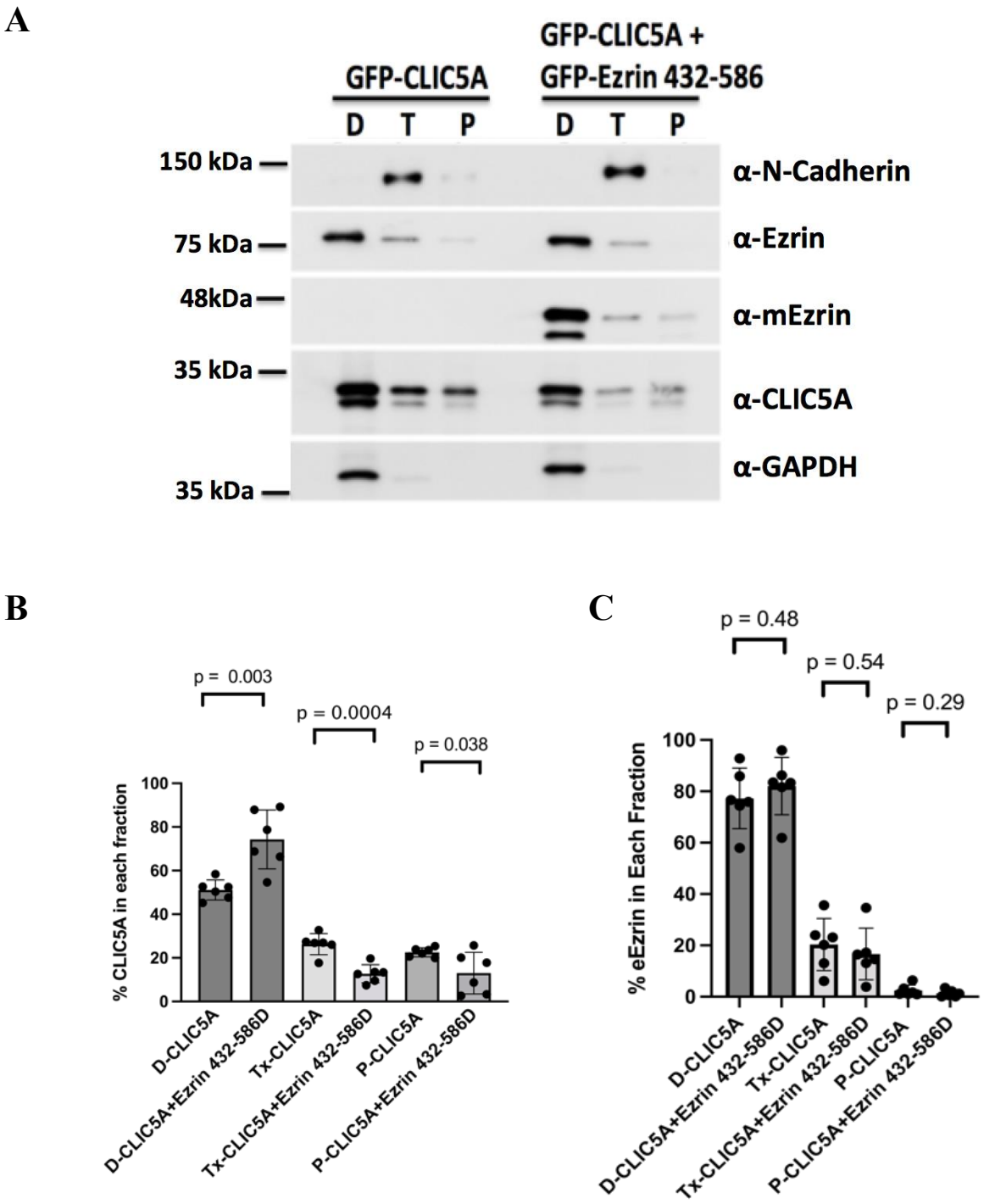

Figure 4.5: Ezrin 432-586 reduces association of CLIC5A with the membrane fraction. A. Differential detergent fractionation of COS-7 cells transfected with GFP-CLIC5A and GFP-ezrin 432-586D (mEzrin). Digitonin-soluble, Triton-X 100 soluble and (Figure 4.5 continues next page)

insoluble aggregates fractions were designated as D, T, and P respectively. **B & C**. The % of total CLIC5A and ezrin in the digitonin (D) (cytoplasmic) fraction, Triton X-100 (T) soluble membrane fraction, and insoluble pellet (P). (100% = sum of D + T + P; n = 3 independent experiments, mean ± SD, * <0.05, ** < 0.01, *** <0.001, two-way ANOVA and post-hoc Bonferroni tests).

Figure 4.6

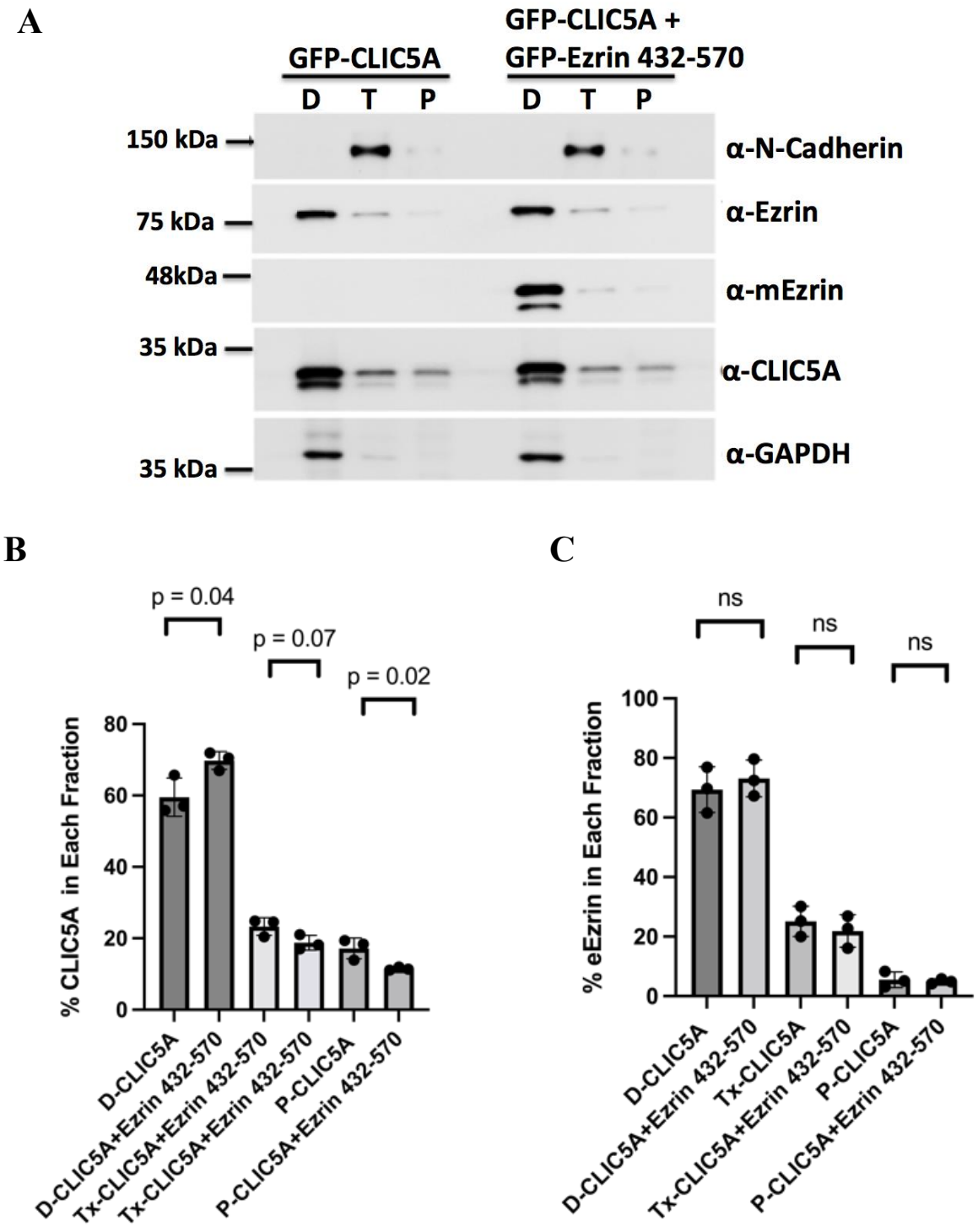

Figure 4.6: Ezrin 432-570 fails to reduce CLIC5A association with the membrane fraction.

A. Differential detergent fractionation followed by western blot (Figure 4.6 continues next page)

of lysates from COS-7 cells transfected with GFP-CLIC5A and GFP-ezrin 432-570 (mEzrin). Digitonin-soluble, Triton-X 100 soluble and insoluble aggregates fractions were designated as D, T, and P respectively. **B & C**. The % of total CLIC5A (left) and ezrin (right) graphs in the digitonin (D) (cytoplasmic) fraction, Triton X-100 (T) soluble membrane fraction, and insoluble pellet (P) or cytoskeletal fraction. (100% = sum of D + T + P; n = 3 independent experiments, mean ± SD, * <0.05, ** < 0.01, *** <0.001, two-way ANOVA and post-hoc Bonferroni tests).

Figure 4.7

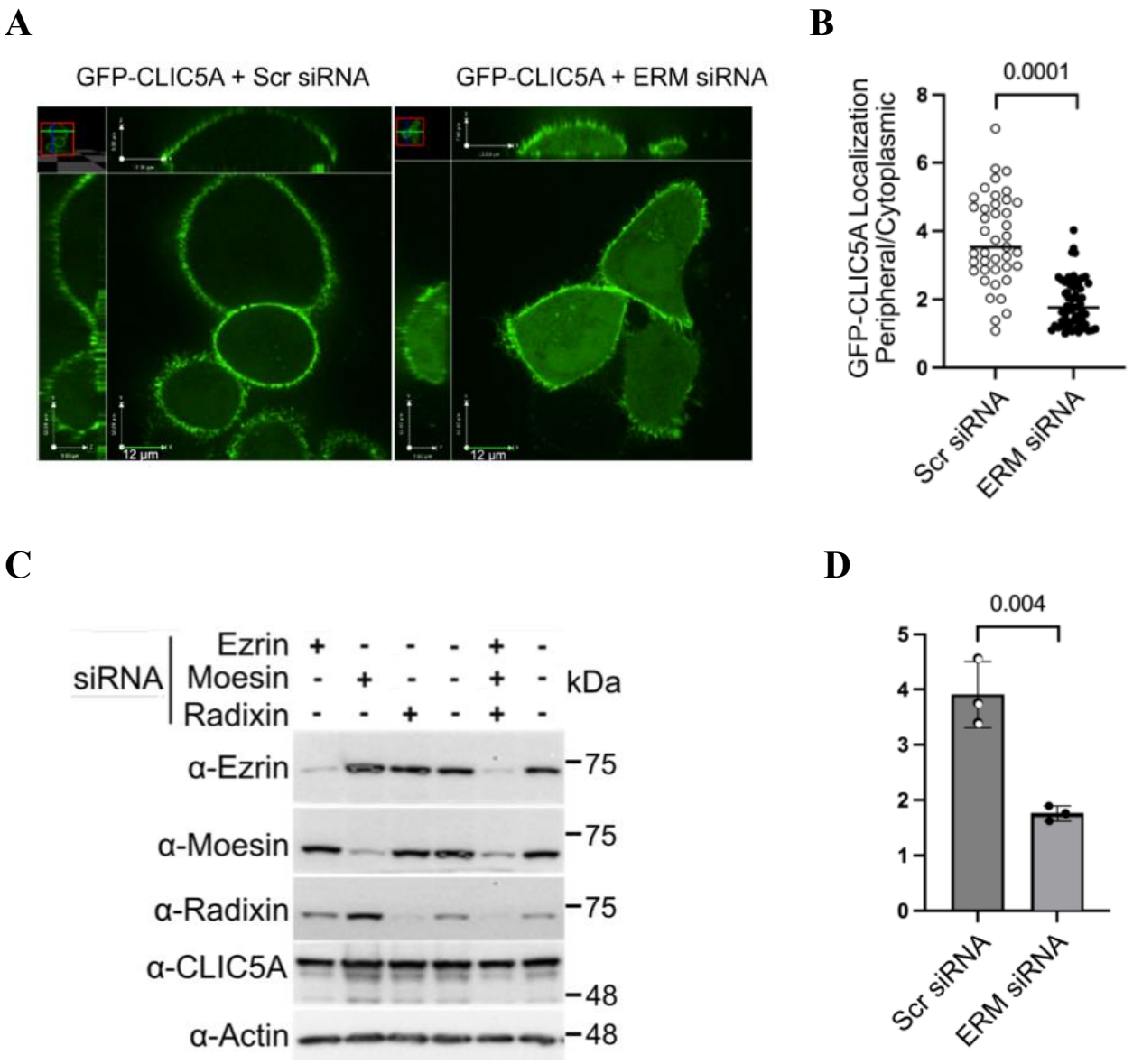

Figure 4.7: Triple ERM knockdown displaces CLIC5A from its peripheral location to cytoplasm. A. GFP-CLIC5A localization in HeLa cells transfected with non-specific scramble (Scr) siRNA or triple ezrin, moesin and radixin siRNA (ERM siRNA). **B.** Quantification of peripheral : cytoplasmic GFP in HeLa cells transfected with Scr or triple ERM siRNA from a single experiment (Student t-test). **C.** WB showing successful individual and triple ERM siRNA mediated knockdown in HeLa cells. **D.** Quantification of Scr or triple ERM siRNA knockdown in HeLa cells (mean ± SD, n = 3 independent experiments, Student t-test).

4.3. Discussion

This component of my thesis work sought to determine whether CLIC5A association with the membrane fraction could be shifted, which would be expected for a peripheral membrane protein. Cell fractionation experiments using glomeruli from CLIC5$^{+/+}$ mice revealed that endogenous CLIC5A is mostly recovered as a soluble protein, although a significant portion was also present in the Triton X-100 soluble "membrane" and the insoluble "cytoskeletal" fractions. The peripheral membrane protein ezrin was consistently most abundant in the membrane and cytoskeletal fractions, and less in the soluble fraction. Since CLIC5A interacts directly with ezrin (Chapter 3) and ezrin binds the integral membrane protein podocalyxin directly and via NHERF2 (184, 233), the presence of endogenous CLIC5A in the Triton X-100 soluble "membrane" fraction could be due to its binding to the ezrin/podocalyxin complex. Ezrin in the membrane fraction could be due to its association with PI4,5P2 and binding to transmembrane proteins like podocalyxin. We think that the recovery of ezrin from the detergent-insoluble "cytoskeletal" fraction is due to the association of active PI4,5P2-bound ezrin with cortical actin. Recovery of some endogenous CLIC5A from this fraction could be due to its association with the ezrin protein complex.

Since I found that the phosphomimetic ezrin fragment ezrin 432-586 (T567D) binds CLIC5A more strongly than wild-type ezrin 432-586 (Figure 3.10) we thought it was possible that changes in phosphorylation would change the association of endogenous CLIC5A with the Triton X-100 soluble and insoluble fractions. But Calyculin-A, which inhibits Ser/Thr phosphatases, and raised the levels of ezrin phosphorylation (Figure 4.2), reduced the cytosolic abundance of CLIC5A only by a very small degree and increased its association with the Triton X-100 membrane fraction by only ~4%, an effect that did not reach statistical significance. Ezrin phosphorylation

is known to stimulate its association with cortical actin (223, 226), and Berryman et al. (422) observed enhanced pull down of CLIC5A by purified GST-ezrin 556-586 protein when actin was added. Therefore, we reasoned that ezrin phosphorylation and actin/ezrin binding might stabilize the ezrin making it more accessible for CLIC5A binding. But enhanced ezrin phosphorylation did not even shift ezrin from the soluble to the membrane or cytoskeletal fractions. So, if the association of CLIC5A with the membrane and cytoskeleton is ezrin-dependent, then the failure of ezrin to shift in these experiments could explain why CLIC5A also moved only very little. Calyculin-A also did not have any effect on the association of the integral membrane proteins nephrin and podocalyxin, nor the peripheral proteins NHERF2 or ezrin with different subcellular fractions. Therefore, the experiment with Calyculin A was not very informative. It is still possible that phosphorylation of ERM proteins that might be partly responsible for a ~4% increase in CLIC5A abundance in the membrane fraction (Figure 4.2), but the change was very small.

While an increase in ezrin phosphorylation did not produce a significant change in the association of endogenous CLIC5A with different subcellular fractions, treatment of isolated glomeruli with Staurosporine resulted in dephosphorylation of ezrin and reduced the association of CLIC5A with the membrane fraction (Figure 4.3). In response to Staurosporine, ezrin dissociated from the insoluble cytoskeletal fraction and shifted to the membrane fraction, consistent with its continued association with PI4,5P2 and dissociation from actin. But Staurosporine would alter the phosphorylation state of many proteins, and even CLIC5A itself could be dephosphorylated and responsible for its shift from the membrane or the membrane bound protein complex. These questions still need to be investigated. Kim et al. (496) reported that a very small portion of ectopically expressed CLIC5A could translocate from the cytosol to

the membrane in COS-7 cells in response to Calyculin-A treatment but that phenomenon was not observed in my studies with endogenous CLIC5A. However, Kim et al (496) observed that the membrane abundance of overexpressed Flag-CLIC5A can be inhibited by Staurosporine-mediated dephosphorylation, consistent with my findings that endogenous CLIC5A in glomeruli can be depleted from the membrane and cytoskeletal fraction with Staurosporine treatment. This portion of the work therefore suggests that CLIC5A membrane localization is sensitive to phosphorylation.

The PLC activator m-3M3FBS-mediated hydrolysis of $P(4,5)P_2$ reduced the abundance of ezrin in HeLa cells and disrupts the association of ezrin with the actin cytoskeleton (189, 206, 213, 214, 226). Also, PLC activator m-3M3FBS treatment of COS-7 cells caused a rapid loss of PI4,5P2 clusters and overexpressed CLIC5A from the dorsal plasma membrane (89). Consistent with those previous findings, I observed that endogenous CLIC5A in glomeruli was displaced from the Triton X-100 membrane fraction by the PLC activator m-3M3FBS (Figure 4.4). Ezrin and NHERF2 were also shifted. The most likely reason for my finding is that the ezrin/actin interaction was disrupted by hydrolysis of PI4,5P2, causing CLIC5A no longer to be associated with the membrane fraction and cytoskeletal fractions. This finding is consistent with the hypothesis that CLIC5A is observed at the cell periphery when the stable ezrin/actin complex is intact. The peripheral membrane protein NHERF2 was also displaced from the membrane by phospholipase C activation, which could be due to displaced ezrin from the membrane periphery though NHERF2 might also lose its interaction with podocalyxin. Though the exact reason for the shift of endogenous CLIC5A from the membrane and cytoskeletal fractions in response to PI4,5P2 hydrolysis cannot be nailed down by these experiments, they do indicate that endogenous CLIC5A can become almost completely soluble, which makes it highly unlikely that

it is an integral membrane-spanning channel. However, since a small portion of endogenous CLIC5A persists in the membrane fraction even in the presence of PLC-mediated PI4,5P2 hydrolysis, the experiments do not completely rule out the possibility that some endogenous CLIC5A might bind to the plasma membrane through a direct interaction with the lipid bilayer.

To further investigate whether the location of CLIC5A in the membrane and cytoskeletal fractions depends on its interaction with ezrin I next turned to studies in cultured cells and overexpressed the phosphomimetic ezrin 432-586 (T567D). This ezrin fragment strongly binds CLIC5A (Figure 3.10) but cannot bind to the plasma membrane because it lacks the FERM domain. In the presence of ezrin 432-586 (T567D) less CLIC5A was found in the Triton X-100 fraction of COS-7 cells than in controls (Figure 4.5). Ezrin 432-570, which cannot bind CLIC5A, did not shift CLIC5A from membrane and cytoskeletal fractions (Figure 4.6). These experiments suggest that binding of CLIC5A to endogenous ezrin is disrupted by ezrin 432-586 (T567D) because this fragment of ezrin competes for CLIC5A binding, retaining it in the cytosol.

We postulated that because of CLIC5A/ezrin direct binding, ezrin might recruit CLIC5A to the apical plasma membrane. However, ezrin silencing in HeLa cells had only minor and inconclusive effects on CLIC5A localization. But when ezrin, radixin, and moesin were silenced simultaneously, a significant portion of GFP-CLIC5A failed to localize to the cell periphery (Figure 4.7), indicating that the interaction of CLIC5A with its ERM partners is partly responsible for its localization near the dorsal plasma membrane. Even so, there still was substantial peripheral GFP-CLIC5A when ezrin, radixin and moesin were silenced. Although it could be argued that this might be due to residual ERM protein expression, it is also possible that additional mechanisms target CLIC5A to its peripheral location. It also may seem surprising that CLIC5A is largely soluble as observed from our cell fractionation studies, yet it does not have a

cytosolic distribution when we observed it with live cell confocal imaging. While formal affinity studies were not done in this study, the affinity of CLIC5A for proteins in the cortical actin cytoskeleton must be low enough for it to be displaced from that location during cell permeabilization with digitonin. Also, since digitonin interacts directly with cholesterol (470), the membrane localization of CLIC5A may be cholesterol-dependent, as previously reported for CLIC1(471). Nevertheless, I can conclude from these experiments that the targeting of CLIC5A to the apical plasma membrane of cells is partially due to its interaction with the ERM proteins.

Therefore, while my data suggest that the location of CLIC5A at the dorsal/apical plasma membrane results from association with components of the cortical actin cytoskeleton complex like ezrin/radixin/moesin, I have not entirely ruled out the possibility of a direct association of CLIC5A with the inner leaflet of the plasma membrane. Taken together with previous findings by Berryman et al. (345) that despite its location at the apical plasma membrane, expressed CLIC5A does not alter chloride ion efflux, it seems safe to conclude that CLIC5A does not function as a plasma membrane-spanning chloride channel.

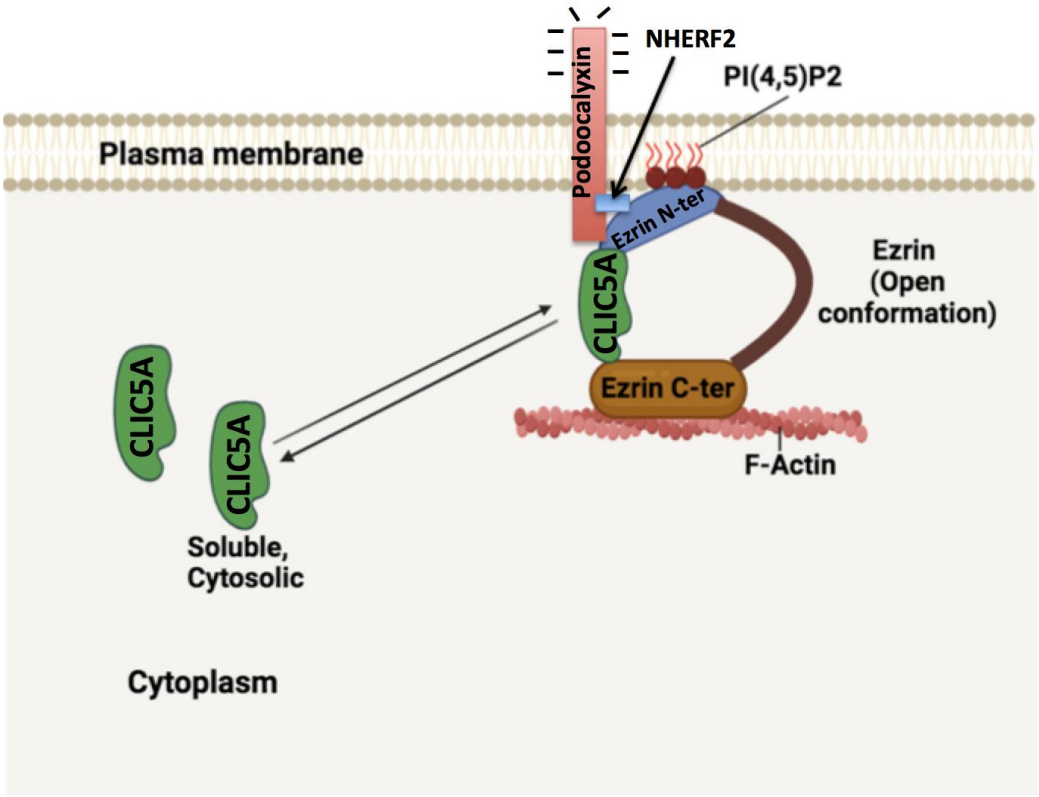

Figure 4.8: Model: CLIC5A can exist as soluble, cytoplasmic protein and also can localize to the cell periphery when bound to open conformation of ezrin, a peripheral membrane protein. CLIC5A at the cell periphery can also dissociate from the ezrin complex and becomes soluble, cytosolic protein. Thus CLIC5A is unlike the membrane spanning channel protein.

Chapter 5

A direct CLIC5A/ezrin interaction accounts for CLIC5A-dependent Rac1 activation and ERM phosphorylation

Chapter 5

A direct CLIC5A/ezrin accounts for CLIC5A-dependent Rac1 activation and ERM phosphorylation

5.1. Introduction

Podocyte foot process motility and remodeling in response to glomerular injury is at least partly mediated by Rac1 activation (123), and in its hyper-activated state Rac1 is involved in the pathogenesis of glomerulosclerosis (472, 473). Inactivating mutations of Rho GDP dissociation inhibitor “ARHGDIA”, and Rho GTPase activating protein "ARHGAP24" cause podocyte Rac1 hyperactivation and FSGS in humans. Podocyte-specific constitutively active Rac1 expression in mice also causes podocyte foot process effacement and FSGS, and ARHGDIA deletion in mice mimics human FSGS (153, 474, 475). Since Rac1 activity at the basal domain enhances cell motility, but CLIC5A is restricted to the apical domain of podocyte foot processes, at least in healthy mice, one might expect Rac1 activation during podocyte remodeling to be CLIC5A-independent. But Tavasoli et al. (86) found that DOCA/salt hypertension-induced podocyte Rac1 and ezrin activation are CLIC5A-dependent, and that hypertension-induced injury is more severe when Rac1 and ezrin activation were blocked in CLIC5-deficient mice. Blattner et al. (476) similarly found more severe glomerular injury in DOCA/Salt hypertensive mice with podocyte-specific Rac1 deletion. Reasoning that CLIC5A provides for location-specific Rac1 activation, we were looking for CLIC5A partners to find out how CLIC5A activates Rac1.

Importantly, the podocalyxin/ezrin complex activity can also enhance cell mobility through its the assembly at the basal domain, followed by dis-assembly, redistribution, and re-assembly of the complex at the apical domain (308, 309, 477, 478). This is an area of interest in oncology, where the podocalyxin/ezrin complex is considered as a potential therapeutic target (479).

Rac1-GTP also binds and activates PI4,5P2 generating kinases (175, 480, 481). The podocyte-predominant CLIC5A stimulates Rac1, which in turn, activates a lipid kinase PIP5K or PIP4K that generates apical plasma membrane PI4,5P2, causing ezrin activation (86, 89). Rac1 inhibition rapidly disrupted CLIC5A-induced PI4,5P2 cluster generation at the plasma membrane (86). Thus, CLIC5A-dependent Rac1 activation results in enhanced PI4,5P2 accumulation at the inner leaflet of the plasma membrane, leading to the open ezrin conformation and its phosphorylation.

This chapter will focus on the mechanism of action of CLIC5A protein and seek to define the potential functional relationship between CLIC5A, Rac1, and ezrin. Therefore, the objective of this chapter is as follows:

To determine how CLIC5A activates Rac1 and ERM proteins.

5.2. Results

5.2.1. CLIC5A, and PI4,5P2 generating kinases are part of the Rac1-GTP complex

Since CLIC5A activates Rac1 and Rac1-GTP binds and activates PIP lipid kinases [PI4,5P2 generating kinases] (175, 480, 481), we determined whether PIP kinases associate with the Rac1-GTP protein complex in cells expressing CLIC5A. We found that immobilized PAK-PBD not only precipitated more Rac1-GTP, but also brought down more PI4P5- and PI5P4-kinases in Flag-CLIC5A-expressing compared to vector-transfected cells. Furthermore, CLIC5A was also precipitated with Rac1-GTP and the PIP kinases (Figure 5.1). The data suggest that CLIC5A expression increases the formation of a protein complex containing CLIC5A and PIP kinases type I (PI4P5KIα) and type II (PI5P4KIIα) along with Rac1-GTP. Since the PAK-PBD interacts specifically with active Rac1-GTP, but not the inactive Rac1-GDP, the data indicate that CLIC5A expression results in Rac1 activation, which in turn brings PI4P5KIα and PI5P4KIIα isoforms and CLIC5A into the Rac1-GTP protein complex. However, these results do not tell us whether any specific PIP kinase isoform is involved in CLIC5A/Rac1-GTP complex.

5.2.2. Association of PI4P5Kα3 isoform with the Rac1-GTP requires CLIC5A

I next determined whether any specific isoform of PIP kinase is associated with the Rac1-GTP/CLIC5A protein complex. The PIP5KIα2 isoform was observed in CLIC5 deficient, but not in CLIC5 wild type kidney cortex lysates. By contrast, endogenous PIP5KIα3 was observed in kidney cortex lysates of the CLIC5 wild type, but not CLIC5 deficient mice (Figure 5.2). Endogenous PIP5KIγ was observed in both the CLIC5 wild type and knockout mice kidney cortex lysates. I also observed that the PIP5KIα3 isoform was precipitated with the Rac1-GTP from CLIC5 wild type, but not from CLIC5 knockout mouse kidney tissue lysates (Figure 5.3). Instead, in the absence of CLIC5A, PIP5KIγ, and PI5P4KIIα2 were precipitated with the Rac1-

GTP, whereas PI5P4KIIα1 was precipitated in both groups (Figure 5.3). Visiting scientist Xin Wang in our laboratory investigated the specificity of particular PIP kinase isoform in the Rac1-GTP complex using the kidney tissue lysates from the CLIC4 deficient, CLIC5 deficient and dual CLIC4/CLIC5 deficient as well as CLIC5 wild type mice (Figure 5.4). Her experiments also showed that PIP5KIα3 failed to precipitate with Rac1-GTP from the kidney cortex lysates of CLIC5 deficient and dual CLIC4/CLIC5 knockout mice, but PIP5KIα3 precipitated with the Rac1-GTP complex from the lysates of CLIC5 wild type and CLIC4 wild type mice (Figure 5.4). Also, PIP5KIγ and PI5P4KIIα2 precipitated with the Rac1-GTP from the CLIC5 knockout mice, and dual CLIC4/CLIC5 knockout mice tissue lysates (Figure 5.4). In the absence of CLIC4 and CLIC5A expression, PIP5KIγ and PI5P4KIIα2 expression increased, and these kinases precipitated with the Rac1-GTP. These findings suggest that CLIC5A-dependent Rac1 activation specifically targets PIP5KIα3, and that compensatory mechanisms lead to greater expression of PIP5KIγ and PI5P4KIIα2 and their association with Rac1-GTP.

Moreover, more phosphorylated ERM proteins (pERM) precipitated with the Rac1-GTP complex from kidney tissue lysates of wild-type mice than from dual CLIC5/CLIC4 deficient mice, indicating that pERM association in the Rac1-GTP complex is at least partly CLIC5 dependent. Our results support a possible mechanism by which CLIC5A-dependent Rac1 activation activates PIP5KIα3 which catalyzes the reaction that produces PI4,5P2 from PI(4)P at the inner leaflet of the plasma membrane, thus triggering ERM open up and leading to ERM phosphorylation.

5.2.3. Ezrin 432-586 expresses in the cytoplasm

Ezrin 432-586 does not have the N-terminus (1-296 aa) which makes it unable to bind to the PI4,5P2 at the cell membrane, while it retains the actin-binding site (ezrin 558-578 aa). As ezrin 432-586 turned out to be the region that strongly binds with CLIC5A in my Y2H mapping

results, I intended to observe the subcellular localization of ezrin 432-586 aa in cells. The live cell confocal imaging of HeLa cells overexpressing GFP-control, GFP-tagged ezrin 432-586 wild type, T567A (phosphorylation-deficient) or T567D (phosphomimetic) mutants showed that GFP-control protein is cytoplasmic as expected. The GFP-ezrin 432-586 wild type and T567A mutant were also found mainly in the cytoplasm but there was some localization at the cell periphery (Figure 5.5). The GFP-ezrin T567D localized more strongly to the cell periphery, although there still was cytoplasmic expression (Figure 5.5). This finding is not unexpected since phosphorylation of ezrin at Thr567 enhances actin binding.

5.2.4. Calyculin-A mediated ezrin phosphorylation increases its binding with CLIC5A

ERM proteins have a critically important phosphorylation site at the highly conserved C-terminal domain (T567 in human ezrin) (Appendix 1: ERM proteins alignment and critical phosphorylation site in ERM proteins). I therefore explored whether ezrin phosphorylation changes its interaction with CLIC5A using the ezrin 432-586 fragment. The Ser/Thr phosphatase inhibitor Calyculin-A significantly increased GFP-ezrin 432-586 aa (wild-type) pull-down by GST-CLIC5A from COS-7 cell lysates compared to vehicle (DMSO) treated cells (Figure 5.6, n = 3 independent experiments). In addition, endogenous ezrin was also pulled down more effectively by GST-CLIC5A in lysates from Calyculin-A treated cells, when compared to vehicle treated cells (Figure 5.6, ezrin blot). Increased pERM abundance in the input (cell lysate) with Calyculin-A treatment serves as proof for effective Calyculin-A treatment (Figure 5.6, pERM blot). Increased pERM was also pulled down by GST-CLIC5A in response to Calyculin-A treatment (Figure 5.6, pERM blot). These results imply that the phosphorylated form of endogenous ezrin, and probably also radixin, and moesin proteins have a stronger affinity for CLIC5A than the unphosphorylated forms.

5.2.5. Staurosporine-mediated dephosphorylation of ezrin reduced CLIC5A/ezrin binding

I next investigated the effect of Staurosporine on CLIC5A/ezrin interaction. Staurosporine is a broad-spectrum inhibitor of protein kinases particularly protein kinase C, cAMP-dependent protein kinase and p60v-src kinase, cyclic AMP-dependent protein kinase (PKA), phosphorylase kinase, ribosomal protein S6 kinase, epidermal growth factor receptor (EGF-R) kinase and Ca2+/calmodulin-dependent protein kinase II (Ca/CaM PKII). I transfected HA-ezrin 432-586 cDNA before treating COS-7 cells with Calyculin-A, or DMSO (vehicle) or Staurosporine, followed by cell lysis, cell lysate preparation, and the lysates were used for GST- or GST-CLIC5A pull down. I found that the overexpressed HA-ezrin 432-586 (~25 kDa) and endogenous ezrin (~75 kDa) were pulled down less effectively by GST-CLIC5A from lysates of Staurosporine-treated cells compare to those from vehicle (DMSO) or Calyculin-A treated cells (Figure 5.7. α-ezrin blot). The α-pERM blot shows that phosphorylated ERM proteins were also pulled down much less by GST-CLIC5A from lysates of Staurosporine treated cells compared to lysates from vehicle (DMSO) or Calyculin-A treated cells. As expected, Calyculin-A mediated phosphorylation caused the most ezrin 432-586 pull down by GST-CLIC5A. These data imply that Staurosporine effectively inhibited protein kinases resulting in dephosphorylation of endogenous ERM proteins and that the dephosphorylated ERM proteins have a lower affinity for CLIC5A.

5.2.6. Phosphomimetic ezrin 1-586 colocalizes with CLIC5A at the cell periphery

When full-length wild-type GFP-ezrin (1-586 aa) was overexpressed in HeLa cells, it localized predominantly in the cytosol (Figure 5.8), consistent with the findings previously described by Auvinen et al. (482). In the same cells, RFP-CLIC5A localized predominantly to the dorsal cell periphery, consistent with the previous findings observed in COS-7 cells (89). Some punctate co-

localization of RFP-CLIC5A with wild-type GFP-ezrin was also observed at the cell periphery (Figure 5.8). By contrast, when the HeLa cells were transfected with GFP-ezrin 1-586 cDNA having the (T567D) phosphomimetic point mutation, it was localized to the cell periphery where it strongly co-localized with RFP-CLIC5A. Phosphorylation of ezrin at the T657 site results in ezrin targeting cortical actin without the necessity of PI4,5P2 binding was previously reported by Fievet et al. (226). This finding supports the theory that CLIC5A interacts with full-length ezrin when the ezrin C-terminus is free of its intramolecular interaction with the ezrin N-terminal FERM domain.

5.2.7. Phosphomimetic ezrin 432-586 T567D enhances its interaction with CLIC5A

To strengthen the observations that ezrin phosphorylation enhances CLIC5A/ezrin binding, I transfected COS-7 cells with the following cDNAs: GFP-ezrin 432-586 wild type, phosphorylation deficient GFP-ezrin 432-586 T567A, and phosphomimetic GFP-ezrin 432-586 T567D point mutants. GST-CLIC5A pulled down significantly more of the GFP-ezrin 432-586 T567D phosphomimetic mutant compared to the GFP-ezrin 432-586 wild type or ezrin 432-586 T567A (Figure 5.9). Moreover, GST-CLIC5A pulled down much less phosphorylation deficient GFP-ezrin T567A even compared to the wild-type form. Together, the findings from Figures 5.6 to Figure 5.9 strongly suggest that ezrin phosphorylation at T567 significantly enhances its affinity for CLIC5A.

5.2.8. Functional consequences of ezrin 432-586 (T567D)/CLIC5A interaction

Because ezrin 432-586 T567D phosphomimetic mutant strongly binds CLIC5A, we reasoned that overexpression of this ezrin fragment in cells might competitively inhibit the CLIC5A/endogenous ezrin interaction. When increasing concentrations of GFP-ezrin 432-586(T567D) were co-expressed with a constant concentration of GFP-CLIC5A in COS-7 cells,

CLIC5A-dependent phosphorylation of endogenous ERM proteins was inhibited in a concentration-dependent fashion, and the association of endogenous ezrin with the insoluble "cytoskeletal" fraction (pellet) was reduced (Figure 5.10). The total ezrin and moesin abundance remained unchanged relative to the actin and GAPDH as loading controls. Similarly, when GFP-ezrin 432-586(T567D) was expressed at an 8-fold excess over GFP-CLIC5A, CLIC5A-stimulated Rac1 activation was significantly reduced (Figure 5.11). The total Rac1 and GFP-CLIC5A abundance did not differ. These data suggest that overexpressed ezrin 432-586 T567D competitively binds overexpressed CLIC5A, reducing CLIC5A-stimulated endogenous ERM phosphorylation and Rac1 activation in a concentration-dependent fashion.

5.2.9. Ezrin 432-570 fails to block CLIC5A-dependent ERM and Rac1 activation

Co-expression of GFP-ezrin 432-570, which does not bind CLIC5A, also at an 8-fold excess over GFP-CLIC5A was undertaken to determine whether it can block CLIC5A-dependent ERM phosphorylation and Rac1 activation. I observed that GFP-ezrin 432-570 aa failed to block CLIC5A-stimulated ERM phosphorylation (Figure 5.12), in keeping with the idea that ezrin 432-570 aa which cannot bind CLIC5A would not interfere with binding of CLIC5A to endogenous ERM proteins or their activation. Moreover, when co-expression of GFP-ezrin 432-570 at an 8-fold excess over GFP-CLIC5A also failed to block CLIC5A-stimulated Rac1 activation (Figure 5.13). This experiment supports the conclusion that ezrin 432-586(T567D), but not ezrin 432-570 can competitively inhibit CLIC5-dependent functions in cells.

5.2.10. CLIC5A requires ezrin for Rac1 activation

It was previously reported by our laboratory that CLIC5A expression activates Rac1and its downstream effector PAK1/3 in cultured cells and *in vivo*, and that but not RhoA or Cdc42 were not stimulated by CLIC5A in cultured cells (86). ERM proteins were previously shown to

facilitate activation of Rho GTPases by binding and sequestering the Rho GDP dissociation inhibitor (Rho-GDI) (234). We therefore determined whether CLIC5A-dependent Rac1 activation requires ezrin. First, we transduced cultured human glomerular endothelial (human glomerular EC) cells with untagged CLIC5A from an adenoviral construct at different MOI (MOI: multiplicity of infection) and observed a concentration-dependent increase in Rac1-GTP abundance (Figure 5.14.A). siRNA-mediated knockdown of endogenous ezrin in these cells (Figure 5.14.B) significantly reduced CLIC5A-stimulated Rac1 activation compared to control siRNA treated cells (Figure 5.14.C). These data suggest that CLIC5A requires endogenous ezrin to activate Rac1, and are consistent with the view that the interaction of CLIC5A with ezrin is required for Rac1 activation.

5.2.11. CLIC5A expression enhances co-immunoprecipitation of Rho GDI with ezrin

The ERM proteins act as a Rho GDI displacement factor (GDF) for Rho GTPases, releasing Rho GTPases from Rho GDI-mediated inhibition (464) and allowing Rho GTPase activation by Rho GEFs (483). Since CLIC5A activates ezrin and ezrin is required for CLIC5A-depenent Rac1 activation, I next determined whether CLIC5A expression enhances Rho GDIα binding to ezrin. HeLa cells were transiently transfected with GFP or GFP-CLIC5A cDNAs, followed by co-immunoprecipitation of endogenous ezrin with using a rabbit α-ezrin antibody. I observed that showed that endogenous ezrin was effectively immunoprecipitated with this antibody, and that Rho GDIα was observed in the ezrin immunoprecipitate from cells expressing GFP-CLIC5A, but not from cells expressing in GFP alone (Figure 5.15). GFP-CLIC5A also precipitated with the ezrin/Rho GDIα complex. These results suggest that the mechanism by which CLIC5A expression increases Rac1 activity is due, at least in part, to sequestration of Rho GDIα by activated ezrin.

Figure 5.1

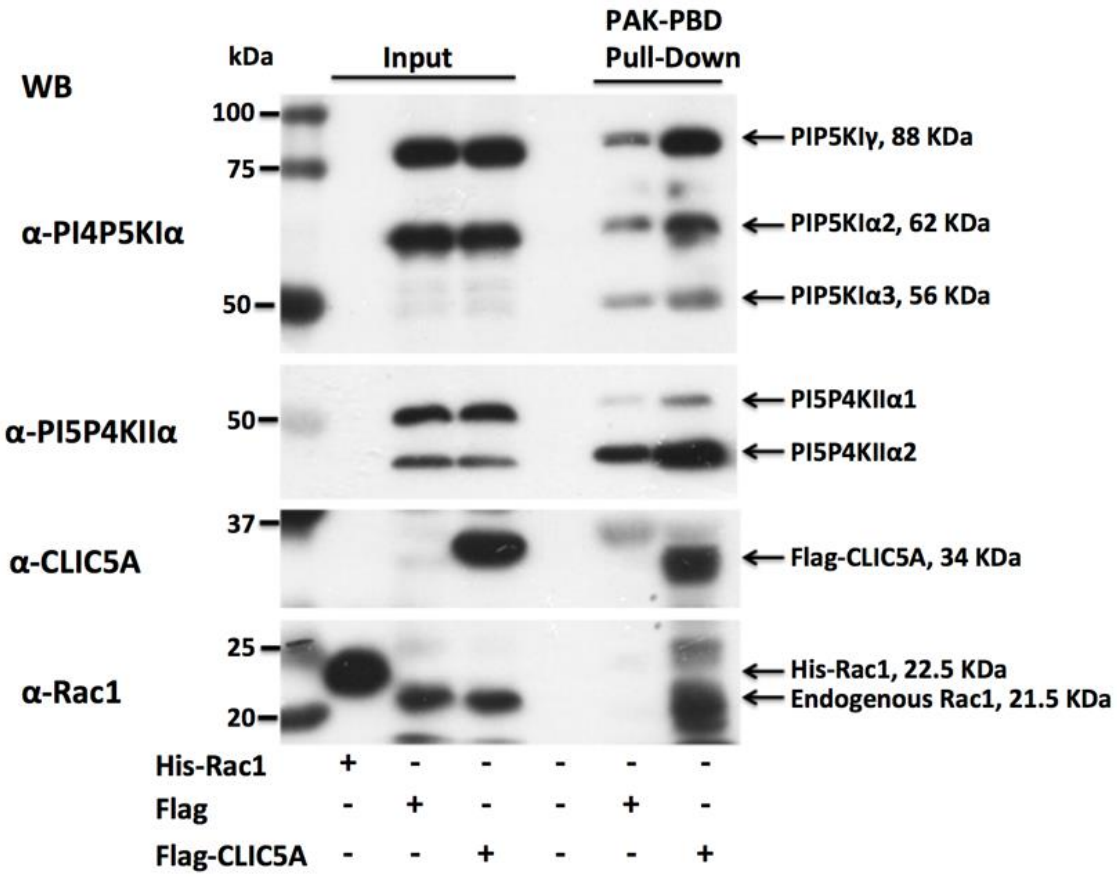

Figure 5.1: CLIC5A, PIP Kinases are part of the Rac1-GTP protein complex. Western blot (WB) with antibodies directed against Rac1, PIP Kinases and CLIC5 showing input (cell lysate) and PAK-PBD pull down results. HEK293 cells were transfected with Flag- or Flag-CLIC5A cDNAs and the cell lysates were incubated with PAK-PBD beads. The beads were precipitated, washed, and bead-associated proteins eluted and detected by WB.

Figure 5.2

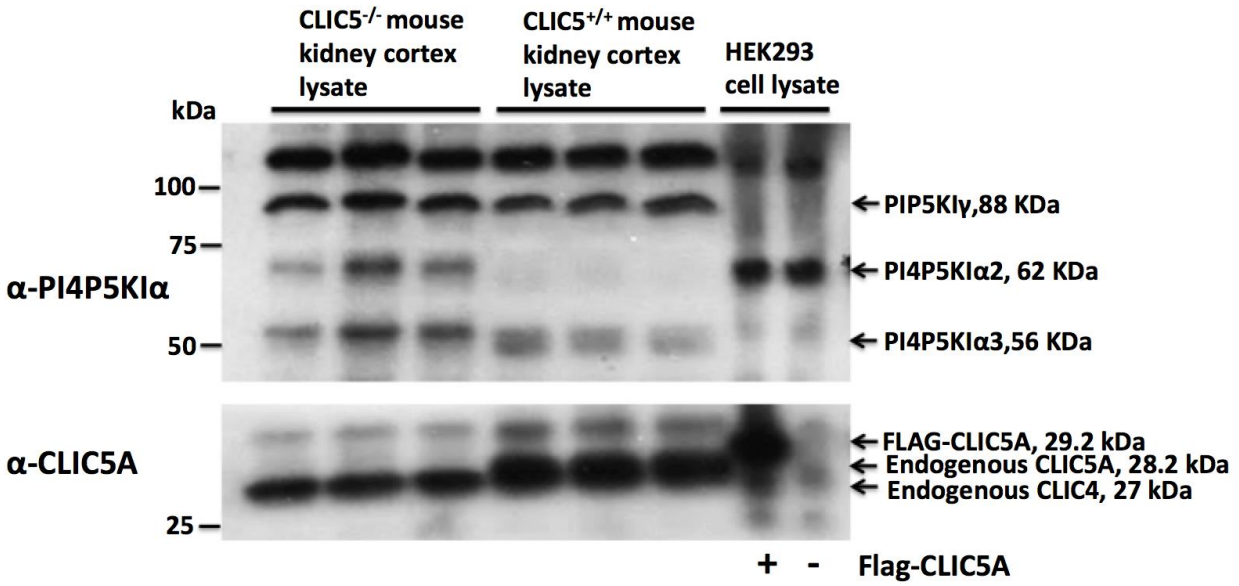

Figure 5.2: CLIC5-deficient mice kidney cortex tissue is enriched with PI4P5KIα2, but not with PI4P5KIα3 isoform. Western blot (WB) analysis with antibodies directed against PI4P5KIα and CLIC5A showing endogenous PI4P5KIα isoforms (top blot) and endogenous CLIC5A (bottom blot).

Figure 5.3

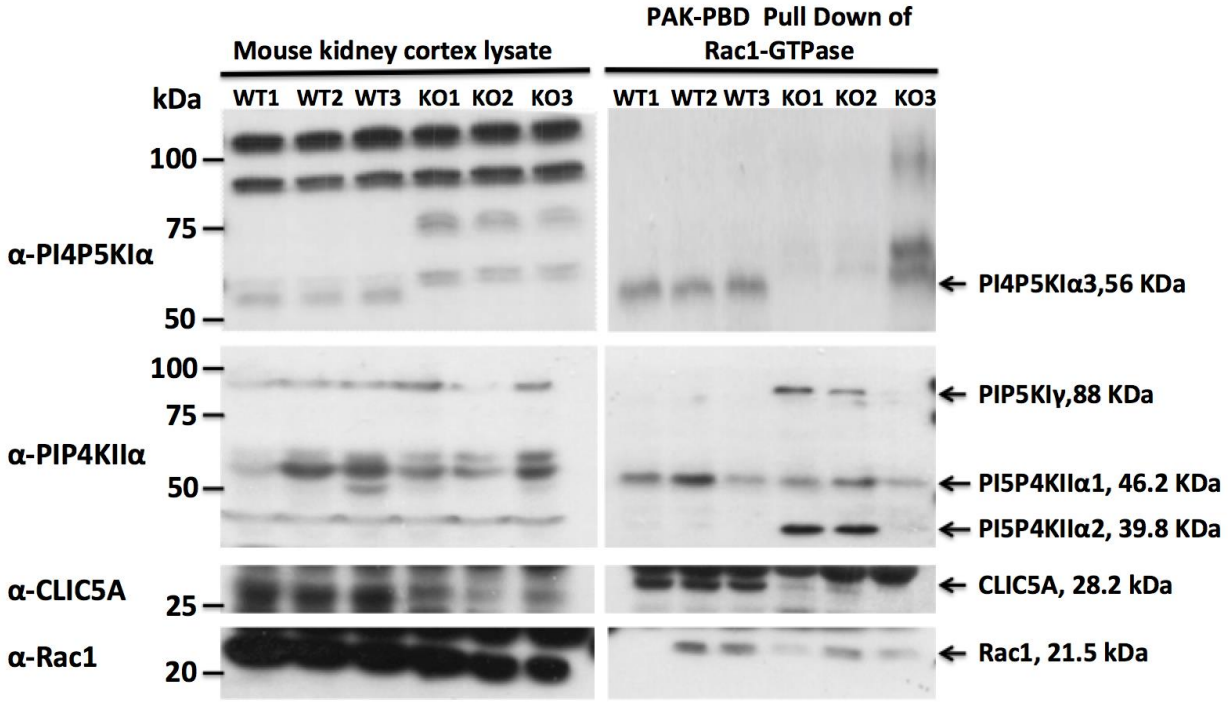

Figure 5.3: *In vivo*, the association of PI4P5Kα3 and Rac1-GTP requires CLIC5A. Rac1-GTP pull-down (PAK-PBD pull down) of PIP Kinases from lysates of kidney cortex from CLIC5A$^{+/+}$ (wild-type 1, 2 and 3 mice) and CLIC5A$^{-/-}$ (knock-out 1, 2 and 3 mice) mice, followed by western blot analysis with antibodies directed against PI4P5KIα, PI5P4KIIα, CLIC5A and Rac1. Each lane represents a distinct mouse.

Figure 5.4

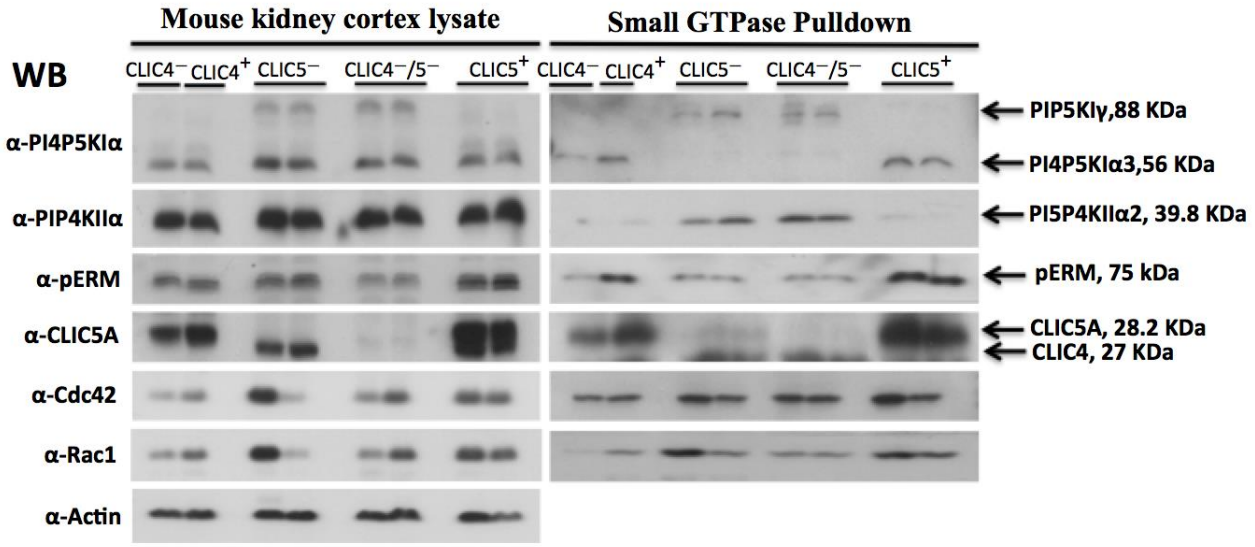

Figure 5.4: *In vivo*, the precipitation of phosphorylated ERM proteins (pERM) and PI4P5Kα3 with the Rac1-GTP complex requires CLIC5A and CLIC4. Small GTPases pull-down of PIP Kinases, pERM, CLIC5A, Cdc42, and Rac1 from lysates of kidney cortex from CLIC4$^{-/-}$or CLIC4$^{+/+}$, CLIC5$^{-/-}$, CLIC4$^{-/-}$/CLIC5$^{-/-}$, CLIC5$^{+/+}$, followed by western blot analysis with antibodies directed against PI4P5KIα, PI5P4KIIα, pERM, CLIC5A, Cdc42, Rac1 and actin. Each lane represents a distinct mouse.

Figure 5.5

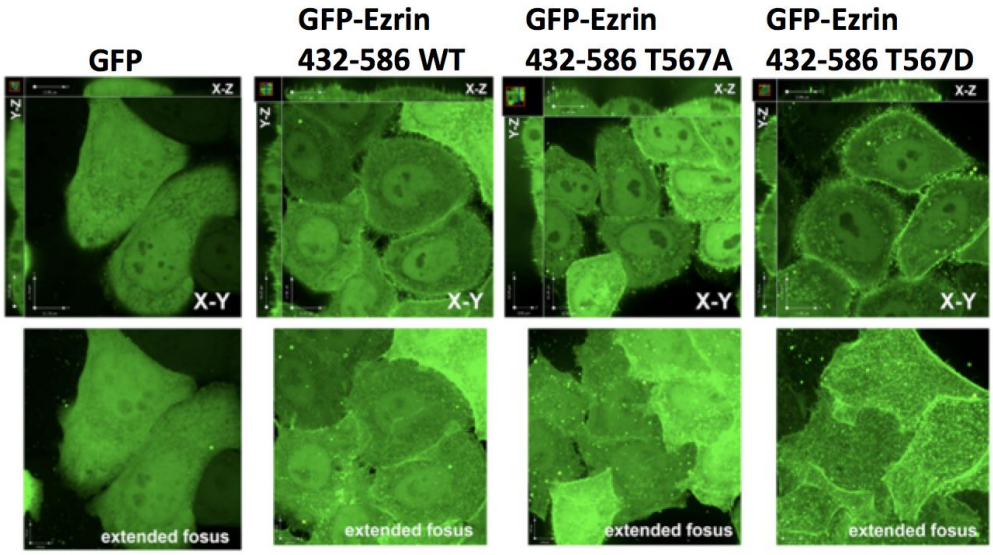

Figure 5.5: Ezrin 432-586 expresses both at the cytoplasm and at or near the cell membrane. Confocal microscopy imaging of cultured HeLa cells transfected with GFP-, or GFP-ezrin 432-586 WT, or GFP-ezrin 432-586 T567A (T for threonine, A for Alanine), GFP-ezrin 432-586 T567D (D for Aspartic acid) cDNA constructs. GFP fluorescence revealed overexpressed proteins. Bottom panels are extended focus of overexpressed proteins.

Figure 5.6

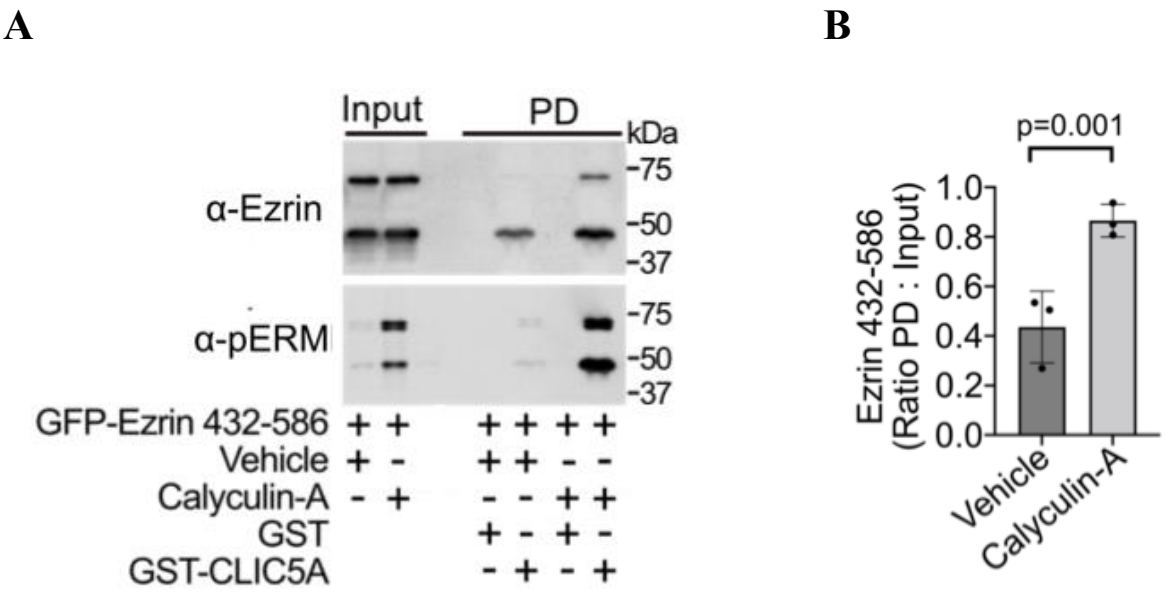

Figure 5.6: Calyculin-A induced ezrin phosphorylation enhances its binding to CLIC5A. A. Western blot with α-ezrin and α-pERM (phosphorylated ERM) antibodies of COS-7 cell lysates (input) and proteins from GST-/GST-CLIC5A pull down from lysates of cells transfected with GFP-ezrin 432-586 cDNA construct cells, treated with vehicle (DMSO) or Calyculin A (50 nM) for 30 minutes prior to cell lysis. **B.** Densitometric quantification of GFP-ezrin 432-586 pulled down by GST-CLIC5A from cells treated without or with Calyculin A (mean ± SD, n = 3 independent experiments).

Figure 5.7

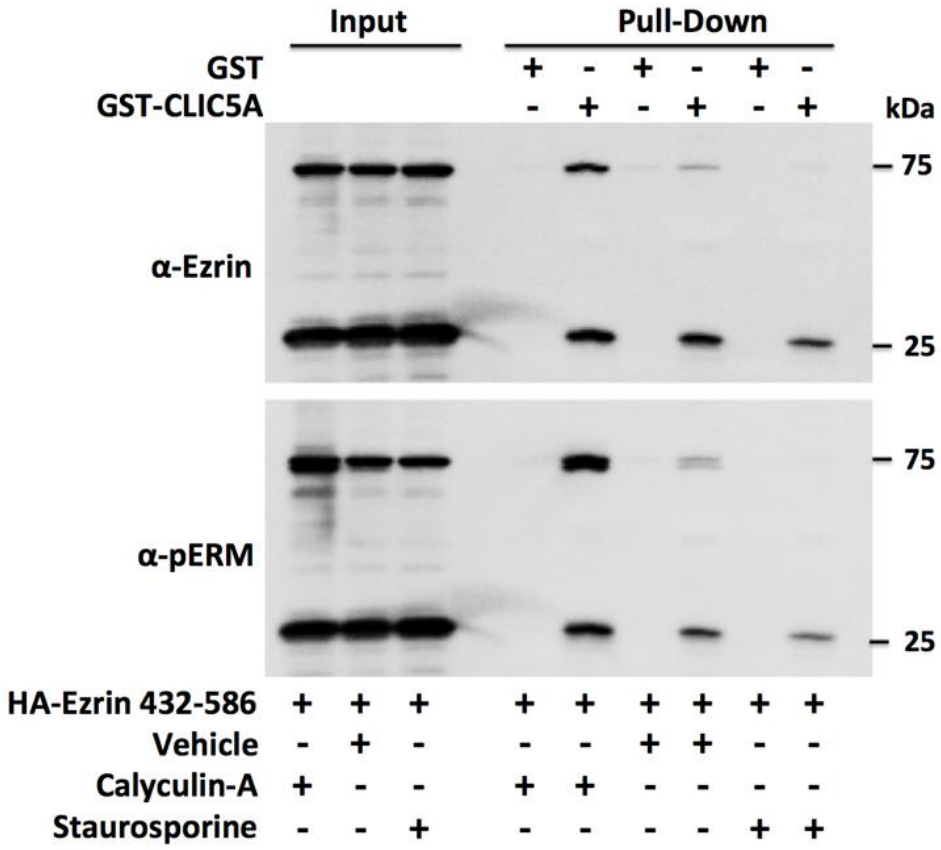

Figure 5.7: Staurosporine mediated inhibition of ezrin phosphorylation reduced ezrin binding to CLIC5A. Western blot with α-ezrin and α-pERM antibodies of COS-7 cell lysates (input) and proteins from GST-/GST-CLIC5A precipitates from lysates of cells transfected with HA-ezrin 432-586 cDNA construct and treated with Calyculin A (50 nM), vehicle (DMSO), or Staurosporine (20 nM) for 30 minutes prior to cell lysis.

Figure 5.8

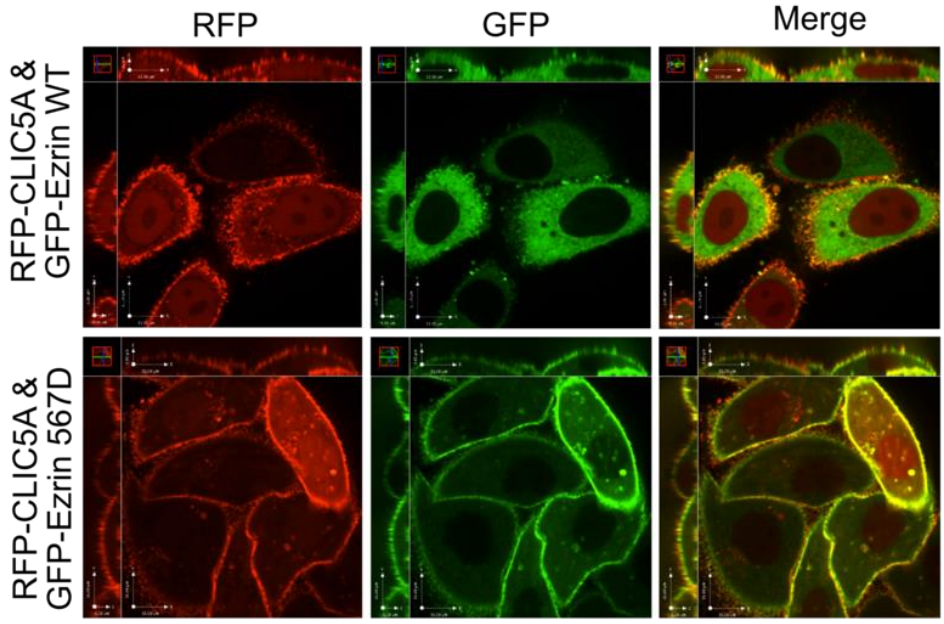

Figure 5.8: CLIC5A colocalizes with phosphomimetic ezrin at the cell periphery. Co-transfection of RFP-CLIC5A and GFP-ezrin 1-586 full-length wild type (WT) or GFP-ezrin 1-586 full-length phosphomimetic (T567D) mutant cDNA constructs in HeLa cells. Co-localization (Merge, yellow) is observed at the cell periphery in HeLa cells expressing RFP-CLIC5A and phosphomimetic ezrin full-length.

Figure 5.9

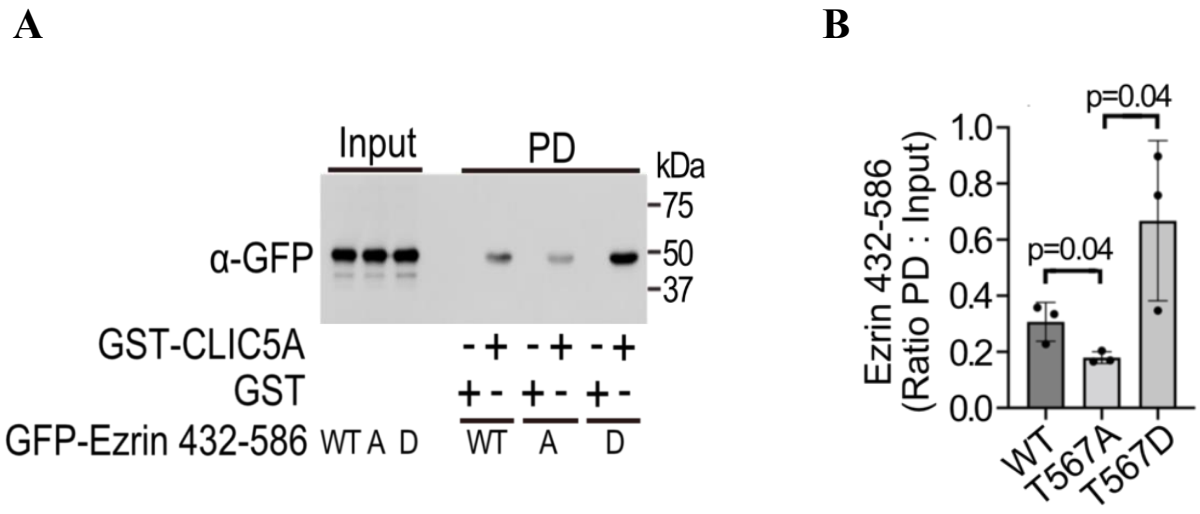

Figure 5.9: Ezrin 432-586 (T567D) phosphomimetic point mutation enhances its association with CLIC5A. A. Western blot with anti-GFP antibody of total cell lysate (Input) and GST or GST-CLIC5A pull-down (PD) from lysates of COS-7 that had been transfected with GFP-ezrin 432-586 (WT), phosphorylation deficient GFP-ezrin 432-586 T567A ("A" for alanine) or phosphomimetic GFP-ezrin 432-586 T567D ("D" for aspartic acid). **B.** Densitometric quantification of the distinct GFP-ezrin 432-586 mutants pulled from the lysates by GST-/GST-CLIC5A immobilized on glutathione bead (mean ± SD, n = 3 independent experiments).

Figure 5.10

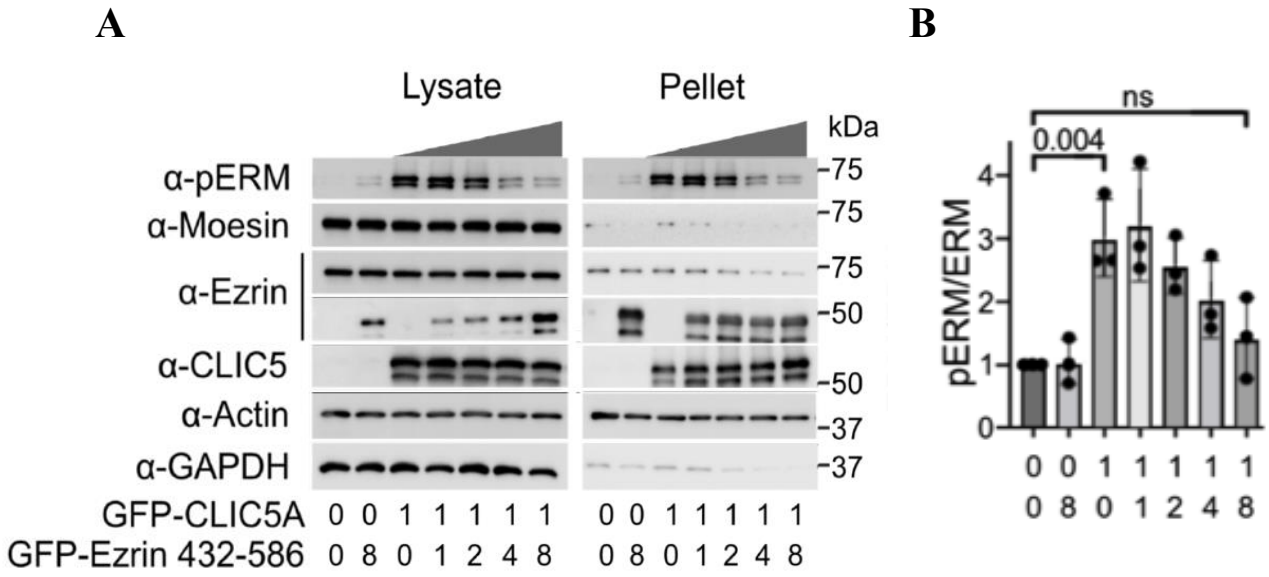

Figure 5.10: Ezrin 432-586 expression inhibits CLIC5A-stimulated ERM phosphorylation. **A.** Representative western blot showing pERM abundance in COS-7 cells transfected with GFP-CLIC5A cDNA with or without a 8-fold excess of GFP-ezrin 432-586 cDNA. GFP-CLIC5A was kept constant and the GFP-CLIC5A : ezrin 432-586 (T567D) transfection ratio was 1:1, 1:2, 1:4 and 1:8. Protein bands showing at around ~48 kDa in ezrin blot represents the over expressed GFP-ezrin 432-586. **B.** Densitometric quantification of the pERM : ezrin ratio (mean ± S.D., n = 3 independent experiments).

Figure 5.11

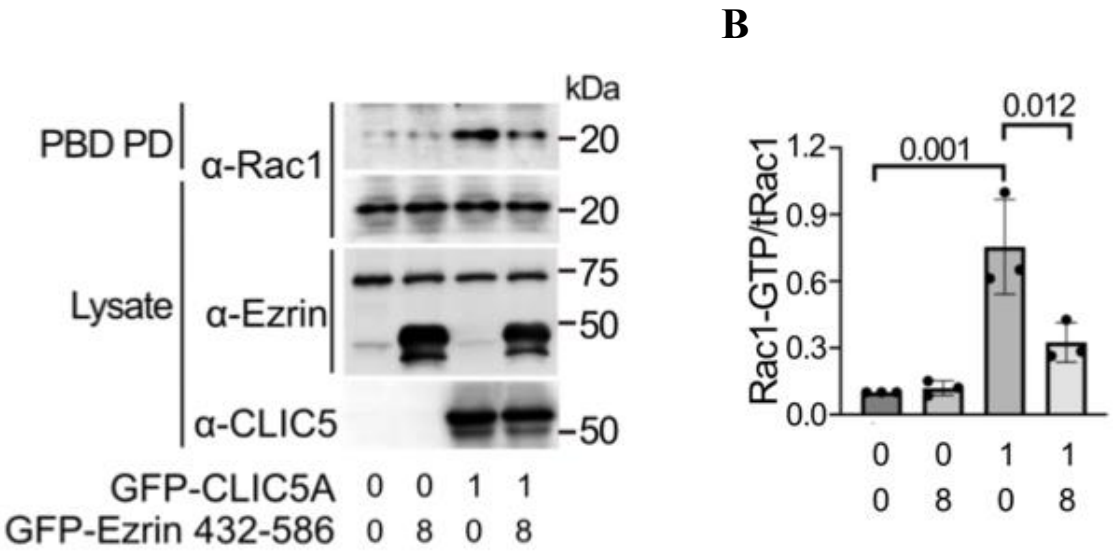

Figure 5.11: Ezrin 432-586 expression blocks CLIC5A-stimulated Rac1 activation. A. Representative anti(α)-Rac1 western blot showing PAK-PBD pull-down (PD) of Rac1-GTP from lysates of COS-7 cells transfected with GFP-CLIC5A cDNA with or without a 8-fold excess of GFP-ezrin 432-586(T567D) cDNA. Protein bands showing at around ~48 kDa in ezrin blot represents the over expressed GFP-ezrin 432-586. **B**. Densitometric quantification of Rac1-GTP/total Rac1 (mean ± S.D., n = 3 independent experiments).

Figure 5.12

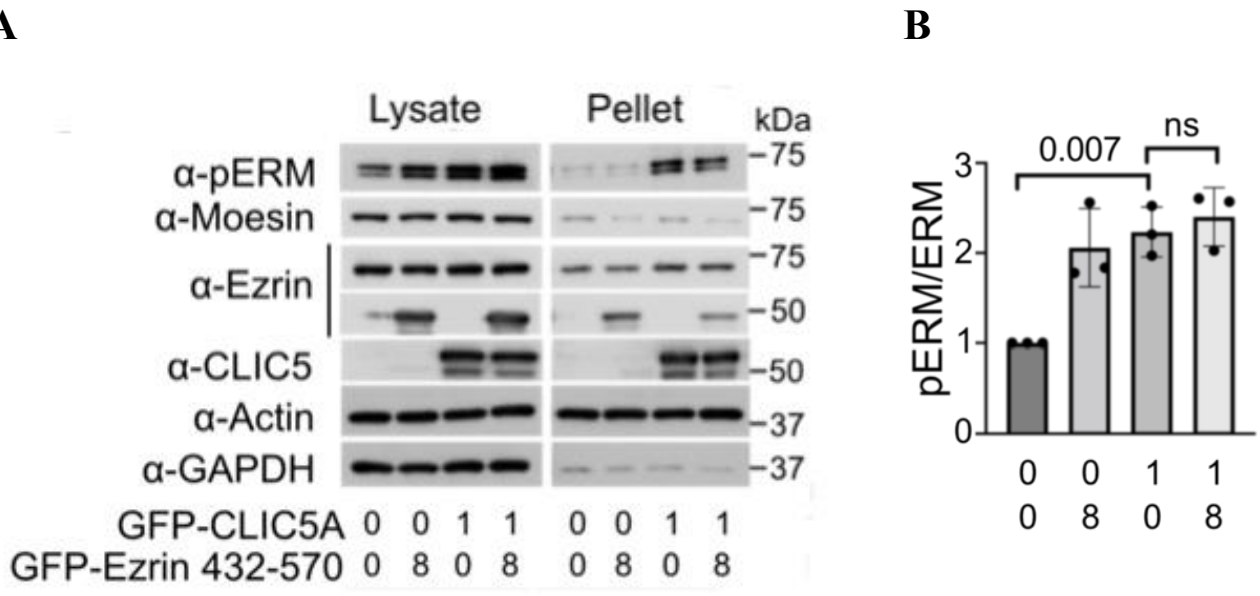

Figure 5.12: Ezrin 432-570 expression failed to block CLIC5A-stimulated ERM phosphorylation. A. Representative western blot showing pERM abundance in COS-7 cells transfected with GFP-CLIC5A cDNA with or without a 8-fold excess of GFP-ezrin 432-570 cDNA. GFP-CLIC5A was kept constant and the GFP-CLIC5A : ezrin 432-570 (T567D) transfection ratio was 1:8. Protein bands showing at around ~48 kDa in ezrin blot represents the over expressed GFP-ezrin 432-570. B. Densitometric quantification of the pERM : ezrin ratio (mean ± S.D., n = 3 independent experiments).

Figure 5.13

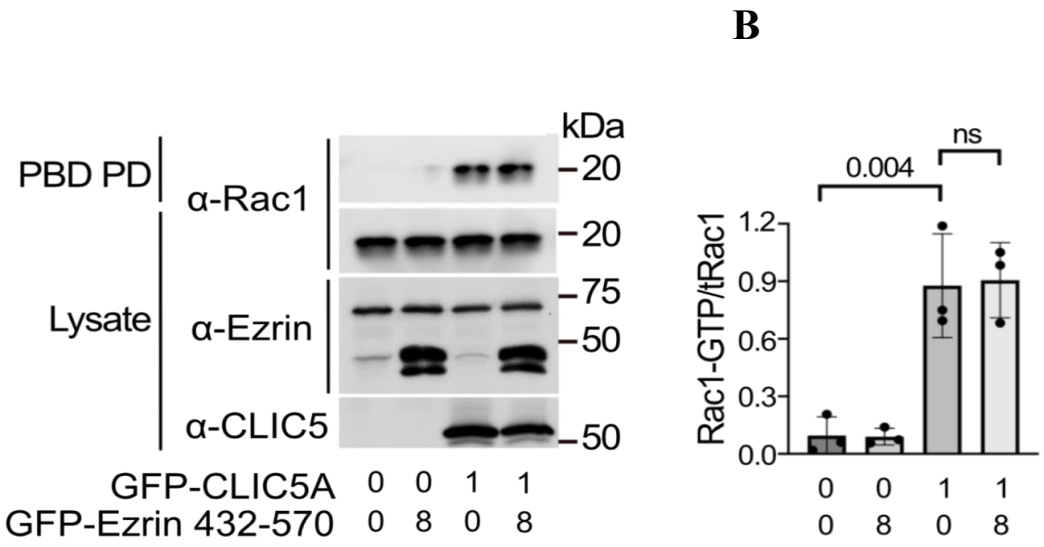

Figure 5.13: Ezrin 432-570 expression failed to block CLIC5A-stimulated Rac1 activation. A. Representative anti(α)-Rac1 western blot showing PAK-PBD pull-down (PD) of Rac1-GTP from lysates of COS-7 cells transfected with GFP-CLIC5A cDNA with or without a 8-fold excess of GFP-ezrin 432-570 cDNA. Protein bands showing at around ~48 kDa in ezrin blot represents the over expressed GFP-ezrin 432-570. **B.** Densitometric quantification of Rac1-GTP/total Rac1 (mean ± S.D., n = 3 independent experiments).

Figure 5.14

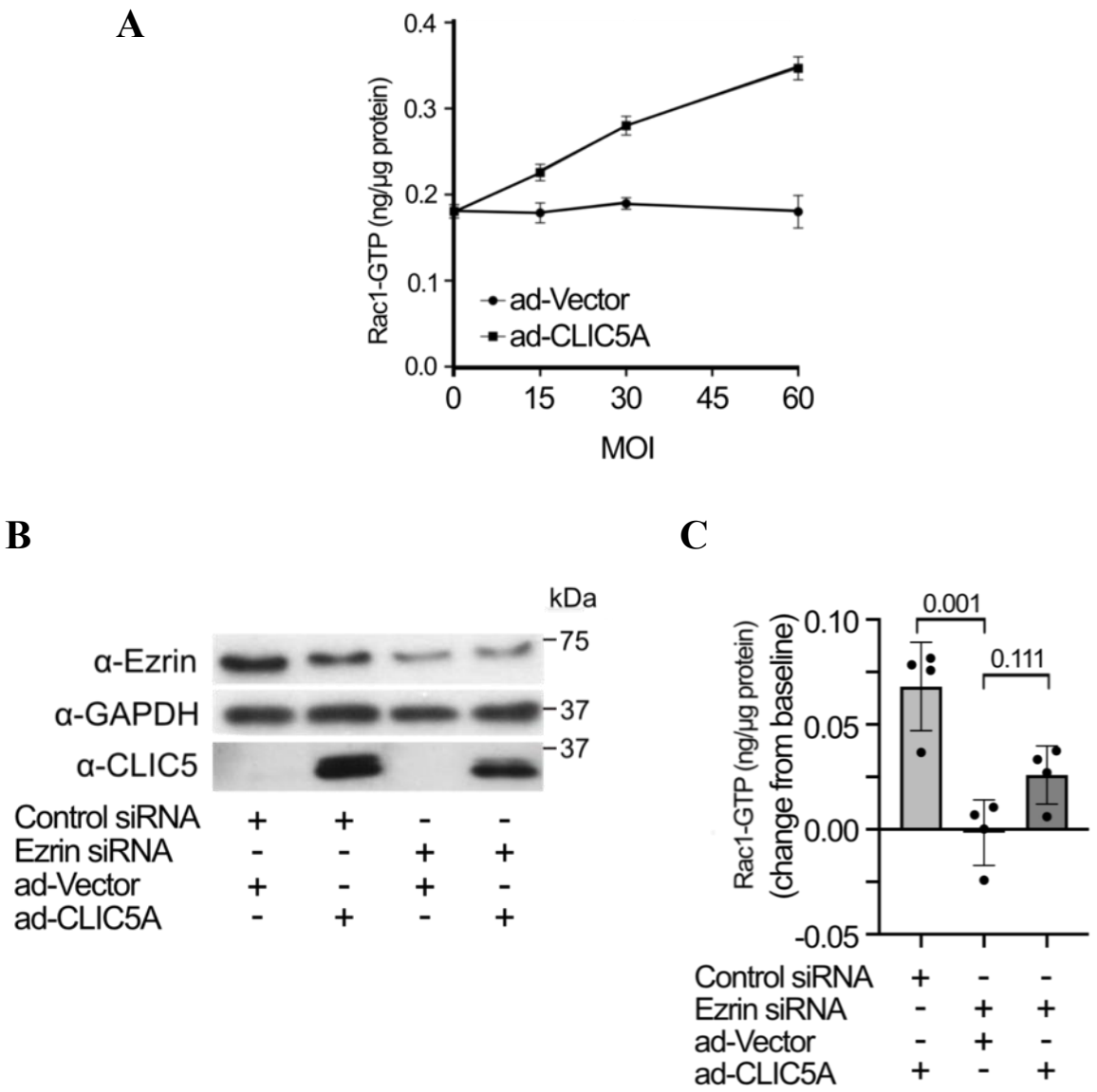

Figure 5.14: Ezrin silencing disrupts CLIC5A-stimulated Rac1 activation. A. Rac1-GTP abundance in human glomerular EC cells determined by Rac1-GTP G-LISA®. The cells were transduced with adenoviral-vector (ad-Vector) or untagged CLIC5A in the same vector (ad-CLIC5A) at an MOI (mean ± SD, n = 3 independent experiments). **B.** Western blot of lysates from human glomerular EC cells transduced with ad-Vector or ad-CLIC5A with or without ezrin–specific siRNA. **C.** Change relative to baseline of Rac1-GTP in human glomerular EC cells transduced with 30 MOI ad-Vector or ad-CLIC5A with or without ezrin–specific siRNA (mean ± SD, n = 4 independent experiments, one-way ANOVA, and Bonferroni's comparisons).

Figure 5.15

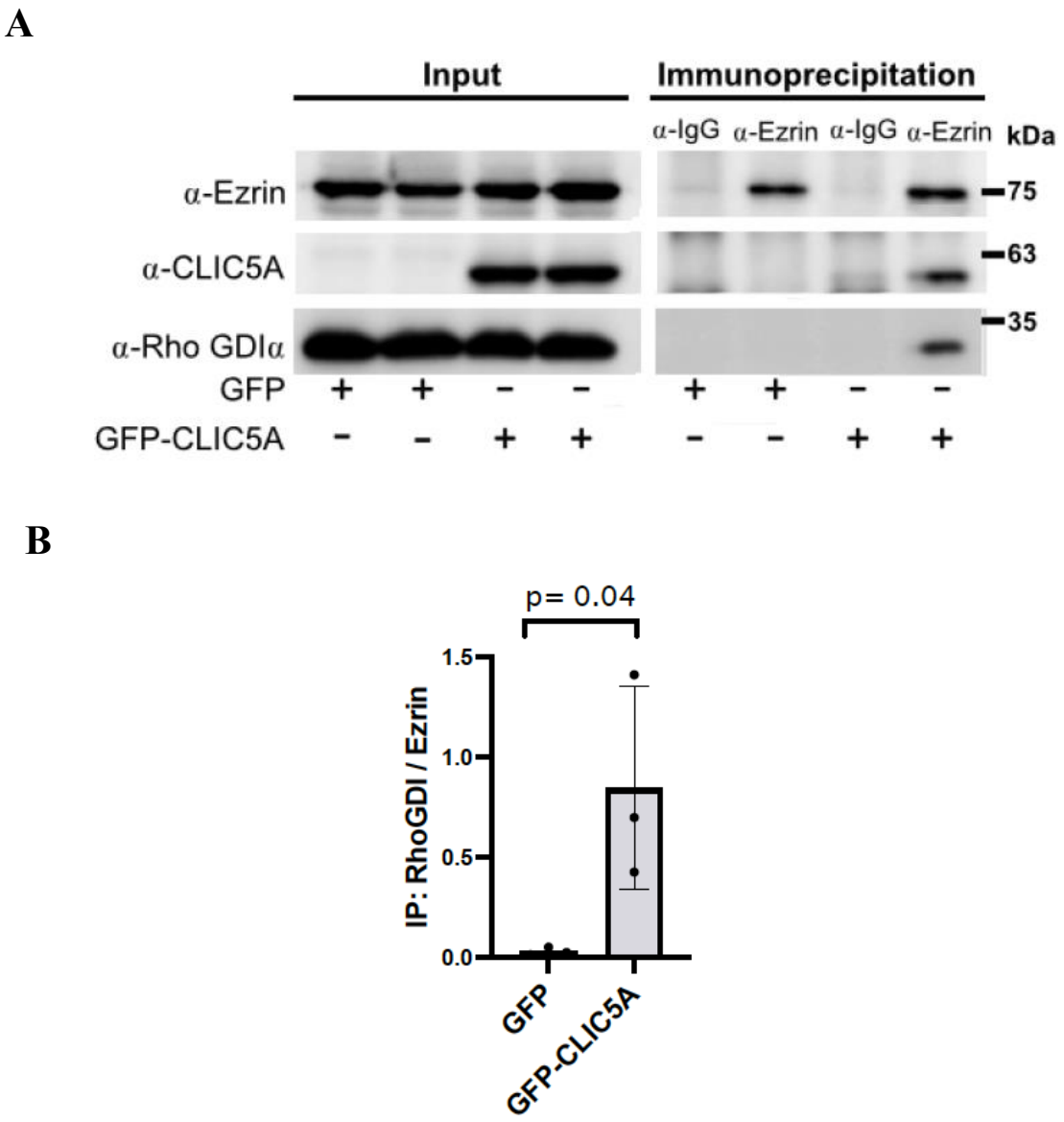

Figure 5.15: CLIC5A enhances ezrin binding to Rho GDI. A. Western blot analysis with α-ezrin, α-CLIC5A and α-RhoGDIα antibodies of lysates (input) from HeLa cells transfected with GFP-or, GFP-CLIC5A cDNAs constructs and proteins from immunoprecipitation of endogenous ezrin using rabbit α-ezrin antibody (100 ng) in HeLa cells. Rabbit α-IgG antibody serves as a negative control. **B.** Densitometric quantification of immunoprecipitated RhoGDIα / ezrin (mean ± SD, n = 3 independent experiments).

5.3. Discussion

Our lab previously reported that CLIC5A expression in COS-7 cells stimulates Rac1, but not Cdc42 or RhoA activity, and that CLIC5A stimulates phosphorylation of the Rac1 effector PAK1,3 in COS-7 cells and in cultured mouse podocytes (86). Rac1-GTP interacts with PAKs which, in turn, trigger signaling cascades that initiate diverse physiological outcomes (484) including cytoskeletal organization, cell growth, and development (485, 486). Rho GTPases also stimulate PI4,5P2 synthesis (487) by interacting directly interact with type 1 PIP5K. In rat liver cytosol and Rac1, but not RhoA or Cdc42, binds and activates type 1 PIP5K (178). Therefore, PIP5K isoforms appear to function downstream of Rac1 (176, 488) to enhance PI4,5P2 synthesis (489). The RhoA effector, Rho-kinase is also involved in RhoA-dependent regulation of PIP5K activity (490), leading to the actin cytoskeleton organization (491).

My data show that CLIC5A expression not only stimulates Rac1 but also increased the association of PIP5K4 and PIP4K5 isoforms with the Rac1-GTP complex (Figure 5.1). This finding implies that CLIC5A expression enhances the synthesis of PI4,5P2 at the inner leaflet of the plasma membrane through Rac1 activation. The PI4P5KIα3 kinase isoform is present in the kidney cortex of $CLIC5^{+/+}$, but not in $CLIC5^{-/-}$ mice, with apparent compensation by greater expression of the PI4P5KIα2 kinase isoform (Figure 5.2). Moreover, PAK-PBD beads pulled down Rac1-GTP and with it the PI4P5KIα3 isoform only from kidney lysates of mice expressing CLIC5A (Figure 5.3, and 5.4). This finding suggests strongly that CLIC5A-dependent Rac1 activation specifically targets the PI4P5KIα3 kinase isoform in kidney cortex tissue. In addition, the observation that PI5P4KIIα2 and PI5P4KIγ were precipitated with the Rac1-GTP from $CLIC5^{-/-}$ but not $CLIC5^{+/+}$ mouse kidney cortex lysates, suggest compensatory mechanisms for $PI4,5P_2$ generation in the absence of CLIC5. Since Rac1-GTP also pulled down pERM and

CLIC5A from kidney lysates of wild-type mice, it seems likely that the PI4P5KIα3 kinase isoform, pERM and Rac1-GTP are all part of the same protein complex.

Theoretically, the phosphomimetic ezrin 432-586 T567D fragment should competitively inhibit the CLIC5A interaction with endogenous ERM proteins because it binds CLIC5A directly and with a high affinity. Consistent with this hypothesis, I found that GST-CLIC5A pulled down GFP-ezrin 432-586 and this interaction was strengthened by Calyculin-A. Conversely, Staurosporine-mediated inhibition of phosphorylation not only reduced the CLIC5A/ezrin 432-586 interaction but also the interaction of endogenous ezrin with CLIC5A. Moreover, the phosphomimetic point mutation replacing threonine to aspartic acid at ezrin 567 site has a significantly greater affinity for CLIC5A than the wild-type or phosphorylation deficient ezrin 432-586 (Figure 5.9). Taken together, these findings imply that CLIC5A gains access to ezrin 432-586 because it is not auto-inhibited by the ezrin N-terminus and that ezrin phosphorylation at Thr 567 enhances CLIC5A/ezrin binding.

We exploited the high affinity of CLIC5A for ezrin 432-586 (T567D) to demonstrate that its overexpression could suppress CLIC5A-induced functional effects while the control-construct ezrin 432-570, which does not bind CLIC5A, could not. We were unable to achieve substantial ezrin knockdown in COS-7 cells, but could reduce ezrin expression in human glomerular endothelial cells, which express CLIC5A in *vivo* (483) but not in culture (87). I overexpressed CLIC5A without a tag in these cells using an adenoviral vector because the transfection efficiency with cDNA is extremely low. Expression of the untagged CLIC5A in the glomerular endothelial cells activated Rac1 in a concentration-dependent fashion, and ezrin knockdown in these cells significantly reduced CLIC5A-stimulated Rac1 activation (Figure 5.14). We can therefore conclude that CLIC5A-stimulated Rac1 activation likely on ezrin.

It is well established that activated ERM proteins directly bind the Rho GDP dissociation inhibitor alpha (ARHGDIA/Rho GDIα) (160, 234). We observed that CLIC5A expression increased Rho GDIα co-immunoprecipitation with ezrin, suggesting that CLIC5A-stimulated ezrin activation causes ezrin to capture Rho GDIα from Rac1, allowing Rac1 to interact with the plasma membrane (492) and relieving the Rho GDIα-mediated inhibitory effect on Rac1.

Therefore, CLIC5A stimulates ezrin-dependent Rac1 activation pathway that in turn activates PI4P5KIα3, which results in phosphorylation of PI4P to generate PI4,5P2. Docking of the ezrin N-terminus on membrane PI4,5P2 in turn prevents its interaction with its own C-terminus. The N-terminus of ezrin can then capture Rho GDIα allowing Rac1 activation by Rac1 GEFs. This signaling pathway therefore seems to be a feed-forward amplification loop, in which CLIC5A by sitting on ezrin facilitates continuous, localized Rac1 activity. Rac-GTP, in turn, activates PI4P5Kα3 to generate PI4,5P_2. The ezrin N-terminus then docks on PI4,5P_2 resulting in the open, active ezrin conformation which binds CLIC5A, gets phosphorylated and captures Rho GDI, activating Rac1, beginning the cycle again.

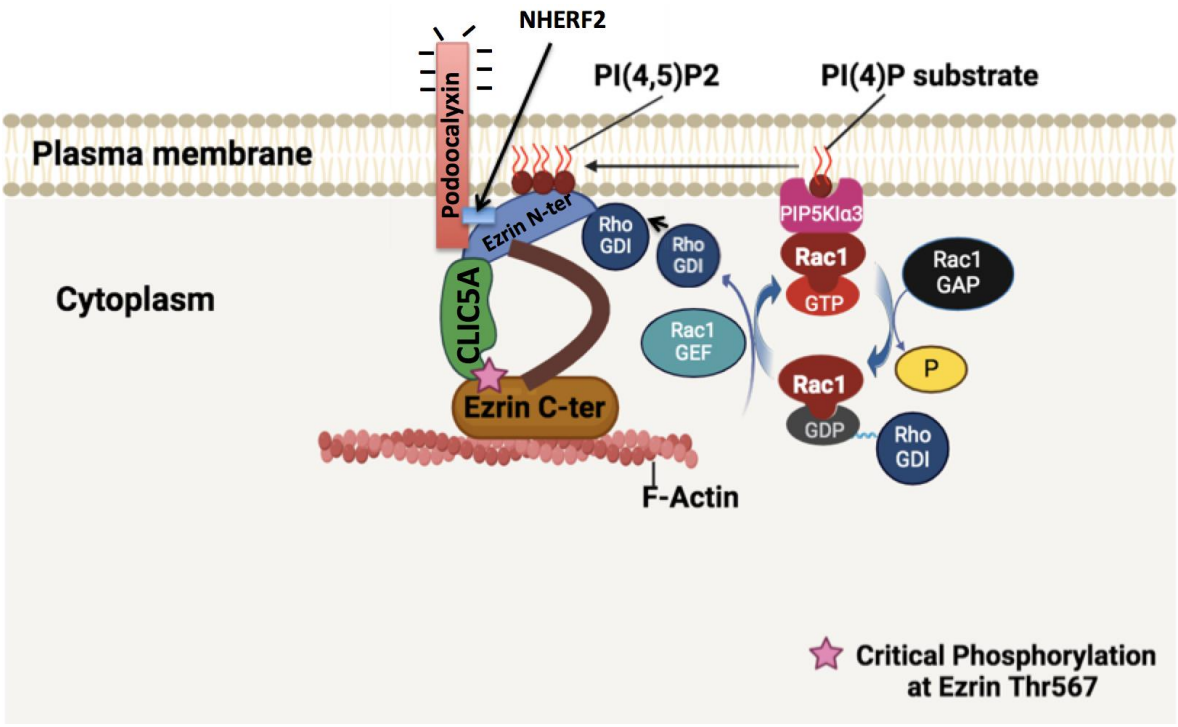

Figure 5.16: Model: CLIC5A expression, followed by CLIC5A/ezrin direct binding stimulates Rho GDI binding to ezrin, which is one of the mechanisms of Rac1 activation. Rac1 activation trigger PI4P5Kα3 kinase to catalyze the reaction for cluster generation of PI4,5P2, which serves a s a docking site for ezrin N–terminus. This results in ezrin open conformation and ezrin C-terminus Thr 567 phosphorylation and ezrin/actin binding. As a result, ezrin open conformation stabilizes. When CLIC5A/endogenous ezrin direct interaction is disrupted with ezrin 432-586 fragment, which has a high affinity for CLIC5A, CLIC5A cannot bind and stimulates ezrin activation/phosphorylation, resulting in ezrin inactive, closed, conformation and CLIC5A becomes soluble, cytosolic.

Chapter 6

CLIC5A reduces taperin isoform 1 nuclear localization and taperin/PP1c enhances ERM phosphorylation

Chapter 6

CLIC5A reduces taperin isoform 1 nuclear localization and taperin/PP1c enhances ERM phosphorylation

6.1. Introduction

Next-generation sequencing (NGS) enabled identification of specific disease-causing gene mutations in the chromosome 9 open reading frame 75 (C9orf75) in two separate families with recessive, non-syndromic hearing loss (432, 433). The protein encoded by the C9orf75 expresses in different tissues, notably in the inner ear hair cells of the cochlea (433, 445, 493), and it was named "taperin" due to it's location in the taper region of inner ear cell stereocilia (433). The gene is now annotated as "TPRN". At the base of the inner ear hair cell stereocilia, CLIC5A stabilizes membrane-actin filament linkages by in a complex with taperin, radixin, myosin IV (MYO6), and protein tyrosine phosphatase receptor type Q (PTPRQ)(428). Taperin forms a dense-core-like structure encircled by an oligomeric ring of Fam65b protein at the taper region of stereocilia (493). Taperin has ~34% amino acid sequence similarity with phostensin and homology searches identified a 58 amino acid stretch of taperin (482–539 aa in human isoform 1) with a 76% similarity to phostensin. The latter is involved in actin dynamics through capping to pointed ends of actin filaments (494, 495). Overexpressed Myc-tagged taperin resulted in rod-like aggregates containing actin in ~53% of COS-7 cells (445), indicating taperin might also regulate actin structures.

Protein kinases and phosphatases are responsible for phosphorylation status of many cellular proteins and mis-regulation of protein phosphorylation is responsible for human diseases. Protein phosphatase one (PP1) catalytic subunits exist as α, β, and γ isoforms in humans. Protein phosphatase 1 catalytic (PP1c) subunits are recruited to dephosphorylate specific substrates

through association with a PP1c interacting protein or regulatory subunits (496-498). Through the interaction with PP1 regulatory subunits, phosphatase activity localizes to specific locations in cells and modulates its activity toward selected substrates (436, 499). Moreover, regulatory subunits often exhibit a preference for one catalytic subunit isoform. Taperin is a PP1 regulatory protein that binds PP1cα, and PP1cγ isoforms, but not PP1cβ, through its KISF motif (434).

Taperin has four isoforms produced through alternative splicing of its primary transcript RNA, and all 4 isoforms were detected by mass spectrometry in HeLa cells (434). Human taperin isoform 1 (1-711 aa) has a calculated molecular weight of ~75.6 kDa. Human taperin isoforms 2 and 3 lack the N-terminal 1-306 aa of isoform 1. Isoform 2 consists of 405 amino acids with a calculated molecular weight of ~44.12 kDa. Isoform 3 is slightly longer with 433 aa and a calculated molecular weight of ~47.3 kDa. It contains a 28 aa insertion (MVRCGGVERW GESDTRASPCVHILSSHFQ) starting at $_{691}$M amino acid relative to the isoform 1 to sequence. Isoform 4 starts at $_{306}$M relative to isoform 1 and consists of 406 amino acids with a calculated molecular weight of ~44.2 kDa. In isoform 4, the translation initiation sequence $_{306}$VMETIP$_{311}$ aa is replaced with $_{306}$MVSITG$_{311}$ (numbering relative to isoform 1). There also are other sequence differences across species. Nonetheless, all taperin isoforms contain the conserved "KISF" PP1c binding motif ($_{577}$KISF$_{580}$ aa relative to human isoform 1).

Bioinformatics analyses of multiple taperin splice variants expressed in vertebrates indicate that the PP1 docking function of taperin is conserved across species and has an ancestral relationship with the PP1- and actin-binding protein phostensin. In the taperin 1 isoform a regulatory region of taperin (8-87 aa) alters the PP1c binding affinity, and a potential phosphorylation site exists at position 241. Recombinant 6XHis-taperin isoform 2 prefers to bind PP1cα over PP1cγ *in vitro* and taperin inhibits PP1cα phosphatase activity towards the phosphorylase A substrate (434). I

showed in chapter 3 that Y2H screening data identified a region in mouse taperin (312-424 aa) as a potential direct interacting site for CLIC5A (Chapter 3, Table 7). In fact, the screen resulted in over 30 positive clones, whereas only 1 positive clone for radixin was observed. It therefore seems highly likely that taperin interact directly with CLIC5A. I postulated that formation of the taperin/CLIC5A complex might regulate ERM phosphorylation. Therefore, experiments in this chapter are designed to investigate the following objectives:

To determine whether CLIC5A and other CLICs interact directly with taperin, and to determine whether taperin alters ERM phosphorylation.

6.2. Results

6.2.1. Endogenous taperin expresses in different cells

First, I aimed to detect the expression of endogenous taperin isoforms in different cell types. Using a mouse monoclonal anti-taperin antibody, western blot analysis of total cell lysates prepared from the glomeruli isolated from CLIC5$^{+/+}$ and CLIC5$^{-/-}$ mice, cultured human podocytes, cultured human glomerular endothelial (human glomerular EC), HeLa, HEK293, and COS-7 cells revealed two major bands at the ~88 kDa, and ~55-58 kDa (Figure 6.1.A). To determine whether these two major bands were actually taperin, I transfected HeLa cells with human taperin siRNA at different concentrations (5 nM, 10 nM, 15 nM, and 20 nM), followed by western blot analysis of cell lysates. The siRNA contains 3 27-mer sequences directed to the 3' end of the taperin open reading frame, common to all 4 isoforms. It turns out that the protein band at ~88 kDa was almost completely knocked down at all concentrations of taperin siRNA, whereas control siRNA treatment did not. This experiment indicates that the protein band at ~88 kDa is the main taperin protein expressed in HeLa cells and its apparent MW is consistent with the full-length taperin isoform 1 (Figure 6.1.B). Surprisingly, the ~55-58 kDa protein band was not knocked down by taperin siRNA, even though the siRNA target sequences are common in all taperin isoforms. This finding suggests that the ~55-58 kDa protein band is not a taperin protein and the mouse taperin antibody detected it non-specifically. However, further analysis of this protein by mass spectrometry might be necessary to be sure that it is not a smaller taperin isoform.

Full-length taperin isoform 1 (1-711 aa) has a calculated molecular weight of 75.5 kDa but runs slower in SDS-PAGE gels and was detected at ~88 kDa on western blots that might be due to post-translational modifications and/or the relatively high density of negatively charged amino

acids in its C-terminal domain. I therefore was able to conclude that the endogenous full-length taperin 1-711 aa is the only taperin protein isoform detected in HeLa cells.

6.2.2. CLIC5A, CLIC4 and CLIC1 interact directly with taperin in Y2H assay

As previously mentioned in chapter 3 that the yeast two-hybrid (Y2H) screening of mouse kidney protein domain library using CLIC5A as bait identified the mouse taperin central domain 312-424 amino acids (aa) as the direct interacting region or CLIC5A (Table 7). Human taperin 272-385 aa has a 78% amino acid sequence identity with this mouse taperin central domain. To confirm the direct interaction between human taperin and CLIC5A, as well as CLIC4 or CLIC1, cDNAs encoding FL CLIC5A (1-251 aa), CLIC5A N-terminal (22-251 aa) and CLIC5A C-terminal (1-232 aa) deletion mutants, FL CLIC4 (1-253 aa) and FL CLIC1 (1-241 aa) were cloned into the pKBKT7 bait vector, while a cDNAs encoding human taperin isoform 1 (1-711 aa), and the taperin 272-385 aa fragment were cloned in to the PGADKT7 prey vector, followed by the Y2H assay. I observed that FL CLIC5A, CLIC4 and CLIC1 all interacted directly with taperin 1-711 and taperin 272-385, as evident from the growth of blue colonies on DDO/X/A plates (Figure 6.2.A and B), confirming the Hybrigenics® screening result. Based on the density of growth of blue colonies, the taperin 272-385 fragment may have a higher affinity for CLIC5A, CLIC4 and CLIC1 compared to full-length taperin isoform 1 (1-711aa). The affinity of CLIC5A and CLIC4 for the taperin 272-385 fragment seemed to be comparable, but fewer colonies were observed for the CLIC1/taperin 272-385 interaction compared to CLIC4 and CLIC5A, suggesting that CLIC1 has a lower affinity for this region than CLIC5A and CLIC4. Also, the CLIC5A produced more blue colonies than CLIC4 and CLIC1 for the interaction with full-length taperin isoform 1 (1-711 aa).

The CLIC5A N-terminal mutant 22-251, and the CLIC5A C-terminal mutant 1-232 failed to interact with taperin 1-711 and taperin 272-385 as evident from the absence of growth of diploid yeast colonies on DDO/X/A plates, indicating that both the N- and C-termini of CLIC5A are necessary for the direct CLIC5A/taperin interaction.

6.2.3. CLIC5A directly binds taperin isoforms *in vitro*

To validate the Y2H assay results, I investigated whether CLIC5A can interact with endogenous taperin expressed in HeLa cells, and with taperin isoforms synthesized *in vitro*. Purified, immobilized GST-CLIC5A pulled down endogenous full-length taperin (~88 kDa) from HeLa cell lysates (Figure 6.3.A). Moreover, TnT transcription/translation-based *in vitro* synthesized HA-taperin 307-711 and HA-taperin 272-385 proteins were pulled down by GST-CLIC5A. HA-ezrin 1-296 was used as a positive control of GST-CLIC5A pull down (Figure 6.3.B). *In vitro* synthesis of full-length HA-taperin 1-711 was less efficient than that of shorter taperin fragments/isoforms. But full-length HA-taperin 1-711 was also pulled down by GST-CLIC5A when I scaled up the reticulocyte lysate input 4-fold (Figure 6.3.C). *In vitro* synthesized HA-taperin 272-385 was pulled equally from the reticulocyte lysates whether treated with or without H_2O_2 (to oxidize protein thiols) (Figure 6.3.D). In addition, GFP-tagged full-length taperin isoform 1 (1-711aa) and taperin isoform 2 (307-711aa) overexpressed in HeLa cells were effectively pulled down by GST-CLIC5A (Figure 6.10). Take together I concluded that CLIC5A binds the taperin isoforms 1 (1-711 aa) and 2 (307-711 aa relative to isoform 1) directly and that the taperin 272-385 aa fragment seem to have a higher affinity for CLIC5A than the full-length taperin isoform 1 (1-711 aa).

6.2.4. Taperin isoforms 1 and 2 localize predominantly to the nucleus

The $_{577}$-KISF-$_{580}$ motif is the primary PP1c binding site in the C-terminus of full-length taperin isoform 1 and is conserved in all taperin isoforms. This motif was mutated to generate $_{577}$KASA$_{580}$ mutants as previously reported by Ferrar et al (434). The GFP-tagged taperin isoform 1 wild type and KASA mutant, and GFP-taperin isoform 2 (307-711 aa) wild type and KASA mutant, GFP-taperin 272-385, GFP-taperin 272-306 were cloned into the pEGFP-C1 vector to study their subcellular localization and co-localization with CLIC5A when overexpressed in HeLa cells.

Live cell confocal microscopy imaging demonstrated that when overexpressed in HeLa cells, GFP-CLIC5A localizes predominantly to the cell membrane as shown as overlap with the CellBrite™ Steady membrane staining (yellow, top panel Figure 6.4). Full-length GFP-taperin isoform 1 (1-711; wild type and KASA mutant) and GFP-taperin isoform 2 (307-711; wild type and KASA mutant) were observed mostly in the nucleus (Figure 6.4). Some GFP-taperin isoform 1 (wild-type and KASA mutant) localized to the cell membrane. By contrast, GFP-taperin isoform 2 (wild-type and KASA mutant) localized exclusively in the cell nucleus, sparing the nucleoli (Figure 6.5).

6.2.5. CLIC5A expression reduced nuclear localization of taperin full-length 1-711, but not taperin 1-306 or taperin 307-711

To determine whether CLIC5A alters the subcellular localization of taperin isoforms HeLa cells co-transfected with full-length RFP-CLIC5A and GFP-taperin constructs. The wild type and KASA mutant GFP-taperin isoform 1 (1-711 aa) were predominantly localized to the nucleoplasm in the presence of the RFP vector control (Figure 6.6.A), but in the presence of RFP-CLIC5A, the localization of full-length and KASA mutant GFP-taperin-1 decreased

substantially, while localization at the cell periphery was retained and GFP-taperin isoform 1 and RFP-CLIC5A co-localized at the cell periphery (Figure 6.6.B). By contrast, the nuclear localization of wild type and KASA mutant GFP-taperin isoform 2 (307-711 aa) was unaffected by RFP-CLIC5A expression, and GFP-taperin isoform 2 did not co-localize with RFP-CLIC5A (Figure 6.6.B). Neither isoform 1 1aperin (1-711 aa) nor isoform 2 taperin (307-711 aa) accumulated in nucleoli.

The sequence from 307 – 711 aa of the taperin isoform 1 is shared by taperin isoform 2, while the sequence from 1-306 is unique for the taperin isoform 1. Since isoform 1, but not isoform 2 partially localized to the cell periphery and only isoform 1 preferentially localized to the periphery in the presence of CLIC5A, we wondered whether the unique region of isoform 1 targets it to the periphery. When a GFP-taperin 1-306 fragment was expressed in HeLa cells, its distribution was the same as that of taperin isoform 1, with predominant localization to the nucleus and partial localization to the cell periphery. But, when RFP-CLIC5A and the GFP-taperin 1-306 fragment were co-expressed in HeLa Cells, there was no reduction of taperin 1-306 abundance in the nucleus (Figure 6.7), unlike the findings for full-length taperin 1-711. This finding suggests that the CLIC5A-induced reduction in nuclear targeting of the taperin isoform 1 requires the CLIC5A binding region beyond residue 306.

We have good evidence indicating that taperin 272-385 sequence contains the CLIC5A binding region and therefore postulated that co-expression of a GFP-tagged taperin 272-385 fragment with RFP-CLIC5A might cause this taperin 272-385 fragment to colocalize with CLIC5A at the cell periphery. We also wondered whether the taperin 272-306 fragment, which does not have the taperin isoform 2 sequence (307-711) might nevertheless interact with CLIC5A. Although expression of GFP-taperin 272-385 and 272-306 fragments resulted in their nuclear and cytosolic

distribution, neither were targeted to the cell periphery and neither co-localized with CLIC5A (Figure 6.8), and no change in their subcellular distribution was observed in the presence of RFP-CLIC5A. These findings indicate that binding to CLIC5A, which we demonstrated for the taperin 272-385 fragment is not sufficient to cause co-localization with CLIC5A at the cell periphery.

6.2.6. Taperin is a protein phosphatase 1 binding protein

As all the four taperin isoforms contain the PP1c binding motif ($_{577}$KISF$_{580}$), we investigated the interaction of taperin isoform 1 (1-711) and isoform 2 (307-711) wild type and KASA mutants with endogenous PP1c. Wild-type and KASA mutants of GFP-taperin isoform 1 (1-711 aa) and isoform 2 (307-711 aa) were expressed in HeLa cells and then immunoprecipitated with an anti-GFP antibody to exclude precipitation of endogenous taperin. PP1c, detected with a pan-PP1c antibody co-immunoprecipitated with wild-type GFP-taperin isoforms 1 and 2, but not with their respective KASA mutants (Figure 6.9 A, B). The findings confirm that the KISF motif is required for the interaction of PP1c with taperin isoforms 1 and 2, consistent with previous findings by Ferrar et al. (434) for taperin isoform 2.

Immobilized GST-CLIC5A also pulled down PP1cα and a small amount of PP1cγ from HeLa cell lysates (Figure 6.10). No difference in the amount of PP1cα and a PP1cγ pulled down by GST-CLIC5A in cells expressing wild type vs. KASA taperin isoform 1. By contrast, expression of wild-type GFP-taperin isoform 2 (307-711aa) resulted in a large increase in PP1cγ co-precipitation with GST-CLIC5A compared with the GFP-taperin isoform 2 KASA mutant (Figure 6.10). This experiment suggests that in HeLa cells, the taperin isoform 2 307-711 specifically binds PP1cγ, allowing it to be pulled down by GST-CLIC5A.However, interpretation of these experiments is complex, because endogenous taperin would also have been pulled down by CLIC5A, and with it PP1cα, obscuring any potential effect of the KASA mutation.

6.2.7. Taperin brings PP1cγ in the CLIC5A containing protein complex

To determine which isoform of PP1c specifically associates with the taperin/CLIC5A protein complex, I performed the GST-/GST-CLIC5A pull down assay using lysates of HeLa cells treated with control siRNA or human taperin siRNA. Endogenous taperin, as well as PP1cα, PP1cβ, and PP1cγ were precipitated by the immobilized GST-CLIC5A from lysates of HeLa cells treated with control siRNA. In HeLa cells treated with taperin siRNA, taperin was not detected on the western blot or in the GST-CLIC5A pull-downs (Figure 6.11). Surprisingly, in the absence of endogenous taperin isoform 1, PP1cα and PP1cβ were still observed in the GST-CLIC5A pull-down proteins, while the pull-down of PP1cγ was significantly reduced (Figure 6.11). These results suggested that CLIC5A can pull-down PP1cα, and PP1cβ independent of taperin, whereas taperin binds PP1cγ allowing it to be co-precipitated by GST-CLIC5A.

6.2.8. CLIC5A binds recombinant, purified PP1c isoforms directly *in vitro*

Because PP1cα was pulled from HeLa cell lysates by GST-CLIC5A even when taperin was silenced, we checked the amino acid sequence of CLIC5A to see if there might be a PP1c binding motif. The usual PP1 binding motif is KVxF (x is any amino acid) is not present in the CLIC5A amino acid sequence. However, some proteins have been identified in which the PP1c binding consensus sequence is KxVxF (500), and CLIC5A has a $_{45}$KGVVF$_{49}$ motif, which is highly conserved among all the CLIC proteins. I therefore determined whether the distinct PP1c isoforms could bind CLIC5A directly. I incubated 100 ng of recombinant, purified PP1cα, PP1c β, or PP1cγ separately incubated with 500 ng GST-, or 1.0 μg of GST-CLIC5A in 500 μl of ice cold Tris-HCl, 20 mM, pH 7.4 buffer for GST-/GST-CLIC5A pull-down assay. GST-CLIC5A effectively pulled down all three PP1c isoforms (PP1cα, or PP1cβ, or PP1cγ) without preference for any one of them (Figure 6.12.A). Moreover, when 1 mM DTT, or 2 mM H_2O_2 were added to

the GST-CLIC5A pull down mixture containing purified PP1cα, or PP1cγ, and both PP1cα, and PP1cγ were still pulled down by the GST-CLIC5A (Figure 6.12 B, C). Therefore, PP1cα, PP1cβ, or PP1cγ can all interact directly with CLIC5A and the oxidation state of CLIC5A does not alter this interaction. This experiment leads me to conclude that both CLIC5A and taperin have PP1c binding sites, and therefore both can bind PP1c. It is therefore possible that taperin and CLIC5A can compete for PP1 catalytic subunits (PP1c). It is also likely that other CLICs bind PP1c directly, since the KGVVF motif is highly conserved. Whether mutation of this motif alters PP1c binding will still need to be determined.

6.2.9. CLIC5A KGAVY mutant does not bind taperin

We then performed site-directed mutagenesis to generate cDNAs of GST-tagged and untagged CLIC5A wild type $_{45}$KGVVF$_{49}$ and mutant $_{45}$KGAVY$_{49}$ (Appendix 2 for PP1 binding motif in CLIC5A). Untransfected HeLa cell lysates were subjected to GST-CLIC5A wild type $_{45}$KGVVF$_{49}$ and GST-CLIC5A $_{45}$KGAVY$_{49}$ mutant pull-down assay. We observed that endogenous taperin was pulled down by the GST-CLIC5A wild type but not by the GST-CLIC5A KGAVY mutant (Figure 13.A), indicating that the putative PP1 binding motif $_{45}$KGVVF$_{49}$ in CLIC5A is actually responsible for the interaction of CLIC5A with taperin.

The untagged CLIC5A wild type and CLIC5A KGAVY mutant were then expressed in HeLa cells followed by pull-down with purified, recombinant GST-ezrin 432-586. Recombinant GST-ezrin 432-586 effectively pulled wild type $_{45}$KGVVF$_{49}$,as well as the CLIC5A mutant $_{45}$KGAVY$_{49}$ from the HeLa cell lysates. However, while endogenous taperin and PP1c were precipitated by immobilized GST-ezrin 432-586 in the presence of wild-type CLIC5A, neither taperin or PP1c were pulled down from lysates of cells expressing the CLIC5A $_{45}$KGAVY$_{49}$ (Figure 6.13.B). These results indicate that endogenous taperin does not associate with the

CLIC5A$_{45}$KGAVY$_{49}$ mutant. The data also suggest that wild-type CLIC5A forms a bridge between ezrin and taperin. Whether CLIC5A KGAVY mutation is responsible for disruption of interaction with PP1c and taperin, or taperin brings PP1c into the CLIC5A/ezrin complex is still unclear.

Live cell imaging experiments with CLIC5A wild type and CLIC5A $_{45}$KGAVY$_{49}$ mutants showed that both localized to the cell periphery (Figure 6.14), and when they were co-expressed in HeLa cells, both strongly colocalized at that location (Figure 6.14), suggesting that the $_{45}$KGAVY$_{49}$ mutation has no role in CLIC5A membrane localization. Importantly, when RFP-CLIC5A $_{45}$KGAVY$_{49}$ was co-expressed with GFP-taperin isoform 1 (1-711) in HeLa cells there was no apparent reduction in the nuclear localization of the taperin isoform 1 (Figure 6.15). Taken together with the findings in Figure 6.13, these data suggest that the CLIC5A $_{45}$KGVVF$_{49}$ (wild type) motif is required for the taperin/CLIC5A interaction and that the $_{45}$KGAVY$_{49}$ mutation in CLIC5A disrupts this interaction.

6.2.10. Taperin knockdown does not change CLIC5A localization at cell periphery

As CLIC5A and taperin bind directly to each other, we wondered whether depletion of endogenous taperin has any effect on CLIC5A localization at cell periphery. Confocal microscopy imaging of HeLa cells transfected with GFP-CLIC5A cDNA, and control or human taperin siRNA (5 nM) showed that GFP-CLIC5A localizes to the cell periphery in both control siRNA treated and taperin siRNA treated cells. (Figure 6.16). Therefore, CLIC5A does not require expression of taperin for its localization at the cell periphery; rather CLIC5A expression reduces taperin 1-711 wild type localization from the nucleus.

6.2.11. Taperin knockdown reduces ERM phosphorylation

As a PP1c regulatory protein, taperin can bind PP1c and can inhibit PP1c phosphatase activity against phosphorylase A (434). We wondered whether taperin/PP1c could act as a phosphatase against ERM proteins, or whether it might inhibit their dephosphorylation due to binding of PP1c in competition with another PP1 targeting subunit. To determine the functional role of taperin in the context of ERM phosphorylation, I co-transfected HeLa cells with GFP- or GFP-CLIC5A cDNAs, followed by control siRNA or human taperin siRNA treatment. I found that GFP-CLIC5A expression stimulated ERM phosphorylation in control siRNA treated cells, consistent with the findings by Al-Momany et al. (89), while siRNA-mediated knockdown of endogenous taperin reduced ERM phosphorylation in both, vector and GFP-CLIC5A transfected cells (Figure 6.17). Moreover, taperin knockdown alone also reduced ERM phosphorylation in the absence of CLIC5A. Therefore, loss of taperin reduces baseline and CLIC5A-stimulated ERM phosphorylation.

Figure 6.1

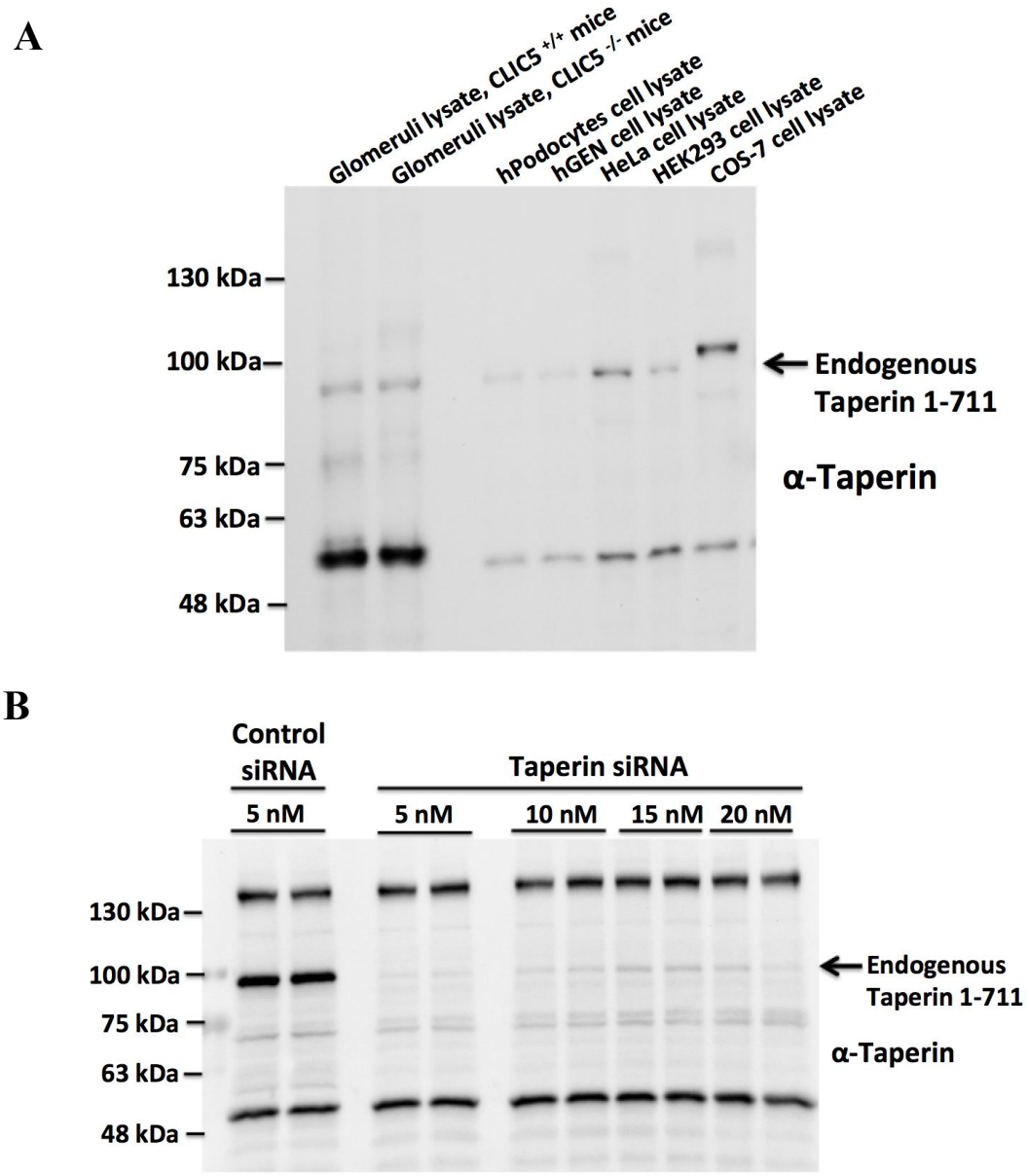

Figure 6.1: Taperin expresses in different cells. A. Western blot analysis with mouse anti(α)-taperin antibody using cell lysates of glomeruli isolated from CLIC5$^{+/+}$ and CLIC5$^{-/-}$ mice, cultured human podocytes, cultured human glomerular endothelial cells (hGEN), HeLa cells, HEK293 cells, and COS-7 cells. **B.** Western blot analysis with mouse α-Taperin antibody showing successful human taperin siRNA-mediated endogenous taperin knockdown in HeLa cells.

Figure 6.2

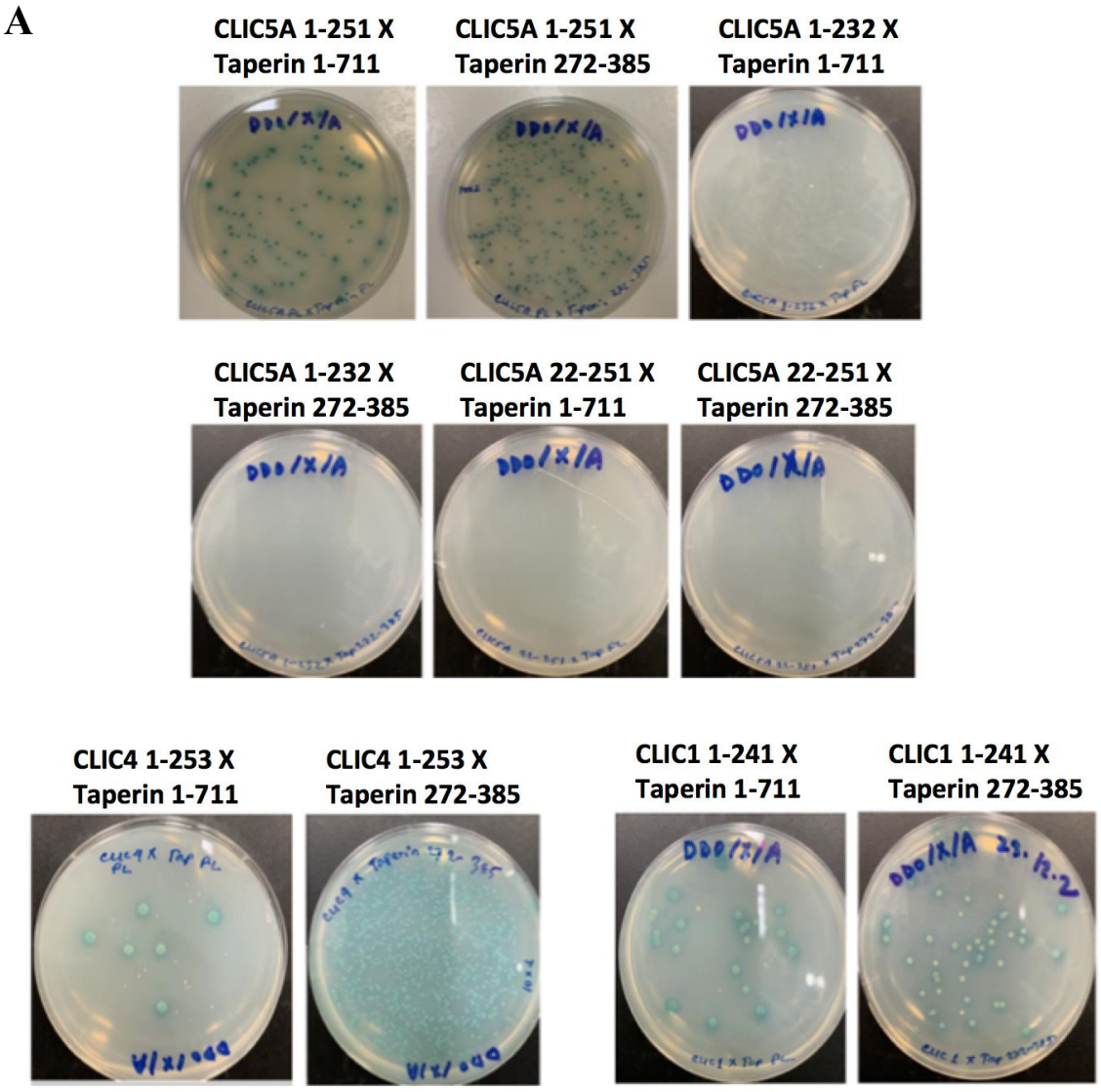

Figure 6.2: CLIC5A, CLIC4 and CLIC1 interact directly with taperin isoforms. A. Yeast two hybrid (Y2H) assay. Yeast colonies expressing untagged CLIC5A 1-251, CLIC5A 22-251 aa, and CLIC5A 1-232 aa in the "bait" vector and taperin 1-711 aa, and taperin 272-385 aa in the "prey" vector. **B.** Yeast two hybrid (Y2H) assay. Yeast colonies expressing untagged CLIC4 (1-253 aa) full-length and CLIC1 (1-241 aa) full-length in the "bait" vector and taperin 1-711 aa, and taperin 272-385 aa in the "prey" vector. Colony growth on DDO/X/A agar plates indicates both bait and prey vectors are present and blue colonies indicate α-galactosidase activity in the presence of X-α-gal due to direct interactions between bait and prey proteins showing Aureobasidin A antibiotic resistance.

Figure 6.3

A

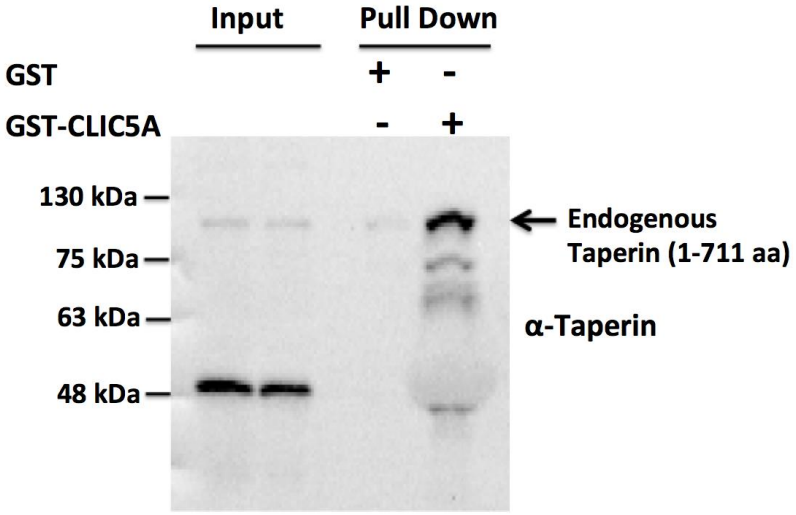

B

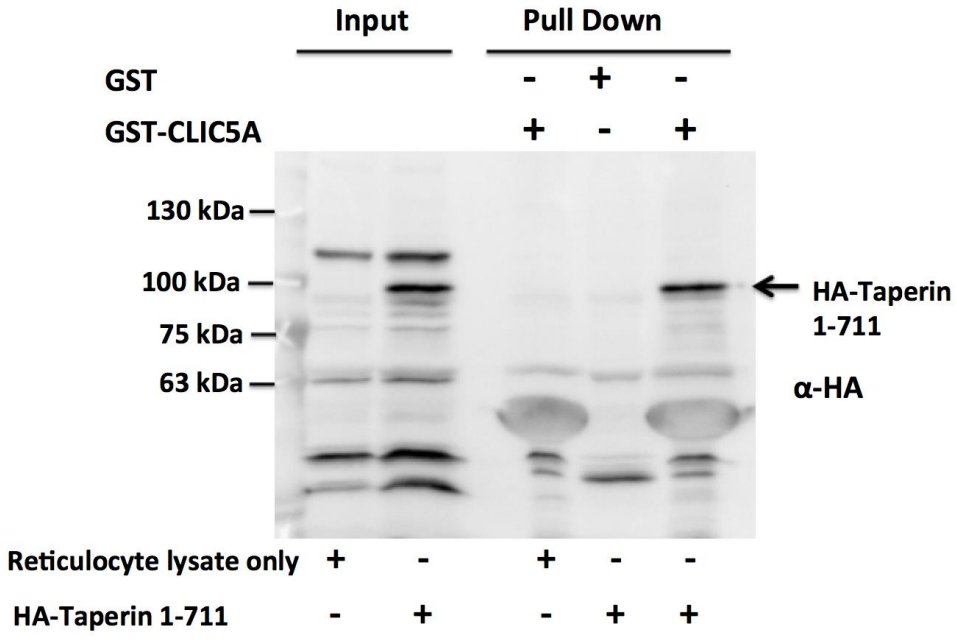

Figure 6.3 continues

C

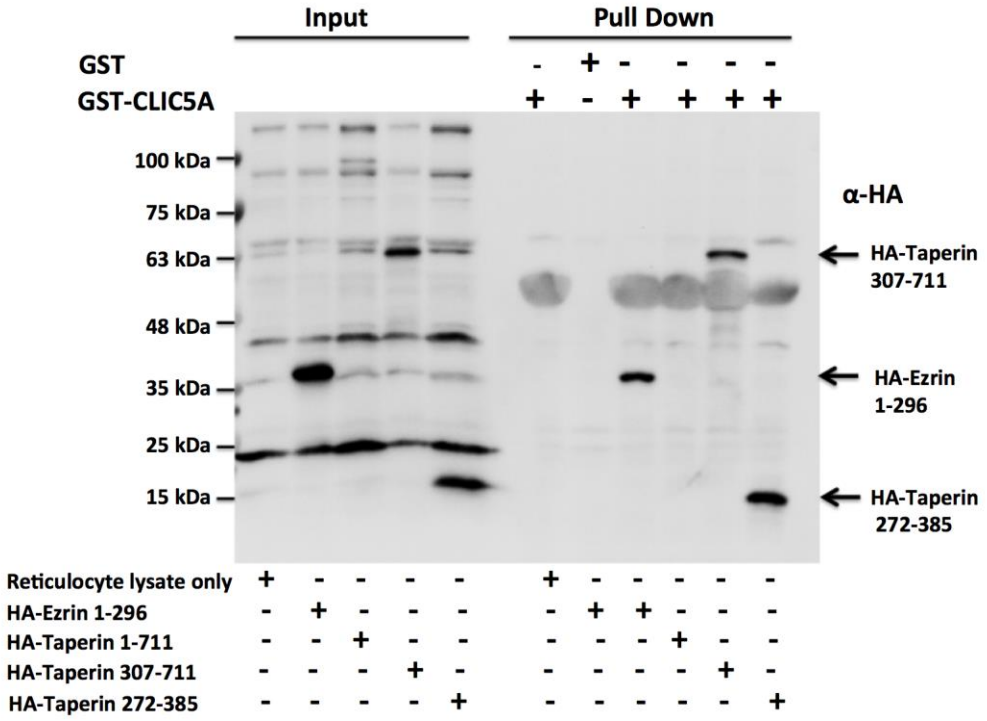

D

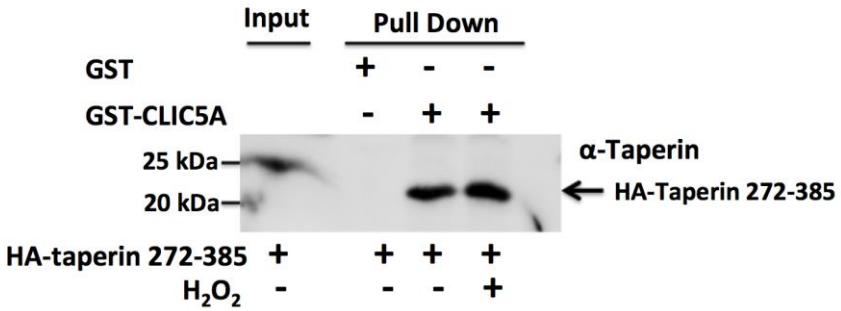

Figure 6.3: CLIC5A interacts directly with taperin *in vitro*. A. Western blot analysis with anti-taperin antibody of HeLa cell lysates (input), and proteins pulled by equimolar amount of immobilized GST-/GST-CLIC5A. **B.** Western blot analysis with α-HA antibody of reticulocyte lysate only, HA-taperin 1-711 aa synthesized *in vitro* (input), and proteins pulled by immobilized GST-/GST-CLIC5A. **C.** Western blot with α-HA antibody of reticulocyte lysate only, HA-taperin 1-711 aa, HA-taperin 307-711 aa, and HA-taperin 272-385 aa synthesized *in vitro* (input), and proteins pulled by equimolar amount of immobilized GST-/GST-CLIC5A. **D.** Western blot analysis with α-HA antibody of HA-taperin 272-385 aa synthesized *in vitro* (with/without 2 mM H_2O_2 treatment) (input), and proteins pulled by immobilized GST-/GST-CLIC5A.

Figure 6.4

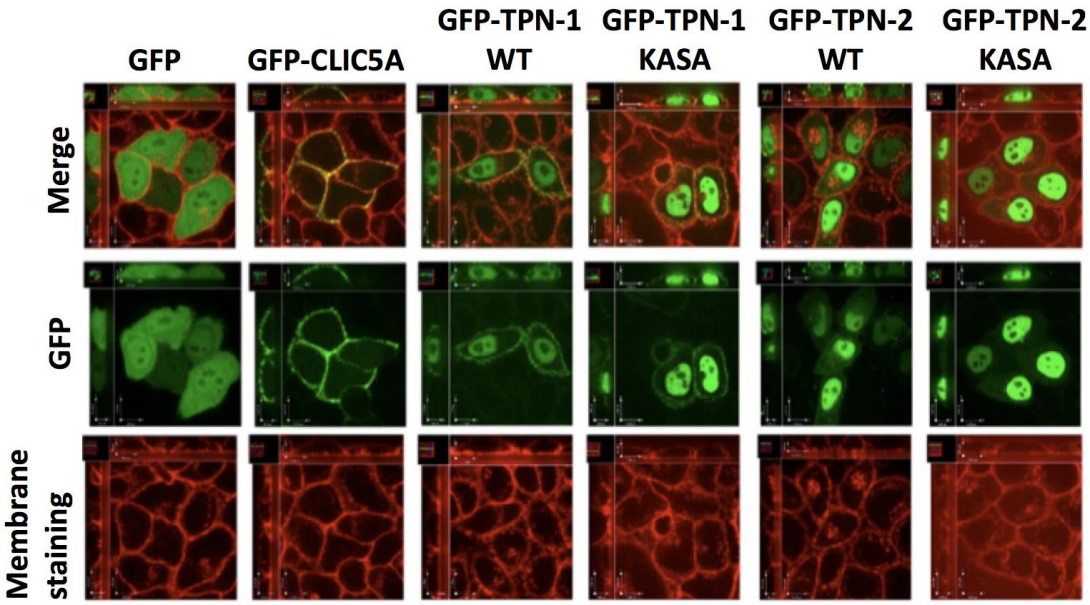

Figure 6.4: Taperin-1 (1-711 aa) and taperin-2 (307-711 aa) isoforms predominantly express at the nucleus. Live cell imaging of HeLa cells transiently transfected with GFP, GFP-CLIC5A, GFP-taperin-1-WT (full-length, wild type, 1-711 aa, codon optimized), GFP-taperin-1-KASA (full-length, KASA mutant, 1-711 aa, codon optimized), GFP-taperin-2-WT (isoform 2, wild type, 307-711 aa), and GFP-taperin-2-KASA (isoform 2, KASA mutant, 307-711 aa) cDNAs. GFP fluorescence shows the subcellular localizations of ectopically expressed proteins (middle panel). Membrane staining is observed at the bottom panel. Membrane-staining merge (yellow) with the overexpressed proteins are shown at the top panel.

Figure 6.5

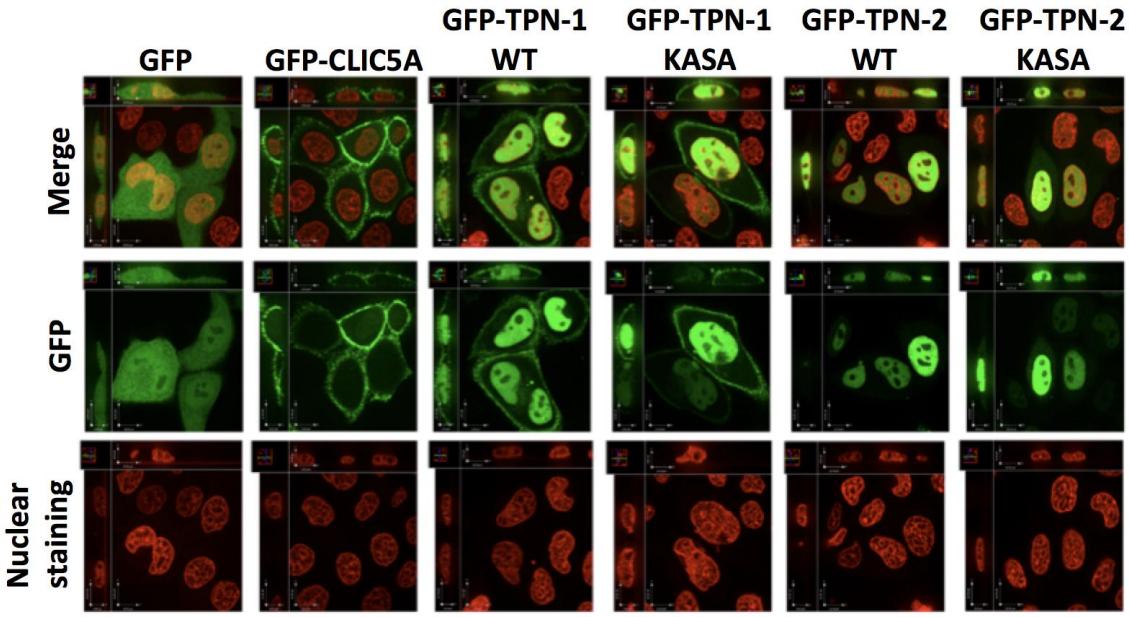

Figure 6.5: Taperin isoform 2 (307-711 aa) localizes predominantly at the nucleus. Live cell confocal microscopy imaging of HeLa cells transiently transfected with GFP, GFPP-CLIC5A, GFP-taperin-1-WT, GFP-Taperin-1-KASA, GFP-taperin-2-WT, and GFP-taperin-2-KASA cDNAs. Subcellular localizations were observed for the ectopically expressed proteins at the middle panel. Nuclear staining was observed at the bottom panel and nuclear staining merge (yellow) with the overexpressed proteins are shown at the top panel. GFP-TPN-1: GFP-taperin 1-711 wild-type (WT) aa (codon optimized); GFP-TPN-2: GFP-taperin 307-711 aa.

Figure 6.6

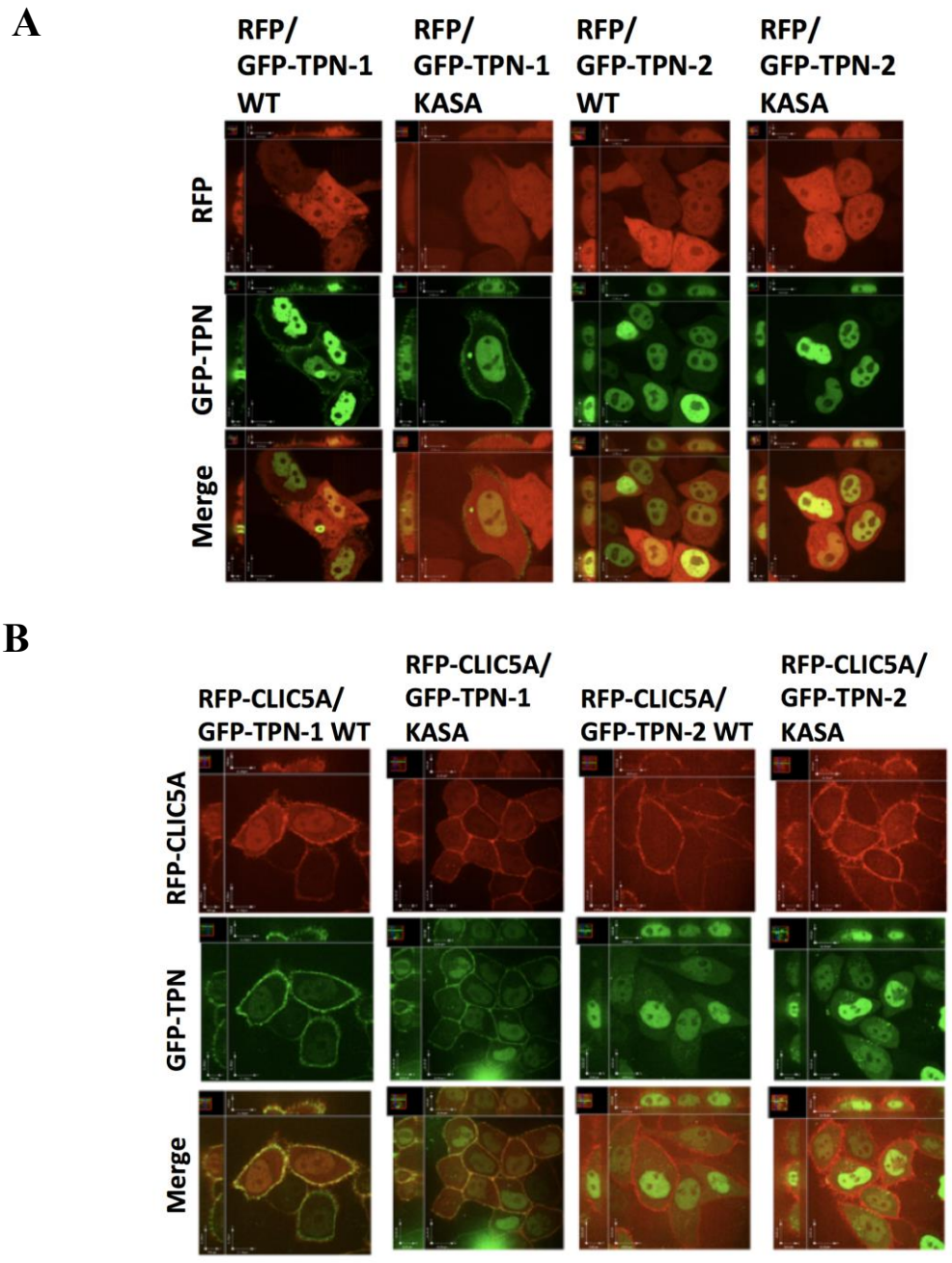

Figure 6.6: CLIC5A expression reduces taperin-1 (1-711 aa) localization from the nucleus. Live cell confocal microscopy imaging of HeLa cells co-transfected with RFP **(A)** or RFP-CLIC5A **(B)**, and GFP-taperin-1 1-711 (WT or KASA mutant), or GFP-taperin-2 (307-711) WT or KASA mutant) cDNAs. Co-localizations (yellow) in the merged image are observed at the cell periphery. GFP-TPN-1: GFP-taperin 1-711 wild-type (WT) aa (codon optimized).

Figure 6.7

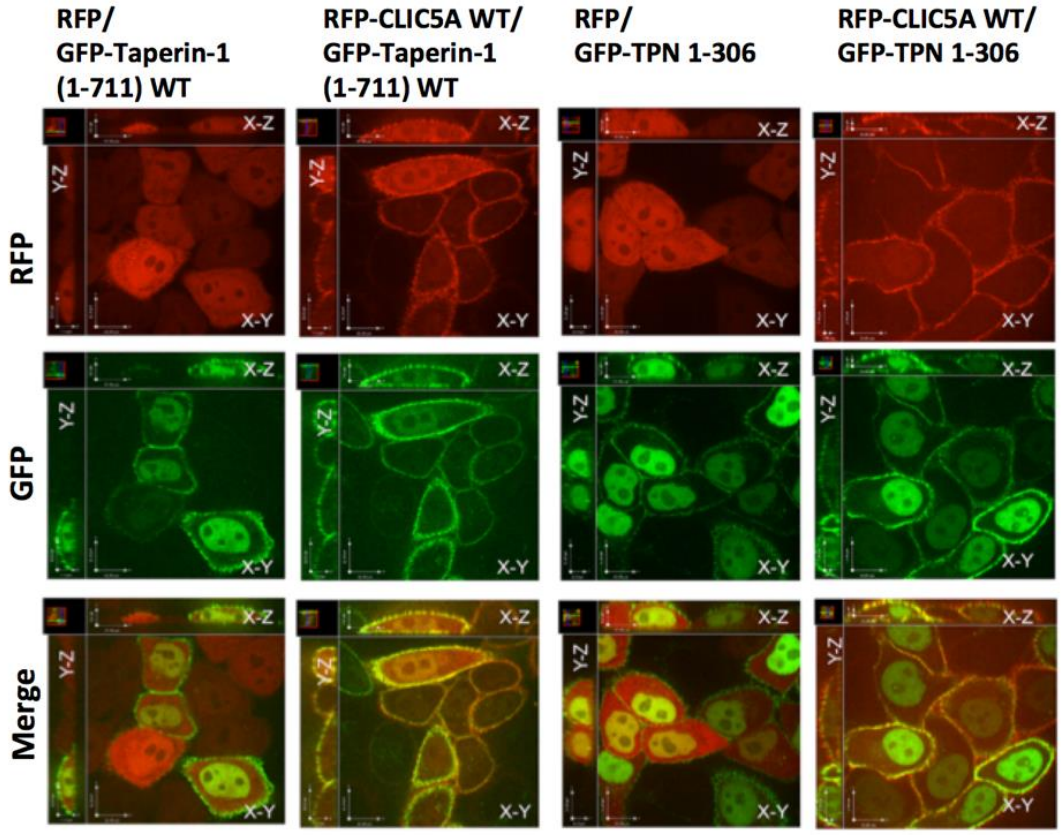

Figure 6.7: CLIC5A expression does not reduce taperin N-terminus (1-306) localization from the nucleus. Live cell confocal microscopy imaging of HeLa cells co-transfected with RFP/GFP-taperin 1-711 WT, or RFP-CLIC5A WT/GFP-taperin 1-711 WT, or RFP/GFP-taperin 1-306, or RFP-CLIC5A WT/GFP-taperin 1-306 cDNAs. Co-localizations (yellow) in the merged image are observed at the nucleus or cell periphery.

Figure 6.8

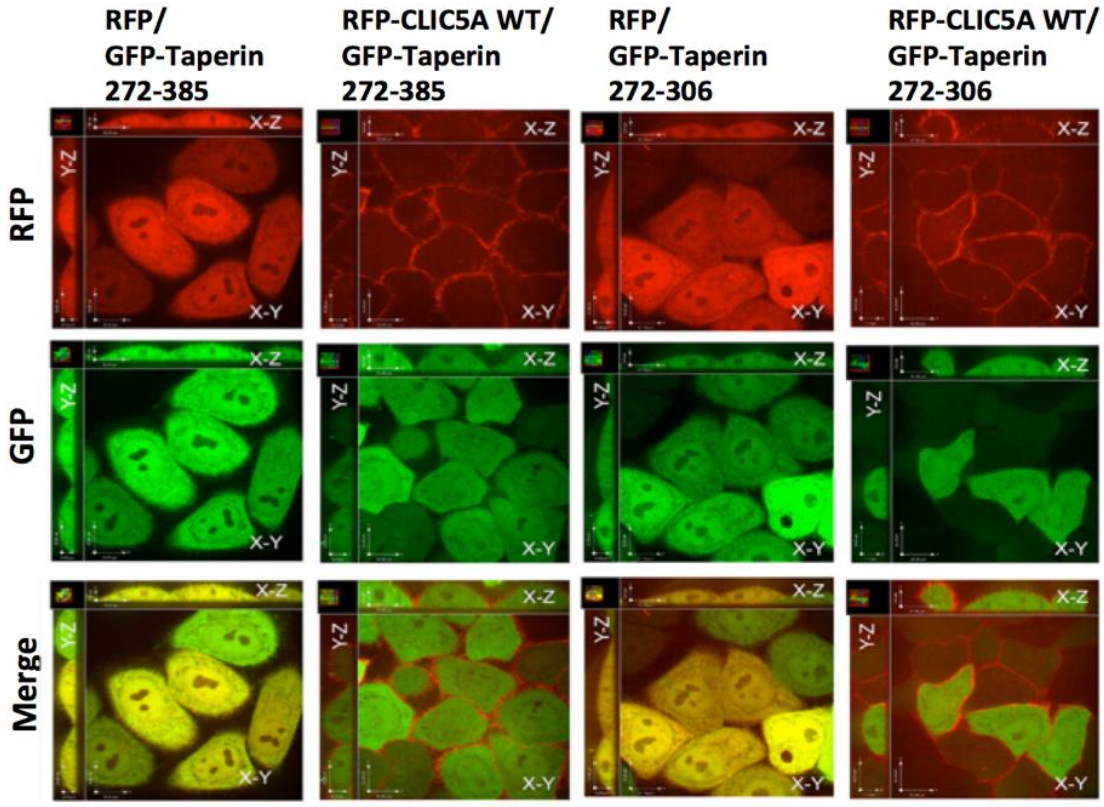

Figure 6.8: CLIC5A expression does not cause cytoplasmic taperin 272-385 or 272-306 to colocalize with CLIC5A at the cell periphery. Live cell confocal microscopy imaging of HeLa cells co-transfected with RFP/ GFP-taperin 272-385, or RFP-CLIC5A WT/GFP-taperin 272-385, or RFP/GFP-taperin 272-306, or RFP-CLIC5A WT/GFP-taperin 272-306 cDNAs. Co-localizations (yellow) in the merged images are observed at the cytoplasm.

Figure 6.9

A

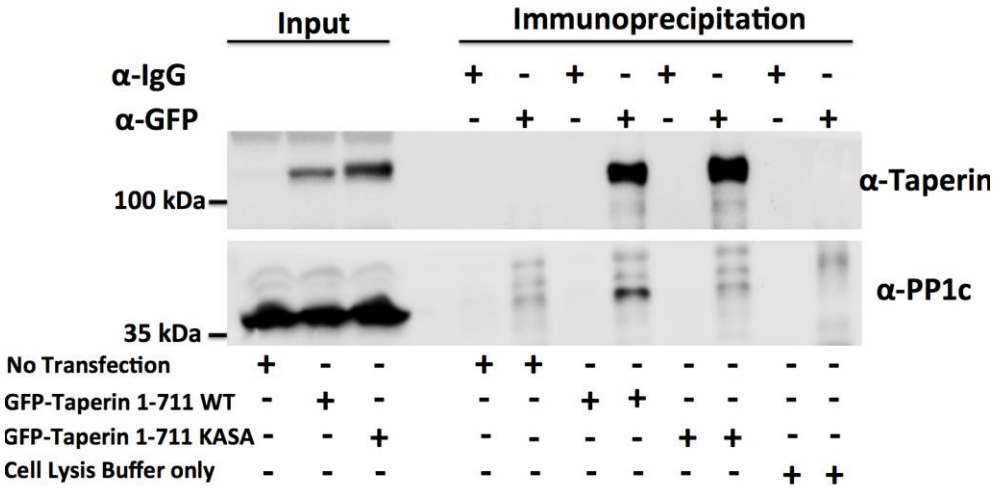

B

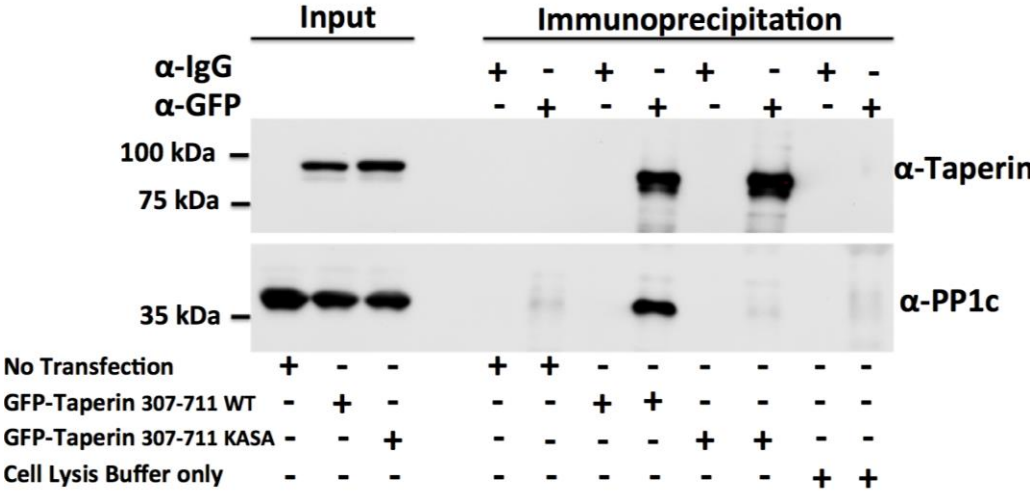

Figure 6.9: Taperin wild types interact with PP1c, but taperin KASA mutants fail to interact with PP1c. A. Immunoprecipitation with anti-GFP antibody of overexpressed GFP-taperin 1-711 WT or KASA mutant (codon optimized) with pan-PP1c proteins in HeLa cells, followed by western blot analysis with α-taperin and α-pan PP1c antibodies. **B.** Immunoprecipitation with anti-GFP antibody of overexpressed GFP-taperin 307-711 WT or GFP-taperin 307-711 KASA mutant with pan-PP1c proteins in HeLa cells, followed by western blot analysis with α-taperin and α-pan PP1c antibodies.

Figure 6.10

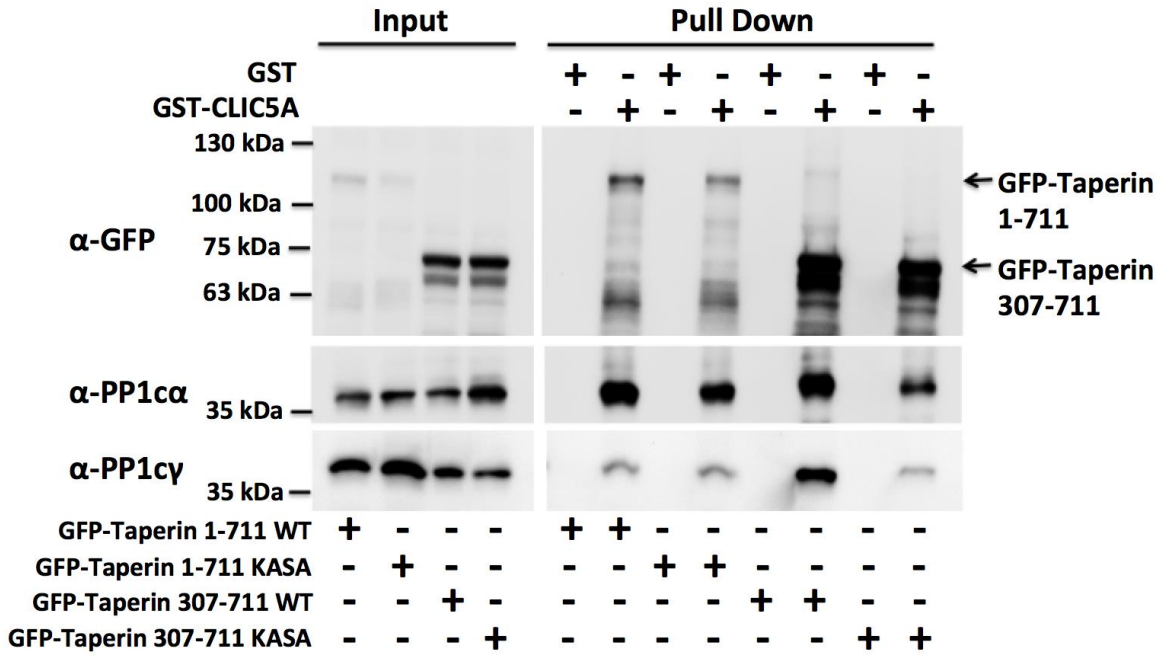

Figure 6.10: Taperin 307-711 KASA mutant failed to interact PP1cγ isoform. Western blot analysis with α-taperin, α-PP1cα and α-PP1cγ antibodies of lysates (input) and proteins of GST-/GST-CLIC5A pull down from HeLa cells transiently transfected with GFP-Tagged taperin 1-711 WT or KASA mutant (codon optimized), and taperin 307-711 WT, and KASA mutant.

Figure 6.11

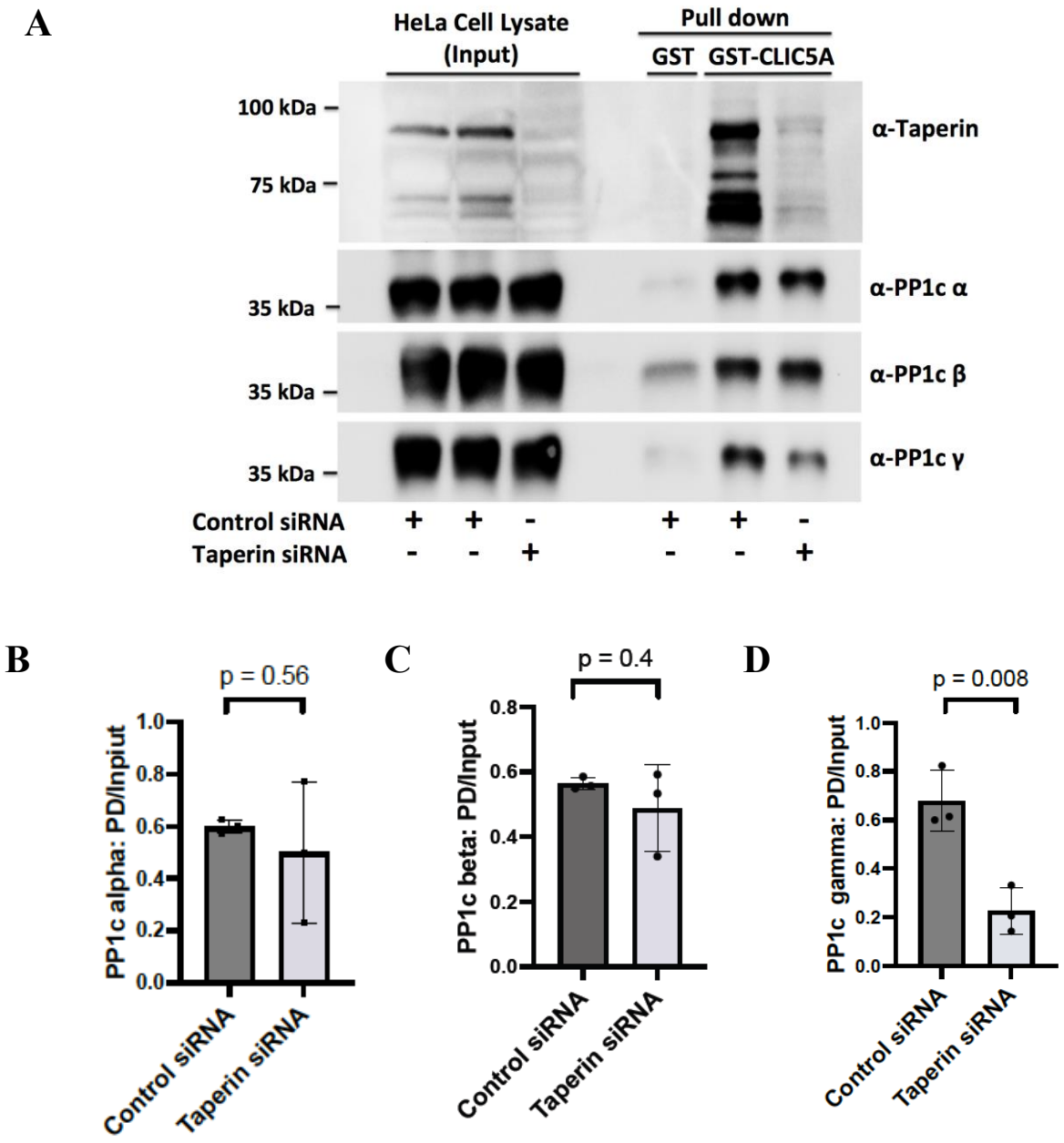

Figure 6.11: PP1cγ isoform specifically associates with the taperin/CLIC5A protein complex. A. Western blot analysis with anti-taperin, α-ezrin, anti-PP1cα, anti-PP1c β, and anti-PP1cγ showing control siRNA and human taperin siRNA-mediated endogenous taperin knock-down in HeLa cells, followed by GST-/GST-CLIC5A pull-down. **B - D**. Densitometric quantification of PP1cα, PP1cβ or PP1cγ pulled down by GST-CLIC5A from HeLa cells transfected with control siRNA and human taperin siRNA.

Figure 6.12

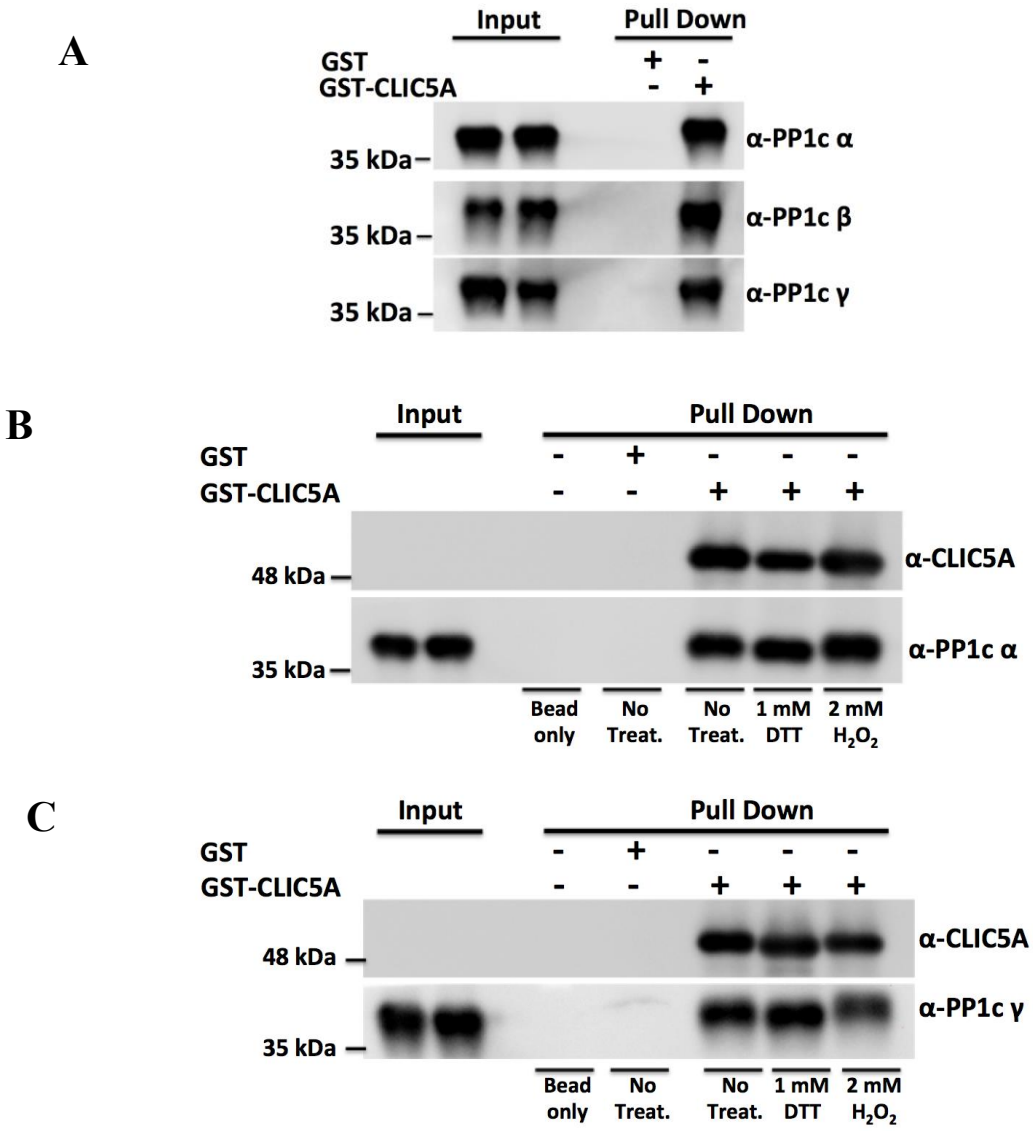

Figure 6.12: CLIC5A interacts directly with the PP1c isoforms *in vitro*. A. WB with α-PP1cα, α-PP1cβ, and α-PP1cγ antibodies. 10 ng Purified protein PP1cα, or PP1cβ, or PP1cγ were used as input. 100 ng of purified protein PP1cα, or PP1cβ, or PP1cγ were incubated at 4°C with 500 ng GST-, or 1.0 µg of GST-CLIC5A in 500 µl of sterilized Tris-HCl, 20 mM, pH 7.4 buffer for GST-/GST-CLIC5A pull-down. **B - C.** WB with α-PP1cα, or α-PP1cγ and α-CLIC5A antibodies. 10 ng purified protein PP1cα or PP1cγ used as input and 100 ng PP1c α or PP1cγ were incubated with 500 ng GST-, or 1.0 µg of GST-CLIC5A in 500 µl of Tris-HCl, 20 mM, pH 7.4 buffer (no treatment, or 1 mM DTT, or 2 mM H_2O_2 added) for GST-/GST-CLIC5A pull-down assay using glutathione bead (50 µl).

Figure 6.13

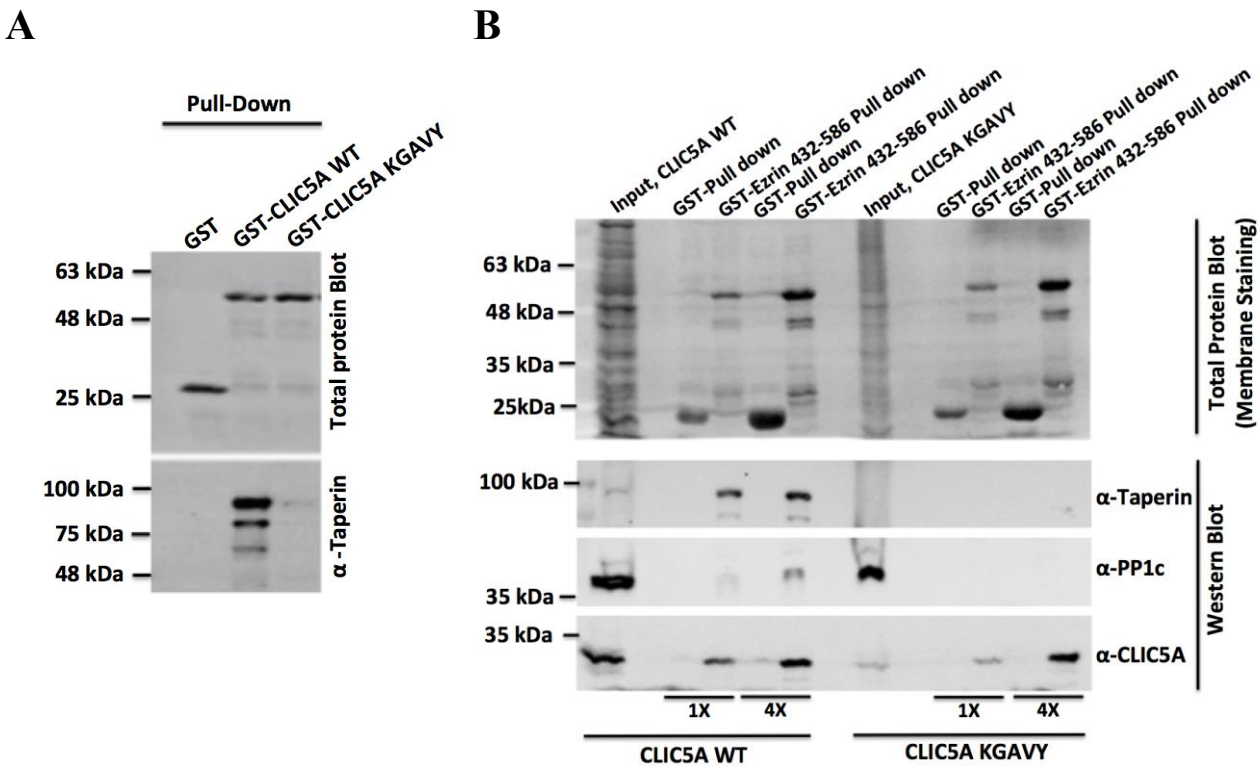

Figure 6.13: CLIC5A KGAVY mutant fails to interact with taperin or PP1c. A. Membrane staining/total protein labelling blot showing GST- and GST-CLIC5A or GST-CLIC5A KGAVY pull-down from untransfected HeLa cells. Endogenous taperin is precipitated only by wild-type GST-CLIC5A, not by GST- or GST-CLIC5A KGAVY. **B.** GST-ezrin 432-586 aa (1X, 4X) pull-down from HeLa cells transfected with untagged CLIC5A or CLIC5A KGAVY**.** Western blot analysis with α-taperin, α-pan PP1c and α-CLIC5A showing input endogenous taperin, endogenous pan-PP1c and ectopically expressed untagged CLIC5A WT and KGAVY mutant. GST-ezrin 432-586 precipitates WT and KGAVY CLIC5A, but taperin and PP1c are only pulled into the complex in the presence of WT CLIC5A.

Figure 6.14

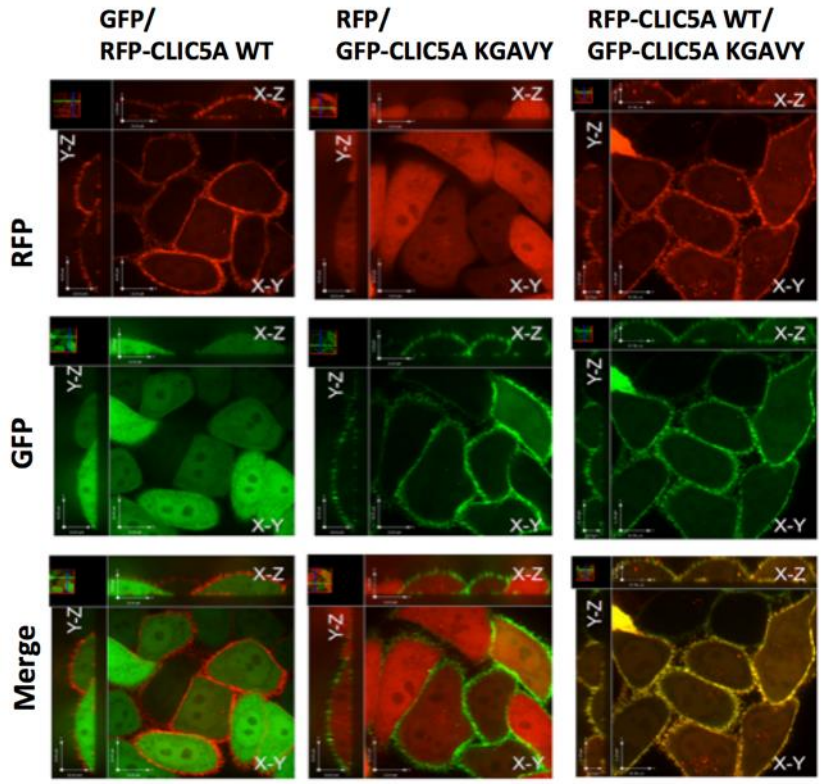

Figure 6.14: KGAVY mutation in CLIC5A does not alter CLIC5A localization at the cell periphery. Live cell confocal microscopy imaging of HeLa cells co-transfected with GFP/RFP-CLIC5A wild type (WT), or RFP/CLIC5A KGAVY mutant, or RFP-CLIC5A WT/GFP-CLIC5A KGAVY cDNAs. Co-localizations (yellow) in the merged image are observed at the cell membrane.

Figure 6.15

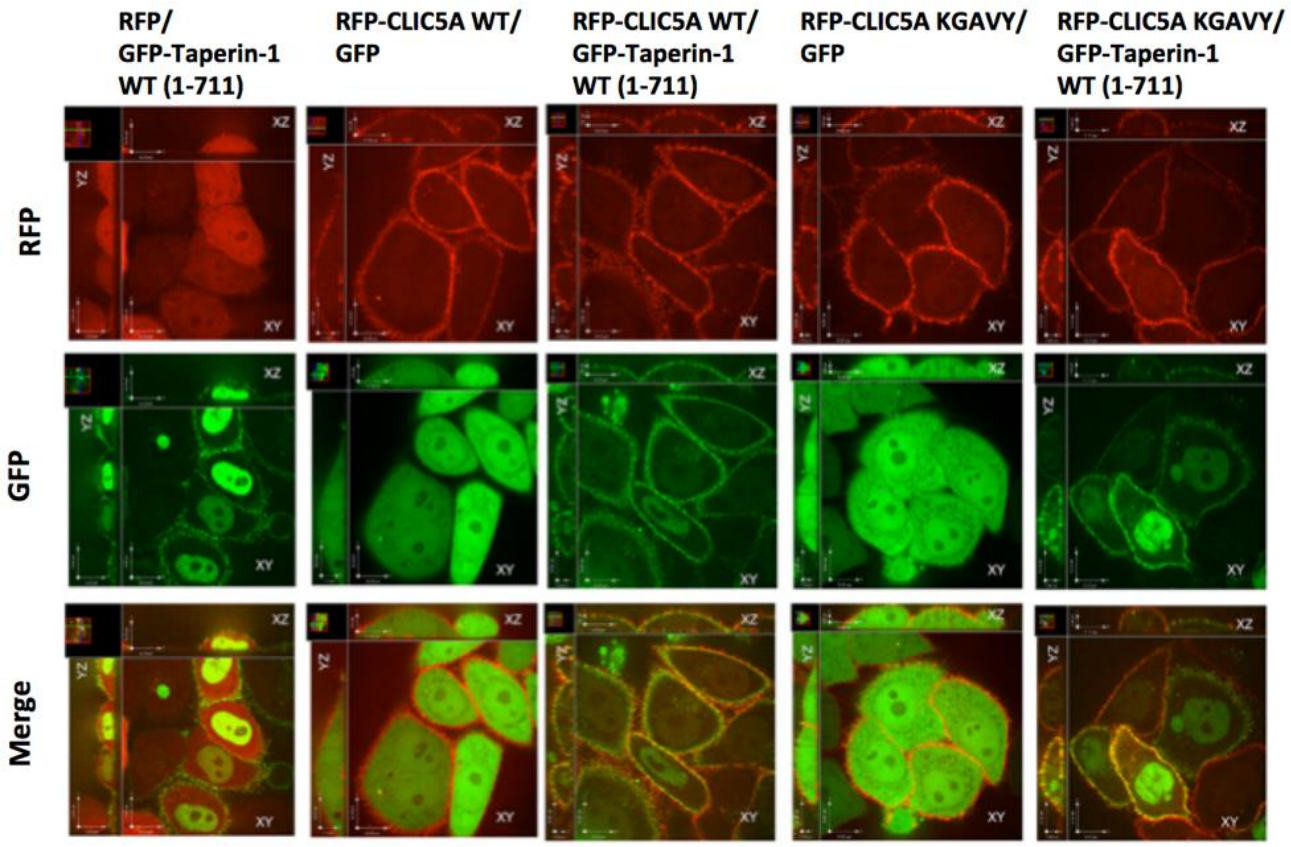

Figure 6.15: CLIC5A KGAVY cannot reduce taperin 1-711 from the nucleus. Live cell confocal microscopy imaging of HeLa cells co-transfected with RFP/GFP-taperin 1-711 wild type (WT), or RFP-CLIC5A WT/GFP, or RFP-CLIC5A WT/ GFP-taperin 1-711 WT, or RFP-CLIC5A KGAVY/GFP, or RFP-CLIC5A KGAVY/GFP-taperin 1-711 WT cDNAs. Co-localizations (yellow) in the merged image are observed at the nucleus or cell membrane.

Figure 6.16

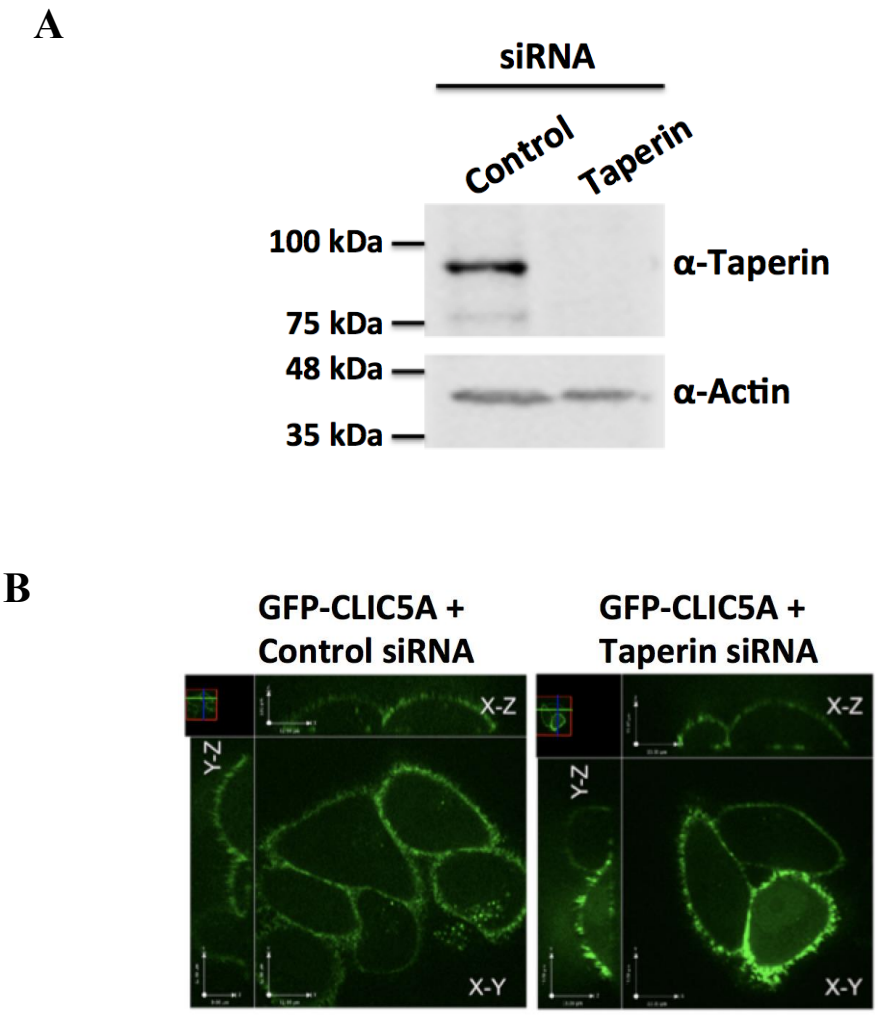

Figure 6.16: Taperin knockdown does not alter CLIC5A localization at the cell periphery. **A.** Western blot analysis with α-taperin, α-actin antibodies of lysates from HeLa cells transfected with control siRNA or human taperin siRNA. **B.** Confocal microscopy imaging of cultured HeLa cells transfected with GFP-CLIC5A cDNA and control siRNA or taperin siRNA.

Figure 6.17

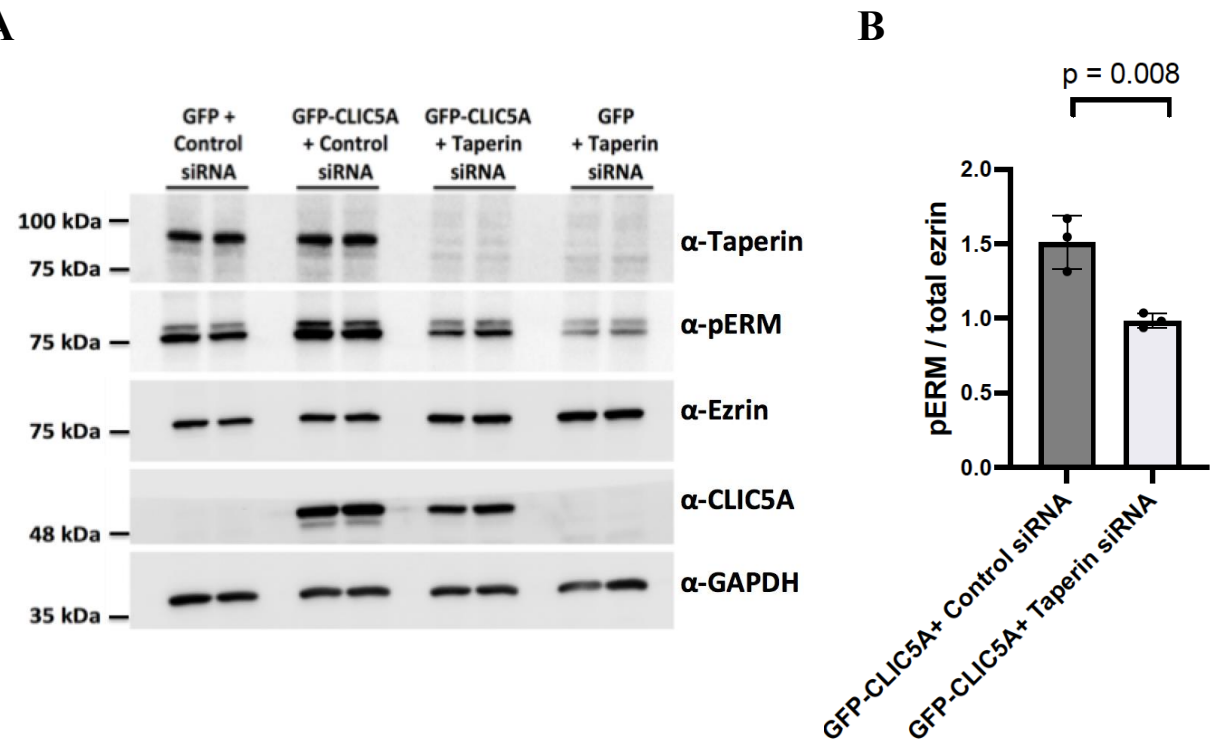

Figure 6.17: Taperin knockdown reduced ERM phosphorylation. A. Western blot analysis with α-taperin, α-pERM, α-ezrin, α-CLIC5A, and α-GAPDH antibodies of lysates from HeLa cells transiently transfected with GFP- or GFP-CLIC5A cDNAs and control siRNA or human taperin siRNA. **B.** Densitometric quantification of pERM/total ezrin (mean ± S.D., n = 3 independent experiments).

6.3. Discussion

Taperin is a ubiquitously expressed PP1 regulatory subunit with multiple splice variants. Human mutations in exon 1 at the DFNB79 locus of the TPRN gene lead to hereditary non-syndromic autosomal recessive deafness (433). *In vivo* and *in vitro* studies have proved that taperin (isoform 2) is a PP1c interacting protein (434) and that it has a preference to dock the PP1α isoform through its KISF PP1c binding motif (434).

On western blots using a mouse monoclonal antibody, I identified the taperin isoform 1 (1-711) unequivocally. The other major ~50 kDa protein detected with the monoclonal mouse anti-taperin antibody was not sensitive to taperin siRNA-mediated silencing (Figure 6.1B). Since the siRNA used in our experiments target the common sequence of isoforms 1-4, it seems unlikely that the ~50 kDa band is the taperin isoform 2. However, two faint bands that reacted with the antibody in the ~ 60 kDa region and were silenced by taperin-specific siRNA were also observed (Figure 6.1B). On subsequent western blots bands below ~ 75 kDa that reacted with the monoclonal anti-taperin antibody, were silenced by taperin-specific siRNA and were pulled down from the lysates and concentrated by GST-CLIC5A (Figures 6.11A, 6.16A) were also observed. It seems likely that these proteins represent smaller isoforms of taperin. Analysis for taperin mRNA species and Mass Spectrometry of the smaller taperin proteins will need to be done to define their identity.

My PCR amplification of taperin isoform 2 was successful, but I could not amplify taperin isoform 1, probably due to the high GC content (~71%) in the nucleotide sequence. Therefore, we undertook to have cDNAs encoding the taperin isoform 1 (wild type and KASA mutants) by the company Gene Script, using codon optimization. The sequence was verified, and correctly encodes the protein sequence of the taperin isoform 1.

The Y2H screen indicated that CLIC5A interacts directly with the mouse taperin isoform 1 central domain (312-424 aa), which is 78% identical with the human taperin isoform 1 sequence at 272-385aa. For subsequent experiments I therefore used cDNAs encoding full-length human taperin isoform 1 1-711 and a human taperin 272-385 fragment as prey to test against CLIC5A, CLIC4 and CLIC1 baits in the Y2H assay. Both, human taperin isoform 1 (1-711aa) and the human taperin 272-385 fragment showed an interaction with CLIC5A, CLIC4 and CLIC1, though the interaction with the taperin 272-385 fragment was stronger (Figure 6.2). I concluded that the 272-385 region in human taperin is the region that binds CLIC5A, CLIC4 and CLIC1 directly. Deletion of parts of N- and C-termini of CLIC5A abolished the interaction with taperin in the Y2H assay. This is similar to our findings in chapter 3 where I showed that these deletion mutants of CLIC5A could not bind ezrin. Taken together with previously published data by Al-Momany et al. (89), the findings indicate that N- and C-terminal deletions of CLIC5A make it non-functional and that intact N- and C-termini of CLIC5A are required for binding to its interacting partners.

taperin isoform 1 (1-711aa) seems to have a much higher affinity for CLIC5A than the ERM proteins. This was evident from the GST-CLIC5A pull-down data and from the Y2H analysis. In fact, the Y2H library screening revealed 32 clones of mouse taperin and only one clone of mouse radixin. The GST-CLIC5A pull-down captured and markedly concentrated endogenous taperin (Figures 6.3A, 6.11A, 6.13B), while the endogenous ERM proteins though highly expressed, and though pulled down, were not concentrated by GST-CLIC5A (Figure 3.8). I used different HA-taperin cDNA constructs cloned into the pGADT7 prey vector for TnT *in vitro* transcription/translation-based synthesis of taperin proteins using the reticulocyte lysates to study the protein-protein direct interaction *in vitro* and found that the taperin isoform 2 and the HA-

taperin 272-385 fragment were readily synthesized and pulled down by GST-CLIC5A. Synthesis of HA-taperin isoform 1 (1-711) was inefficient when compared to HA-taperin isoform 2 (307-711aa) the or the taperin 272-385aa fragment, but when I scaled up the volume of reticulocyte lysate from 40 µl to 160 µl for the GST-CLIC5A pull down assay I found that *in vitro* synthesized HA-taperin isoform 1 (1-711aa) was effectively pulled from solution and by GST-CLIC5A (Figure 6.3B). Because CLIC proteins transition from a folded to an unfolded conformation in response to oxidation, I also treated the pull-down mixture of *in vitro* synthesized HA-taperin 272-385 and immobilized GST-CLIC5A with H_2O_2 and found that it did not affect the efficiency of GST-CLIC5A pull down of HA-taperin 272-385.

Live cell imaging with GFP-tagged taperin isoform 1 (1-711aa), the N-terminus of taperin isoform 1 (1-306aa), and taperin isoform 2 (307-711aa) revealed that their localization is predominantly nuclear, consistent with the findings observed by Ferrar et al. (434) for taperin isoform 2 (307-711aa). The NLStradamus® online NLS prediction software detected nuclear localization signals in the taperin 1 isoform (1-711) at amino acids 25-28 and 142-193, but not in the taperin 2 sequence. In general nuclear export requires 4 closely spaced hydrophobic residues (typically leucine with an arrangement of LxxxLxxLxL), though isoleucine, methionine, valine and phenylalanine can also support nuclear export. No regions with the typical arrangement are present in the taperin 1-711 sequence, though there is one region with an atypical arrangement of 4 leucine residues ($_{312}$**L**GD**L**QARA**L**AS**L**$_{323}$**)**, interestingly located in the identified CLIC5A binding region. Whether this sequence supports nuclear export will require future investigation. However, we observed a fraction of GFP-taperin isoform 1 (1-711) as well as its 1-306 aa N-terminal fragment also localized to the cell periphery. By contrast, the GFP-taperin isoform 2 localized exclusively to the nucleus and was never found at the cell periphery. Therefore,

targeting of a fraction of the taperin isoform 1 to the cell periphery is mediated by the N-terminal 1-306 aa region.

Importantly, when RFP-CLIC5A and different GFP-taperin proteins were co-expressed in HeLa cells we observed that the taperin isoform 1 (1-711aa) was now found predominantly at the cell periphery where it co-localized strongly with RFP-CLIC5A, and that its nuclear localization was substantially diminished compared to cells not expressing CLIC5A. This reduction in nuclear localization was also observed when the KASA mutant of the taperin isoform 1 was co-expressed with RFP-CLIC5A. Using photobleaching microscopy, Ferrar et al. (434) previously concluded that the GFP-taperin isoform 2 can exit the nucleus. However, we observed that RFP-CLIC5A expression did not change the nucleoplasmic localization of GFP-taperin isoform 2 nor the GFP tagged taperin 272-385 fragment, the region that binds CLIC5A. The finding that RFP-CLIC5A expression did not reduce the nuclear localization of taperin 272-385 aa or 272-306 aa suggests that both, an intact N-terminus (1-306) and the CLIC5A binding region (272-385) are required to reduce the nuclear localization of the taperin isoform 1. The mechanism by which CLIC5A expression causes the taperin isoform 1 to exit the nucleus, while the taperin isoform 2 (307-711aa) is retained could be due to a nuclear export signal in the N-terminal 1-306 region, but so far, such a sequence has not been identified. The CLIC5A-dependent shift of the taperin 1 isoform from nucleus to the cell periphery may be functionally important and will require further evaluation.

Our approach to study the interaction of taperin with PP1c isoforms, and of mutating the KISF motif was based on previously published work by Ferrar et al. (434). Using the Bimolecular Fluorescence Complementation (BiFC) assay with the NIPP1 protein as a control, they demonstrated that EYFP-PP1γ-taperin 307-711 wild type formed a competent fluorophore in

living cells, emitting a clear nuclear EYFP signal [direct vicinity (<10 nm)], similar to the positive control NYFP-NIPP1, whereas the EYFP signal was completely abolished in case of taperin 307-711 KASA mutant, indicated that KASA mutant with the PP1c binding motif mutated cannot bind PP1c (434). They also reported that overexpressed taperin 307-711 recruits most of the nuclear PP1cγ isoform, including the nucleolar pool to the nucleoplasm of the cell where taperin is expressed and found that mutation of the PP1 binding site from KISF to KASA prevented this relocalization of PP1γ. My experiments showing that the taperin isoform 2 (307-711aa) prefers PP1cγ, at least when expressed in HeLa cells (Figure 6.10), is consistent with those observations.

We expected that GST-CLIC5A would pull taperin from cell lysates, and that PP1c would be co-precipitated because CLIC5A directly binds taperin, and taperin directly binds PP1c. Indeed, GST-CLIC5A co-precipitated the endogenous the taperin 1 isoform as well as PP1c (Figure 6.10). However, when I knocked down taperin using siRNA, endogenous PP1cα and PP1cβ were still pulled from the HeLa cell lysates, even though there was little or no taperin in the precipitate (Figure 6.11). This finding was surprising and indicated that PP1cα and PP1cβ can interact with GST-CLIC5A in a taperin-independent fashion. Sequence analysis showed that CLICs share a potential PP1c binding motif ($_{45}$KGVVF$_{49}$ for CLIC5A), and we found that GST-CLIC5A can precipitate all three recombinant, purified PP1c isoforms *in vitro*, in the absence of other proteins. In a separate set of experiments, GST-ezrin 432-586 was used for a "reciprocal" pull-down of WT and $_{45}$KGAVY$_{49}$ mutant CLIC5A expressed in HeLa cells. The GST-ezrin 432-586 fragment pulled WT CLIC5A as well as endogenous taperin and PP1c proteins from HeLa cell lysates. But while the GST-ezrin 432-586 fragment also pulled the $_{45}$KGAVY$_{49}$ mutant CLIC5A from cell lysates taperin and PP1c were not co-precipitated with the $_{45}$KGAVY$_{49}$

mutant CLIC5A. This experiment indicates that the KGVVF motif of CLIC5A, and probably also the other CLICs, is necessary for its interaction with taperin. We expected that the mutation would knock out PP1c binding to CLIC5A, and PP1c was also absent from the complex containing the $_{45}$KGAVY$_{49}$ mutant CLIC5A, but whether this was due to its inability to bind to CLIC5A or the fact that taperin was not pulled down is unclear. It is possible that CLIC5A, and other CLICs are substrates for taperin/PP1c and that the PP1c catalytic subunit transfers to the CLIC5A substrate from taperin. It is also conceivable that taperin/CLIC5A and PP1c form a heteromer, but it seems unlikely that a single PP1c molecule binds taperin and CLIC5A simultaneously. In our live cell imaging experiments, the presence of the $_{45}$KGAVY$_{49}$ mutation in CLIC5A had no effect on its peripheral localization, but unlike wild-type CLIC5A, the the $_{45}$KGAVY$_{49}$ mutant CLIC5A did not reduce the nuclear localization of GFP-taperin isoform 1 (1-711) (Figure 6.15). We think therefore, we have inadvertently produced a CLIC5A mutant that cannot bind taperin, though it was our intent to mutate a PP1c binding motif. More work is needed to determine whether this mutation also eliminates the CLIC5A/PP1c interaction. Also, the functional role(s) of the interactions between CLIC5A, taperin and the PP1 catalytic subunits need further investigation.

The preference of taperin for PP1cγ in the CLIC5A-bound form of taperin raises the possibility that CLIC5A-bound taperin binds and inhibits the PP1cγ phosphatase activity in the CLIC5A/ezrin complex to protect CLIC5A-dependent ERM phosphorylation. It is already proven that taperin inhibits PP1cα phosphatase activity against the glycogen phosphorylase A substrate (434). However, since the taperin knockdown also inhibited basal ERM phosphorylation, the effect of taperin on ERM phosphorylation is not CLIC5A-dependent. It is more likely that taperin competes for PP1c subunits, thereby inhibiting the function of other PP1

holoenzyme(s) toward the ERMs. Another possibility might be that taperin inhibits PP1c under the basal conditions and that an unknown stimulus activates the taperin/PP1c phosphatase activity against ERM proteins.

Finally, unlike triple ERM silencing (Chapter 4), siRNA mediated taperin knockdown did not change the peripheral CLIC5A localization (Figure 6.14), indicating that CLIC5A localization at or near the cell membrane is independent of taperin.

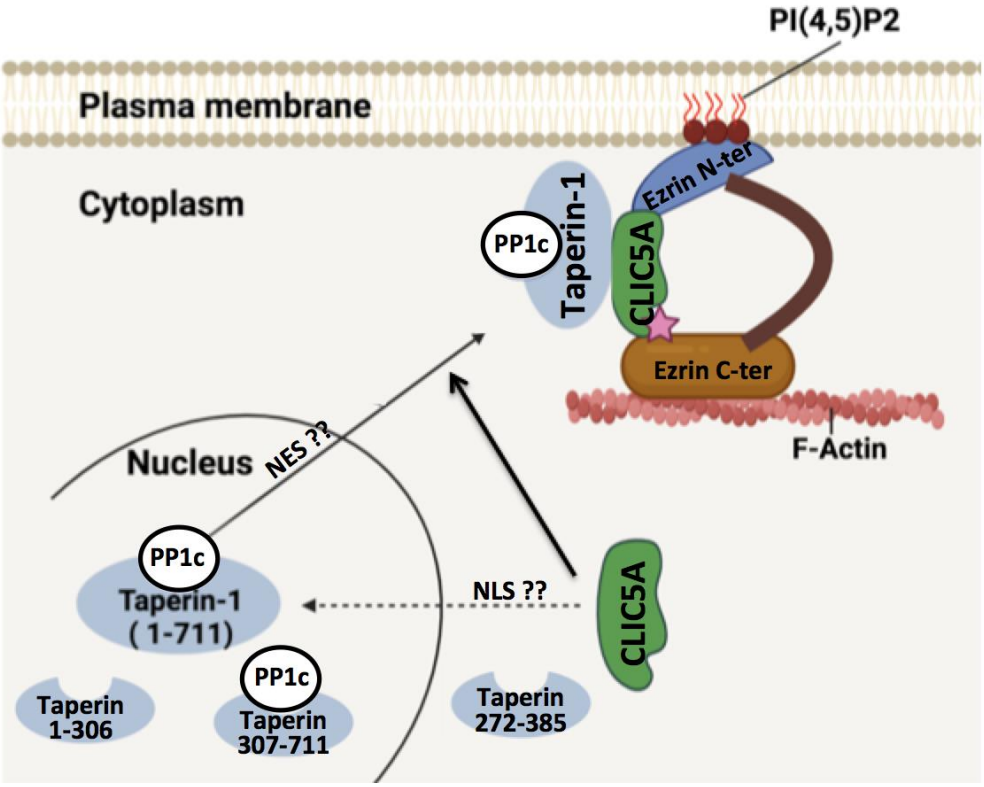

Figure 6.18: Model: CLIC5A expression abolishes taperin full-length (1-711) localization from the nucleus. CLIC5A and taperin 1-711 colocalizes at the cell periphery. CLIC5A might facilitate taperin move out of the nucleus into the CLIC5A/ezrin complex where it colocalizes with CLIC5A, or CLIC5A/taperin forms a complex in the cytoplasm, which prevents full-length taperin to go to the nucleus, but CLIC5A has no effect on nuclear localization of taperin 1-306 or 307-711. taperin 1-711, 1-306, and 307-711 and CLIC5A might have nuclear localization signal (NLS) and taperin full-length might have an additional nuclear export signal (NES).

Chapter 7

Overall Discussion and Future Directions

Chapter 7

Overall discussion and future directions

7.1. Overall discussion

This thesis provides experimental evidence for molecular mechanisms that underlie the CLIC5A-dependent Rac1 GTPase activation and ERM phosphorylation. While previous studies reported controversial ion-conductance of CLIC5A *in vitro* (345), CLIC5A-stimulated ERM phosphorylation (89) and Rac1 activation (86), how CLIC5A activates Rac1 and phosphorylates ERM proteins was not known.

In this thesis, I present data in chapter 3 that even though CLIC5A and ezrin are part of the Rac1-GTP complex, Rac1 is not a direct interacting partner of CLIC5A. Direct activation of Rac1 and probably other small GTPases by CLIC5A and other CLICs is therefore highly unlikely. However, radixin, ezrin, and moesin turn out to be direct interacting partners of CLIC5A. For ezrin, I showed that this interaction is strongest for the C-terminal 432-586 domain and that deletion of the last 16 amino acids of the ezrin C-terminus completely abolish the interaction. Furthermore, my work shows that phosphorylation of ezrin at the conserved T567 residue enhances CLIC5A binding. The actin-binding site of ezrin has been mapped to the 558-585 region of its carboxy terminus (207), so deletion of its last 16 amino acids should disrupt actin binding as well. Actin was also shown to enhance the interaction of CLIC5A with a carboxyterminal fragment of ezrin (422). The possibility that ezrin/actin complex formation is necessary for CLIC5A binding to ezrin, still needs to be investigated.

I also found that full-length ezrin (1-586 aa) does not interact directly with CLIC5A in the Y2H assay, or when I synthesized full-length ezrin *in vitro*. This is not a surprise, since ERM proteins take on a "closed", inactive conformation due to intramolecular binding their N- and C-

termini. Binding of the N-terminus to PI4,5P_2 is necessary to free the C-terminus so it can be phosphorylated and bind actin, and in this study, CLIC5A. Full-length ezrin did, however, co-immunoprecipitate with CLIC5A when both proteins were present in cells, indicating that they interact in the living cell. It is also likely that CLIC5A-stimulated ERM phosphorylation enhanced CLIC5A binding. The ezrin N-terminal domain (1-296) also did not interact directly with CLIC5A in yeast cells, but when it was synthesized in vitro or expressed in cells, GST-CLIC5A was able to bind to it. We think that docking of this ezrin fragment to the PI4,5P2 at the cell membrane, might have made it unavailable to bind to CLIC5A in the yeast cells. The findings in this thesis therefore suggest that the interaction of CLIC5A with ezrin, though direct, are not due to interactions between short, sequence-specific motifs in either protein, but that they require the complete CLIC5A protein and may involve both C- and N-termini of ERM proteins. The exact biochemical mechanism of their interaction and the functional consequences of this interaction therefore still need further investigation.

In chapter 4, I showed that endogenous, native CLIC5A expressed in mouse glomeruli is predominantly soluble, that Ser/Thr phosphatase inhibition could not increase its membrane localization, but that Staurosporine and Phospholipase C activation decreased its association with the membrane and cytoskeletal fractions. Therefore, endogenous CLIC5A can move fairly rapidly from the membrane to the soluble fraction, which is not the behaviour expected from an integral membrane protein or membrane–spanning chloride channel. Furthermore, in cultured cells, association of expressed CLIC5A with the membrane fraction was reduced by the ezrin 432-586 fragment and endogenous ERM knockdown reduced CLIC5A localization at the cell periphery, suggesting that the CLIC5A localization at or near the cell membrane is at least partly due to its interaction with ERM proteins, and that CLIC5A, like the ERM proteins, is a peripheral

membrane protein. While the cell fractionation studies indicate that CLIC5A is mostly a soluble protein, it is still possible that binding of digitonin to membrane cholesterol disrupted the association of CLIC5A with plasma membrane lipids, as previously reported for CLIC1 (471). Therefore, while our data suggest that location of CLIC5A at the dorsal/apical plasma membrane results from association with components of the cortical actin cytoskeleton like ezrin/radixin/moesin, we have not entirely ruled out the possibility of a direct association of CLIC5A with the inner leaflet of the plasma membrane.

In chapter 5, I observed that CLIC5A-stimulated Rac1-GTP formation increased the association of type 1 PI4P5 and type 2 PI5P4 lipid kinases with the Rac1-GTP. This was not surprising since it is known that PI4,5P_2 generating kinases are activated by small GTPases. Interestingly however, deletion of CLIC5 in mice resulted in a dramatic change not only of expression of specific PIPK isoforms in the kidney, but also in their association with Rac1-GTP. The PI4P5K1α3 isoform was much more abundant in kidney lysates of wild type than in CLIC5 deficient mice. By contrast, the PI4P5Kα2 isoform was more much more abundant in kidney tissue lysates of CLIC5 deficient mice than in wild-type mice. Moreover, the PI4P5K1α3 isoform co-precipitated with Rac1-GTP in wild-type, but not in CLIC5 deficient mice. Instead, in the CLIC5 deficient mice PI4P5Kα2 and PI4P5KIγ were co-precipitated with Rac-GTP. The PI4P5Kα2 or PI4P5KIγ isoforms were not observed in the Rac1-GTP complexes pulled from kidney lysates of wild type mice. Therefore, endogenous CLIC5 in the kidney seems to targets Rac1-GTP specifically to the PI4P5K1α3 isoform, and two other PI4,5P_2 generating kinases substitute for the loss of PI4P5K1α3 activity when CLIC5A is deleted in mice. The finding that there may be a high degree of specificity to CLIC5-dependent Rac1-mediated PIPK activation is very exciting. But exactly how a specific PIPK isoform could be targeted by CLIC5 is unclear.

It is also noteworthy that this type of specificity was not observed when CLIC5A was overexpressed in cultured cells, so overexpression studies might not be helpful for such work. In addition, deletion of CLIC4 did not seem to disrupt the association of Rac-GTP with any of the PIP kinase isoforms we studied. Much more work is therefore needed to define how CLIC5 causes activation of the specific PI4P5K1α3 isoform by Rac1-GTP.

In Chapter 5, I also determined whether CLIC5A-stimulated Rac1 activation requires CLIC5A binding to ezrin. I found that ezrin phosphorylation at Thr567 significantly enhanced CLIC5A binding and that the phosphomimetic ezrin 432-586 T567D fragment, which binds CLIC5A with high affinity competitively inhibited CLIC5A-dependent endogenous ERM phosphorylation and Rac1 activation. This suggested that CLIC5A must bind directly to endogenous ERM proteins to promote their phosphorylation and Rac1 activation. I also found that ezrin silencing reduced CLIC5A-stimulated Rac1 activation significantly, indicating that CLIC5A-stimulated Rac1 activation is ezrin-dependent. CLIC5A expression also markedly enhanced co-immunoprecipitation of Rho GDI with ezrin. Taken together, I interpret these findings to indicate that the CLIC5A/ezrin direct interaction triggers Rho GDI recruitment by ezrin, which would relieve Rho GDI-mediated inhibition of Rac1 activation. All together my data suggest strongly that the CLIC5A/ezrin direct interaction is required for Rac1 activation and ERM phosphorylation.

One of the limitations of my work is the fact that I used CLIC5A overexpression cultured HEK293 cells, HeLa cells and COS-7 cells to study CLIC5A functions. These cells are all null for CLIC5A at baseline, so the work was not confounded by endogenous CLIC5A. It would have been desirable to do more of the studies in cultured human podocytes and glomerular endothelial cells because they express CLIC5A at high levels *in vivo*. However, cultured

podocytes and glomerular endothelial cells also do not express CLIC5A, and the transfection efficiency of these cells with cDNA is very low. The set of experiments done with cultured glomerular endothelial cells (Figure 5.14) used expression of CLIC5A from an adenoviral vector, and findings in these cells were consistent with those in the other cell types. Moreover, findings presented in this thesis are also consistent with previous results from this laboratory which showed that ERM phosphorylation and Rac1 activation glomeruli in mouse glomerular podocytes in vivo requires CLIC5 (89) (86).

In chapter 6, I proved a direct interaction of the PP1c regulatory protein taperin with CLIC5A, CLIC4 and CLIC1. I found that CLIC5A interacts with both, taperin 1 (1-711aa) and taperin 2 (307-711 aa) isoforms and mapped the interaction to the region between amino acids 272-385 of human taperin. Furthermore, mutation of the $_{45}$KGVVF$_{49}$ motif in CLIC5A to $_{45}$KGAVY$_{49}$ abolished taperin/CLIC5A binding. The most exciting finding in this part of the thesis was that taperin isoform 1 (1-711 aa) localizes strongly to the nucleus and partially to the cell periphery, and that CLIC5A expression substantially curtails its nuclear, but not its peripheral localization. This is in contrast to the taperin isoform 2 which localizes exclusively to the nucleus and whose nuclear localization was not changed by CLIC5A, even though it can bind CLIC5A directly. The observation that the CLIC5A $_{45}$KGAVY$_{49}$ mutant could not reduce the nuclear localization of the taperin isoform 1 (1-711aa) from the nucleus indicates that the effect of CLIC5A on the nuclear localization of the taperin 1 isoform depends on their direct interaction.

As had been reported before (434), I observed that taperin binds PP1c and that mutation of the KISF motif in the C-terminal domain of taperin abolishes PP1c binding. The interaction of both taperin isoforms with PP1c did not depend on CLIC5A (Figure 6.9). For the taperin isoform

2, but not isoform 1, I was able to establish that it binds PP1cγ in preference over the PP1cα or PP1cβ isoforms (Figure 6.10). The GST-CLIC5A pull-down studies must be interpreted with some caution, because any soluble taperin in cell lysates and its associated PP1c would be pulled down by GST-CLIC5A, due to the relatively high affinity of the CLIC5A/taperin interaction. While the GFP-tagged taperin isoform 1 co-localized with CLIC5A at the cell periphery, I did not establish any co-localization of the two proteins in the cell nuclei. It is therefore unclear whether CLIC5A interacts with the taperin isoform 2 in the nuclei. It turns out that the $_{45}$KGVVF$_{49}$ motif of CLIC5A, which is conserved in all CLICs, represents a potential PP1c binding motif. I found that GST-CLIC5A can pull all PP1c isoforms from cell lysates, even when taperin is silenced, and CLIC5A can bind the purified PP1c α, β, and γ isoforms *in vitro* independent of taperin. So, CLIC5A itself could be a PP1c binding protein. Whether this finding is of functional significance is still unclear and needs further exploration. Taperin depletion had no effect on CLIC5A localization to the cell periphery. Endogenous taperin and PP1c were pulled from cell lysates by the C-terminal ezrin 432-586 fragment together with expressed wild-type, but CLIC5A but not the CLIC5A $_{45}$KGAVY$_{49}$ mutant. These findings suggest that CLIC5A does not require taperin for localization at the cell periphery but rather that CLIC5A may pull taperin/PP1c into the CLIC5A/ezrin complex at the cell periphery. Finally, I found that silencing of endogenous taperin in HeLa cells reduced ERM phosphorylation. If taperin/PP1c functioned as an ERM phosphatase, I would have expected enhanced ERM phosphorylation upon taperin silencing. It is known that distinct PP1c binding proteins in cells compete for PP1 catalytic subunits. The reduction of ERM phosphorylation when taperin was silenced most likely reflects, enhanced activity of a distinct, ERM-specific phosphatase because of reduced competition by taperin for PP1c. It is also conceivable that taperin more specifically inhibits ERM

dephosphorylation by binding and inhibiting PP1c. Further work is required to explore these possibilities.

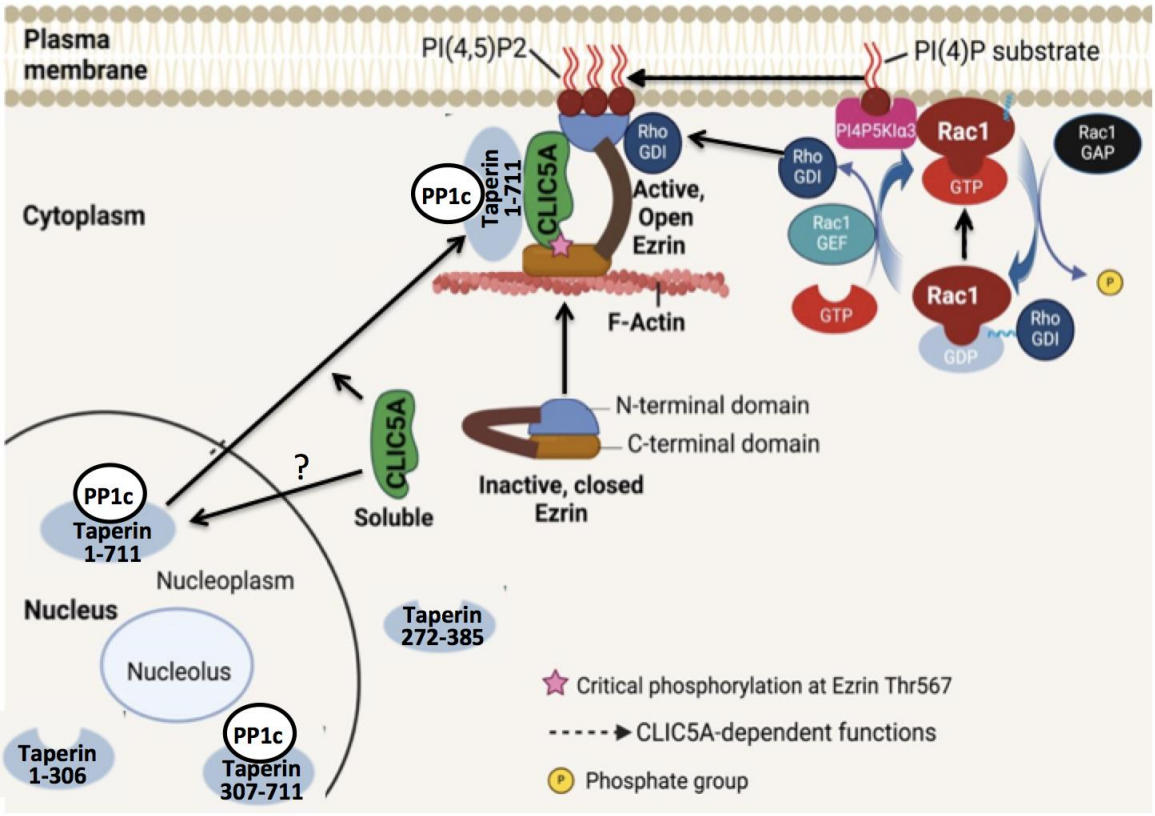

Figure 7.1: Proposed model. CLIC5A-stimulates Rac1, which activates PI4P5KIα3. PI4P5KIα3 catalyzes phosphorylation of the substrate PI(4)P to produce PI4,5P2. CLIC5A-dependent accumulation of PI4,5P2 at the inner leaflet of the plasma membrane triggers ezrin FERM domain (N-terminus) docking on PI4,5P2, making the C-terminus of ezrin available for CLIC5A binding. CLIC5A binds directly and strongly to the phosphorylated (pThr 567) ezrin C-terminus. CLIC5A/ezrin binding enhances Rho GDI sequestration by ezrin, leading to Rac1 activation (Rac1-GTP), which again binds and activates PI4P5KIα3 leading to PI4,5P2 synthesis. Therefore, CLIC5A/ezrin binding is required for CLIC5A-depedenent Rac1 activation. This is a feed forward amplification loop. CLIC5A reduces the nuclear localization of the taperin 1 isoform (1-711aa) and brings the taperin isoform 1 into the CLIC5A/ezrin complex at the cell periphery. Taperin may enhance ERM phosphorylation by inhibiting PP1c activity toward the ERM proteins.

7.2. Future directions

While I have shown the direct interaction of CLIC5A with ERM proteins, and our lab previously showed that CLIC5A specifically activated ezrin in glomerular podocytes, to what degree other CLIC proteins promote ERM protein activation still needs to be investigated. We also know that CLIC4 and moesin are predominant in endothelial cells, that CLIC4 associates with ezrin and moesin in proximal tubule cells and that CLIC4 deletion in mice causes a major disruption of proximal tubule brush border microvilli. Therefore, other CLICs might have specificity toward specific ERM proteins. Also, identifying the direct interacting partners of other CLICs might give valuable information about the specificity of CLICs towards particular binding partners and will pave the way for determining novel biological functions in different subcellular locations.

CLIC5A does not behave like integral membrane protein. Therefore, it is highly likely that other CLICs behave like CLIC5A as mostly soluble cytosolic protein that can associate with the protein complex at the cell periphery, a hypothesis that can be considered. Therefore, investigating the subcellular abundance using fractionation assay in mouse glomeruli and subcellular localizations using confocal microscopy imaging of other CLICs will give us insight into the nature of CLIC proteins. As ERM triple siRNA mediated knockdown can partially displace CLIC5A from the cell periphery, similar approach on other CLICs also give us the information about the sensitivity of CLICs towards any particular ERM siRNA or triple ERM knockdown.

The NetPhos® protein phosphorylation prediction tool indicates that there are several potential Ser, Thr and Tyr phosphorylation sites in CLIC5 proteins, as detailed in the MSc thesis of J.-S. Kim (426). My analysis suggests that $_{97}$Thr, $_{111}$Ser, $_{171}$Ser, $_{249}$Ser, $_{151}$Tyr and $_{241}$Tyr of

human CLIC5A have the highest probability of being phosphorylated. Given that CLIC5A interacts with the PP1c regulatory subunit taperin, it will be important to explore whether CLIC5A might be a substrate for taperin/PP1c. If phosphorylation sites can be identified, it will be important to determine whether they are conserved in other CLICs and whether they are functionally significant. Since the peripheral localization of CLIC5A is at least partly phosphorylation-dependent, it would be worthwhile to determine phosphorylation might result in translocation from the cytosol to ERM protein complexes at the cell periphery. Good phospho-tyrosine specific antibodies are widely used, but unfortunately, good pan-specific antibodies to study Ser/Thr phosphorylation are not available. So, one might attempt immunoprecipitation of endogenous CLIC5A from glomerular lysates treated with and without phosphatase inhibitors followed by western blot analysis with anti-phospho-Ser/Thre and anti-phospho-Tyr antibodies, using the CLIC5 deficient mice as controls. If this approach does not give decisive evidence, then phospho-proteomic analysis of human podocyte lysates transduced with adenoviral vector CLIC5A cDNAs, and glomerular lysates from CLIC5 wild type and knock out mice might be a robust approach to solve this mystery. Metabolic labeling using [γ-32P]ATP as a kinase substrate can be another approach to determine if CLIC5A and other CLICs are phosphorylated in cells. If CLICs are phosphorylated, then this can be validated by site-directed mutagenesis of CLICs of the putative phosphorylation sites to make phosphorylation-deficient mutants. The function (ERM phosphorylation, Rac1 activation, taperin binding) and subcellular localization can then be studied. It would then also be important to define the kinase signaling pathways that stimulate CLIC phosphorylation and to determine whether dephosphorylation of the Ser/Thr sites is carried out by taperin/PP1c. If CLIC5A and other CLICs are not phosphorylated with biological importance, their putative SH2 domain could indicate unexplored protein-protein interactions.

CLIC3 has oxidoreductase enzyme activity (501), as there is significant sequence homology of CLICs with Ω-class glutathione s-transferases. The clue is the presence of reactive cysteine situated in the conserved thioredoxin motif of CLICs. However, similar oxidoreductase activity has not been described for other CLICs in a biologically relevant context, though proteomic studies indicate that CLIC5A, CLIC4, and CLIC1 are all reactive to a cysteine-labeling reagent (502). Therefore, determining the oxidoreductase activity of all CLICs and comparing with the H_2O_2 treatment in living cells could be interesting.

The investigations of CLIC5A-depedent functions were not entirely conducted *in vivo* or in cultured podocytes and in glomerular endothelial cells. I tried cDNA transfection in cultured mouse podocytes and glomerular endothelial cells, but these cells are resistant to uptake cDNAs. Moreover, cultured mouse podocytes and human glomerular endothelial cells do not express endogenous CLIC5A, and podocalyxin, and thus cannot form the CLIC5A/ezrin/podocalyxin complex at the cell periphery. That was the reason why I used COS-7 cells, HEK293 cells and HeLa cells which are suitable for cDNA transfection. However, transducing human cultured podocytes and endothelial cells with adenoviral vectors containing CLIC5A, its functional mutants, and podocalyxin is feasible and would be of great interest. Most important in would be to answer the question whether expression of CLIC5A and podocalyxin in these cells plays a role in inducing their characteristic ultrastructural phenotypes; formation of foot processes by podocytes and transcellular pores/fenestrae by the glomerular endothelial cells.

It will also be also important to pay some attention to NHERF2 in future studies. NHERF2 links the transmembrane protein podocalyxin to the peripheral membrane protein ezrin. NHERF2 furthermore recruits a Rac1 GEF that facilitates Rac1 activation. But we do not know whether CLIC5A stimulates Rac1 GEF binding to NHERF2 in the ezrin complex.

Immunoprecipitation of expressed NHERF2 from lysates of HeLa cells and cultured human podocytes expressing CLIC5A or not would be useful to explore this mechanism. In addition, determining whether a Rac-GEF can be co-immunoprecipitation with endogenous NHERF2 from wild-type and CLIC5 deficient glomeruli would define whether such a mechanism might exist in mice, *in vivo*.

Shank2 was also identified as a direct interacting partner of CLIC5A as observed from our Hybrigenics® screening data (Table 7). Shank2 is one of the master organizers of the post-synaptic densities of central nervous system (503). Shank2 is expressed in podocytes and its deletion in podocytes causes proteinuria in mice (504). Shank2 regulates Rac1/Cdc42 activation (505, 506) by recruiting the Rac1 and Cdc42 specific Rho GEF p21-Activated kinase (PAK)-interacting exchange factor "βPix" (507, 508). βPix is highly expressed in podocytes and βPix/Shank2/NHERF3 forms macromolecular complex when expressed endogenously in kidney (509). Since Shank2 is a known adaptor of Rac1 GEFs, and Rac1 is activated by CLIC5A, and since neither CLIC5A nor ezrin is a Rac1 GEF, the question remains how Shank2 is involved in CLIC5A-dependent localized Rac1 activation in the ezrin complex. I am reasonably confident that the Shank2/CLIC5A interaction will turn out to be positive and significant, since the Y2H library screening results are robust, and because Shank2 is functional in podocytes (504). The objectives are to map the minimum direct interacting regions of Shank2 that binds CLIC5A and to define whether Shank2 mediates CLIC5A-stimulated Rac1 activation. A key limitation of this proposal is that there are many Rac1 GEFs, so the focus on ARHGEF7/βPix is clearly a best guess. If Shank2 is indeed required for CLIC5A-induced Rac1 activation, but βPix is not brought into the complex, an approach to find the appropriate GEF(s) would be to again use Y2H library screening of the mouse kidney library with Shank2 as the bait, or to immunoprecipitate Shank2

from glomeruli lysate, followed by Mass Spectrometry to identify co-immunoprecipitated proteins. Another objective is to define whether Shank2 regulates the function of the podocalyxin/ezrin/NHERF/CLIC5A complex *in vivo*. Shank2 flox/flox mice in which Shank2 can be deleted selectively in podocytes are currently available for pre-order from Jackson Labs, so it will be possible to determine whether podocyte-specific Shank2 deletion can disrupt the CLIC5A/ezrin/podocalyxin complex *in vivo*. Role of Shank2 in CLIC5A-dependent functions will most likely define new components of the CLIC5A/ezrin/podocalyxin signaling complex in podocytes and the mechanism of localized CLIC5A–dependent Rac1 activation in this complex. Rac1 hyperactivation causes pathologic podocyte remodeling, for instance in diabetes. If βPix is found in the CLIC5A/Shank2 complex, mapping of the Shank2/βPix interaction will also be worthwhile. The outcome of this study will also help define the mechanism of CLIC protein action, away from the old theory that they are membrane-spanning chloride channels, to their most likely function as ERM-associated adaptors or chaperones that cause localized Rac1 activation. In tumor cells, ezrin/NHERF2/podocalyxin complexes are located in the basal domain and induce cellular mobility (308, 477, 478), making this multi-protein complex a potential therapeutic target (479).

CLIC5A also interacts directly with taperin isoforms 1 and 2 and reduces the nuclear localization of the taperin 1 isoform (1-711). In future work, the specific nuclear localization and nuclear export motifs in the taperin and CLIC5A sequences need to be identified and their function tested with site-directed mutants that disrupt these sequences. The relationship of the CLIC5A binding site on taperin to the nuclear localization and export sequences needs to be clarified. For these studies, a simple cell fractionation approach to isolate nuclei separate from cytosol would be a first good approach, because in the live cell imaging studies we only see the

GFP tag, and would not know whether fragments of taperin cleaved from the GFP-tagged N-terminus might be present. Nonetheless, dynamic imaging studies with photobleaching of GFP-tagged taperin isoforms 1 and 2, with the GFP tag either at the N- or the C-terminus should be informative. We also do not know whether other CLICs can alter the taperin subcellular localization. HeLa cells express endogenous CLIC1 and CLIC4 but the GFP-tagged taperin 1 isoform is mostly in the nucleus in the presence of these two CLICs. Whether knocking down the endogenous CLIC 1 and CLIC4 alters taperin subcellular localization will be of interest.

As taperin isoforms 1 and 2 are predominantly nuclear, they might influence transcription of specific genes. To identify transcription factors in HeLa cells with or without taperin siRNA knockdown, I would propose the chromatin immunoprecipitation (ChIP) assays combined with sequencing. ChIP sequencing (ChIP-Seq) is a powerful method for identifying DNA binding sites for transcription factors and other proteins. ChIP relies on the use of an antibody to isolate, or precipitate, a certain protein, histone, transcription factor, or cofactor and its bound chromatin from a protein mixture that was extracted from cells or tissues.

We also should determine whether taperin binds and inhibits or activates PP1cγ phosphatase activity to regulate phosphorylation of CLIC5A, other CLIC proteins or other targets. Phospho-proteomics employing in HeLa cells treated with or without human taperin siRNA would be the most straightforward first step, followed by rescue with wild-type and KASA mutant taperin 1 or 2 isoforms. It will also be important to determine whether taperin knockdown disrupts the CLIC5A/ERM proteins interaction. I showed that taperin knockdown reduces ERM phosphorylation in cells expressing CLIC5A, therefore it is highly likely that taperin knockdown also disrupts the CLIC5A/ERM proteins interaction. The same question needs to be examined for other CLICs. It will also be important to determine whether taperin

deficiency reduces CLIC5A-dependent Rac1 activation and generation of PI4,5P2 clusters at the inner leaflet of the plasma membrane. Kidney cortex lysates and glomerular lysates from taperin wild type and taperin deficient mice expressing CLIC5A can be used to conduct the PAK-PBD pull down assay to detect the Rac1-GTP abundance and the G-LISA assay to quantify the amount of Rac1-GTP. The PAK-PBD pull down assay can also be used to define whether there is a change in the PI4,5P_2-generating kinases in the taperin ko mice. Furthermore, the abundance of podocalyxin, ezrin, and NHERF2 in glomeruli, their association with the cytoskeleton and the phosphorylation state of ERM and PAK proteins should be studied in the taperin deficient mice. Whether taperin deficiency results in glomerular ultrastructural abnormalities should be determined. Finally, whether the taperin deficient mice have glomerular filtration barrier defects and are more susceptible to glomerular injury by hypertension, diabetes and Adriamycin should be determined. In cultured cells, expression of CLIC5A with or without taperin knockdown can also be used to determine whether taperin is important for Rac1 activation, association of Rac1-GTP with PI4,5P_2 generating kinases and/or the CLIC5A-dependent increase in PI4,5P_2 apical membrane clusters. To observe the cluster accumulation of PI4,5P2 at the plasma membrane, HeLa cells would be co-transfected with GFP-CLIC5A and the surface potential biosensor GFP-KRAS or the PI4,5P2 reporter GFP-PH-PLC as previously reported from this lab (89) with and without taperin silencing. My expectation is that taperin knockdown in cells expressing CLIC5A will reduce CLIC5A-dependent Rac1 activation as well as PI4,5P_2 generation, and I predict that taperin will be required to stabilize CLIC5A/ezrin complex formation at the cell periphery.

To determine taperin/CLICs colocalization *in* cultured human podocytes, and in glomeruli *in vivo*, confocal immunofluorescence microscopy with different CLIC and taperin antibodies as well as co-immunoprecipitation studies can be performed. To strengthen the claim

that taperin belongs to the CLIC5A/ezrin complex in podocytes, lysates of glomeruli isolated from $CLIC5^{+/+}$ and $CLIC5^{-/-}$ mice should be subjected to immunoprecipitation with anti-ezrin antibody to see whether CLIC5A, taperin and PP1c co-precipitate with ezrin. Also, confocal immunofluorescence microscopy using kidney sections and anti-ezrin, anti-CLIC5A, and anti-taperin to define the degree of colocalization of CLIC5A, ezrin and taperin in renal glomeruli of $CLIC5^{+/+}$ and $CLIC5^{-/-}$ mice can be done. To determine whether taperin deficiency reduces CLIC5A-dependent ERM phosphorylation *in vivo* and disrupts the CLIC5A/ezrin/podocalyxin complex in renal glomeruli, taperin and CLIC5A wild type and dual knockout mouse kidney sections can be used for confocal immunofluorescence microscopy using pERM antibody, CLIC5 antibody, and podocalyxin antibody. This will also strengthen the claim that taperin is part of the CLIC5A/ezrin/podocalyxin complex in renal glomeruli.

Rac1 activation in hypertension is CLIC5A dependent and CLIC5A deficiency worsens glomerular injury in hypertensive mice (86). However, whether Rac1 activation is CLIC5A-dependent in diabetic nephropathy is not known. We also do not know whether CLIC5A can be a part of the ezrin/podocalyxin complex at basal domain of podocyte foot processes during podocyte remodeling, for instance in diabetic mice. Whether the presence or absence of CLIC5A protects hypertensive diabetic mice from the development of diabetic nephropathy and whether CLIC5A function is reduced in diabetes make podocytes more susceptible to injury should be studied.

Destabilization of podocytes due to Rac1 hyperactivation is emerging as a major mechanism that leads to progressive glomerular sclerosis. Since CLIC5A is expressed at such extremely high levels in glomerular podocytes, it was critically important to define how it activates Rac1 to gain insights into processes that control podocyte remodeling. I believe that the

work I have done, the proposed work, along with work by many others studying podocytes, will eventually lead to targeted interruption of glomerular injury and prevent proteinuria.

References:

1. **Quaggin SE, and Kreidberg JA**. Development of the renal glomerulus: good neighbors and good fences. *Development* 135: 609-620, 2008.
2. **Jin R, Grunkemeier GL, Brown JR, and Furnary AP**. Estimated glomerular filtration rate and renal function. *Ann Thorac Surg* 86: 1-3, 2008.
3. **Saran R, Li Y, Robinson B, Abbott KC, Agodoa LY, Ayanian J, Bragg-Gresham J, Balkrishnan R, Chen JL, Cope E, Eggers PW, Gillen D, Gipson D, Hailpern SM, Hall YN, He K, Herman W, Heung M, Hirth RA, Hutton D, Jacobsen SJ, Kalantar-Zadeh K, Kovesdy CP, Lu Y, Molnar MZ, Morgenstern H, Nallamothu B, Nguyen DV, O'Hare AM, Plattner B, Pisoni R, Port FK, Rao P, Rhee CM, Sakhuja A, Schaubel DE, Selewski DT, Shahinian V, Sim JJ, Song P, Streja E, Kurella Tamura M, Tentori F, White S, Woodside K, and Hirth RA**. US Renal Data System 2015 Annual Data Report: Epidemiology of Kidney Disease in the United States. *Am J Kidney Dis* 67: Svii, S1-305, 2016.
4. **Ballermann BJ, Nystrom J, and Haraldsson B**. The Glomerular Endothelium Restricts Albumin Filtration. *Front Med (Lausanne)* 8: 766689, 2021.
5. **Haraldsson B, Nystrom J, and Deen WM**. Properties of the glomerular barrier and mechanisms of proteinuria. *Physiol Rev* 88: 451-487, 2008.
6. **Mogensen CE**. Microalbuminuria in prediction and prevention of diabetic nephropathy in insulin-dependent diabetes mellitus patients. *J Diabetes Complications* 9: 337-349, 1995.
7. **Tisher CC, Madsen KM, and Verlander JW**. Structural adaptation of the collecting duct to acid-base disturbances. *Contrib Nephrol* 95: 168-177, 1991.
8. **Atherton JC**. Renal physiology. *Br J Anaesth* 44: 236-245, 1972.
9. **Blount MA, Sim JH, Zhou R, Martin CF, Lu W, Sands JM, and Klein JD**. Expression of transporters involved in urine concentration recovers differently after cessation of lithium treatment. *Am J Physiol Renal Physiol* 298: F601-608, 2010.
10. **Knepper MA**. Molecular physiology of urinary concentrating mechanism: regulation of aquaporin water channels by vasopressin. *Am J Physiol* 272: F3-12, 1997.
11. **Melkikh AV, and Sutormina MI**. Model of active transport of ions in cardiac cell. *J Theor Biol* 252: 247-254, 2008.
12. **Puelles VG, Hoy WE, Hughson MD, Diouf B, Douglas-Denton RN, and Bertram JF**. Glomerular number and size variability and risk for kidney disease. *Curr Opin Nephrol Hypertens* 20: 7-15, 2011.
13. **Thomson SC, and Blantz RC**. A new role for charge of the glomerular capillary membrane. *J Am Soc Nephrol* 21: 2011-2013, 2010.
14. **Chang RL, Deen WM, Robertson CR, and Brenner BM**. Permselectivity of the glomerular capillary wall: III. Restricted transport of polyanions. *Kidney Int* 8: 212-218, 1975.
15. **Schlondorff D**. The glomerular mesangial cell: an expanding role for a specialized pericyte. *FASEB J* 1: 272-281, 1987.
16. **Olivetti G, Anversa P, Rigamonti W, Vitali-Mazza L, and Loud AV**. Morphometry of the renal corpuscle during normal postnatal growth and compensatory hypertrophy. A light microscope study. *J Cell Biol* 75: 573-585, 1977.
17. **Sakai T, and Kriz W**. The structural relationship between mesangial cells and basement membrane of the renal glomerulus. *Anat Embryol (Berl)* 176: 373-386, 1987.

18. **Bjarnegard M, Enge M, Norlin J, Gustafsdottir S, Fredriksson S, Abramsson A, Takemoto M, Gustafsson E, Fassler R, and Betsholtz C**. Endothelium-specific ablation of PDGFB leads to pericyte loss and glomerular, cardiac and placental abnormalities. *Development* 131: 1847-1857, 2004.
19. **Nagai T, Yokomori H, Yoshimura K, Fujimaki K, Nomura M, Hibi T, and Oda M**. Actin filaments around endothelial fenestrae in rat hepatic sinusoidal endothelial cells. *Med Electron Microsc* 37: 252-255, 2004.
20. **Ballermann BJ**. Glomerular endothelial cell differentiation. *Kidney Int* 67: 1668-1671, 2005.
21. **Salmon AH, and Satchell SC**. Endothelial glycocalyx dysfunction in disease: albuminuria and increased microvascular permeability. *J Pathol* 226: 562-574, 2012.
22. **Rostgaard J, and Qvortrup K**. Sieve plugs in fenestrae of glomerular capillaries--site of the filtration barrier? *Cells Tissues Organs* 170: 132-138, 2002.
23. **Curry FE, and Adamson RH**. Endothelial glycocalyx: permeability barrier and mechanosensor. *Ann Biomed Eng* 40: 828-839, 2012.
24. **Hjalmarsson C, Johansson BR, and Haraldsson B**. Electron microscopic evaluation of the endothelial surface layer of glomerular capillaries. *Microvasc Res* 67: 9-17, 2004.
25. **Kriz W, and Lemley KV**. A potential role for mechanical forces in the detachment of podocytes and the progression of CKD. *J Am Soc Nephrol* 26: 258-269, 2015.
26. **Eremina V, Baelde HJ, and Quaggin SE**. Role of the VEGF--a signaling pathway in the glomerulus: evidence for crosstalk between components of the glomerular filtration barrier. *Nephron Physiol* 106: p32-37, 2007.
27. **Liu A, Dardik A, and Ballermann BJ**. Neutralizing TGF-beta1 antibody infusion in neonatal rat delays in vivo glomerular capillary formation 1. *Kidney Int* 56: 1334-1348, 1999.
28. **Pino RM**. The cell surface of a restrictive fenestrated endothelium. II. Dynamics of cationic ferritin binding and the identification of heparin and heparan sulfate domains on the choriocapillaris. *Cell Tissue Res* 243: 157-164, 1986.
29. **Pino RM**. The cell surface of a restrictive fenestrated endothelium. I. Distribution of lectin-receptor monosaccharides on the choriocapillaris. *Cell Tissue Res* 243: 145-155, 1986.
30. **Cao R, Eriksson A, Kubo H, Alitalo K, Cao Y, and Thyberg J**. Comparative evaluation of FGF-2-, VEGF-A-, and VEGF-C-induced angiogenesis, lymphangiogenesis, vascular fenestrations, and permeability. *Circ Res* 94: 664-670, 2004.
31. **Jeansson M, Bjorck K, Tenstad O, and Haraldsson B**. Adriamycin alters glomerular endothelium to induce proteinuria. *J Am Soc Nephrol* 20: 114-122, 2009.
32. **Ballermann BJ, and Obeidat M**. Tipping the balance from angiogenesis to fibrosis in CKD. *Kidney Int Suppl (2011)* 4: 45-52, 2014.
33. **Noris M, and Remuzzi G**. Atypical hemolytic-uremic syndrome. *N Engl J Med* 361: 1676-1687, 2009.
34. **Coppo P, and Veyradier A**. Thrombotic microangiopathies: towards a pathophysiology-based classification. *Cardiovasc Hematol Disord Drug Targets* 9: 36-50, 2009.
35. **Pollak MR, Quaggin SE, Hoenig MP, and Dworkin LD**. The glomerulus: the sphere of influence. *Clin J Am Soc Nephrol* 9: 1461-1469, 2014.

36. **Abrahamson DR**. Origin of the glomerular basement membrane visualized after in vivo labeling of laminin in newborn rat kidneys. *J Cell Biol* 100: 1988-2000, 1985.
37. **Lennon R, Byron A, Humphries JD, Randles MJ, Carisey A, Murphy S, Knight D, Brenchley PE, Zent R, and Humphries MJ**. Global analysis reveals the complexity of the human glomerular extracellular matrix. *J Am Soc Nephrol* 25: 939-951, 2014.
38. **Byron A, Randles MJ, Humphries JD, Mironov A, Hamidi H, Harris S, Mathieson PW, Saleem MA, Satchell SC, Zent R, Humphries MJ, and Lennon R**. Glomerular cell cross-talk influences composition and assembly of extracellular matrix. *J Am Soc Nephrol* 25: 953-966, 2014.
39. **St John PL, and Abrahamson DR**. Glomerular endothelial cells and podocytes jointly synthesize laminin-1 and -11 chains. *Kidney Int* 60: 1037-1046, 2001.
40. **Noakes PG, Miner JH, Gautam M, Cunningham JM, Sanes JR, and Merlie JP**. The renal glomerulus of mice lacking s-laminin/laminin beta 2: nephrosis despite molecular compensation by laminin beta 1. *Nat Genet* 10: 400-406, 1995.
41. **Jarad G, Cunningham J, Shaw AS, and Miner JH**. Proteinuria precedes podocyte abnormalities inLamb2-/- mice, implicating the glomerular basement membrane as an albumin barrier. *J Clin Invest* 116: 2272-2279, 2006.
42. **Kashtan CE**. Alport syndromes: phenotypic heterogeneity of progressive hereditary nephritis. *Pediatr Nephrol* 14: 502-512, 2000.
43. **Rossi M, Morita H, Sormunen R, Airenne S, Kreivi M, Wang L, Fukai N, Olsen BR, Tryggvason K, and Soininen R**. Heparan sulfate chains of perlecan are indispensable in the lens capsule but not in the kidney. *EMBO J* 22: 236-245, 2003.
44. **Harvey SJ, Jarad G, Cunningham J, Rops AL, van der Vlag J, Berden JH, Moeller MJ, Holzman LB, Burgess RW, and Miner JH**. Disruption of glomerular basement membrane charge through podocyte-specific mutation of agrin does not alter glomerular permselectivity. *Am J Pathol* 171: 139-152, 2007.
45. **Hamano Y, Okude T, Shirai R, Sato I, Kimura R, Ogawa M, Ueda Y, Yokosuka O, Kalluri R, and Ueda S**. Lack of collagen XVIII/endostatin exacerbates immune-mediated glomerulonephritis. *J Am Soc Nephrol* 21: 1445-1455, 2010.
46. **van den Hoven MJ, Wijnhoven TJ, Li JP, Zcharia E, Dijkman HB, Wismans RG, Rops AL, Lensen JF, van den Heuvel LP, van Kuppevelt TH, Vlodavsky I, Berden JH, and van der Vlag J**. Reduction of anionic sites in the glomerular basement membrane by heparanase does not lead to proteinuria. *Kidney Int* 73: 278-287, 2008.
47. **Groffen AJ, Ruegg MA, Dijkman H, van de Velden TJ, Buskens CA, van den Born J, Assmann KJ, Monnens LA, Veerkamp JH, and van den Heuvel LP**. Agrin is a major heparan sulfate proteoglycan in the human glomerular basement membrane. *J Histochem Cytochem* 46: 19-27, 1998.
48. **Rennke HG, and Venkatachalam MA**. Glomerular permeability: in vivo tracer studies with polyanionic and polycationic ferritins. *Kidney Int* 11: 44-53, 1977.
49. **Rennke HG, and Venkatachalam MA**. Structural determinants of glomerular permselectivity. *Fed Proc* 36: 2519-2526, 1977.
50. **Goldberg S, Harvey SJ, Cunningham J, Tryggvason K, and Miner JH**. Glomerular filtration is normal in the absence of both agrin and perlecan-heparan sulfate from the glomerular basement membrane. *Nephrol Dial Transplant* 24: 2044-2051, 2009.
51. **Pavenstadt H, Kriz W, and Kretzler M**. Cell biology of the glomerular podocyte. *Physiol Rev* 83: 253-307, 2003.

52. **Ichimura K, Kurihara H, and Sakai T**. Actin filament organization of foot processes in rat podocytes. *J Histochem Cytochem* 51: 1589-1600, 2003.
53. **Andrews PM**. Investigations of cytoplasmic contractile and cytoskeletal elements in the kidney glomerulus. *Kidney Int* 20: 549-562, 1981.
54. **Reiser J, Kriz W, Kretzler M, and Mundel P**. The glomerular slit diaphragm is a modified adherens junction. *J Am Soc Nephrol* 11: 1-8, 2000.
55. **Huber TB, and Benzing T**. The slit diaphragm: a signaling platform to regulate podocyte function. *Curr Opin Nephrol Hypertens* 14: 211-216, 2005.
56. **Grahammer F, Schell C, and Huber TB**. The podocyte slit diaphragm--from a thin grey line to a complex signalling hub. *Nat Rev Nephrol* 9: 587-598, 2013.
57. **George B, and Holzman LB**. Signaling from the podocyte intercellular junction to the actin cytoskeleton. *Semin Nephrol* 32: 307-318, 2012.
58. **Beltcheva O, Martin P, Lenkkeri U, and Tryggvason K**. Mutation spectrum in the nephrin gene (NPHS1) in congenital nephrotic syndrome. *Hum Mutat* 17: 368-373, 2001.
59. **Donoviel DB, Freed DD, Vogel H, Potter DG, Hawkins E, Barrish JP, Mathur BN, Turner CA, Geske R, Montgomery CA, Starbuck M, Brandt M, Gupta A, Ramirez-Solis R, Zambrowicz BP, and Powell DR**. Proteinuria and perinatal lethality in mice lacking NEPH1, a novel protein with homology to NEPHRIN. *Mol Cell Biol* 21: 4829-4836, 2001.
60. **Inoue T, Yaoita E, Kurihara H, Shimizu F, Sakai T, Kobayashi T, Ohshiro K, Kawachi H, Okada H, Suzuki H, Kihara I, and Yamamoto T**. FAT is a component of glomerular slit diaphragms. *Kidney Int* 59: 1003-1012, 2001.
61. **Ciani L, Patel A, Allen ND, and ffrench-Constant C**. Mice lacking the giant protocadherin mFAT1 exhibit renal slit junction abnormalities and a partially penetrant cyclopia and anophthalmia phenotype. *Mol Cell Biol* 23: 3575-3582, 2003.
62. **Saito A, Miyauchi N, Hashimoto T, Karasawa T, Han GD, Kayaba M, Sumi T, Tomita M, Ikezumi Y, Suzuki K, Koitabashi Y, Shimizu F, and Kawachi H**. Neurexin-1, a presynaptic adhesion molecule, localizes at the slit diaphragm of the glomerular podocytes in kidneys. *Am J Physiol Regul Integr Comp Physiol* 300: R340-348, 2011.
63. **Hashimoto T, Karasawa T, Saito A, Miyauchi N, Han GD, Hayasaka K, Shimizu F, and Kawachi H**. Ephrin-B1 localizes at the slit diaphragm of the glomerular podocyte. *Kidney Int* 72: 954-964, 2007.
64. **Kerjaschki D, Sharkey DJ, and Farquhar MG**. Identification and characterization of podocalyxin--the major sialoprotein of the renal glomerular epithelial cell. *J Cell Biol* 98: 1591-1596, 1984.
65. **Gelberg H, Healy L, Whiteley H, Miller LA, and Vimr E**. In vivo enzymatic removal of alpha 2-->6-linked sialic acid from the glomerular filtration barrier results in podocyte charge alteration and glomerular injury. *Lab Invest* 74: 907-920, 1996.
66. **Langham RG, Kelly DJ, Cox AJ, Thomson NM, Holthofer H, Zaoui P, Pinel N, Cordonnier DJ, and Gilbert RE**. Proteinuria and the expression of the podocyte slit diaphragm protein, nephrin, in diabetic nephropathy: effects of angiotensin converting enzyme inhibition. *Diabetologia* 45: 1572-1576, 2002.
67. **Doublier S, Salvidio G, Lupia E, Ruotsalainen V, Verzola D, Deferrari G, and Camussi G**. Nephrin expression is reduced in human diabetic nephropathy: evidence for a distinct role for glycated albumin and angiotensin II. *Diabetes* 52: 1023-1030, 2003.

68. **Tian D, Jacobo SM, Billing D, Rozkalne A, Gage SD, Anagnostou T, Pavenstadt H, Hsu HH, Schlondorff J, Ramos A, and Greka A**. Antagonistic regulation of actin dynamics and cell motility by TRPC5 and TRPC6 channels. *Sci Signal* 3: ra77, 2010.
69. **Riehle M, Buscher AK, Gohlke BO, Kassmann M, Kolatsi-Joannou M, Brasen JH, Nagel M, Becker JU, Winyard P, Hoyer PF, Preissner R, Krautwurst D, Gollasch M, Weber S, and Harteneck C**. TRPC6 G757D Loss-of-Function Mutation Associates with FSGS. *J Am Soc Nephrol* 27: 2771-2783, 2016.
70. **Kaplan JM, Kim SH, North KN, Rennke H, Correia LA, Tong HQ, Mathis BJ, Rodriguez-Perez JC, Allen PG, Beggs AH, and Pollak MR**. Mutations in ACTN4, encoding alpha-actinin-4, cause familial focal segmental glomerulosclerosis. *Nat Genet* 24: 251-256, 2000.
71. **Brown EJ, Schlondorff JS, Becker DJ, Tsukaguchi H, Tonna SJ, Uscinski AL, Higgs HN, Henderson JM, and Pollak MR**. Mutations in the formin gene INF2 cause focal segmental glomerulosclerosis. *Nat Genet* 42: 72-76, 2010.
72. **Pollak MR**. The genetic basis of FSGS and steroid-resistant nephrosis. *Semin Nephrol* 23: 141-146, 2003.
73. **Lowik MM, Groenen PJ, Levtchenko EN, Monnens LA, and van den Heuvel LP**. Molecular genetic analysis of podocyte genes in focal segmental glomerulosclerosis--a review. *Eur J Pediatr* 168: 1291-1304, 2009.
74. **Kuppe C, Grone HJ, Ostendorf T, van Kuppevelt TH, Boor P, Floege J, Smeets B, and Moeller MJ**. Common histological patterns in glomerular epithelial cells in secondary focal segmental glomerulosclerosis. *Kidney Int* 88: 990-998, 2015.
75. **Wiggins RC**. The spectrum of podocytopathies: a unifying view of glomerular diseases. *Kidney Int* 71: 1205-1214, 2007.
76. **Wharram BL, Goyal M, Wiggins JE, Sanden SK, Hussain S, Filipiak WE, Saunders TL, Dysko RC, Kohno K, Holzman LB, and Wiggins RC**. Podocyte depletion causes glomerulosclerosis: diphtheria toxin-induced podocyte depletion in rats expressing human diphtheria toxin receptor transgene. *J Am Soc Nephrol* 16: 2941-2952, 2005.
77. **Fukuda A, Chowdhury MA, Venkatareddy MP, Wang SQ, Nishizono R, Suzuki T, Wickman LT, Wiggins JE, Muchayi T, Fingar D, Shedden KA, Inoki K, and Wiggins RC**. Growth-dependent podocyte failure causes glomerulosclerosis. *J Am Soc Nephrol* 23: 1351-1363, 2012.
78. **Asanuma K, and Mundel P**. The role of podocytes in glomerular pathobiology. *Clin Exp Nephrol* 7: 255-259, 2003.
79. **Rahilly MA, and Fleming S**. Differential expression of integrin alpha chains by renal epithelial cells. *J Pathol* 167: 327-334, 1992.
80. **Kreidberg JA, and Symons JM**. Integrins in kidney development, function, and disease. *Am J Physiol Renal Physiol* 279: F233-242, 2000.
81. **Kreidberg JA**. Functions of alpha3beta1 integrin. *Curr Opin Cell Biol* 12: 548-553, 2000.
82. **Kreidberg JA, Donovan MJ, Goldstein SL, Rennke H, Shepherd K, Jones RC, and Jaenisch R**. Alpha 3 beta 1 integrin has a crucial role in kidney and lung organogenesis. *Development* 122: 3537-3547, 1996.
83. **Regele HM, Fillipovic E, Langer B, Poczewki H, Kraxberger I, Bittner RE, and Kerjaschki D**. Glomerular expression of dystroglycans is reduced in minimal change

nephrosis but not in focal segmental glomerulosclerosis. *J Am Soc Nephrol* 11: 403-412, 2000.
84. **Raats CJ, van den Born J, Bakker MA, Oppers-Walgreen B, Pisa BJ, Dijkman HB, Assmann KJ, and Berden JH**. Expression of agrin, dystroglycan, and utrophin in normal renal tissue and in experimental glomerulopathies. *Am J Pathol* 156: 1749-1765, 2000.
85. **Wegner B, Al-Momany A, Kulak SC, Kozlowski K, Obeidat M, Jahroudi N, Paes J, Berryman M, and Ballermann BJ**. CLIC5A, a component of the ezrin-podocalyxin complex in glomeruli, is a determinant of podocyte integrity. *Am J Physiol Renal Physiol* 298: F1492-1503, 2010.
86. **Tavasoli M, Li L, Al-Momany A, Zhu LF, Adam BA, Wang Z, and Ballermann BJ**. The chloride intracellular channel 5A stimulates podocyte Rac1, protecting against hypertension-induced glomerular injury. *Kidney Int* 89: 833-847, 2016.
87. **Tavasoli M, Al-Momany A, Wang X, Li L, Edwards JC, and Ballermann BJ**. Both CLIC4 and CLIC5A activate ERM proteins in glomerular endothelium. *Am J Physiol Renal Physiol* 311: F945-F957, 2016.
88. **Takeda T, McQuistan T, Orlando RA, and Farquhar MG**. Loss of glomerular foot processes is associated with uncoupling of podocalyxin from the actin cytoskeleton. *J Clin Invest* 108: 289-301, 2001.
89. **Al-Momany A, Li L, Alexander RT, and Ballermann BJ**. Clustered PI(4,5)P(2) accumulation and ezrin phosphorylation in response to CLIC5A. *J Cell Sci* 127: 5164-5178, 2014.
90. **Wennerberg K, Rossman KL, and Der CJ**. The Ras superfamily at a glance. *J Cell Sci* 118: 843-846, 2005.
91. **Takai Y, Sasaki T, and Matozaki T**. Small GTP-binding proteins. *Physiol Rev* 81: 153-208, 2001.
92. **Pereira-Leal JB, Hume AN, and Seabra MC**. Prenylation of Rab GTPases: molecular mechanisms and involvement in genetic disease. *FEBS Lett* 498: 197-200, 2001.
93. **Vetter IR, and Wittinghofer A**. The guanine nucleotide-binding switch in three dimensions. *Science* 294: 1299-1304, 2001.
94. **Bourne HR, Sanders DA, and McCormick F**. The GTPase superfamily: conserved structure and molecular mechanism. *Nature* 349: 117-127, 1991.
95. **Mosteller RD, Han J, and Broek D**. Identification of residues of the H-ras protein critical for functional interaction with guanine nucleotide exchange factors. *Mol Cell Biol* 14: 1104-1112, 1994.
96. **Crechet JB, Bernardi A, and Parmeggiani A**. Distal switch II region of Ras2p is required for interaction with guanine nucleotide exchange factor. *J Biol Chem* 271: 17234-17240, 1996.
97. **Cherfils J, and Zeghouf M**. Regulation of small GTPases by GEFs, GAPs, and GDIs. *Physiol Rev* 93: 269-309, 2013.
98. **Parri M, and Chiarugi P**. Rac and Rho GTPases in cancer cell motility control. *Cell Commun Signal* 8: 23, 2010.
99. **Miyazaki K, Komatsu S, and Ikebe M**. Dynamics of RhoA and ROKalpha translocation in single living cells. *Cell Biochem Biophys* 45: 243-254, 2006.
100. **Dvorsky R, and Ahmadian MR**. Always look on the bright site of Rho: structural implications for a conserved intermolecular interface. *EMBO Rep* 5: 1130-1136, 2004.

101. **Roberts PJ, Mitin N, Keller PJ, Chenette EJ, Madigan JP, Currin RO, Cox AD, Wilson O, Kirschmeier P, and Der CJ**. Rho Family GTPase modification and dependence on CAAX motif-signaled posttranslational modification. *J Biol Chem* 283: 25150-25163, 2008.
102. **Ridley AJ, Paterson HF, Johnston CL, Diekmann D, and Hall A**. The small GTP-binding protein rac regulates growth factor-induced membrane ruffling. *Cell* 70: 401-410, 1992.
103. **Ridley AJ, and Hall A**. The small GTP-binding protein rho regulates the assembly of focal adhesions and actin stress fibers in response to growth factors. *Cell* 70: 389-399, 1992.
104. **Hall A, and Nobes CD**. Rho GTPases: molecular switches that control the organization and dynamics of the actin cytoskeleton. *Philos Trans R Soc Lond B Biol Sci* 355: 965-970, 2000.
105. **Hall A**. Rho GTPases and the actin cytoskeleton. *Science* 279: 509-514, 1998.
106. **Su LF, Knoblauch R, and Garabedian MJ**. Rho GTPases as modulators of the estrogen receptor transcriptional response. *J Biol Chem* 276: 3231-3237, 2001.
107. **Ridley AJ**. Rho GTPases and actin dynamics in membrane protrusions and vesicle trafficking. *Trends Cell Biol* 16: 522-529, 2006.
108. **Ridley AJ**. Rho proteins: linking signaling with membrane trafficking. *Traffic* 2: 303-310, 2001.
109. **Ho HY, Rohatgi R, Lebensohn AM, Le M, Li J, Gygi SP, and Kirschner MW**. Toca-1 mediates Cdc42-dependent actin nucleation by activating the N-WASP-WIP complex. *Cell* 118: 203-216, 2004.
110. **Villalonga P, and Ridley AJ**. Rho GTPases and cell cycle control. *Growth Factors* 24: 159-164, 2006.
111. **Yoshizaki H, Ohba Y, Kurokawa K, Itoh RE, Nakamura T, Mochizuki N, Nagashima K, and Matsuda M**. Activity of Rho-family GTPases during cell division as visualized with FRET-based probes. *J Cell Biol* 162: 223-232, 2003.
112. **Ellenbroek SI, and Collard JG**. Rho GTPases: functions and association with cancer. *Clin Exp Metastasis* 24: 657-672, 2007.
113. **Jaffe AB, and Hall A**. Rho GTPases: biochemistry and biology. *Annu Rev Cell Dev Biol* 21: 247-269, 2005.
114. **Tao Y, Chen YC, Li YY, Yang SQ, and Xu WR**. Localization and translocation of RhoA protein in the human gastric cancer cell line SGC-7901. *World J Gastroenterol* 14: 1175-1181, 2008.
115. **Wheeler AP, and Ridley AJ**. Why three Rho proteins? RhoA, RhoB, RhoC, and cell motility. *Exp Cell Res* 301: 43-49, 2004.
116. **Schaefer A, Reinhard NR, and Hordijk PL**. Toward understanding RhoGTPase specificity: structure, function and local activation. *Small GTPases* 5: 6, 2014.
117. **Wu D, Asiedu M, and Wei Q**. Myosin-interacting guanine exchange factor (MyoGEF) regulates the invasion activity of MDA-MB-231 breast cancer cells through activation of RhoA and RhoC. *Oncogene* 28: 2219-2230, 2009.
118. **Narumiya S, Tanji M, and Ishizaki T**. Rho signaling, ROCK and mDia1, in transformation, metastasis and invasion. *Cancer Metastasis Rev* 28: 65-76, 2009.
119. **Sadok A, and Marshall CJ**. Rho GTPases: masters of cell migration. *Small GTPases* 5: e29710, 2014.

120. **Tapon N, and Hall A**. Rho, Rac and Cdc42 GTPases regulate the organization of the actin cytoskeleton. *Curr Opin Cell Biol* 9: 86-92, 1997.
121. **Scott RP, Hawley SP, Ruston J, Du J, Brakebusch C, Jones N, and Pawson T**. Podocyte-specific loss of Cdc42 leads to congenital nephropathy. *J Am Soc Nephrol* 23: 1149-1154, 2012.
122. **Zhu L, Jiang R, Aoudjit L, Jones N, and Takano T**. Activation of RhoA in podocytes induces focal segmental glomerulosclerosis. *J Am Soc Nephrol* 22: 1621-1630, 2011.
123. **Babelova A, Jansen F, Sander K, Lohn M, Schafer L, Fork C, Ruetten H, Plettenburg O, Stark H, Daniel C, Amann K, Pavenstadt H, Jung O, and Brandes RP**. Activation of Rac-1 and RhoA contributes to podocyte injury in chronic kidney disease. *PLoS One* 8: e80328, 2013.
124. **Peng F, Wu D, Gao B, Ingram AJ, Zhang B, Chorneyko K, McKenzie R, and Krepinsky JC**. RhoA/Rho-kinase contribute to the pathogenesis of diabetic renal disease. *Diabetes* 57: 1683-1692, 2008.
125. **Huang Z, Zhang L, Chen Y, Zhang H, Yu C, Zhou F, Zhang Z, Jiang L, Li R, Ma J, Li Z, Lai Y, Lin T, Zhao X, Zhang Q, Zhang B, Ye Z, Liu S, Wang W, Liang X, Liao R, and Shi W**. RhoA deficiency disrupts podocyte cytoskeleton and induces podocyte apoptosis by inhibiting YAP/dendrin signal. *BMC Nephrol* 17: 66, 2016.
126. **Erickson JW, Zhang C, Kahn RA, Evans T, and Cerione RA**. Mammalian Cdc42 is a brefeldin A-sensitive component of the Golgi apparatus. *J Biol Chem* 271: 26850-26854, 1996.
127. **Osmani N, Peglion F, Chavrier P, and Etienne-Manneville S**. Cdc42 localization and cell polarity depend on membrane traffic. *J Cell Biol* 191: 1261-1269, 2010.
128. **Ridley AJ, Schwartz MA, Burridge K, Firtel RA, Ginsberg MH, Borisy G, Parsons JT, and Horwitz AR**. Cell migration: integrating signals from front to back. *Science* 302: 1704-1709, 2003.
129. **Gupta GP, and Massague J**. Cancer metastasis: building a framework. *Cell* 127: 679-695, 2006.
130. **Cerione RA**. Cdc42: new roads to travel. *Trends Cell Biol* 14: 127-132, 2004.
131. **Bishop AL, and Hall A**. Rho GTPases and their effector proteins. *Biochem J* 348 Pt 2: 241-255, 2000.
132. **Murphy NP, Binti Ahmad Mokhtar AM, Mott HR, and Owen D**. Molecular subversion of Cdc42 signalling in cancer. *Biochem Soc Trans* 49: 1425-1442, 2021.
133. **Schmidt A, and Hall A**. Guanine nucleotide exchange factors for Rho GTPases: turning on the switch. *Genes Dev* 16: 1587-1609, 2002.
134. **Edwards DC, Sanders LC, Bokoch GM, and Gill GN**. Activation of LIM-kinase by Pak1 couples Rac/Cdc42 GTPase signalling to actin cytoskeletal dynamics. *Nat Cell Biol* 1: 253-259, 1999.
135. **Machesky LM, and Insall RH**. Signaling to actin dynamics. *J Cell Biol* 146: 267-272, 1999.
136. **Kim AS, Kakalis LT, Abdul-Manan N, Liu GA, and Rosen MK**. Autoinhibition and activation mechanisms of the Wiskott-Aldrich syndrome protein. *Nature* 404: 151-158, 2000.
137. **Pollard TD, and Borisy GG**. Cellular motility driven by assembly and disassembly of actin filaments. *Cell* 112: 453-465, 2003.

138. **Huang Z, Zhang L, Chen Y, Zhang H, Zhang Q, Li R, Ma J, Li Z, Yu C, Lai Y, Lin T, Zhao X, Zhang B, Ye Z, Liu S, Wang W, Liang X, Liao R, and Shi W**. Cdc42 deficiency induces podocyte apoptosis by inhibiting the Nwasp/stress fibers/YAP pathway. *Cell Death Dis* 7: e2142, 2016.
139. **Pan Y, Jiang S, Hou Q, Qiu D, Shi J, Wang L, Chen Z, Zhang M, Duan A, Qin W, Zen K, and Liu Z**. Dissection of Glomerular Transcriptional Profile in Patients With Diabetic Nephropathy: SRGAP2a Protects Podocyte Structure and Function. *Diabetes* 67: 717-730, 2018.
140. **Lin J, Shi Y, Peng H, Shen X, Thomas S, Wang Y, Truong LD, Dryer SE, Hu Z, and Xu J**. Loss of PTEN promotes podocyte cytoskeletal rearrangement, aggravating diabetic nephropathy. *J Pathol* 236: 30-40, 2015.
141. **Shen J, Wang R, He Z, Huang H, He X, Zhou J, Yan Y, Shen S, Shao X, Shen X, Weng C, Lin W, and Chen J**. NMDA receptors participate in the progression of diabetic kidney disease by decreasing Cdc42-GTP activation in podocytes. *J Pathol* 240: 149-160, 2016.
142. **Didsbury J, Weber RF, Bokoch GM, Evans T, and Snyderman R**. rac, a novel ras-related family of proteins that are botulinum toxin substrates. *J Biol Chem* 264: 16378-16382, 1989.
143. **Fagerberg L, Hallstrom BM, Oksvold P, Kampf C, Djureinovic D, Odeberg J, Habuka M, Tahmasebpoor S, Danielsson A, Edlund K, Asplund A, Sjostedt E, Lundberg E, Szigyarto CA, Skogs M, Takanen JO, Berling H, Tegel H, Mulder J, Nilsson P, Schwenk JM, Lindskog C, Danielsson F, Mardinoglu A, Sivertsson A, von Feilitzen K, Forsberg M, Zwahlen M, Olsson I, Navani S, Huss M, Nielsen J, Ponten F, and Uhlen M**. Analysis of the human tissue-specific expression by genome-wide integration of transcriptomics and antibody-based proteomics. *Mol Cell Proteomics* 13: 397-406, 2014.
144. **Bosco EE, Mulloy JC, and Zheng Y**. Rac1 GTPase: a "Rac" of all trades. *Cell Mol Life Sci* 66: 370-374, 2009.
145. **Westwick JK, Lambert QT, Clark GJ, Symons M, Van Aelst L, Pestell RG, and Der CJ**. Rac regulation of transformation, gene expression, and actin organization by multiple, PAK-independent pathways. *Mol Cell Biol* 17: 1324-1335, 1997.
146. **Choy E, Chiu VK, Silletti J, Feoktistov M, Morimoto T, Michaelson D, Ivanov IE, and Philips MR**. Endomembrane trafficking of ras: the CAAX motif targets proteins to the ER and Golgi. *Cell* 98: 69-80, 1999.
147. **DerMardirossian C, and Bokoch GM**. GDIs: central regulatory molecules in Rho GTPase activation. *Trends Cell Biol* 15: 356-363, 2005.
148. **Ugolev Y, Berdichevsky Y, Weinbaum C, and Pick E**. Dissociation of Rac1(GDP).RhoGDI complexes by the cooperative action of anionic liposomes containing phosphatidylinositol 3,4,5-trisphosphate, Rac guanine nucleotide exchange factor, and GTP. *J Biol Chem* 283: 22257-22271, 2008.
149. **Hsu YH, Lin WL, Hou YT, Pu YS, Shun CT, Chen CL, Wu YY, Chen JY, Chen TH, and Jou TS**. Podocalyxin EBP50 ezrin molecular complex enhances the metastatic potential of renal cell carcinoma through recruiting Rac1 guanine nucleotide exchange factor ARHGEF7. *Am J Pathol* 176: 3050-3061, 2010.
150. **Pasapera AM, Plotnikov SV, Fischer RS, Case LB, Egelhoff TT, and Waterman CM**. Rac1-dependent phosphorylation and focal adhesion recruitment of myosin IIA regulates migration and mechanosensing. *Curr Biol* 25: 175-186, 2015.

151. **Yu H, Suleiman H, Kim AH, Miner JH, Dani A, Shaw AS, and Akilesh S**. Rac1 activation in podocytes induces rapid foot process effacement and proteinuria. *Mol Cell Biol* 33: 4755-4764, 2013.
152. **Ronco P**. Proteinuria: is it all in the foot? *J Clin Invest* 117: 2079-2082, 2007.
153. **Shibata S, Nagase M, Yoshida S, Kawarazaki W, Kurihara H, Tanaka H, Miyoshi J, Takai Y, and Fujita T**. Modification of mineralocorticoid receptor function by Rac1 GTPase: implication in proteinuric kidney disease. *Nat Med* 14: 1370-1376, 2008.
154. **Akilesh S, Suleiman H, Yu H, Stander MC, Lavin P, Gbadegesin R, Antignac C, Pollak M, Kopp JB, Winn MP, and Shaw AS**. Arhgap24 inactivates Rac1 in mouse podocytes, and a mutant form is associated with familial focal segmental glomerulosclerosis. *J Clin Invest* 121: 4127-4137, 2011.
155. **Robins R, Baldwin C, Aoudjit L, Cote JF, Gupta IR, and Takano T**. Rac1 activation in podocytes induces the spectrum of nephrotic syndrome. *Kidney Int* 92: 349-364, 2017.
156. **Robins R, Baldwin C, Aoudjit L, Gupta IR, and Takano T**. Loss of Rho-GDIalpha sensitizes podocytes to lipopolysaccharide-mediated injury. *Am J Physiol Renal Physiol* 308: F1207-1216, 2015.
157. **Maier M, Baldwin C, Aoudjit L, and Takano T**. The Role of Trio, a Rho Guanine Nucleotide Exchange Factor, in Glomerular Podocytes. *Int J Mol Sci* 19: 2018.
158. **Auguste D, Maier M, Baldwin C, Aoudjit L, Robins R, Gupta IR, and Takano T**. Disease-causing mutations of RhoGDIalpha induce Rac1 hyperactivation in podocytes. *Small GTPases* 7: 107-121, 2016.
159. **Polat OK, Isaeva E, Sudhini YR, Knott B, Zhu K, Noben M, Suresh Kumar V, Endlich N, Mangos S, Reddy TV, Samelko B, Wei C, Altintas MM, Dryer SE, Sever S, Staruschenko A, and Reiser J**. The small GTPase regulatory protein Rac1 drives podocyte injury independent of cationic channel protein TRPC5. *Kidney Int* 103: 1056-1062, 2023.
160. **Hatano R, Takeda A, Abe Y, Kawaguchi K, Kazama I, Matsubara M, and Asano S**. Loss of ezrin expression reduced the susceptibility to the glomerular injury in mice. *Sci Rep* 8: 4512, 2018.
161. **Yonemura S, Tsukita S, and Tsukita S**. Direct involvement of ezrin/radixin/moesin (ERM)-binding membrane proteins in the organization of microvilli in collaboration with activated ERM proteins. *J Cell Biol* 145: 1497-1509, 1999.
162. **Viswanatha R, Bretscher A, and Garbett D**. Dynamics of ezrin and EBP50 in regulating microvilli on the apical aspect of epithelial cells. *Biochem Soc Trans* 42: 189-194, 2014.
163. **Kondo T, Takeuchi K, Doi Y, Yonemura S, Nagata S, and Tsukita S**. ERM (ezrin/radixin/moesin)-based molecular mechanism of microvillar breakdown at an early stage of apoptosis. *J Cell Biol* 139: 749-758, 1997.
164. **Downes CP, Gray A, and Lucocq JM**. Probing phosphoinositide functions in signaling and membrane trafficking. *Trends Cell Biol* 15: 259-268, 2005.
165. **Wang M, Bond NJ, Letcher AJ, Richardson JP, Lilley KS, Irvine RF, and Clarke JH**. Genomic tagging reveals a random association of endogenous PtdIns5P 4-kinases IIalpha and IIbeta and a partial nuclear localization of the IIalpha isoform. *Biochem J* 430: 215-221, 2010.
166. **Loijens JC, Boronenkov IV, Parker GJ, and Anderson RA**. The phosphatidylinositol 4-phosphate 5-kinase family. *Adv Enzyme Regul* 36: 115-140, 1996.

167. **Honda A, Nogami M, Yokozeki T, Yamazaki M, Nakamura H, Watanabe H, Kawamoto K, Nakayama K, Morris AJ, Frohman MA, and Kanaho Y**. Phosphatidylinositol 4-phosphate 5-kinase alpha is a downstream effector of the small G protein ARF6 in membrane ruffle formation. *Cell* 99: 521-532, 1999.
168. **Saltel F, Mortier E, Hytonen VP, Jacquier MC, Zimmermann P, Vogel V, Liu W, and Wehrle-Haller B**. New PI(4,5)P2- and membrane proximal integrin-binding motifs in the talin head control beta3-integrin clustering. *J Cell Biol* 187: 715-731, 2009.
169. **Liepina I, Czaplewski C, Janmey P, and Liwo A**. Molecular dynamics study of a gelsolin-derived peptide binding to a lipid bilayer containing phosphatidylinositol 4,5-bisphosphate. *Biopolymers* 71: 49-70, 2003.
170. **Amano T, Tanabe K, Eto T, Narumiya S, and Mizuno K**. LIM-kinase 2 induces formation of stress fibres, focal adhesions and membrane blebs, dependent on its activation by Rho-associated kinase-catalysed phosphorylation at threonine-505. *Biochem J* 354: 149-159, 2001.
171. **Walter LM, Franz P, Lindner R, Tsiavaliaris G, Hensel N, and Claus P**. Profilin2a-phosphorylation as a regulatory mechanism for actin dynamics. *FASEB J* 34: 2147-2160, 2020.
172. **Romarowski A, Battistone MA, La Spina FA, Puga Molina Ldel C, Luque GM, Vitale AM, Cuasnicu PS, Visconti PE, Krapf D, and Buffone MG**. PKA-dependent phosphorylation of LIMK1 and Cofilin is essential for mouse sperm acrosomal exocytosis. *Dev Biol* 405: 237-249, 2015.
173. **McLean MA, Stephen AG, and Sligar SG**. PIP2 Influences the Conformational Dynamics of Membrane-Bound KRAS4b. *Biochemistry* 58: 3537-3545, 2019.
174. **Reversi A, Loeser E, Subramanian D, Schultz C, and De Renzis S**. Plasma membrane phosphoinositide balance regulates cell shape during Drosophila embryo morphogenesis. *J Cell Biol* 205: 395-408, 2014.
175. **van Hennik PB, ten Klooster JP, Halstead JR, Voermans C, Anthony EC, Divecha N, and Hordijk PL**. The C-terminal domain of Rac1 contains two motifs that control targeting and signaling specificity. *J Biol Chem* 278: 39166-39175, 2003.
176. **Tolias KF, Hartwig JH, Ishihara H, Shibasaki Y, Cantley LC, and Carpenter CL**. Type Ialpha phosphatidylinositol-4-phosphate 5-kinase mediates Rac-dependent actin assembly. *Curr Biol* 10: 153-156, 2000.
177. **Tolias KF, Couvillon AD, Cantley LC, and Carpenter CL**. Characterization of a Rac1- and RhoGDI-associated lipid kinase signaling complex. *Mol Cell Biol* 18: 762-770, 1998.
178. **Tolias KF, Cantley LC, and Carpenter CL**. Rho family GTPases bind to phosphoinositide kinases. *J Biol Chem* 270: 17656-17659, 1995.
179. **Chatah NE, and Abrams CS**. G-protein-coupled receptor activation induces the membrane translocation and activation of phosphatidylinositol-4-phosphate 5-kinase I alpha by a Rac- and Rho-dependent pathway. *J Biol Chem* 276: 34059-34065, 2001.
180. **Chong LD, Traynor-Kaplan A, Bokoch GM, and Schwartz MA**. The small GTP-binding protein Rho regulates a phosphatidylinositol 4-phosphate 5-kinase in mammalian cells. *Cell* 79: 507-513, 1994.
181. **Yamamoto M, Hilgemann DH, Feng S, Bito H, Ishihara H, Shibasaki Y, and Yin HL**. Phosphatidylinositol 4,5-bisphosphate induces actin stress-fiber formation and inhibits membrane ruffling in CV1 cells. *J Cell Biol* 152: 867-876, 2001.

182. **Nystrom J, Fierlbeck W, Granqvist A, Kulak SC, and Ballermann BJ**. A human glomerular SAGE transcriptome database. *BMC Nephrol* 10: 13, 2009.
183. **Sengoelge G, Luo W, Fine D, Perschl AM, Fierlbeck W, Haririan A, Sorensson J, Rehman TU, Hauser P, Trevick JS, Kulak SC, Wegner B, and Ballermann BJ**. A SAGE-based comparison between glomerular and aortic endothelial cells. *Am J Physiol Renal Physiol* 288: F1290-1300, 2005.
184. **Orlando RA, Takeda T, Zak B, Schmieder S, Benoit VM, McQuistan T, Furthmayr H, and Farquhar MG**. The glomerular epithelial cell anti-adhesin podocalyxin associates with the actin cytoskeleton through interactions with ezrin. *J Am Soc Nephrol* 12: 1589-1598, 2001.
185. **Bretscher A, Edwards K, and Fehon RG**. ERM proteins and merlin: integrators at the cell cortex. *Nat Rev Mol Cell Biol* 3: 586-599, 2002.
186. **Fehon RG, McClatchey AI, and Bretscher A**. Organizing the cell cortex: the role of ERM proteins. *Nat Rev Mol Cell Biol* 11: 276-287, 2010.
187. **Conboy J**. Molecular cloning and characterization of the gene coding for red cell membrane skeletal protein 4.1. *Biorheology* 24: 673-687, 1987.
188. **Chishti AH, Kim AC, Marfatia SM, Lutchman M, Hanspal M, Jindal H, Liu SC, Low PS, Rouleau GA, Mohandas N, Chasis JA, Conboy JG, Gascard P, Takakuwa Y, Huang SC, Benz EJ, Jr., Bretscher A, Fehon RG, Gusella JF, Ramesh V, Solomon F, Marchesi VT, Tsukita S, Tsukita S, Hoover KB, and et al.** The FERM domain: a unique module involved in the linkage of cytoplasmic proteins to the membrane. *Trends Biochem Sci* 23: 281-282, 1998.
189. **Hamada K, Shimizu T, Matsui T, Tsukita S, and Hakoshima T**. Structural basis of the membrane-targeting and unmasking mechanisms of the radixin FERM domain. *EMBO J* 19: 4449-4462, 2000.
190. **Pearson MA, Reczek D, Bretscher A, and Karplus PA**. Structure of the ERM protein moesin reveals the FERM domain fold masked by an extended actin binding tail domain. *Cell* 101: 259-270, 2000.
191. **Arpin M, Chirivino D, Naba A, and Zwaenepoel I**. Emerging role for ERM proteins in cell adhesion and migration. *Cell Adh Migr* 5: 199-206, 2011.
192. **Ivetic A, and Ridley AJ**. Ezrin/radixin/moesin proteins and Rho GTPase signalling in leucocytes. *Immunology* 112: 165-176, 2004.
193. **Tsukita S, and Yonemura S**. Cortical actin organization: lessons from ERM (ezrin/radixin/moesin) proteins. *J Biol Chem* 274: 34507-34510, 1999.
194. **Berryman M, Franck Z, and Bretscher A**. Ezrin is concentrated in the apical microvilli of a wide variety of epithelial cells whereas moesin is found primarily in endothelial cells. *J Cell Sci* 105 (Pt 4): 1025-1043, 1993.
195. **Bretscher A**. Purification of the intestinal microvillus cytoskeletal proteins villin, fimbrin, and ezrin. *Methods Enzymol* 134: 24-37, 1986.
196. **Bretscher A**. Purification of an 80,000-dalton protein that is a component of the isolated microvillus cytoskeleton, and its localization in nonmuscle cells. *J Cell Biol* 97: 425-432, 1983.
197. **Saotome I, Curto M, and McClatchey AI**. Ezrin is essential for epithelial organization and villus morphogenesis in the developing intestine. *Dev Cell* 6: 855-864, 2004.

198. **Lankes W, Griesmacher A, Grunwald J, Schwartz-Albiez R, and Keller R**. A heparin-binding protein involved in inhibition of smooth-muscle cell proliferation. *Biochem J* 251: 831-842, 1988.
199. **Lankes WT, and Furthmayr H**. Moesin: a member of the protein 4.1-talin-ezrin family of proteins. *Proc Natl Acad Sci U S A* 88: 8297-8301, 1991.
200. **Ingraffea J, Reczek D, and Bretscher A**. Distinct cell type-specific expression of scaffolding proteins EBP50 and E3KARP: EBP50 is generally expressed with ezrin in specific epithelia, whereas E3KARP is not. *Eur J Cell Biol* 81: 61-68, 2002.
201. **Liu X, Yang T, Suzuki K, Tsukita S, Ishii M, Zhou S, Wang G, Cao L, Qian F, Taylor S, Oh MJ, Levitan I, Ye RD, Carnegie GK, Zhao Y, Malik AB, and Xu J**. Moesin and myosin phosphatase confine neutrophil orientation in a chemotactic gradient. *J Exp Med* 212: 267-280, 2015.
202. **Tsukita S, Hieda Y, and Tsukita S**. A new 82-kD barbed end-capping protein (radixin) localized in the cell-to-cell adherens junction: purification and characterization. *J Cell Biol* 108: 2369-2382, 1989.
203. **Kawaguchi K, Yoshida S, Hatano R, and Asano S**. Pathophysiological Roles of Ezrin/Radixin/Moesin Proteins. *Biol Pharm Bull* 40: 381-390, 2017.
204. **Kitajiri S, Fukumoto K, Hata M, Sasaki H, Katsuno T, Nakagawa T, Ito J, Tsukita S, and Tsukita S**. Radixin deficiency causes deafness associated with progressive degeneration of cochlear stereocilia. *J Cell Biol* 166: 559-570, 2004.
205. **Pataky F, Pironkova R, and Hudspeth AJ**. Radixin is a constituent of stereocilia in hair cells. *Proc Natl Acad Sci U S A* 101: 2601-2606, 2004.
206. **Niggli V, Andreoli C, Roy C, and Mangeat P**. Identification of a phosphatidylinositol-4,5-bisphosphate-binding domain in the N-terminal region of ezrin. *FEBS Lett* 376: 172-176, 1995.
207. **Turunen O, Wahlstrom T, and Vaheri A**. Ezrin has a COOH-terminal actin-binding site that is conserved in the ezrin protein family. *J Cell Biol* 126: 1445-1453, 1994.
208. **Ben-Aissa K, Patino-Lopez G, Belkina NV, Maniti O, Rosales T, Hao JJ, Kruhlak MJ, Knutson JR, Picart C, and Shaw S**. Activation of moesin, a protein that links actin cytoskeleton to the plasma membrane, occurs by phosphatidylinositol 4,5-bisphosphate (PIP2) binding sequentially to two sites and releasing an autoinhibitory linker. *J Biol Chem* 287: 16311-16323, 2012.
209. **Algrain M, Turunen O, Vaheri A, Louvard D, and Arpin M**. Ezrin contains cytoskeleton and membrane binding domains accounting for its proposed role as a membrane-cytoskeletal linker. *J Cell Biol* 120: 129-139, 1993.
210. **Gary R, and Bretscher A**. Ezrin self-association involves binding of an N-terminal domain to a normally masked C-terminal domain that includes the F-actin binding site. *Mol Biol Cell* 6: 1061-1075, 1995.
211. **Barret C, Roy C, Montcourrier P, Mangeat P, and Niggli V**. Mutagenesis of the phosphatidylinositol 4,5-bisphosphate (PIP(2)) binding site in the NH(2)-terminal domain of ezrin correlates with its altered cellular distribution. *J Cell Biol* 151: 1067-1080, 2000.
212. **Gobel V, Barrett PL, Hall DH, and Fleming JT**. Lumen morphogenesis in C. elegans requires the membrane-cytoskeleton linker erm-1. *Dev Cell* 6: 865-873, 2004.
213. **Canals D, Roddy P, and Hannun YA**. Protein phosphatase 1alpha mediates ceramide-induced ERM protein dephosphorylation: a novel mechanism independent of

phosphatidylinositol 4, 5-biphosphate (PIP2) and myosin/ERM phosphatase. *J Biol Chem* 287: 10145-10155, 2012.
214. **Hao JJ, Liu Y, Kruhlak M, Debell KE, Rellahan BL, and Shaw S**. Phospholipase C-mediated hydrolysis of PIP2 releases ERM proteins from lymphocyte membrane. *J Cell Biol* 184: 451-462, 2009.
215. **Rasmussen M, Alexander RT, Darborg BV, Mobjerg N, Hoffmann EK, Kapus A, and Pedersen SF**. Osmotic cell shrinkage activates ezrin/radixin/moesin (ERM) proteins: activation mechanisms and physiological implications. *Am J Physiol Cell Physiol* 294: C197-212, 2008.
216. **Yonemura S, Matsui T, Tsukita S, and Tsukita S**. Rho-dependent and -independent activation mechanisms of ezrin/radixin/moesin proteins: an essential role for polyphosphoinositides in vivo. *J Cell Sci* 115: 2569-2580, 2002.
217. **Matsui T, Maeda M, Doi Y, Yonemura S, Amano M, Kaibuchi K, Tsukita S, and Tsukita S**. Rho-kinase phosphorylates COOH-terminal threonines of ezrin/radixin/moesin (ERM) proteins and regulates their head-to-tail association. *J Cell Biol* 140: 647-657, 1998.
218. **Tran Quang C, Gautreau A, Arpin M, and Treisman R**. Ezrin function is required for ROCK-mediated fibroblast transformation by the Net and Dbl oncogenes. *EMBO J* 19: 4565-4576, 2000.
219. **Ng T, Parsons M, Hughes WE, Monypenny J, Zicha D, Gautreau A, Arpin M, Gschmeissner S, Verveer PJ, Bastiaens PI, and Parker PJ**. Ezrin is a downstream effector of trafficking PKC-integrin complexes involved in the control of cell motility. *EMBO J* 20: 2723-2741, 2001.
220. **Shiue H, Musch MW, Wang Y, Chang EB, and Turner JR**. Akt2 phosphorylates ezrin to trigger NHE3 translocation and activation. *J Biol Chem* 280: 1688-1695, 2005.
221. **Nakamura F, Amieva MR, and Furthmayr H**. Phosphorylation of threonine 558 in the carboxyl-terminal actin-binding domain of moesin by thrombin activation of human platelets. *J Biol Chem* 270: 31377-31385, 1995.
222. **Baumgartner M, Sillman AL, Blackwood EM, Srivastava J, Madson N, Schilling JW, Wright JH, and Barber DL**. The Nck-interacting kinase phosphorylates ERM proteins for formation of lamellipodium by growth factors. *Proc Natl Acad Sci U S A* 103: 13391-13396, 2006.
223. **Simons PC, Pietromonaco SF, Reczek D, Bretscher A, and Elias L**. C-terminal threonine phosphorylation activates ERM proteins to link the cell's cortical lipid bilayer to the cytoskeleton. *Biochem Biophys Res Commun* 253: 561-565, 1998.
224. **Gautreau A, Louvard D, and Arpin M**. Morphogenic effects of ezrin require a phosphorylation-induced transition from oligomers to monomers at the plasma membrane. *J Cell Biol* 150: 193-203, 2000.
225. **Roch F, Polesello C, Roubinet C, Martin M, Roy C, Valenti P, Carreno S, Mangeat P, and Payre F**. Differential roles of PtdIns(4,5)P2 and phosphorylation in moesin activation during Drosophila development. *J Cell Sci* 123: 2058-2067, 2010.
226. **Fievet BT, Gautreau A, Roy C, Del Maestro L, Mangeat P, Louvard D, and Arpin M**. Phosphoinositide binding and phosphorylation act sequentially in the activation mechanism of ezrin. *J Cell Biol* 164: 653-659, 2004.
227. **Yonemura S, Hirao M, Doi Y, Takahashi N, Kondo T, Tsukita S, and Tsukita S**. Ezrin/radixin/moesin (ERM) proteins bind to a positively charged amino acid cluster in the

juxta-membrane cytoplasmic domain of CD44, CD43, and ICAM-2. *J Cell Biol* 140: 885-895, 1998.
228. **Wang Z, and Schey KL**. Aquaporin-0 interacts with the FERM domain of ezrin/radixin/moesin proteins in the ocular lens. *Invest Ophthalmol Vis Sci* 52: 5079-5087, 2011.
229. **Zhang M, Bohlson SS, Dy M, and Tenner AJ**. Modulated interaction of the ERM protein, moesin, with CD93. *Immunology* 115: 63-73, 2005.
230. **Weinman EJ, Hall RA, Friedman PA, Liu-Chen LY, and Shenolikar S**. The association of NHERF adaptor proteins with g protein-coupled receptors and receptor tyrosine kinases. *Annu Rev Physiol* 68: 491-505, 2006.
231. **Reczek D, Berryman M, and Bretscher A**. Identification of EBP50: A PDZ-containing phosphoprotein that associates with members of the ezrin-radixin-moesin family. *J Cell Biol* 139: 169-179, 1997.
232. **Fukasawa H, Obayashi H, Schmieder S, Lee J, Ghosh P, and Farquhar MG**. Phosphorylation of podocalyxin (Ser415) Prevents RhoA and ezrin activation and disrupts its interaction with the actin cytoskeleton. *Am J Pathol* 179: 2254-2265, 2011.
233. **Takeda T**. Podocyte cytoskeleton is connected to the integral membrane protein podocalyxin through Na+/H+-exchanger regulatory factor 2 and ezrin. *Clin Exp Nephrol* 7: 260-269, 2003.
234. **Takahashi K, Sasaki T, Mammoto A, Takaishi K, Kameyama T, Tsukita S, and Takai Y**. Direct interaction of the Rho GDP dissociation inhibitor with ezrin/radixin/moesin initiates the activation of the Rho small G protein. *J Biol Chem* 272: 23371-23375, 1997.
235. **Takahashi K, Sasaki T, Mammoto A, Hotta I, Takaishi K, Imamura H, Nakano K, Kodama A, and Takai Y**. Interaction of radixin with Rho small G protein GDP/GTP exchange protein Dbl. *Oncogene* 16: 3279-3284, 1998.
236. **Takai Y, Sasaki T, Tanaka K, and Nakanishi H**. Rho as a regulator of the cytoskeleton. *Trends Biochem Sci* 20: 227-231, 1995.
237. **Yaku H, Sasaki T, and Takai Y**. The Dbl oncogene product as a GDP/GTP exchange protein for the Rho family: its properties in comparison with those of Smg GDS. *Biochem Biophys Res Commun* 198: 811-817, 1994.
238. **Ozaki K, Tanaka K, Imamura H, Hihara T, Kameyama T, Nonaka H, Hirano H, Matsuura Y, and Takai Y**. Rom1p and Rom2p are GDP/GTP exchange proteins (GEPs) for the Rho1p small GTP binding protein in Saccharomyces cerevisiae. *EMBO J* 15: 2196-2207, 1996.
239. **Hart MJ, Eva A, Evans T, Aaronson SA, and Cerione RA**. Catalysis of guanine nucleotide exchange on the CDC42Hs protein by the dbl oncogene product. *Nature* 354: 311-314, 1991.
240. **Polesello C, Delon I, Valenti P, Ferrer P, and Payre F**. Dmoesin controls actin-based cell shape and polarity during Drosophila melanogaster oogenesis. *Nat Cell Biol* 4: 782-789, 2002.
241. **Jankovics F, Sinka R, Lukacsovich T, and Erdelyi M**. MOESIN crosslinks actin and cell membrane in Drosophila oocytes and is required for OSKAR anchoring. *Curr Biol* 12: 2060-2065, 2002.

242. **Van Furden D, Johnson K, Segbert C, and Bossinger O**. The C. elegans ezrin-radixin-moesin protein ERM-1 is necessary for apical junction remodelling and tubulogenesis in the intestine. *Dev Biol* 272: 262-276, 2004.
243. **Pilot F, Philippe JM, Lemmers C, and Lecuit T**. Spatial control of actin organization at adherens junctions by a synaptotagmin-like protein Btsz. *Nature* 442: 580-584, 2006.
244. **Louvet S, Aghion J, Santa-Maria A, Mangeat P, and Maro B**. Ezrin becomes restricted to outer cells following asymmetrical division in the preimplantation mouse embryo. *Dev Biol* 177: 568-579, 1996.
245. **Dard N, Louvet-Vallee S, Santa-Maria A, and Maro B**. Phosphorylation of ezrin on threonine T567 plays a crucial role during compaction in the mouse early embryo. *Dev Biol* 271: 87-97, 2004.
246. **Dard N, Louvet S, Santa-Maria A, Aghion J, Martin M, Mangeat P, and Maro B**. In vivo functional analysis of ezrin during mouse blastocyst formation. *Dev Biol* 233: 161-173, 2001.
247. **Molnar C, and de Celis JF**. Independent roles of Drosophila Moesin in imaginal disc morphogenesis and hedgehog signalling. *Mech Dev* 123: 337-351, 2006.
248. **Speck O, Hughes SC, Noren NK, Kulikauskas RM, and Fehon RG**. Moesin functions antagonistically to the Rho pathway to maintain epithelial integrity. *Nature* 421: 83-87, 2003.
249. **Naba A, Reverdy C, Louvard D, and Arpin M**. Spatial recruitment and activation of the Fes kinase by ezrin promotes HGF-induced cell scattering. *EMBO J* 27: 38-50, 2008.
250. **McClatchey AI, and Fehon RG**. Merlin and the ERM proteins--regulators of receptor distribution and signaling at the cell cortex. *Trends Cell Biol* 19: 198-206, 2009.
251. **Morales FC, Takahashi Y, Momin S, Adams H, Chen X, and Georgescu MM**. NHERF1/EBP50 head-to-tail intramolecular interaction masks association with PDZ domain ligands. *Mol Cell Biol* 27: 2527-2537, 2007.
252. **Crepaldi T, Gautreau A, Comoglio PM, Louvard D, and Arpin M**. Ezrin is an effector of hepatocyte growth factor-mediated migration and morphogenesis in epithelial cells. *J Cell Biol* 138: 423-434, 1997.
253. **Legg JW, Lewis CA, Parsons M, Ng T, and Isacke CM**. A novel PKC-regulated mechanism controls CD44 ezrin association and directional cell motility. *Nat Cell Biol* 4: 399-407, 2002.
254. **Hunter KW**. Ezrin, a key component in tumor metastasis. *Trends Mol Med* 10: 201-204, 2004.
255. **Ren L, Hong SH, Cassavaugh J, Osborne T, Chou AJ, Kim SY, Gorlick R, Hewitt SM, and Khanna C**. The actin-cytoskeleton linker protein ezrin is regulated during osteosarcoma metastasis by PKC. *Oncogene* 28: 792-802, 2009.
256. **Orian-Rousseau V, Morrison H, Matzke A, Kastilan T, Pace G, Herrlich P, and Ponta H**. Hepatocyte growth factor-induced Ras activation requires ERM proteins linked to both CD44v6 and F-actin. *Mol Biol Cell* 18: 76-83, 2007.
257. **Orian-Rousseau V, and Ponta H**. Adhesion proteins meet receptors: a common theme? *Adv Cancer Res* 101: 63-92, 2008.
258. **Meder D, Shevchenko A, Simons K, and Fullekrug J**. Gp135/podocalyxin and NHERF-2 participate in the formation of a preapical domain during polarization of MDCK cells. *J Cell Biol* 168: 303-313, 2005.

259. **Belbin TJ, Singh B, Smith RV, Socci ND, Wreesmann VB, Sanchez-Carbayo M, Masterson J, Patel S, Cordon-Cardo C, Prystowsky MB, and Childs G**. Molecular profiling of tumor progression in head and neck cancer. *Arch Otolaryngol Head Neck Surg* 131: 10-18, 2005.
260. **Elliott BE, Meens JA, SenGupta SK, Louvard D, and Arpin M**. The membrane cytoskeletal crosslinker ezrin is required for metastasis of breast carcinoma cells. *Breast Cancer Res* 7: R365-373, 2005.
261. **Elliott BE, Qiao H, Louvard D, and Arpin M**. Co-operative effect of c-Src and ezrin in deregulation of cell-cell contacts and scattering of mammary carcinoma cells. *J Cell Biochem* 92: 16-28, 2004.
262. **Clucas J, and Valderrama F**. ERM proteins in cancer progression. *J Cell Sci* 127: 267-275, 2014.
263. **Hugo C, Nangaku M, Shankland SJ, Pichler R, Gordon K, Amieva MR, Couser WG, Furthmayr H, and Johnson RJ**. The plasma membrane-actin linking protein, ezrin, is a glomerular epithelial cell marker in glomerulogenesis, in the adult kidney and in glomerular injury. *Kidney Int* 54: 1934-1944, 1998.
264. **Roselli S, Gribouval O, Boute N, Sich M, Benessy F, Attie T, Gubler MC, and Antignac C**. Podocin localizes in the kidney to the slit diaphragm area. *Am J Pathol* 160: 131-139, 2002.
265. **Cunningham R, Esmaili A, Brown E, Biswas RS, Murtazina R, Donowitz M, Dijkman HB, van der Vlag J, Hogema BM, De Jonge HR, Shenolikar S, Wade JB, and Weinman EJ**. Urine electrolyte, mineral, and protein excretion in NHERF-2 and NHERF-1 null mice. *Am J Physiol Renal Physiol* 294: F1001-1007, 2008.
266. **Wasik AA, Koskelainen S, Hyvonen ME, Musante L, Lehtonen E, Koskenniemi K, Tienari J, Vaheri A, Kerjaschki D, Szalay C, Revesz C, Varmanen P, Nyman TA, Hamar P, Holthofer H, and Lehtonen S**. Ezrin is down-regulated in diabetic kidney glomeruli and regulates actin reorganization and glucose uptake via GLUT1 in cultured podocytes. *Am J Pathol* 184: 1727-1739, 2014.
267. **Harvey SJ, Jarad G, Cunningham J, Goldberg S, Schermer B, Harfe BD, McManus MT, Benzing T, and Miner JH**. Podocyte-specific deletion of dicer alters cytoskeletal dynamics and causes glomerular disease. *J Am Soc Nephrol* 19: 2150-2158, 2008.
268. **Hatano R, Fujii E, Segawa H, Mukaisho K, Matsubara M, Miyamoto K, Hattori T, Sugihara H, and Asano S**. Ezrin, a membrane cytoskeletal cross-linker, is essential for the regulation of phosphate and calcium homeostasis. *Kidney Int* 83: 41-49, 2013.
269. **Schelling JR, and Abu Jawdeh BG**. Regulation of cell survival by Na+/H+ exchanger-1. *Am J Physiol Renal Physiol* 295: F625-632, 2008.
270. **McRobert EA, Gallicchio M, Jerums G, Cooper ME, and Bach LA**. The amino-terminal domains of the ezrin, radixin, and moesin (ERM) proteins bind advanced glycation end products, an interaction that may play a role in the development of diabetic complications. *J Biol Chem* 278: 25783-25789, 2003.
271. **Khan S, Wu KL, Sedor JR, Abu Jawdeh BG, and Schelling JR**. The NHE1 Na+/H+ exchanger regulates cell survival by activating and targeting ezrin to specific plasma membrane domains. *Cell Mol Biol (Noisy-le-grand)* 52: 115-121, 2006.
272. **Gallicchio MA, McRobert EA, Tikoo A, Cooper ME, and Bach LA**. Advanced glycation end products inhibit tubulogenesis and migration of kidney epithelial cells in an ezrin-dependent manner. *J Am Soc Nephrol* 17: 414-421, 2006.

273. **Vanni C, Parodi A, Mancini P, Visco V, Ottaviano C, Torrisi MR, and Eva A**. Phosphorylation-independent membrane relocalization of ezrin following association with Dbl in vivo. *Oncogene* 23: 4098-4106, 2004.
274. **Bourguignon LY**. Hyaluronan-mediated CD44 activation of RhoGTPase signaling and cytoskeleton function promotes tumor progression. *Semin Cancer Biol* 18: 251-259, 2008.
275. **Martin-Villar E, Megias D, Castel S, Yurrita MM, Vilaro S, and Quintanilla M**. Podoplanin binds ERM proteins to activate RhoA and promote epithelial-mesenchymal transition. *J Cell Sci* 119: 4541-4553, 2006.
276. **Samarin S, and Nusrat A**. Regulation of epithelial apical junctional complex by Rho family GTPases. *Front Biosci (Landmark Ed)* 14: 1129-1142, 2009.
277. **Doyonnas R, Nielsen JS, Chelliah S, Drew E, Hara T, Miyajima A, and McNagny KM**. Podocalyxin is a CD34-related marker of murine hematopoietic stem cells and embryonic erythroid cells. *Blood* 105: 4170-4178, 2005.
278. **Horvat R, Hovorka A, Dekan G, Poczewski H, and Kerjaschki D**. Endothelial cell membranes contain podocalyxin--the major sialoprotein of visceral glomerular epithelial cells. *J Cell Biol* 102: 484-491, 1986.
279. **Kelley TW, Huntsman D, McNagny KM, Roskelley CD, and Hsi ED**. Podocalyxin: a marker of blasts in acute leukemia. *Am J Clin Pathol* 124: 134-142, 2005.
280. **Miettinen A, Solin ML, Reivinen J, Juvonen E, Vaisanen R, and Holthofer H**. Podocalyxin in rat platelets and megakaryocytes. *Am J Pathol* 154: 813-822, 1999.
281. **Nielsen JS, and McNagny KM**. The role of podocalyxin in health and disease. *J Am Soc Nephrol* 20: 1669-1676, 2009.
282. **Sassetti C, Tangemann K, Singer MS, Kershaw DB, and Rosen SD**. Identification of podocalyxin-like protein as a high endothelial venule ligand for L-selectin: parallels to CD34. *J Exp Med* 187: 1965-1975, 1998.
283. **Vitureira N, Andres R, Perez-Martinez E, Martinez A, Bribian A, Blasi J, Chelliah S, Lopez-Domenech G, De Castro F, Burgaya F, McNagny K, and Soriano E**. Podocalyxin is a novel polysialylated neural adhesion protein with multiple roles in neural development and synapse formation. *PLoS One* 5: e12003, 2010.
284. **Snyder KA, Hughes MR, Hedberg B, Brandon J, Hernaez DC, Bergqvist P, Cruz F, Po K, Graves ML, Turvey ME, Nielsen JS, Wilkins JA, McColl SR, Babcook JS, Roskelley CD, and McNagny KM**. Podocalyxin enhances breast tumor growth and metastasis and is a target for monoclonal antibody therapy. *Breast Cancer Res* 17: 46, 2015.
285. **Takeda T, Go WY, Orlando RA, and Farquhar MG**. Expression of podocalyxin inhibits cell-cell adhesion and modifies junctional properties in Madin-Darby canine kidney cells. *Mol Biol Cell* 11: 3219-3232, 2000.
286. **Kerjaschki D**. Dysfunctions of cell biological mechanisms of visceral epithelial cell (podocytes) in glomerular diseases. *Kidney Int* 45: 300-313, 1994.
287. **Mundel P, and Kriz W**. Structure and function of podocytes: an update. *Anat Embryol (Berl)* 192: 385-397, 1995.
288. **Orlando RA, Takeda T, Zak B, Schmieder S, Benoit VM, McQuistan T, Furthmayr H, and Farquhar MG**. The glomerular epithelial cell anti-adhesin podocalyxin associates with the actin cytoskeleton through interactions with ezrin. *J Am Soc Nephrol* 12: 1589-1598, 2001.

289. **Yun CH, Lamprecht G, Forster DV, and Sidor A**. NHE3 kinase A regulatory protein E3KARP binds the epithelial brush border Na+/H+ exchanger NHE3 and the cytoskeletal protein ezrin. *J Biol Chem* 273: 25856-25863, 1998.
290. **Manser E, Loo TH, Koh CG, Zhao ZS, Chen XQ, Tan L, Tan I, Leung T, and Lim L**. PAK kinases are directly coupled to the PIX family of nucleotide exchange factors. *Mol Cell* 1: 183-192, 1998.
291. **Doyonnas R, Kershaw DB, Duhme C, Merkens H, Chelliah S, Graf T, and McNagny KM**. Anuria, omphalocele, and perinatal lethality in mice lacking the CD34-related protein podocalyxin. *J Exp Med* 194: 13-27, 2001.
292. **Min SY, Ha DS, and Ha TS**. Puromycin aminonucleoside triggers apoptosis in podocytes by inducing endoplasmic reticulum stress. *Kidney Res Clin Pract* 37: 210-221, 2018.
293. **Refaeli I, Hughes MR, Wong AK, Bissonnette MLZ, Roskelley CD, Wayne Vogl A, Barbour SJ, Freedman BS, and McNagny KM**. Distinct Functional Requirements for Podocalyxin in Immature and Mature Podocytes Reveal Mechanisms of Human Kidney Disease. *Sci Rep* 10: 9419, 2020.
294. **Ichimura K, Powell R, Nakamura T, Kurihara H, Sakai T, and Obara T**. Podocalyxin regulates pronephric glomerular development in zebrafish. *Physiol Rep* 1: 2013.
295. **Galeano B, Klootwijk R, Manoli I, Sun M, Ciccone C, Darvish D, Starost MF, Zerfas PM, Hoffmann VJ, Hoogstraten-Miller S, Krasnewich DM, Gahl WA, and Huizing M**. Mutation in the key enzyme of sialic acid biosynthesis causes severe glomerular proteinuria and is rescued by N-acetylmannosamine. *J Clin Invest* 117: 1585-1594, 2007.
296. **Refaeli I, Hughes MR, and McNagny KM**. The first identified heterozygous nonsense mutations in podocalyxin offer new perspectives on the biology of podocytopathies. *Clin Sci (Lond)* 133: 443-447, 2019.
297. **Pierchala BA, Munoz MR, and Tsui CC**. Proteomic analysis of the slit diaphragm complex: CLIC5 is a protein critical for podocyte morphology and function. *Kidney Int* 78: 868-882, 2010.
298. **Casey G, Neville PJ, Liu X, Plummer SJ, Cicek MS, Krumroy LM, Curran AP, McGreevy MR, Catalona WJ, Klein EA, and Witte JS**. Podocalyxin variants and risk of prostate cancer and tumor aggressiveness. *Hum Mol Genet* 15: 735-741, 2006.
299. **Sizemore S, Cicek M, Sizemore N, Ng KP, and Casey G**. Podocalyxin increases the aggressive phenotype of breast and prostate cancer cells in vitro through its interaction with ezrin. *Cancer Res* 67: 6183-6191, 2007.
300. **Kreimann EL, Morales FC, de Orbeta-Cruz J, Takahashi Y, Adams H, Liu TJ, McCrea PD, and Georgescu MM**. Cortical stabilization of beta-catenin contributes to NHERF1/EBP50 tumor suppressor function. *Oncogene* 26: 5290-5299, 2007.
301. **Pan Y, Wang L, and Dai JL**. Suppression of breast cancer cell growth by Na+/H+ exchanger regulatory factor 1 (NHERF1). *Breast Cancer Res* 8: R63, 2006.
302. **Shibata T, Chuma M, Kokubu A, Sakamoto M, and Hirohashi S**. EBP50, a beta-catenin-associating protein, enhances Wnt signaling and is over-expressed in hepatocellular carcinoma. *Hepatology* 38: 178-186, 2003.
303. **Song J, Bai J, Yang W, Gabrielson EW, Chan DW, and Zhang Z**. Expression and clinicopathological significance of oestrogen-responsive ezrin-radixin-moesin-binding phosphoprotein 50 in breast cancer. *Histopathology* 51: 40-53, 2007.

304. **Martin-Belmonte F, and Mostov K**. Regulation of cell polarity during epithelial morphogenesis. *Curr Opin Cell Biol* 20: 227-234, 2008.
305. **Zhu L, Crothers J, Jr., Zhou R, and Forte JG**. A possible mechanism for ezrin to establish epithelial cell polarity. *Am J Physiol Cell Physiol* 299: C431-443, 2010.
306. **Economou CG, Kitsiou PV, Tzinia AK, Panagopoulou E, Marinos E, Kershaw DB, Kerjaschki D, and Tsilibary EC**. Enhanced podocalyxin expression alters the structure of podocyte basal surface. *J Cell Sci* 117: 3281-3294, 2004.
307. **Fernandez D, Horrillo A, Alquezar C, Gonzalez-Manchon C, Parrilla R, and Ayuso MS**. Control of cell adhesion and migration by podocalyxin. Implication of Rac1 and Cdc42. *Biochem Biophys Res Commun* 432: 302-307, 2013.
308. **Flores-Tellez TN, Lopez TV, Vasquez Garzon VR, and Villa-Trevino S**. Co-Expression of Ezrin-CLIC5-Podocalyxin Is Associated with Migration and Invasiveness in Hepatocellular Carcinoma. *PLoS One* 10: e0131605, 2015.
309. **Wang J, Zhao Y, Qi R, Zhu X, Huang C, Cheng S, Wang S, and Qi X**. Prognostic role of podocalyxin-like protein expression in various cancers: A systematic review and meta-analysis. *Oncotarget* 8: 52457-52464, 2017.
310. **Bryant DM, Roignot J, Datta A, Overeem AW, Kim M, Yu W, Peng X, Eastburn DJ, Ewald AJ, Werb Z, and Mostov KE**. A molecular switch for the orientation of epithelial cell polarization. *Dev Cell* 31: 171-187, 2014.
311. **Ashley RH**. Challenging accepted ion channel biology: p64 and the CLIC family of putative intracellular anion channel proteins (Review). *Mol Membr Biol* 20: 1-11, 2003.
312. **Elter A, Hartel A, Sieben C, Hertel B, Fischer-Schliebs E, Luttge U, Moroni A, and Thiel G**. A plant homolog of animal chloride intracellular channels (CLICs) generates an ion conductance in heterologous systems. *J Biol Chem* 282: 8786-8792, 2007.
313. **Littler DR, Harrop SJ, Brown LJ, Pankhurst GJ, Mynott AV, Luciani P, Mandyam RA, Mazzanti M, Tanda S, Berryman MA, Breit SN, and Curmi PM**. Comparison of vertebrate and invertebrate CLIC proteins: the crystal structures of Caenorhabditis elegans EXC-4 and Drosophila melanogaster DmCLIC. *Proteins* 71: 364-378, 2008.
314. **Berry KL, Bulow HE, Hall DH, and Hobert O**. A C. elegans CLIC-like protein required for intracellular tube formation and maintenance. *Science* 302: 2134-2137, 2003.
315. **Berry KL, and Hobert O**. Mapping functional domains of chloride intracellular channel (CLIC) proteins in vivo. *J Mol Biol* 359: 1316-1333, 2006.
316. **Littler DR, Harrop SJ, Goodchild SC, Phang JM, Mynott AV, Jiang L, Valenzuela SM, Mazzanti M, Brown LJ, Breit SN, and Curmi PM**. The enigma of the CLIC proteins: Ion channels, redox proteins, enzymes, scaffolding proteins? *FEBS Lett* 584: 2093-2101, 2010.
317. **Glickman J, Croen K, Kelly S, and Al-Awqati Q**. Golgi membranes contain an electrogenic H+ pump in parallel to a chloride conductance. *J Cell Biol* 97: 1303-1308, 1983.
318. **al-Awqati Q, Landry D, Akabas M, Redhead C, Edelman A, and Edwards J**. Purification of the epithelial Cl channel. *Adv Exp Med Biol* 290: 235-238; discussion 238-240, 1991.
319. **Landry DW, Reitman M, Cragoe EJ, Jr., and Al-Awqati Q**. Epithelial chloride channel. Development of inhibitory ligands. *J Gen Physiol* 90: 779-798, 1987.
320. **Landry DW, Akabas MH, Redhead C, Edelman A, Cragoe EJ, Jr., and Al-Awqati Q**. Purification and reconstitution of chloride channels from kidney and trachea. *Science* 244: 1469-1472, 1989.

321. **Landry D, Sullivan S, Nicolaides M, Redhead C, Edelman A, Field M, al-Awqati Q, and Edwards J**. Molecular cloning and characterization of p64, a chloride channel protein from kidney microsomes. *J Biol Chem* 268: 14948-14955, 1993.
322. **Edwards JC, Tulk B, and Schlesinger PH**. Functional expression of p64, an intracellular chloride channel protein. *J Membr Biol* 163: 119-127, 1998.
323. **Redhead CR, Edelman AE, Brown D, Landry DW, and al-Awqati Q**. A ubiquitous 64-kDa protein is a component of a chloride channel of plasma and intracellular membranes. *Proc Natl Acad Sci U S A* 89: 3716-3720, 1992.
324. **al-Awqati Q**. Chloride channels of intracellular organelles. *Curr Opin Cell Biol* 7: 504-508, 1995.
325. **Harrop SJ, DeMaere MZ, Fairlie WD, Reztsova T, Valenzuela SM, Mazzanti M, Tonini R, Qiu MR, Jankova L, Warton K, Bauskin AR, Wu WM, Pankhurst S, Campbell TJ, Breit SN, and Curmi PM**. Crystal structure of a soluble form of the intracellular chloride ion channel CLIC1 (NCC27) at 1.4-A resolution. *J Biol Chem* 276: 44993-45000, 2001.
326. **Dulhunty A, Gage P, Curtis S, Chelvanayagam G, and Board P**. The glutathione transferase structural family includes a nuclear chloride channel and a ryanodine receptor calcium release channel modulator. *J Biol Chem* 276: 3319-3323, 2001.
327. **Board PG, Coggan M, Chelvanayagam G, Easteal S, Jermiin LS, Schulte GK, Danley DE, Hoth LR, Griffor MC, Kamath AV, Rosner MH, Chrunyk BA, Perregaux DE, Gabel CA, Geoghegan KF, and Pandit J**. Identification, characterization, and crystal structure of the Omega class glutathione transferases. *J Biol Chem* 275: 24798-24806, 2000.
328. **Tulk BM, Schlesinger PH, Kapadia SA, and Edwards JC**. CLIC-1 functions as a chloride channel when expressed and purified from bacteria. *J Biol Chem* 275: 26986-26993, 2000.
329. **Tulk BM, Kapadia S, and Edwards JC**. CLIC1 inserts from the aqueous phase into phospholipid membranes, where it functions as an anion channel. *Am J Physiol Cell Physiol* 282: C1103-1112, 2002.
330. **Warton K, Tonini R, Fairlie WD, Matthews JM, Valenzuela SM, Qiu MR, Wu WM, Pankhurst S, Bauskin AR, Harrop SJ, Campbell TJ, Curmi PM, Breit SN, and Mazzanti M**. Recombinant CLIC1 (NCC27) assembles in lipid bilayers via a pH-dependent two-state process to form chloride ion channels with identical characteristics to those observed in Chinese hamster ovary cells expressing CLIC1. *J Biol Chem* 277: 26003-26011, 2002.
331. **Tonini R, Ferroni A, Valenzuela SM, Warton K, Campbell TJ, Breit SN, and Mazzanti M**. Functional characterization of the NCC27 nuclear protein in stable transfected CHO-K1 cells. *FASEB J* 14: 1171-1178, 2000.
332. **Valenzuela SM, Mazzanti M, Tonini R, Qiu MR, Warton K, Musgrove EA, Campbell TJ, and Breit SN**. The nuclear chloride ion channel NCC27 is involved in regulation of the cell cycle. *J Physiol* 529 Pt 3: 541-552, 2000.
333. **Littler DR, Harrop SJ, Fairlie WD, Brown LJ, Pankhurst GJ, Pankhurst S, DeMaere MZ, Campbell TJ, Bauskin AR, Tonini R, Mazzanti M, Breit SN, and Curmi PM**. The intracellular chloride ion channel protein CLIC1 undergoes a redox-controlled structural transition. *J Biol Chem* 279: 9298-9305, 2004.
334. **Singh H, and Ashley RH**. Redox regulation of CLIC1 by cysteine residues associated with the putative channel pore. *Biophys J* 90: 1628-1638, 2006.

335. **Cromer BA, Gorman MA, Hansen G, Adams JJ, Coggan M, Littler DR, Brown LJ, Mazzanti M, Breit SN, Curmi PM, Dulhunty AF, Board PG, and Parker MW**. Structure of the Janus protein human CLIC2. *J Mol Biol* 374: 719-731, 2007.
336. **Ueno Y, Ozaki S, Umakoshi A, Yano H, Choudhury ME, Abe N, Sumida Y, Kuwabara J, Uchida R, Islam A, Ogawa K, Ishimaru K, Yorozuya T, Kunieda T, Watanabe Y, Takada Y, and Tanaka J**. Chloride intracellular channel protein 2 in cancer and non-cancer human tissues: relationship with tight junctions. *Tissue Barriers* 7: 1593775, 2019.
337. **Lecat S, Matthes HW, Pepperkok R, Simpson JC, and Galzi JL**. A Fluorescent Live Imaging Screening Assay Based on Translocation Criteria Identifies Novel Cytoplasmic Proteins Implicated in G Protein-coupled Receptor Signaling Pathways. *Mol Cell Proteomics* 14: 1385-1399, 2015.
338. **Singh H**. Two decades with dimorphic Chloride Intracellular Channels (CLICs). *FEBS Lett* 584: 2112-2121, 2010.
339. **Kawai S, Fujii T, Shimizu T, Sukegawa K, Hashimoto I, Okumura T, Nagata T, Sakai H, and Fujii T**. Pathophysiological properties of CLIC3 chloride channel in human gastric cancer cells. *J Physiol Sci* 70: 15, 2020.
340. **Qian Z, Okuhara D, Abe MK, and Rosner MR**. Molecular cloning and characterization of a mitogen-activated protein kinase-associated intracellular chloride channel. *J Biol Chem* 274: 1621-1627, 1999.
341. **Littler DR, Assaad NN, Harrop SJ, Brown LJ, Pankhurst GJ, Luciani P, Aguilar MI, Mazzanti M, Berryman MA, Breit SN, and Curmi PM**. Crystal structure of the soluble form of the redox-regulated chloride ion channel protein CLIC4. *FEBS J* 272: 4996-5007, 2005.
342. **Singh H, and Ashley RH**. CLIC4 (p64H1) and its putative transmembrane domain form poorly selective, redox-regulated ion channels. *Mol Membr Biol* 24: 41-52, 2007.
343. **Singh H, Cousin MA, and Ashley RH**. Functional reconstitution of mammalian 'chloride intracellular channels' CLIC1, CLIC4 and CLIC5 reveals differential regulation by cytoskeletal actin. *FEBS J* 274: 6306-6316, 2007.
344. **Proutski I, Karoulias N, and Ashley RH**. Overexpressed chloride intracellular channel protein CLIC4 (p64H1) is an essential component of novel plasma membrane anion channels. *Biochem Biophys Res Commun* 297: 317-322, 2002.
345. **Berryman M, Bruno J, Price J, and Edwards JC**. CLIC-5A functions as a chloride channel in vitro and associates with the cortical actin cytoskeleton in vitro and in vivo. *J Biol Chem* 279: 34794-34801, 2004.
346. **Edwards JC, and Kapadia S**. Regulation of the bovine kidney microsomal chloride channel p64 by p59fyn, a Src family tyrosine kinase. *J Biol Chem* 275: 31826-31832, 2000.
347. **Nishizawa T, Nagao T, Iwatsubo T, Forte JG, and Urushidani T**. Molecular cloning and characterization of a novel chloride intracellular channel-related protein, parchorin, expressed in water-secreting cells. *J Biol Chem* 275: 11164-11173, 2000.
348. **Griffon N, Jeanneteau F, Prieur F, Diaz J, and Sokoloff P**. CLIC6, a member of the intracellular chloride channel family, interacts with dopamine D(2)-like receptors. *Brain Res Mol Brain Res* 117: 47-57, 2003.
349. **Friedli M, Guipponi M, Bertrand S, Bertrand D, Neerman-Arbez M, Scott HS, Antonarakis SE, and Reymond A**. Identification of a novel member of the CLIC family, CLIC6, mapping to 21q22.12. *Gene* 320: 31-40, 2003.

350. **Ponnalagu D, and Singh H**. Anion Channels of Mitochondria. *Handb Exp Pharmacol* 240: 71-101, 2017.
351. **Milton RH, Abeti R, Averaimo S, DeBiasi S, Vitellaro L, Jiang L, Curmi PM, Breit SN, Duchen MR, and Mazzanti M**. CLIC1 function is required for beta-amyloid-induced generation of reactive oxygen species by microglia. *J Neurosci* 28: 11488-11499, 2008.
352. **Ferofontov A, Strulovich R, Marom M, Giladi M, and Haitin Y**. Inherent flexibility of CLIC6 revealed by crystallographic and solution studies. *Sci Rep* 8: 6882, 2018.
353. **Littler DR, Brown LJ, Breit SN, Perrakis A, and Curmi PM**. Structure of human CLIC3 at 2 A resolution. *Proteins* 78: 1594-1600, 2010.
354. **Jentsch TJ, and Pusch M**. CLC Chloride Channels and Transporters: Structure, Function, Physiology, and Disease. *Physiol Rev* 98: 1493-1590, 2018.
355. **Jentsch TJ, Stein V, Weinreich F, and Zdebik AA**. Molecular structure and physiological function of chloride channels. *Physiol Rev* 82: 503-568, 2002.
356. **Ulmasov B, Bruno J, Oshima K, Cheng YW, Holly SP, Parise LV, Egan TM, and Edwards JC**. CLIC1 null mice demonstrate a role for CLIC1 in macrophage superoxide production and tissue injury. *Physiol Rep* 5: 2017.
357. **Olotu F, Medina-Carmona E, Serrano-Sanchez A, Ossa F, El-Hamdaoui A, Bishop OT, Ortega-Roldan JL, and Abdul-Salam VB**. Structure-based discovery and in vitro validation of inhibitors of chloride intracellular channel 4 protein. *Comput Struct Biotechnol J* 21: 688-701, 2023.
358. **Aguilera O, Quiros LM, and Fierro JF**. Transferrins selectively cause ion efflux through bacterial and artificial membranes. *FEBS Lett* 548: 5-10, 2003.
359. **de Planque MR, Raussens V, Contera SA, Rijkers DT, Liskamp RM, Ruysschaert JM, Ryan JF, Separovic F, and Watts A**. beta-Sheet structured beta-amyloid(1-40) perturbs phosphatidylcholine model membranes. *J Mol Biol* 368: 982-997, 2007.
360. **Kagan BL, Azimov R, and Azimova R**. Amyloid peptide channels. *J Membr Biol* 202: 1-10, 2004.
361. **Patel N, Ramachandran S, Azimov R, Kagan BL, and Lal R**. Ion Channel Formation by Tau Protein: Implications for Alzheimer's Disease and Tauopathies. *Biochemistry* 54: 7320-7325, 2015.
362. **Suginta W, Karoulias N, Aitken A, and Ashley RH**. Chloride intracellular channel protein CLIC4 (p64H1) binds directly to brain dynamin I in a complex containing actin, tubulin and 14-3-3 isoforms. *Biochem J* 359: 55-64, 2001.
363. **Argenzio E, and Moolenaar WH**. Emerging biological roles of Cl- intracellular channel proteins. *J Cell Sci* 129: 4165-4174, 2016.
364. **Argenzio E, Margadant C, Leyton-Puig D, Janssen H, Jalink K, Sonnenberg A, and Moolenaar WH**. CLIC4 regulates cell adhesion and beta1 integrin trafficking. *J Cell Sci* 127: 5189-5203, 2014.
365. **Stoychev SH, Nathaniel C, Fanucchi S, Brock M, Li S, Asmus K, Woods VL, Jr., and Dirr HW**. Structural dynamics of soluble chloride intracellular channel protein CLIC1 examined by amide hydrogen-deuterium exchange mass spectrometry. *Biochemistry* 48: 8413-8421, 2009.
366. **Peter B, Polyansky AA, Fanucchi S, and Dirr HW**. A Lys-Trp cation-pi interaction mediates the dimerization and function of the chloride intracellular channel protein 1 transmembrane domain. *Biochemistry* 53: 57-67, 2014.

367. **Legg-E'silva D, Achilonu I, Fanucchi S, Stoychev S, Fernandes M, and Dirr HW**. Role of arginine 29 and glutamic acid 81 interactions in the conformational stability of human chloride intracellular channel 1. *Biochemistry* 51: 7854-7862, 2012.
368. **Hare JE, Goodchild SC, Breit SN, Curmi PM, and Brown LJ**. Interaction of Human Chloride Intracellular Channel Protein 1 (CLIC1) with Lipid Bilayers: A Fluorescence Study. *Biochemistry* 55: 3825-3833, 2016.
369. **Fanucchi S, Adamson RJ, and Dirr HW**. Formation of an unfolding intermediate state of soluble chloride intracellular channel protein CLIC1 at acidic pH. *Biochemistry* 47: 11674-11681, 2008.
370. **Al Khamici H, Brown LJ, Hossain KR, Hudson AL, Sinclair-Burton AA, Ng JP, Daniel EL, Hare JE, Cornell BA, Curmi PM, Davey MW, and Valenzuela SM**. Members of the chloride intracellular ion channel protein family demonstrate glutaredoxin-like enzymatic activity. *PLoS One* 10: e115699, 2015.
371. **Valenzuela SM, Martin DK, Por SB, Robbins JM, Warton K, Bootcov MR, Schofield PR, Campbell TJ, and Breit SN**. Molecular cloning and expression of a chloride ion channel of cell nuclei. *J Biol Chem* 272: 12575-12582, 1997.
372. **Tulk BM, and Edwards JC**. NCC27, a homolog of intracellular Cl- channel p64, is expressed in brush border of renal proximal tubule. *Am J Physiol* 274: F1140-1149, 1998.
373. **Chen JI, Hannan NJ, Mak Y, Nicholls PK, Zhang J, Rainczuk A, Stanton PG, Robertson DM, Salamonsen LA, and Stephens AN**. Proteomic characterization of midproliferative and midsecretory human endometrium. *J Proteome Res* 8: 2032-2044, 2009.
374. **Qiu MR, Jiang L, Matthaei KI, Schoenwaelder SM, Kuffner T, Mangin P, Joseph JE, Low J, Connor D, Valenzuela SM, Curmi PM, Brown LJ, Mahaut-Smith M, Jackson SP, and Breit SN**. Generation and characterization of mice with null mutation of the chloride intracellular channel 1 gene. *Genesis* 48: 127-136, 2010.
375. **Salao K, Jiang L, Li H, Tsai VW, Husaini Y, Curmi PM, Brown LJ, Brown DA, and Breit SN**. CLIC1 regulates dendritic cell antigen processing and presentation by modulating phagosome acidification and proteolysis. *Biol Open* 5: 620-630, 2016.
376. **Jiang L, Salao K, Li H, Rybicka JM, Yates RM, Luo XW, Shi XX, Kuffner T, Tsai VW, Husaini Y, Wu L, Brown DA, Grewal T, Brown LJ, Curmi PM, and Breit SN**. Intracellular chloride channel protein CLIC1 regulates macrophage function through modulation of phagosomal acidification. *J Cell Sci* 125: 5479-5488, 2012.
377. **Tung JJ, Hobert O, Berryman M, and Kitajewski J**. Chloride intracellular channel 4 is involved in endothelial proliferation and morphogenesis in vitro. *Angiogenesis* 12: 209-220, 2009.
378. **Ulmasov B, Bruno J, Gordon N, Hartnett ME, and Edwards JC**. Chloride intracellular channel protein-4 functions in angiogenesis by supporting acidification of vacuoles along the intracellular tubulogenic pathway. *Am J Pathol* 174: 1084-1096, 2009.
379. **Chalothorn D, Zhang H, Smith JE, Edwards JC, and Faber JE**. Chloride intracellular channel-4 is a determinant of native collateral formation in skeletal muscle and brain. *Circ Res* 105: 89-98, 2009.
380. **Heiss NS, and Poustka A**. Genomic structure of a novel chloride channel gene, CLIC2, in Xq28. *Genomics* 45: 224-228, 1997.

381. **El-Hattab AW, Schaaf CP, Fang P, Roeder E, Kimonis VE, Church JA, Patel A, and Cheung SW**. Clinical characterization of int22h1/int22h2-mediated Xq28 duplication/deletion: new cases and literature review. *BMC Med Genet* 16: 12, 2015.
382. **Andersen EF, Baldwin EE, Ellingwood S, Smith R, and Lamb AN**. Xq28 duplication overlapping the int22h-1/int22h-2 region and including RAB39B and CLIC2 in a family with intellectual and developmental disability. *Am J Med Genet A* 164A: 1795-1801, 2014.
383. **Sugimoto K, Nishioka R, Ikeda A, Mise A, Takahashi H, Yano H, Kumon Y, Ohnishi T, and Tanaka J**. Activated microglia in a rat stroke model express NG2 proteoglycan in peri-infarct tissue through the involvement of TGF-beta1. *Glia* 62: 185-198, 2014.
384. **Burns AR, Zheng Z, Soubra SH, Chen J, and Rumbaut RE**. Transendothelial flow inhibits neutrophil transmigration through a nitric oxide-dependent mechanism: potential role for cleft shear stress. *Am J Physiol Heart Circ Physiol* 293: H2904-2910, 2007.
385. **Witham S, Takano K, Schwartz C, and Alexov E**. A missense mutation in CLIC2 associated with intellectual disability is predicted by in silico modeling to affect protein stability and dynamics. *Proteins* 79: 2444-2454, 2011.
386. **Dejana E, Orsenigo F, Molendini C, Baluk P, and McDonald DM**. Organization and signaling of endothelial cell-to-cell junctions in various regions of the blood and lymphatic vascular trees. *Cell Tissue Res* 335: 17-25, 2009.
387. **Bates DO**. Vascular endothelial growth factors and vascular permeability. *Cardiovasc Res* 87: 262-271, 2010.
388. **Martin TA, and Jiang WG**. Loss of tight junction barrier function and its role in cancer metastasis. *Biochim Biophys Acta* 1788: 872-891, 2009.
389. **Miyamoto K, Kusumi T, Sato F, Kawasaki H, Shibata S, Ohashi M, Hakamada K, Sasaki M, and Kijima H**. Decreased expression of claudin-1 is correlated with recurrence status in esophageal squamous cell carcinoma. *Biomed Res* 29: 71-76, 2008.
390. **Forster C**. Tight junctions and the modulation of barrier function in disease. *Histochem Cell Biol* 130: 55-70, 2008.
391. **Ozaki S, Umakoshi A, Yano H, Ohsumi S, Sumida Y, Hayase E, Usa E, Islam A, Choudhury ME, Nishi Y, Yamashita D, Ohtsuka Y, Nishikawa M, Inoue A, Suehiro S, Kuwabara J, Watanabe H, Takada Y, Watanabe Y, Nakano I, Kunieda T, and Tanaka J**. Chloride intracellular channel protein 2 is secreted and inhibits MMP14 activity, while preventing tumor cell invasion and metastasis. *Neoplasia* 23: 754-765, 2021.
392. **Miyazaki H, Shiozaki A, Niisato N, Ohsawa R, Itoi H, Ueda Y, Otsuji E, Yamagishi H, Iwasaki Y, Nakano T, Nakahari T, and Marunaka Y**. Chloride ions control the G1/S cell-cycle checkpoint by regulating the expression of p21 through a p53-independent pathway in human gastric cancer cells. *Biochem Biophys Res Commun* 366: 506-512, 2008.
393. **Hiraoka K, Miyazaki H, Niisato N, Iwasaki Y, Kawauchi A, Miki T, and Marunaka Y**. Chloride ion modulates cell proliferation of human androgen-independent prostatic cancer cell. *Cell Physiol Biochem* 25: 379-388, 2010.
394. **Dozynkiewicz MA, Jamieson NB, Macpherson I, Grindlay J, van den Berghe PV, von Thun A, Morton JP, Gourley C, Timpson P, Nixon C, McKay CJ, Carter R, Strachan D, Anderson K, Sansom OJ, Caswell PT, and Norman JC**. Rab25 and CLIC3 collaborate to promote integrin recycling from late endosomes/lysosomes and drive cancer progression. *Dev Cell* 22: 131-145, 2012.

395. **Chen M, Zhang S, Wen X, Cao H, and Gao Y**. Prognostic value of CLIC3 mRNA overexpression in bladder cancer. *PeerJ* 8: e8348, 2020.
396. **Kim KH, Choi BK, Song KM, Cha KW, Kim YH, Lee H, Han IS, and Kwon BS**. CRIg signals induce anti-intracellular bacterial phagosome activity in a chloride intracellular channel 3-dependent manner. *Eur J Immunol* 43: 667-678, 2013.
397. **Murthi P, Stevenson JL, Money TT, Borg AJ, Brennecke SP, and Gude NM**. Placental CLIC3 is increased in fetal growth restriction and pre-eclampsia affected human pregnancies. *Placenta* 33: 741-744, 2012.
398. **Gronich N, Kumar A, Zhang Y, Efimov IR, and Soldatov NM**. Molecular remodeling of ion channels, exchangers and pumps in atrial and ventricular myocytes in ischemic cardiomyopathy. *Channels (Austin)* 4: 101-107, 2010.
399. **Duncan RR, Westwood PK, Boyd A, and Ashley RH**. Rat brain p64H1, expression of a new member of the p64 chloride channel protein family in endoplasmic reticulum. *J Biol Chem* 272: 23880-23886, 1997.
400. **Chuang JZ, Chou SY, and Sung CH**. Chloride intracellular channel 4 is critical for the epithelial morphogenesis of RPE cells and retinal attachment. *Mol Biol Cell* 21: 3017-3028, 2010.
401. **Chou SY, Hsu KS, Otsu W, Hsu YC, Luo YC, Yeh C, Shehab SS, Chen J, Shieh V, He GA, Marean MB, Felsen D, Ding A, Poppas DP, Chuang JZ, and Sung CH**. CLIC4 regulates apical exocytosis and renal tube luminogenesis through retromer- and actin-mediated endocytic trafficking. *Nat Commun* 7: 10412, 2016.
402. **Padmakumar V, Masiuk KE, Luger D, Lee C, Coppola V, Tessarollo L, Hoover SB, Karavanova I, Buonanno A, Simpson RM, and Yuspa SH**. Detection of differential fetal and adult expression of chloride intracellular channel 4 (CLIC4) protein by analysis of a green fluorescent protein knock-in mouse line. *BMC Dev Biol* 14: 24, 2014.
403. **Fernandez-Salas E, Sagar M, Cheng C, Yuspa SH, and Weinberg WC**. p53 and tumor necrosis factor alpha regulate the expression of a mitochondrial chloride channel protein. *J Biol Chem* 274: 36488-36497, 1999.
404. **Suh KS, Mutoh M, Mutoh T, Li L, Ryscavage A, Crutchley JM, Dumont RA, Cheng C, and Yuspa SH**. CLIC4 mediates and is required for Ca2+-induced keratinocyte differentiation. *J Cell Sci* 120: 2631-2640, 2007.
405. **Suh KS, Mutoh M, Gerdes M, and Yuspa SH**. CLIC4, an intracellular chloride channel protein, is a novel molecular target for cancer therapy. *J Investig Dermatol Symp Proc* 10: 105-109, 2005.
406. **Bonilha VL, Rayborn ME, Saotome I, McClatchey AI, and Hollyfield JG**. Microvilli defects in retinas of ezrin knockout mice. *Exp Eye Res* 82: 720-729, 2006.
407. **Tung JJ, and Kitajewski J**. Chloride intracellular channel 1 functions in endothelial cell growth and migration. *J Angiogenes Res* 2: 23, 2010.
408. **Edwards JC, Bruno J, Key P, and Cheng YW**. Absence of chloride intracellular channel 4 (CLIC4) predisposes to acute kidney injury but has minimal impact on recovery. *BMC Nephrol* 15: 54, 2014.
409. **Rodriguez C, Gonzalez-Diez M, Badimon L, and Martinez-Gonzalez J**. Sphingosine-1-phosphate: A bioactive lipid that confers high-density lipoprotein with vasculoprotection mediated by nitric oxide and prostacyclin. *Thromb Haemost* 101: 665-673, 2009.

410. **Mendelson K, Evans T, and Hla T**. Sphingosine 1-phosphate signalling. *Development* 141: 5-9, 2014.
411. **Mao Y, Kleinjan ML, Jilishitz I, Swaminathan B, Obinata H, Komarova YA, Bayless KJ, Hla T, and Kitajewski JK**. CLIC1 and CLIC4 mediate endothelial S1P receptor signaling to facilitate Rac1 and RhoA activity and function. *Sci Signal* 14: 2021.
412. **Fernandez-Salas E, Suh KS, Speransky VV, Bowers WL, Levy JM, Adams T, Pathak KR, Edwards LE, Hayes DD, Cheng C, Steven AC, Weinberg WC, and Yuspa SH**. mtCLIC/CLIC4, an organellular chloride channel protein, is increased by DNA damage and participates in the apoptotic response to p53. *Mol Cell Biol* 22: 3610-3620, 2002.
413. **Yokoyama R, Kubota A, Kojima H, Tanaka T, Mutoh M, and Terasaki M**. Detection of Cells Displaying High Expression of CLIC4 in Tumor Tissue of Patients With Colorectal Cancer. *In Vivo* 35: 3165-3173, 2021.
414. **Ponsioen B, van Zeijl L, Langeslag M, Berryman M, Littler D, Jalink K, and Moolenaar WH**. Spatiotemporal regulation of chloride intracellular channel protein CLIC4 by RhoA. *Mol Biol Cell* 20: 4664-4672, 2009.
415. **Strippoli P, D'Addabbo P, Lenzi L, Giannone S, Canaider S, Casadei R, Vitale L, Carinci P, and Zannotti M**. Segmental paralogy in the human genome: a large-scale triplication on 1p, 6p, and 21q. *Mamm Genome* 13: 456-462, 2002.
416. **Hattori M, Fujiyama A, Taylor TD, Watanabe H, Yada T, Park HS, Toyoda A, Ishii K, Totoki Y, Choi DK, Groner Y, Soeda E, Ohki M, Takagi T, Sakaki Y, Taudien S, Blechschmidt K, Polley A, Menzel U, Delabar J, Kumpf K, Lehmann R, Patterson D, Reichwald K, Rump A, Schillhabel M, Schudy A, Zimmermann W, Rosenthal A, Kudoh J, Schibuya K, Kawasaki K, Asakawa S, Shintani A, Sasaki T, Nagamine K, Mitsuyama S, Antonarakis SE, Minoshima S, Shimizu N, Nordsiek G, Hornischer K, Brant P, Scharfe M, Schon O, Desario A, Reichelt J, Kauer G, Blocker H, Ramser J, Beck A, Klages S, Hennig S, Riesselmann L, Dagand E, Haaf T, Wehrmeyer S, Borzym K, Gardiner K, Nizetic D, Francis F, Lehrach H, Reinhardt R, Yaspo ML, Chromosome m, and sequencing c**. The DNA sequence of human chromosome 21. *Nature* 405: 311-319, 2000.
417. **Loyo-Celis V, Patel D, Sanghvi S, Kaur K, Ponnalagu D, Zheng Y, Bindra S, Bhachu HR, Deschenes I, Gururaja Rao S, and Singh H**. Biophysical characterization of chloride intracellular channel 6 (CLIC6). *J Biol Chem* 299: 105349, 2023.
418. **Urushidani T, Chow D, and Forte JG**. Redistribution of a 120 kDa phosphoprotein in the parietal cell associated with stimulation. *J Membr Biol* 168: 209-220, 1999.
419. **Schlesinger PH, Blair HC, Teitelbaum SL, and Edwards JC**. Characterization of the osteoclast ruffled border chloride channel and its role in bone resorption. *J Biol Chem* 272: 18636-18643, 1997.
420. **Edwards JC, Cohen C, Xu W, and Schlesinger PH**. c-Src control of chloride channel support for osteoclast HCl transport and bone resorption. *J Biol Chem* 281: 28011-28022, 2006.
421. **Forgac M**. Vacuolar ATPases: rotary proton pumps in physiology and pathophysiology. *Nat Rev Mol Cell Biol* 8: 917-929, 2007.
422. **Berryman M, and Bretscher A**. Identification of a novel member of the chloride intracellular channel gene family (CLIC5) that associates with the actin cytoskeleton of placental microvilli. *Mol Biol Cell* 11: 1509-1521, 2000.
423. **Chabardes-Garonne D, Mejean A, Aude JC, Cheval L, Di Stefano A, Gaillard MC, Imbert-Teboul M, Wittner M, Balian C, Anthouard V, Robert C, Segurens B, Wincker P,**

Weissenbach J, Doucet A, and Elalouf JM. A panoramic view of gene expression in the human kidney. *Proc Natl Acad Sci U S A* 100: 13710-13715, 2003.
424. **Shanks RA, Larocca MC, Berryman M, Edwards JC, Urushidani T, Navarre J, and Goldenring JR**. AKAP350 at the Golgi apparatus. II. Association of AKAP350 with a novel chloride intracellular channel (CLIC) family member. *J Biol Chem* 277: 40973-40980, 2002.
425. **Gagnon LH, Longo-Guess CM, Berryman M, Shin JB, Saylor KW, Yu H, Gillespie PG, and Johnson KR**. The chloride intracellular channel protein CLIC5 is expressed at high levels in hair cell stereocilia and is essential for normal inner ear function. *J Neurosci* 26: 10188-10198, 2006.
426. **Kim J-S**. The translocation of CLIC5A to membranes as a peripheral protein. In: *Medicine*. Edmonton, Alberta: University of Alberta, 2018, p. 150.
427. **Frolenkov GI, Belyantseva IA, Friedman TB, and Griffith AJ**. Genetic insights into the morphogenesis of inner ear hair cells. *Nat Rev Genet* 5: 489-498, 2004.
428. **Salles FT, Andrade LR, Tanda S, Grati M, Plona KL, Gagnon LH, Johnson KR, Kachar B, and Berryman MA**. CLIC5 stabilizes membrane-actin filament linkages at the base of hair cell stereocilia in a molecular complex with radixin, taperin, and myosin VI. *Cytoskeleton (Hoboken)* 71: 61-78, 2014.
429. **Seco CZ, Oonk AM, Dominguez-Ruiz M, Draaisma JM, Gandia M, Oostrik J, Neveling K, Kunst HP, Hoefsloot LH, del Castillo I, Pennings RJ, Kremer H, Admiraal RJ, and Schraders M**. Progressive hearing loss and vestibular dysfunction caused by a homozygous nonsense mutation in CLIC5. *Eur J Hum Genet* 23: 189-194, 2015.
430. **Yasuda K, Park HC, Ratliff B, Addabbo F, Hatzopoulos AK, Chander P, and Goligorsky MS**. Adriamycin nephropathy: a failure of endothelial progenitor cell-induced repair. *Am J Pathol* 176: 1685-1695, 2010.
431. **Schenk J, and McNeill JH**. The pathogenesis of DOCA-salt hypertension. *J Pharmacol Toxicol Methods* 27: 161-170, 1992.
432. **Li Y, Pohl E, Boulouiz R, Schraders M, Nurnberg G, Charif M, Admiraal RJ, von Ameln S, Baessmann I, Kandil M, Veltman JA, Nurnberg P, Kubisch C, Barakat A, Kremer H, and Wollnik B**. Mutations in TPRN cause a progressive form of autosomal-recessive nonsyndromic hearing loss. *Am J Hum Genet* 86: 479-484, 2010.
433. **Rehman AU, Morell RJ, Belyantseva IA, Khan SY, Boger ET, Shahzad M, Ahmed ZM, Riazuddin S, Khan SN, Riazuddin S, and Friedman TB**. Targeted capture and next-generation sequencing identifies C9orf75, encoding taperin, as the mutated gene in nonsyndromic deafness DFNB79. *Am J Hum Genet* 86: 378-388, 2010.
434. **Ferrar T, Chamousset D, De Wever V, Nimick M, Andersen J, Trinkle-Mulcahy L, and Moorhead GB**. Taperin (c9orf75), a mutated gene in nonsyndromic deafness, encodes a vertebrate specific, nuclear localized protein phosphatase one alpha (PP1alpha) docking protein. *Biol Open* 1: 128-139, 2012.
435. **Lehner B, Semple JI, Brown SE, Counsell D, Campbell RD, and Sanderson CM**. Analysis of a high-throughput yeast two-hybrid system and its use to predict the function of intracellular proteins encoded within the human MHC class III region. *Genomics* 83: 153-167, 2004.
436. **Moorhead GB, Trinkle-Mulcahy L, Nimick M, De Wever V, Campbell DG, Gourlay R, Lam YW, and Lamond AI**. Displacement affinity chromatography of protein phosphatase one (PP1) complexes. *BMC Biochem* 9: 28, 2008.

437. **Lim DJ, and Anniko M**. Developmental morphology of the mouse inner ear. A scanning electron microscopic observation. *Acta Otolaryngol Suppl* 422: 1-69, 1985.
438. **Zuo J**. Transgenic and gene targeting studies of hair cell function in mouse inner ear. *J Neurobiol* 53: 286-305, 2002.
439. **Goodyear R, and Richardson G**. Distribution of the 275 kD hair cell antigen and cell surface specialisations on auditory and vestibular hair bundles in the chicken inner ear. *J Comp Neurol* 325: 243-256, 1992.
440. **Hasson T**. Unconventional myosins, the basis for deafness in mouse and man. *Am J Hum Genet* 61: 801-805, 1997.
441. **Hasson T, Gillespie PG, Garcia JA, MacDonald RB, Zhao Y, Yee AG, Mooseker MS, and Corey DP**. Unconventional myosins in inner-ear sensory epithelia. *J Cell Biol* 137: 1287-1307, 1997.
442. **Sakaguchi H, Tokita J, Naoz M, Bowen-Pope D, Gov NS, and Kachar B**. Dynamic compartmentalization of protein tyrosine phosphatase receptor Q at the proximal end of stereocilia: implication of myosin VI-based transport. *Cell Motil Cytoskeleton* 65: 528-538, 2008.
443. **Goodyear RJ, Legan PK, Wright MB, Marcotti W, Oganesian A, Coats SA, Booth CJ, Kros CJ, Seifert RA, Bowen-Pope DF, and Richardson GP**. A receptor-like inositol lipid phosphatase is required for the maturation of developing cochlear hair bundles. *J Neurosci* 23: 9208-9219, 2003.
444. **Self T, Sobe T, Copeland NG, Jenkins NA, Avraham KB, and Steel KP**. Role of myosin VI in the differentiation of cochlear hair cells. *Dev Biol* 214: 331-341, 1999.
445. **Liu C, Luo N, Tung CY, Perrin BJ, and Zhao B**. GRXCR2 Regulates Taperin Localization Critical for Stereocilia Morphology and Hearing. *Cell Rep* 25: 1268-1280 e1264, 2018.
446. **Gluzman Y**. SV40-transformed simian cells support the replication of early SV40 mutants. *Cell* 23: 175-182, 1981.
447. **Shaw G, Morse S, Ararat M, and Graham FL**. Preferential transformation of human neuronal cells by human adenoviruses and the origin of HEK 293 cells. *FASEB J* 16: 869-871, 2002.
448. **Hsu SH, Schacter BZ, Delaney NL, Miller TB, McKusick VA, Kennett RH, Bodmer JG, Young D, and Bodmer WF**. Genetic characteristics of the HeLa cell. *Science* 191: 392-394, 1976.
449. **Pabst R, and Sterzel RB**. Cell renewal of glomerular cell types in normal rats. An autoradiographic analysis. *Kidney Int* 24: 626-631, 1983.
450. **Sakairi T, Abe Y, Kajiyama H, Bartlett LD, Howard LV, Jat PS, and Kopp JB**. Conditionally immortalized human podocyte cell lines established from urine. *Am J Physiol Renal Physiol* 298: F557-567, 2010.
451. **Mundel P, Reiser J, Zuniga Mejia Borja A, Pavenstadt H, Davidson GR, Kriz W, and Zeller R**. Rearrangements of the cytoskeleton and cell contacts induce process formation during differentiation of conditionally immortalized mouse podocyte cell lines. *Exp Cell Res* 236: 248-258, 1997.
452. **Jat PS, Noble MD, Ataliotis P, Tanaka Y, Yannoutsos N, Larsen L, and Kioussis D**. Direct derivation of conditionally immortal cell lines from an H-2Kb-tsA58 transgenic mouse. *Proc Natl Acad Sci U S A* 88: 5096-5100, 1991.

453. **Truett GE, Heeger P, Mynatt RL, Truett AA, Walker JA, and Warman ML**. Preparation of PCR-quality mouse genomic DNA with hot sodium hydroxide and tris (HotSHOT). *Biotechniques* 29: 52, 54, 2000.
454. **Harlow EL, D.** . *Antibodies, A Laboratory Manual*. Cold Spring Harbor, NY: Cold Spring Harbor Laboratory Press, 1988, p. 74.
455. **Li L, Kozlowski K, Wegner B, Rashid T, Yeung T, Holmes C, and Ballermann BJ**. Phosphorylation of TIMAP by glycogen synthase kinase-3beta activates its associated protein phosphatase 1. *J Biol Chem* 282: 25960-25969, 2007.
456. **Burbelo PD, Drechsel D, and Hall A**. A conserved binding motif defines numerous candidate target proteins for both Cdc42 and Rac GTPases. *J Biol Chem* 270: 29071-29074, 1995.
457. **Rops AL, van der Vlag J, Jacobs CW, Dijkman HB, Lensen JF, Wijnhoven TJ, van den Heuvel LP, van Kuppevelt TH, and Berden JH**. Isolation and characterization of conditionally immortalized mouse glomerular endothelial cell lines. *Kidney Int* 66: 2193-2201, 2004.
458. **Pelham HR, and Jackson RJ**. An efficient mRNA-dependent translation system from reticulocyte lysates. *Eur J Biochem* 67: 247-256, 1976.
459. **Lamb RF, Ozanne BW, Roy C, McGarry L, Stipp C, Mangeat P, and Jay DG**. Essential functions of ezrin in maintenance of cell shape and lamellipodial extension in normal and transformed fibroblasts. *Curr Biol* 7: 682-688, 1997.
460. **Schwartz-Albiez R, Merling A, Spring H, Moller P, and Koretz K**. Differential expression of the microspike-associated protein moesin in human tissues. *Eur J Cell Biol* 67: 189-198, 1995.
461. **Takeuchi K, Sato N, Kasahara H, Funayama N, Nagafuchi A, Yonemura S, Tsukita S, and Tsukita S**. Perturbation of cell adhesion and microvilli formation by antisense oligonucleotides to ERM family members. *J Cell Biol* 125: 1371-1384, 1994.
462. **Jiang L, Phang JM, Yu J, Harrop SJ, Sokolova AV, Duff AP, Wilk KE, Alkhamici H, Breit SN, Valenzuela SM, Brown LJ, and Curmi PM**. CLIC proteins, ezrin, radixin, moesin and the coupling of membranes to the actin cytoskeleton: a smoking gun? *Biochim Biophys Acta* 1838: 643-657, 2014.
463. **Briggs JW, Ren L, Nguyen R, Chakrabarti K, Cassavaugh J, Rahim S, Bulut G, Zhou M, Veenstra TD, Chen Q, Wei JS, Khan J, Uren A, and Khanna C**. The ezrin metastatic phenotype is associated with the initiation of protein translation. *Neoplasia* 14: 297-310, 2012.
464. **Hirao M, Sato N, Kondo T, Yonemura S, Monden M, Sasaki T, Takai Y, Tsukita S, and Tsukita S**. Regulation mechanism of ERM (ezrin/radixin/moesin) protein/plasma membrane association: possible involvement of phosphatidylinositol turnover and Rho-dependent signaling pathway. *J Cell Biol* 135: 37-51, 1996.
465. **Ishihara H, Martin BL, Brautigan DL, Karaki H, Ozaki H, Kato Y, Fusetani N, Watabe S, Hashimoto K, Uemura D, and et al.** Calyculin A and okadaic acid: inhibitors of protein phosphatase activity. *Biochem Biophys Res Commun* 159: 871-877, 1989.
466. **Tamaoki T, Nomoto H, Takahashi I, Kato Y, Morimoto M, and Tomita F**. Staurosporine, a potent inhibitor of phospholipid/Ca++dependent protein kinase. *Biochem Biophys Res Commun* 135: 397-402, 1986.
467. **Tamaoki T**. Use and specificity of staurosporine, UCN-01, and calphostin C as protein kinase inhibitors. *Methods Enzymol* 201: 340-347, 1991.

468. **Bae YS, Lee TG, Park JC, Hur JH, Kim Y, Heo K, Kwak JY, Suh PG, and Ryu SH**. Identification of a compound that directly stimulates phospholipase C activity. *Mol Pharmacol* 63: 1043-1050, 2003.
469. **Wills RC, and Hammond GRV**. PI(4,5)P2: signaling the plasma membrane. *Biochem J* 479: 2311-2325, 2022.
470. **Fan HY, and Heerklotz H**. Digitonin does not flip across cholesterol-poor membranes. *J Colloid Interface Sci* 504: 283-293, 2017.
471. **Hossain KR, Holt SA, Le Brun AP, Al Khamici H, and Valenzuela SM**. X-ray and Neutron Reflectivity Study Shows That CLIC1 Undergoes Cholesterol-Dependent Structural Reorganization in Lipid Monolayers. *Langmuir* 33: 12497-12509, 2017.
472. **Heasman SJ, and Ridley AJ**. Mammalian Rho GTPases: new insights into their functions from in vivo studies. *Nat Rev Mol Cell Biol* 9: 690-701, 2008.
473. **Kistler AD, Altintas MM, and Reiser J**. Podocyte GTPases regulate kidney filter dynamics. *Kidney Int* 81: 1053-1055, 2012.
474. **Gee HY, Saisawat P, Ashraf S, Hurd TW, Vega-Warner V, Fang H, Beck BB, Gribouval O, Zhou W, Diaz KA, Natarajan S, Wiggins RC, Lovric S, Chernin G, Schoeb DS, Ovunc B, Frishberg Y, Soliman NA, Fathy HM, Goebel H, Hoefele J, Weber LT, Innis JW, Faul C, Han Z, Washburn J, Antignac C, Levy S, Otto EA, and Hildebrandt F**. ARHGDIA mutations cause nephrotic syndrome via defective RHO GTPase signaling. *J Clin Invest* 123: 3243-3253, 2013.
475. **Gupta IR, Baldwin C, Auguste D, Ha KC, El Andalousi J, Fahiminiya S, Bitzan M, Bernard C, Akbari MR, Narod SA, Rosenblatt DS, Majewski J, and Takano T**. ARHGDIA: a novel gene implicated in nephrotic syndrome. *J Med Genet* 50: 330-338, 2013.
476. **Blattner SM, Hodgin JB, Nishio M, Wylie SA, Saha J, Soofi AA, Vining C, Randolph A, Herbach N, Wanke R, Atkins KB, Gyung Kang H, Henger A, Brakebusch C, Holzman LB, and Kretzler M**. Divergent functions of the Rho GTPases Rac1 and Cdc42 in podocyte injury. *Kidney Int* 84: 920-930, 2013.
477. **Wu H, Yang L, Liao D, Chen Y, Wang W, and Fang J**. Podocalyxin regulates astrocytoma cell invasion and survival against temozolomide. *Exp Ther Med* 5: 1025-1029, 2013.
478. **Frose J, Chen MB, Hebron KE, Reinhardt F, Hajal C, Zijlstra A, Kamm RD, and Weinberg RA**. Epithelial-Mesenchymal Transition Induces Podocalyxin to Promote Extravasation via Ezrin Signaling. *Cell Rep* 24: 962-972, 2018.
479. **Itai S, Ohishi T, Kaneko MK, Yamada S, Abe S, Nakamura T, Yanaka M, Chang YW, Ohba SI, Nishioka Y, Kawada M, Harada H, and Kato Y**. Anti-podocalyxin antibody exerts antitumor effects via antibody-dependent cellular cytotoxicity in mouse xenograft models of oral squamous cell carcinoma. *Oncotarget* 9: 22480-22497, 2018.
480. **Weernink PA, Meletiadis K, Hommeltenberg S, Hinz M, Ishihara H, Schmidt M, and Jakobs KH**. Activation of type I phosphatidylinositol 4-phosphate 5-kinase isoforms by the Rho GTPases, RhoA, Rac1, and Cdc42. *J Biol Chem* 279: 7840-7849, 2004.
481. **van den Bout I, and Divecha N**. PIP5K-driven PtdIns(4,5)P2 synthesis: regulation and cellular functions. *J Cell Sci* 122: 3837-3850, 2009.
482. **Auvinen E, Kivi N, and Vaheri A**. Regulation of ezrin localization by Rac1 and PIPK in human epithelial cells. *Exp Cell Res* 313: 824-833, 2007.

483. **Sasaki T, and Takai Y**. The Rho small G protein family-Rho GDI system as a temporal and spatial determinant for cytoskeletal control. *Biochem Biophys Res Commun* 245: 641-645, 1998.
484. **Manser E, Leung T, Salihuddin H, Zhao ZS, and Lim L**. A brain serine/threonine protein kinase activated by Cdc42 and Rac1. *Nature* 367: 40-46, 1994.
485. **Bokoch GM**. Biology of the p21-activated kinases. *Annu Rev Biochem* 72: 743-781, 2003.
486. **Etienne-Manneville S, and Hall A**. Rho GTPases in cell biology. *Nature* 420: 629-635, 2002.
487. **Ren XD, and Schwartz MA**. Regulation of inositol lipid kinases by Rho and Rac. *Curr Opin Genet Dev* 8: 63-67, 1998.
488. **Shibasaki Y, Ishihara H, Kizuki N, Asano T, Oka Y, and Yazaki Y**. Massive actin polymerization induced by phosphatidylinositol-4-phosphate 5-kinase in vivo. *J Biol Chem* 272: 7578-7581, 1997.
489. **Hartwig JH, Bokoch GM, Carpenter CL, Janmey PA, Taylor LA, Toker A, and Stossel TP**. Thrombin receptor ligation and activated Rac uncap actin filament barbed ends through phosphoinositide synthesis in permeabilized human platelets. *Cell* 82: 643-653, 1995.
490. **Weernink PA, Guo Y, Zhang C, Schmidt M, Von Eichel-Streiber C, and Jakobs KH**. Control of cellular phosphatidylinositol 4,5-bisphosphate levels by adhesion signals and rho GTPases in NIH 3T3 fibroblasts involvement of both phosphatidylinositol-4-phosphate 5-kinase and phospholipase C. *Eur J Biochem* 267: 5237-5246, 2000.
491. **Amano M, Chihara K, Kimura K, Fukata Y, Nakamura N, Matsuura Y, and Kaibuchi K**. Formation of actin stress fibers and focal adhesions enhanced by Rho-kinase. *Science* 275: 1308-1311, 1997.
492. **Hodge RG, and Ridley AJ**. Regulating Rho GTPases and their regulators. *Nat Rev Mol Cell Biol* 17: 496-510, 2016.
493. **Zhao B, Wu Z, and Muller U**. Murine Fam65b forms ring-like structures at the base of stereocilia critical for mechanosensory hair cell function. *Elife* 5: 2016.
494. **Kao SC, Chen CY, Wang SL, Yang JJ, Hung WC, Chen YC, Lai NS, Liu HT, Huang HL, Chen HC, Lin TH, and Huang HB**. Identification of phostensin, a PP1 F-actin cytoskeleton targeting subunit. *Biochem Biophys Res Commun* 356: 594-598, 2007.
495. **Lai NS, Wang TF, Wang SL, Chen CY, Yen JY, Huang HL, Li C, Huang KY, Liu SQ, Lin TH, and Huang HB**. Phostensin caps to the pointed end of actin filaments and modulates actin dynamics. *Biochem Biophys Res Commun* 387: 676-681, 2009.
496. **Virshup DM, and Shenolikar S**. From promiscuity to precision: protein phosphatases get a makeover. *Mol Cell* 33: 537-545, 2009.
497. **Shi Y**. Serine/threonine phosphatases: mechanism through structure. *Cell* 139: 468-484, 2009.
498. **Moorhead GB, De Wever V, Templeton G, and Kerk D**. Evolution of protein phosphatases in plants and animals. *Biochem J* 417: 401-409, 2009.
499. **Hendrickx A, Beullens M, Ceulemans H, Den Abt T, Van Eynde A, Nicolaescu E, Lesage B, and Bollen M**. Docking motif-guided mapping of the interactome of protein phosphatase-1. *Chem Biol* 16: 365-371, 2009.

500. **Nasa I, Moorhead GB, and Kettenbach AN**. Use of Mitotic Protein Kinase Inhibitors and Phospho-Specific Antibodies to Monitor Protein Phosphorylation During the Cell Cycle. *Methods Mol Biol* 2329: 205-221, 2021.
501. **Hernandez-Fernaud JR, Ruengeler E, Casazza A, Neilson LJ, Pulleine E, Santi A, Ismail S, Lilla S, Dhayade S, MacPherson IR, McNeish I, Ennis D, Ali H, Kugeratski FG, Al Khamici H, van den Biggelaar M, van den Berghe PV, Cloix C, McDonald L, Millan D, Hoyle A, Kuchnio A, Carmeliet P, Valenzuela SM, Blyth K, Yin H, Mazzone M, Norman JC, and Zanivan S**. Secreted CLIC3 drives cancer progression through its glutathione-dependent oxidoreductase activity. *Nat Commun* 8: 14206, 2017.
502. **Weerapana E, Simon GM, and Cravatt BF**. Disparate proteome reactivity profiles of carbon electrophiles. *Nat Chem Biol* 4: 405-407, 2008.
503. **Braude JP, Vijayakumar S, Baumgarner K, Laurine R, Jones TA, Jones SM, and Pyott SJ**. Deletion of Shank1 has minimal effects on the molecular composition and function of glutamatergic afferent postsynapses in the mouse inner ear. *Hear Res* 321: 52-64, 2015.
504. **Dobrinskikh E, Lewis L, Brian Doctor R, Okamura K, Lee MG, Altmann C, Faubel S, Kopp JB, and Blaine J**. Shank2 Regulates Renal Albumin Endocytosis. *Physiol Rep* 3: 2015.
505. **Sarowar T, and Grabrucker AM**. Actin-Dependent Alterations of Dendritic Spine Morphology in Shankopathies. *Neural Plast* 2016: 8051861, 2016.
506. **Carbonetto S**. A blueprint for research on Shankopathies: a view from research on autism spectrum disorder. *Dev Neurobiol* 74: 85-112, 2014.
507. **Park E, Na M, Choi J, Kim S, Lee JR, Yoon J, Park D, Sheng M, and Kim E**. The Shank family of postsynaptic density proteins interacts with and promotes synaptic accumulation of the beta PIX guanine nucleotide exchange factor for Rac1 and Cdc42. *J Biol Chem* 278: 19220-19229, 2003.
508. **Lee JS, Lee YM, Kim JY, Park HW, Grinstein S, Orlowski J, Kim E, Kim KH, and Lee MG**. BetaPix up-regulates Na+/H+ exchanger 3 through a Shank2-mediated protein-protein interaction. *J Biol Chem* 285: 8104-8113, 2010.
509. **Staruschenko A, and Sorokin A**. Role of betaPix in the Kidney. *Front Physiol* 3: 154, 2012.

Appendices

1. Multiple sequence alignment of human ezrin, human radixin and human moesin

```
CLUSTAL O(1.2.4) multiple sequence alignment


Ezrin       MPKPINVRVTTMDAELEFAIQPNTTGKQLFDQVVKTIGLREVWYFGLHYVDNKGFPTWLK      60
Radixin     MPKPINVRVTTMDAELEFAIQPNTTGKQLFDQVVKTVGLREVWFFGLQYVDSKGYSTWLK      60
Moesin      MPKTISVRVTTMDAELEFAIQPNTTGKQLFDQVVKTIGLREVWFFGLQYQDTKGFSTWLK      60
            *** *.*******************************:******:***:* *.**: ****

Ezrin       LDKKVSAQEVRKENPLQFKFRAKFYPEDVAEELIQDITQKLFFLQVKEGILSDEIYCPPE      120
Radixin     LNKKVTQQDVKKENPLQFKFRAKFFPEDVSEELIQEITQRLFFLQVKEAILNDEIYCPPE      120
Moesin      LNKKVTAQDVRKESPLLFKFRAKFYPEDVSEELIQDITQRLFFLQVKEGILNDDIYCPPE      120
            *:***: *:*:**.** *******:****:*****:***:********.**.*:******

Ezrin       TAVLLGSYAVQAKFGDYNKEVHKSGYLSSERLIPQRVMDQHKLTRDQWEDRIQVWHAEHR      180
Radixin     TAVLLASYAVQAKYGDYNKEIHKPGYLANDRLLPQRVLEQHKLTKEQWEERIQNWHEEHR      180
Moesin      TAVLLASYAVQSKYGDFNKEVHKSGYLAGDKLLPQRVLEQHKLNKDQWEERIQVWHEEHR      180
            *****.*****:*:**:***:** ***:.::*:****::****.::***:*** ** ***

Ezrin       GMLKDNAMLEYLKIAQDLEMYGINYFEIKNKKGTDLWLGVDALGLNIYEKDDKLTPKIGF      240
Radixin     GMLREDSMMEYLKIAQDLEMYGVNYFEIKNKKGTELWLGVDALGLNIYEHDDKLTPKIGF      240
Moesin      GMLREDAVLEYLKIAQDLEMYGVNYFSIKNKKGSELWLGVDALGLNIYEQNDRLTPKIGF      240
            ***::::::**************:***.******::***************::*:*******

Ezrin       PWSEIRNISFNDKKFVIKPIDKKAPDFVFYAPRLRINKRILQLCMGNHELYMRRRKPDTI      300
Radixin     PWSEIRNISFNDKKFVIKPIDKKAPDFVFYAPRLRINKRILALCMGNHELYMRRRKPDTI      300
Moesin      PWSEIRNISFNDKKFVIKPIDKKAPDFVFYAPRLRINKRILALCMGNHELYMRRRKPDTI      300
            **************************************** ******************

Ezrin       EVQQMKAQAREEKHQKQLERQQLETEKKRRETVEREKEQMMREKEELMLRLQDYEEKTKK      360
Radixin     EVQQMKAQAREEKHQKQLERAQLENEKEKREIAEKEKERIEREKEELMERLKQIEEQTIK      360
Moesin      EVQQMKAQAREEKHQKQMERAMLENEKKKREMAEKEKEKIEREKEELMERLKQIEEQTKK      360
            *****************:**  **.**::** .*:***:: ******* **:: **:* *

Ezrin       AERELSEQIQRALQLEEERKRAQEEAERLEADRMAALRAKEELERQAVDQIKSQEQLAAE      420
Radixin     AQKELEEQTRKALELDQERKRAKEEAERLEKERRAAEEAKSAIAKQAADQMKNQEQLAAE      420
Moesin      AQQELEEQTRRALELEQERKRAQSEAEKLAKERQEAEEAKEALLQASRDQKKTQEQLALE      420
            *::**.** ::**:*::*****:.***:*  :*  * .**. : : : ** *.***** *

Ezrin       LAEYTAKIALLEEARRRKEDEVEEWQHRAKEAQDDLVKTKEELHLVMTAPPPPPPPVYEP      480
Radixin     LAEFTAKIALLEEAKKKKEEEATEWQHKAFAAQEDLEKTKEELKTVMSAPPPPPPPPVIP      480
Moesin      MAELTARISQLEMARQKKESEAVEWQQKAQMVQEDLEKTRAELKTAMSTPH------VAE      474
            :** **:*: ** *:::**.*. ***::*  .*:** **: **: .*::*

Ezrin       VSYHVQESLQDEGAEPTGYSAELSSEGIRDDRNEEKRITEAEKNERVQRQLLTLSSELSQ      540
Radixin     PTENEHDEHDEN---NAEASAELSNEGVMNHRSEEERVTETQKNERVKKQLQALSSELAQ      537
Moesin      PAENEQDEQDEN---GAEASADLRADAMAKDRSEEERTTEAEKNERVQKHLKALTSELAN      531
             : : ::. :::    :  **:*  :.: ..*.**:* **::*****:::* :*:***::

Ezrin       ARDENKRTHNDIIHNENMRQGRDKYKTLRQIRQGNTKQRIDEFEAL     586
Radixin     ARDETKKTQNDVLHAENVKAGRDKYKTLRQIRQGNTKQRIDEFEAM     583
Moesin      ARDESKKTANDMIHAENMRLGRDKYKTLRQIRQGNTKQRIDEFESM     577
            ****.*:* **::* **:: *************************::
```

Appendix 1: Clustal Omega multiple sequence alignment (Sievers et al. 2011. Mol Syst Biol. 11; 7:539; and Goujon et al. 2010, Nucleic Acids Res. 2010. 38 (Web Server issue): W695-9) of human ezrin (NCBI reference sequence: NP_001104547.1), human radixin (NCBI reference

sequence: AAH47109.1), and human moesin (NCBI reference sequence: NP_002435.1) proteins. asterisk sign indicates identical/conserved amino acids, (appendix 1 continues next page) while gap indicates non-identical amino acids, : colon sign indicates conservation between groups of strongly similar properties, . period sign indicates conservation between groups of weekly similar properties and red arrow (bold) indicates critical phosphorylation site (Ezrin Thr567, radixin Thr564, and moesin Thr558). Red amino acids represent small, hydrophobic (including aromatic) amino acids, blue amino acids represent acidic amino acids, magenta amino acids represent basic amino acids, and green amino acids represent polar, hydroxyl amino acids.

2. Multiple sequence alignment of human CLIC5A, human CLIC1, and human CLIC4

```
CLUSTAL O(1.2.4) multiple sequence alignment


CLIC1       -----------MAEEQPQVELFVKAGSDGAKIGNCPFSQRLFMVLWLKGVTFNVTTVDTK        49
CLIC5A      MT---DSATANGDDRDPEIELFVKAGIDGESIGNCPFSQRLFMILWLKGVVFNVTTVDLK        57
CLIC4       MALSMPLNGLKEEDKEPLIELFVKAGSDGESIGNCPFSQRLFMILWLKGVVFSVTTVDLK        60
                         :.:* :******* ** .***********:******.*.***** *

CLIC1       RRTETVQKLCPGGQLPFLLYGTEVHTDTNKIEEFLEAVLCPPRYPKLAALNPESNTAGLD        109
CLIC5A      RKPADLHNLAPGTHPPFLTFNGDVKTDVNKIEEFLEETLTPEKYPKLAAKHRESNTAGID        117
CLIC4       RKPADLQNLAPGTHPPFITFNSEVKTDVNKIEEFLEEVLCPPKYLKLSPKHPESNTAGMD        120
            *:   :::*.** : **: :. :*:**.******** .* * :* **:  : ******:*

CLIC1       IFAKFSAYIKNSNPALNDNLEKGLLKALKVLDNYLTSPLPEEVDETSAEDEGVSQRKFLD        169
CLIC5A      IFSKFSAYIKNTKQQNNAALERGLTKALKKLDDYLNTPLPEEIDANTCGEDKGSRRKFLD        177
CLIC4       IFAKFSAYIKNSRPEANEALERGLLKTLQKLDEYLNSPLPDEIDENSMEDIKFSTRKFLD        180
            **:********:.   *  **:** *:*: **:**.:***:*:* .:  :   * *****

CLIC1       GNELTLADCNLLPKLHIVQVVCKKYRGFTIPEAFRGVHRYLSNAYAREEFASTCPDDEEI        229
CLIC5A      GDELTLADCNLLPKLHVVKIVAKKYRNYDIPAEMTGLWRYLKNAYARDEFTNTCAADSEI        237
CLIC4       GNEMTLADCNLLPKLHIVKVVAKKYRNFDIPKEMTGIWRYLTNAYSRDEFTNTCPSDKEV        240
            *:*:************:*::*.****.: **  : *: ***.***:*:**:.**  *.*:

CLIC1       ELAYEQVAKALK--      241
CLIC5A      ELAYADVAKRLSRS      251
CLIC4       EIAYSDVAKRLTK-      253
            *:** :*** *.
```

Appendix 2: Clustal Omega multiple sequence alignment (Sievers et al. 2011. Mol Syst Biol. 11; 7:539; and Goujon et al. 2010, Nucleic Acids Res. 2010. 38 (Web Server issue): W695-9) of human CLIC5A (NCBI reference sequence: ABG46342.1), human CLIC1 (NCBI reference sequence: UQL51164.1), and human CLIC4 (NCBI reference sequence: CAG38532.1) protein

sequencess. Black underline indicates PP1c binding motif ($_{45}$-KGVVF-$_{49}$ in CLIC5A). asterisk sign indicates identical/conserved amino acids, (appendix 2 continues next page), while gap indicates non-identical amino acids, : colon sign indicates conservation between groups of strongly similar properties, . period sign indicates conservation between groups of weekly similar properties and red arrow (bold) indicates critical phosphorylation site (ezrin Thr567, radixin Thr564, and moesin Thr558). Red amino acids represent small, hydrophobic (including aromatic) amino acids, blue amino acids represent acidic amino acids, magenta amino acids represent basic amino acids, and green amino acids represent polar, hydroxyl amino acids.

UNIVERSITY OF ALBERTA

RESEARCH ETHICS OFFICE

308 Campus Tower
Edmonton, AB, Canada T6G 1K8
Tel: 780.492.0459
uab.ca/reo

Notice of Approval for Renewal

Date:	September 4, 2018
Study ID:	AUP00000222
Study Title:	CLIC5 and TIMAP study
Principal Investigator:	Barbara Ballermann
Approval Expiry Date:	Tuesday, September 17, 2019

Funding Source:

RSO or Project ID	Agency/Sponsor Name
RES0024007	Division of Nephrology, University of Alberta
G099001279	General Research
RES0020991	Kidney Foundation of Canada
RES0028395	Heart And Stroke Foundation Of Canada

Thank you for submitting a renewal to the Animal Care and Use Committee. Your application for renewal was reviewed and is approved by the committee.

Approved Animal Number: 70 Mice

The Canadian Council on Animal Care (CCAC) requires annual renewal of ethics approval for research projects using animals, and a Full Renewal in the 4th year. These renewals must be approved by the ACUC prior to the anniversary or expiration date of this approval. The University of Alberta's Animal Welfare Assurance Number is #A5070-01.

Any changes to this approved protocol must be submitted as an amendment online.

You will be sent electronic reminders to renew your ethics approval 90, 60, 45, and 30 days prior to the expiry date. To allow time for the review process, we recommend you submit your renewal **2 months** prior to the expiry date of this approval. If you do not have a renewal underway before that date, the animal facility and RSO will be notified the study is due to expire, you **will not** be able to order animals, and you may be asked to submit a new animal use application.

All approved animal use protocols are subject to Post-Approval Monitoring (PAM). PAM is a vital part of a robust and effective animal care and use program and it takes many forms including researcher self-assessment, veterinary reports, facility consultation, tracking cage-level care and animal health, scheduled and unannounced lab visits, observation, and education. Post-approval monitoring is a shared responsibility of animal users, ACUCs, veterinarians and animal care staff and the Research Ethics Office. If you have any questions about PAM, please contact Donna Taylor, PAM Coordinator, at 780--492-6828 or donna.taylor@ualberta.ca.

Sincerely,

Mary Hitt, PhD
Acting Chair, ACUC: Health Sciences 2

UNIVERSITY OF ALBERTA

RESEARCH ETHICS OFFICE

308 Campus Tower
Edmonton, AB, Canada T6G 1K8
Tel: 780.492.0459
uab.ca/reo

Notice of Approval for Renewal

Date:	December 5, 2019
Study ID:	AUP00000222
Study Title:	CLIC5 and TIMAP study
Principal Investigator:	Barbara Ballermann
Approval Expiry Date:	Tuesday, September 17, 2020

Funding Source:

RSO or Project ID	Agency/Sponsor Name
RES0029405	NSERC - Natural Sciences And Engineering Research Council
G099001279	General research

Thank you for submitting a renewal to the Animal Care and Use Committee. Your application for renewal was reviewed and is approved by the committee with a caveat as described in an email sent on December 5, 2019.

Approved Animal Number: 238 Mice

The Canadian Council on Animal Care (CCAC) requires annual renewal of ethics approval for research projects using animals, and a Full Renewal in the 4th year. These renewals must be approved by the ACUC prior to the anniversary or expiration date of this approval. The University of Alberta's Animal Welfare Assurance Number is #A5070-01.

Any changes to this approved protocol must be submitted as an amendment online.

You will be sent electronic reminders to renew your ethics approval 90, 60, 45, and 30 days prior to the expiry date. To allow time for the review process, we recommend you submit your renewal **2 months** prior to the expiry date of this approval. If you do not have a renewal underway before that date, the animal facility and RSO will be notified the study is due to expire, you **will not** be able to order animals, and you may be asked to submit a new animal use application.

All approved animal use protocols are subject to Post-Approval Monitoring (PAM). PAM is a vital part of a robust and effective animal care and use program and it takes many forms including researcher self-assessment, veterinary reports, facility consultation, tracking cage-level care and animal health, scheduled and unannounced lab visits, observation, and education. Post-approval monitoring is a shared responsibility of animal users, ACUCs, veterinarians and animal care staff and the Research Ethics Office. If you have any questions about PAM, please contact Donna Taylor, PAM Coordinator, at 780--492-6828 or donna.taylor@ualberta.ca.

Sincerely,

Frances Plane, PhD
Chair, ACUC: Health Sciences 2

UNIVERSITY OF ALBERTA

RESEARCH ETHICS OFFICE

308 Campus Tower
Edmonton, AB, Canada T6G 1K8
Tel: 780.492.0459
uab.ca/reo

Notice of Approval for Renewal

Date:	October 29, 2020
Study ID:	AUP00000222
Study Title:	CLIC5 and TIMAP functions in Glomerular Endothelial cell development and differentiation and Breeding Colony
Principal Investigator:	Barbara Ballermann
Approval Expiry Date:	Friday, September 17, 2021

Funding Source:

Project ID	Agency/Sponsor Name
RES0047576	Canadian Institutes of Health Research
RES0029405	NSERC
G099001279	MULTI SPONSOR

Thank you for submitting a renewal to the Animal Care and Use Committee. Your application for renewal was reviewed and is approved by the committee.

Approved Animal Numbers:

Species	#Re-used	#New Requested	Total # Approved for current protocol year
Mouse	0	146	146

The Canadian Council on Animal Care (CCAC) requires annual renewal of ethics approval for research projects using animals, and a Full Renewal in the 4th year. These renewals must be approved by the ACUC prior to the anniversary or expiration date of this approval. The University of Alberta's Animal Welfare Assurance Number is #A5070-01.

Any changes to this approved protocol must be submitted as an amendment online.

You will be sent electronic reminders to renew your ethics approval 90, 60, 45, and 30 days prior to the expiry date. To allow time for the review process, we recommend you submit your renewal **2 months** prior to the expiry date of this approval. If you do not have a renewal underway before that date, the animal facility and RSO will be notified the study is due to expire, you **will not** be able to order animals, and you may be asked to submit a new animal use application.

All approved animal use protocols are subject to Post-Approval Monitoring (PAM). PAM is a vital part of a robust and effective animal care and use program and it takes many forms including researcher self-assessment, veterinary reports, facility consultation, tracking cage-level care and animal health, scheduled and unannounced lab visits, observation, and education. Post-approval monitoring is a shared responsibility of animal users, ACUCs, veterinarians and animal care staff and the Research Ethics Office. If you have any questions about PAM, please contact Donna Taylor, PAM Coordinator, at 780--492-6828 or donna.taylor@ualberta.ca.

Sincerely,

Frances Plane, PhD

Chair, ACUC: Health Sciences 2

UNIVERSITY OF ALBERTA

RESEARCH ETHICS OFFICE

2-01 North Power Plant (NPP)
11312 - 89 Ave NW
Edmonton, Alberta, Canada T6G 2N2
Tel: 780.492.0459
www.uab.ca/reo

Notice of Approval for Renewal

Date:	September 20, 2021
Study ID:	AUP00000222
Study Title:	CLIC5 and TIMAP functions in Glomerular Endothelial cell development and differentiation and Breeding Colony
Principal Investigator:	Barbara Ballermann
Approval Expiry Date:	Saturday, September 17, 2022

Funding Source:

Project ID	Agency/Sponsor Name
RES0047576	Canadian Institutes of Health Research
RES0029405	NSERC
G099001279	MULTI SPONSOR

Thank you for submitting a renewal to the Animal Care and Use Committee. Your application for renewal was reviewed and is approved by the committee.

Approved Animal Numbers:

Species	#Re-used	#New Requested	Total # Approved for current protocol year
Mouse	0	50	50

The Canadian Council on Animal Care (CCAC) requires annual renewal of ethics approval for research projects using animals, and a Full Renewal in the 4th year. These renewals must be approved by the ACUC prior to the anniversary or expiration date of this approval. The University of Alberta's Animal Welfare Assurance Number is #A5070-01.

Any changes to this approved protocol must be submitted as an amendment online.

You will be sent electronic reminders to renew your ethics approval 90, 60, 45, and 30 days prior to the expiry date. To allow time for the review process, we recommend you submit your renewal **2 months** prior to the expiry date of this approval. If you do not have a renewal underway before that date, the animal facility and RSO will be notified the study is due to expire, you **will not** be able to order animals, and you may be asked to submit a new animal use application.

All approved animal use protocols are subject to Post-Approval Monitoring (PAM). PAM is a vital part of a robust and effective animal care and use program and it takes many forms including researcher self-assessment, veterinary reports, facility consultation, tracking cage-level care and animal health, scheduled and unannounced lab visits, observation, and education. Post-approval monitoring is a shared responsibility of animal users, ACUCs, veterinarians and animal care staff and the Research Ethics Office. If you have any questions about PAM, please contact Donna Taylor, PAM Coordinator, at 780--492-6828 or donna.taylor@ualberta.ca.

Sincerely,

Frances Plane, PhD

Chair, ACUC: Health Sciences 2

UNIVERSITY OF ALBERTA

RESEARCH ETHICS OFFICE

2-01 North Power Plant (NPP)
11312 - 89 Ave NW
Edmonton, Alberta, Canada T6G 2N2
Tel: 780.492.0459
www.uab.ca/reo

Notice of Approval for Renewal

Date:	October 19, 2022
Renewal ID:	AUP00000222_REN10
Study ID:	AUP00000222
Study Title:	CLIC5 and TIMAP functions in Glomerular Endothelial cell development and differentiation and Breeding Colony
Principal Investigator:	Barbara Ballermann
Approval Expiry Date:	Sunday, September 17, 2023

Funding Source:

Project ID	Agency/Sponsor Name
RES0047576	Canadian Institutes of Health Research
RES0029405	NSERC
G099001279	MULTI SPONSOR

Thank you for submitting a renewal to the Animal Care and Use Committee. Your application for renewal was reviewed and is approved by the committee.

Approved Animal Numbers:

Species	#Re-used	#New Requested	Total # Approved for current protocol year
Mouse	0	50	50

The Canadian Council on Animal Care (CCAC) requires annual renewal of ethics approval for research projects using animals, and a Full Renewal in the 4th year. These renewals must be approved by the ACUC prior to the anniversary or expiration date of this approval. The University of Alberta's Animal Welfare Assurance Number is #A5070-01.

Any changes to this approved protocol must be submitted as an amendment online.

You will be sent electronic reminders to renew your ethics approval 90, 60, 45, and 30 days prior to the expiry date. To allow time for the review process, we recommend you submit your renewal **2 months** prior to the expiry date of this approval. If you do not have a renewal underway before that date, the animal facility and RSO will be notified the study is due to expire, you **will not** be able to order animals, and you may be asked to submit a new animal use application.

All approved animal use protocols are subject to Post-Approval Monitoring (PAM). PAM is a vital part of a robust and effective animal care and use program and it takes many forms including researcher self-assessment, veterinary reports, facility consultation, tracking cage-level care and animal health, scheduled and unannounced lab visits, observation, and education. Post-approval monitoring is a shared responsibility of animal users, ACUCs, veterinarians and animal care staff and the Research Ethics Office. If you have any questions about PAM, please contact Pamela Raposo - Senior Officer Animal Care and Use, at 780-492-6828 or praposo@ualberta.ca.

Sincerely,

Catherine Chan, PhD

Chair, ACUC: Health Sciences 2

UNIVERSITY OF ALBERTA

RESEARCH ETHICS OFFICE

2-01 North Power Plant (NPP)
11312 - 89 Ave NW
Edmonton, Alberta, Canada T6G 2N2
Tel: 780.492.0459
www.uab.ca/reo

Notice of Approval for Renewal

Date:	November 9, 2023
Renewal ID:	AUP00000222_REN11
Study ID:	AUP00000222
Study Title:	CLIC5 and TIMAP functions in Glomerular Endothelial cell development and differentiation and Breeding Colony
Principal Investigator:	Barbara Ballermann
Approval Expiry Date:	Thursday, October 31, 2024

Funding Source:

Project ID	Agency/Sponsor Name
RES0047576	Canadian Institutes of Health Research

Thank you for submitting a renewal to the Animal Care and Use Committee. Your application for renewal was reviewed and is approved by the committee.

Approved Animal Numbers:

Species	#Re-used	#New Requested	Total # Approved for current protocol year
Mouse	0	0	0

The Canadian Council on Animal Care (CCAC) requires annual renewal of ethics approval for research projects using animals, and a Full Renewal in the 4th year. These renewals must be approved by the ACUC prior to the anniversary or expiration date of this approval. The University of Alberta's Animal Welfare Assurance Number is #A5070-01.

Any changes to this approved protocol must be submitted as an amendment online.

You will be sent electronic reminders to renew your ethics approval 90, 60, 45, and 30 days prior to the expiry date. To allow time for the review process, we recommend you submit your renewal **2 months** prior to the expiry date of this approval. If you do not have a renewal underway before that date, the animal facility and RSO will be notified the study is due to expire, you **will not** be able to order animals, and you may be asked to submit a new animal use application.

All approved animal use protocols are subject to Post-Approval Monitoring (PAM). PAM is a vital part of a robust and effective animal care and use program and it takes many forms including researcher self-assessment, veterinary reports, facility consultation, tracking cage-level care and animal health, scheduled and unannounced lab visits, observation, and education. Post-approval monitoring is a shared responsibility of animal users, ACUCs, veterinarians and animal care staff and the Research Ethics Office. If you have any questions about PAM, please contact Pamela Raposo - Senior Officer Animal Care and Use, at 780-492-6828 or praposo@ualberta.ca.

Sincerely,

Catherine Chan, PhD
Chair, ACUC: Health Sciences 2